Characterisation of the bZIP Transcription Factor Hac1 Key Domains in Transcriptional Repression of Early Meiotic Genes

SAGINI, HANAN,ABDUALRAHMAN,M

Abstract

In *Saccharomyces cerevisiae*, accumulation of unfolded proteins in the endoplasmic reticulum promotes *HAC1* mRNA splicing by the transmembrane kinase-endoribonuclease Ire1.Spliced Hac1 consists of 238 amino acids ($Hac1^{i}$), compared to its unspliced form of 230 amino acids ($Hac1^{u}$). $Hac1^{i}$ negatively regulates differentiation in response to nitrogen starvation, such as meiosis. $Hac1^{i}$ represses transcription of early meiotic genes (EMGs) under the control of URS1 promoter element. URS1 sites act as repressor sequences during mitosis and function as activator sites during meiosis. Recruitment of Rpd3L histone deacetylase complex by Ume6-Ime1 to URS1 facilitates repression of EMGs by $Hac1^{i}$ in response to nitrogen starvation, interfering with sporulation.

The bZIP transcription factor $Hac1^{i}$ consists of a DNA-binding domain, leucine zipper domain, and a C-terminal transactivation domain. These domains share highly conserved residues with other well studied bZIP transcription factors, such as Gcn4. Here we observe the effect of different Hac1 constructs in regulating EMGs transcription through USR1 in nitrogen sensing. We constructed and characterised $Hac1^{u}$, and three classes of point mutants in the different domains of the $Hac1^{i}$ transcription factor, $Hac1^{i}$-N49L mutation in the DNA-binding domain, $Hac1^{i}$-L67P/L74P/V81P mutants in the leucine zipper, and a S238A mutation in the transactivation domain requirement. Experiments with URS1-*lacZ* reporter genes demonstrated that $Hac1^{i}$ has higher repression potential than $Hac1^{u}$ and requires its transactivation domain for repression of EMGs in response to nitrogen starvation. $Hac1^{i}$ bZIP mutant residues partially disrupt repression of EMGs transcription by $Hac1^{i}$; consequently, these point mutations interfere with binding of Hac1 to DNA, dimerisation of Hac1, and transcriptional activation by Hac1. Data from these T_4C-URS1-*lacZ* reporter experiments were confirmed using northern analysis of EMGs such as *IME2*, *HOP1*, and *SPO13*. Further northern analysis eliminated several known constituents of Rpd3L histone deacetylase complex (*DEP1*, *CTI6*, *RXT2*, *RXT3*, *PHO23*, *SDS3*, *SAP30*), as transcriptional targets of $Hac1^{i}$. In summary, $Hac1^{i}$, its bZIP domain key residues, and its transactivation domain are required to repress transcription of EMG via URS1 in response to nutrient sensing. Overall, the findings provided novel insights into how Hac1 represses early meiotic genes via the bZIP characteristics in *S. cerevisiae*. Future work will investigate and develop methods to screen and identify $Hac1^{i}$ potential targets involved in negatively regulating EMGs in response to nitrogen starvation. And characterisation whether Hac1 inhibits nucleosomal acetylation in the promoters of EMGs.

Characterisation of the bZIP Transcription Factor Hac1 Key Domains in Transcriptional Repression of Early Meiotic Genes

Hanan Abdulrahman Sagini

This thesis is submitted as part of the requirements for the award of
Degree of Doctor of Philosophy

Department of Biosciences
Durham University
April 2022

TABLE OF CONTENTS

1 INTRODUCATION 1

1.1 The endoplasmic reticulum and the unfolded protein response 2

1.1.1 The endoplasmic reticulum 2

1.1.2 The unfolded protein response 4

1.1.3 IRE1 4

1.1.4 *HAC1* mRNA splicing by the Ire1 RNase domain 5

1.1.5 $Hac1^{i}$ triggers the UPR 6

1.1.6 Hac1 half-life and the UPR 7

1.2 Hac1 domains 10

1.2.1 $Hac1^{i}$ transactivation domain 10

1.2.2 Hac1 bZIP transcription domain 11

1.2.3 Disruption in the bZIP domain 15

1.3 *HAC1* mRNA translational fail-safe 16

1.3.1 Leaky splicing of $HAC1^{u}$ mRNA 16

1.3.2 Leaky translation of $HAC1^{u}$ mRNA 17

1.4 Nutrient sensing pathways in *S. cerevisiae* 17

1.4.1 Carbon sensing pathway 18

1.4.2 Nitrogen sensing pathway 19

1.4.3 The TOR signalling pathway 20

1.5 *Saccharomyces cerevisiae* differentiation responses 23

1.5.1 Master regulators of differentiation 25

1.5.2 Pseudohyphal growth 25

1.5.3 Meiosis (sporulation) 32

1.6 Unfolded protein response pathway's involvement in nutrient sensing and developmental programs 52

1.6.1 The UPR pathway's role in nutrient sensing and differentiation 52

1.6.2 Basal activity of the UPR during vegetative growth 54

1.7 Aims 56

2 MATERIALS AND METHODS 58

2.1 Materials 58
2.1.1 Reagents 58
2.1.2 Buffers and Solutions 63
2.1.3 RNA Buffers and Solutions 70
2.1.4 Yeast, Bacterial Strains and Plasmids 76
2.1.5 Primers 79
2.1.6 Antibodies 83
2.2 Methods 84
2.2.1 Microbiology 84
2.2.2 Molecular Biology 91
2.2.3 Plasmid DNA, and RNA Quantification 94
2.2.4 *In vitro* DNA Manipulation 95
2.2.5 Chemical Transformation of *E. coli* 100
2.2.6 Transformation of *Saccharomyces cerevisiae* 101
2.2.7 Protein Biochemistry 102
2.2.8 Immunoprecipitation (IP) 105
2.2.9 RNA Methods 109
2.2.10 Statistical Analysis 113
3 Production of HAC1 Mutants to Investigate HAC1 Domains Key Residue Functions 114
3.1 Rationale 114
3.2 Construction of *HAC1^u*, an Intron-less Form of *HAC1* mRNA 115
3.3 Construction of pRS303-HA-*HAC1^i* 118
3.4 Mutation of the Conserved Asparagine Residue in the Basic Region of Hac1^i 119
3.4.1 Multiple Mutations in the Leucine Zipper Region 120
3.4.2 Mutation of the Hac1^i S238 Residue Located in the Transactivation Domain 120
3.5 Discussion 121
4 Hac1 Mutant Derivatives in Regulation of UPRE-Controlled Genes 124
4.1 Rationale 124
4.2 Hac1^i is Required to Efficiently Activate UPRE-controlled genes 125

4.3 Hac1^{i} Requires Specific Residues in the bZIP Domain to Activate the UPRE-controlled plasmid....126

4.4 Discussion....128

5 Hac1 bZIP Conserved Residues Play a Role in Transcription Regulation of EMGs by Hac1^{i} 130

5.1 Rationale 130

5.2 238 aa Hac1 represses URS1 activation significantly stronger than 230 aa Hac1 131

5.3 N49 Invariant Asparagine within the DNA-Binding Region is Required to Repress Transcription of EMGs by Hac1^{i} 134

5.4 Point Mutations in the Leucine Zipper Domain Mitigate Transcriptional Repression on URS1 by Hac1^{i}....136

5.5 S238 is Required for Efficient URS1 Element Transcription Repression Mediated by Hac1^{i}....139

5.6 Repression of EMGs Requires Specific Residues Within the Domains of the bZIP Transcription Factor Hac1 141

6 Experiments to Measure Steady-State Levels of Hac1 and Hac1 Variants....146

6.1 Rationale 146

6.2 Experiments to Extract and Detect Hac1^{i}....147

6.3 Experiments to Optimise Measurement of Steady-State Levels of Hac1^{i}...149

6.3.1 Hac1^{i} Fractionation by Ammonium Sulfate $(NH_4)_2SO_4$....149

6.3.2 Hac1^{i} Immunoprecipitation Using Capture of the anti-HA antibody With Protein A Coupled to Agarose Beads 157

6.3.3 Hac1^{i} Immunoprecipitation Using Magnetic Beads 159

6.4 Discussion....168

7 Transcription of Known Components of RPD3L (HDA) are not regulated by Hac1^{i} 171

7.1 Rationale 171

7.2 Hac1^{i} is not required to transcribe known constituents of HDAC (*DEP1, CTI6, RXT2, RXT3, PHO23, SDS3, SAP30*) 172

7.3 Discussion....173

8 Conclusion and Future Work.....174

9 BIBLIOGRAPHY 181

TABLE OF TABLES

Table 2-1 Media reagents....58
Table 2-2 Chemical reagents....60
Table 2-3 Commonly used buffers and solutions and their protocol....63
Table 2-4 Specialist used buffers and solutions and their protocol....67
Table 2-5 Buffers and solutions used for RNA work and their protocol....70
Table 2-6 List of Enzymes....75
Table 2-7 List of Kits....75
Table 2-8 Yeast Strain....76
Table 2-9 Bacterial Strains....77
Table 2-10 Plasmid List....78
Table 2-11 Oligonucleotides for cloning....79
Table 2-12 Oligodeoxynucleotides to amplify DNA fragment for target RNA....81
Table 2-13 Antibodies....83
Table 2-14 Liquid media for *Saccharomyces cerevisiae*....85
Table 2-15 Solidified media for *Saccharomyces cerevisiae*....88
Table 2-16 PCR (Overlap extension)....95
Table 2-17 Cycling parameters for the QuikChange II XL method....97
Table 2-18 DNA Template Amplification....109

TABLE OF FIGURES

Figure 1-1 Protein folding and quality control in the endoplasmic reticulum in yeast. 3
Figure 1-2 ER stress and the unfolded response signalling pathway. 8
Figure 1-3 The *HAC1* gene is *Saccharomyces cerevisiae*. 9
Figure 1-4 A schematic illustration showing the Hac1^{i} bZIP transcription factor's characteristic domains..... 11
Figure 1-5 structure of the yeast bZIP homodimer, GCN4 (blue α -helices) bound to DNA (red helices). 14
Figure 1-6 Nutrient sensing signalling pathways in *S. cerevisiae*. 22
Figure 1-7 An illustration depicting the life cycle of *Saccharomyces cerevisiae* and alternative fates for haploid and diploid yeast. 24
Figure 1-8 The MAPK and PKA signalling pathway involved in pseudohyphal growth. .. 27
Figure 1-9 Schematic structure of the IME1 5′ untranslated region showing IME1 promoter regulation by different stimuli. 33
Figure 1-10 Model for the signal network that controls meiotic initiation in *S. cerevisiae*. 34
Figure 1-11 Interaction of transcriptional regulators, histone-modifying enzymes, and chromatin remodelling complexes in regulation of early meiotic genes. 42
Figure 1-12 A model showing of a nitrogen-sensing pathway. 55
Figure 3-1 *HAC1^{u}* intron deletion strategy. 117
Figure 3-2 Structure of Hac1^{i} bZIP domain, composed of the DNA-binding region and leucine zipper dimerization region, in addition to the transactivation domain at the C-terminus. 123
Figure 4-1 Hac1 mutant derivatives in regulation of UPRE-*lacZ*. 127
Figure 5-1 Hac1 bZIP conserved residues play a role in mediating transcription of URS1-*CYC1-lacZ*. 133
Figure 5-2 The invariant asparagine within the DNA-binding region is required to negatively regulate transcription of URS1-*CYC1-lacZ*. 135
Figure 5-3 The leucine zipper mutant has a role in regulating repression of URS1-*CYC1-lacZ*. 138
Figure 5-4 The transactivation domain residue Ser-238 plays a role in repressing URS1-*CYC1-lacZ*. 140
Figure 5-5 Hac1 conserved residues are required for negative regulation of EMGs during nitrogen starvation. 143
Figure 6-1 Coomassie Blue staining and destaining of whole cell extracts expressing EV and mutant Hac1 proteins. 148

Figure 6-2 Hac1^{i} $(NH_4)_2SO_4$ fractionation. 151
Figure 6-3 Fractionation scheme to observe Hac1^{i} precipitation.....153
Figure 6-4 Ammonium sulfate ($(NH_4)_2SO_4$) fractionation of HA-tagged p2UG-Hac1^{i} using different $(NH_4)_2SO_4$ concentrations. 156
Figure 6-5 Hac1^{i} Immunoprecipitation with α-HA antibodies. 159
Figure 6-6 Hac1^{i} Immunoprecipitation using magnetic beads (Method optimisation) 161
Figure 6-7 Hac1^{i} Immunoprecipitation using magnetic beads.....166
Figure 7-1 Hac1^{i} is not required to regulate early meiotic genes repression through known components of the Rpd3L complex. 173

LIST OF ABBREVIATIONS

$(NH_4)_2SO_4$	Ammonium sulfate
3′ BE	cis-acting bipartite element at *HAC1*^{u} 3′UTR
3′ UTR	Three prime untranslated region
5′ UTR	Five prime untranslated region
A_{600}nm	Absorbance measured at 600 nm wavelength
aa	Amino acid
AP-1	Activator protein 1
APC/C	Anaphase-promoting complex/cyclosome
APS	Ammonium persulphate
ATP	Adenosine 5′-triphosphate
BCY1	Bypass of CYclic-AMP requirement
BIP	HSP70 molecular chaperone
bp	Base pair
BSA	Bovine serum albumin
bZIP	Basic leucine zipper
C-SPO	Complete sporulation medium
C-terminus	Carboxyl-terminus
cAMP	cyclic adenosine monophosphate
CDC20	Cell Division Cycle
$CHCl_3$	Chloroform
CIAP	Calf intestine alkaline phosphatase
CTI6	Cyc8-Tup1 Interacting protein
CYC1	Cytochrome c, isoform 1
d	Days
DEP1	Disability in regulation of expression of genes involved in phospholipid biosynthesis
DEPC	Diethyl Pyrocarbonate
DNA	Deoxyribonucleic acid
dNTP	Deoxynucleotide triphosphates
DOC	Deoxycorticosterone
DTT	Dithiothreitol
EDTA	Ethylenediaminetetraacetic acid
EMG	Early meiotic genes
ER	Endoplasmic reticulum

ERAD	Endoplasmic reticulum-associated degradation
EtOH	Ethanol
FOS	proto-oncogene
g	Gram
GCN4	General Control Nonderepressible
GPCR	G protein coupled receptor
h	Hour
HA	Human influenza hemagglutinin
HAC1	Homologue of ATF/CREB1
HAT	Histone acetyltransferases
HDAC	Histone deacetylases
HOP1	Homolog pairing
IME1	Inducer of meiosis 1
IME2	Inducer of meiosis 2
IP	Immunoprecipitation
IRE1	Inositol requiring enzyme 1
JUN	proto-oncogene
KAR2	Karyogamy
Kb	Kilobases
kDa	kilo Dalton (unit in mass)
l	Litre
LB	Lennox broth or lysogeny broth
M	Molar
MAPK	A mitogen-activated protein kinase
mg	Milligrams
min	Minute
ml	Millilitre
mM	Millimolar
N-terminus	Amino terminus
NCR	Nitrogen catabolite repression
NDR	Nitrogen discrimination pathway
ng	Nanogram
nt	Nucleotides
o/n	Overnight
^{o}C	Degree Celsius

ORF	Open reading frame
PCR	Polymerase chain reaction
PEST	Peptide sequence that is rich in proline (P), glutamic acid (E), serine (S), and threonine (T)
PHO23	Phosphate metabolism
PKA	Protein kinase A
PMSF	Phenylmethylsulfonyl fluoride
PSP2	Pre-sporulation medium
RLB	Reporter lysis buffer
RNA	Ribonucleic acid
RNase	Endoribonuclease
RPD3	Histone deacetylase of RPD3-SIN3 complex
Rpm	Revolutions per minute
RT	Room temperature
RXT2	Component of the histone deacetylase Rpd3L complex
SAGA	Histone acetyltransferase, chromatin-modifying complex
SAP30	Sin3-Associated Polypeptide
SD	Synthetic dextrose medium
SDS	Sodium dodecyl sulphate
sec	Second
SIN3	Switch independent
SPO13	Sporulation
ss	Splice site
SSC	Saline-sodium citrate
T_4C	An enhancer on nonfermentable carbon source
TCEP	Tris(2-carboxyethyl)phosphine
Tm	Tunicamycin
U	Units
UAS	Upstream activating sequence
UME6	Unscheduled meiotic gene expression
UPR	Unfolded protein response
UPRE	Unfolded protein response element
URS1	Upstream repressing site 1
UV	Ultraviolet
Vol	Volume

YPD	Yeast extract peptone dextrose medium
β-gal	β-galactosidase
Δ	Deletion
λ	wavelength
µg	microgram
µM	micromolar

DECLARATION

I confirm that this thesis is my own work and that it contains no material previously submitted for a degree in this or any other institute. All data are my own other than those represented in the following figure: 1.5. It will also be stipulated in the text where research is not my individual contribution.

STATEMENT OF COPYRIGHT

ACKNOWLEDGMENTS

Foremost, I would like to express the deepest appreciation to my supervisor; Dr Martin Schröder. I cannot emphasise enough how much his direction, supervision, and commitment to my project helped with the final product outcome. His endless support throughout my ups and downs really shaped my PhD project, personal skills, and growth. Dr Martin's devotion to his research, stressing on ER-stress (pun not intended), has left me with a new attitude towered research and what it means to be committed to an art. Gratefully filled with different emotions, I tip my hat to Dr Martin Schröder for his tolerance and encouragement.

I also want to thank my lab 2 mates for their delightful company and respect, especially: Max Brown and Amnah Obidan. They both have supported me and helped when I needed a hand, when my tow hands weren't enough. It was enlightening and great to meet everyone in the bioscience department and Durham University.

I am also grateful to my thesis committee members, Dr Akis (Iakowos) Karakesisoglou and Professor Carrie A. Ambler for their attention, understanding, and encouragement during my time at Durham University.

In addition, without the first pond in this chess game (more like boxing) being moved by the University of Jeddah, supported by the Royal Embassy of Saudi Arabia Cultural Bureau, I would not have had the opportunity and fanatical support to continue my dreams of higher education. So, thanks for believing in me.

Finally, I would like to give a warm thanks to my family and friends for their constant source of inspiration.

I know you are waiting for my acknowledgment of Covid-19 virus; however, I think it acknowledged itself more than enough worldwide. See it even tricked me into mentioning Covid-19 in my thesis. So, stay safe everyone.

DEDICATION

All my accomplishments and overcoming's throughout my PhD are attributed solely to "Alla". With his guidance and mercy, I am where I am today. I am excited to see what my future holds with his grace and mercy.

I also then, dedicate this accomplishment to my parents, without their love, support, supplications, and belief in me I would not have reached the finishing line of this project. My dad's hot chocolate and mom's jokes truly motivated me through the past year of writing.

Family is a word with various meanings, each of which supported and pushed me to believe in myself, no matter how difficult things seemed. Therefore, Hend, Abdualrahim, Taha, Azhar, and Tasneem I appreciate with all my heart everything you'll have done for me.

During my time at Durham University, like many, the road to success appeared bleak and far sometimes; however, with the support and encouragement of my friends: Wajnat Tunsi, Duaa Hajawi, Sibal Orhan, Betul Dogan-Akkas, Naema Al Nofeli, and Amnah Obidan, I was able to overcome the hurdles that came my way.

1 INTRODUCATION

The endoplasmic reticulum (ER) is responsible for folding of membrane and secretory proteins. ER stress can be caused by accumulation of mis- or unfolded proteins. ER stress triggers activation of the unfolded protein response (UPR). In the yeast UPR signalling pathway, the ER-located transmembrane protein Ire1 promotes splicing of the *HAC1* pre-mRNA (*HAC1*^{u}) to generate the translatable transcription factor mRNA (*HAC1*^{i}). Hac1^{i} is a basic leucine-zipper (bZIP)-containing factor which promotes transcription of ER-resident molecular chaperones and upregulates ER-associated protein degradation (ERAD). Thus, alleviating ER stress and restoring homeostasis. Homeostasis indicates an unstressed cell, or does it? There is nothing such as a completely unstressed cell, but more of a minimally stressed cell. Interestingly, yeast defective in the UPR and ERAD display decreased cell viability. Yeast in exponentially growing cultures display minimal levels of *HAC1* mRNA splicing. These observations suggest that under normal conditions "unstressed" cells contain sufficient unfolded proteins to activate the UPR. Furthermore, normal growth conditions are also nitrogen-rich; hence, *HAC1* splicing is also regulated by nitrogen availability. In nitrogen-rich conditions, *HAC1* mRNA is regulated to synthesise functional Hac1^{i}, whereas in complete nitrogen starvation *HAC1* splicing stops. This change in the yeast nutritional statues demands a response. Diploid budding yeast respond by promoting either of two differentiation programs during nitrogen starvation, pseudohyphal growth or sporulation. These two programs are negatively regulated by Hac1^{i}. Consequently, increased synthesis of Hac1^{i} in nitrogen-rich conditions represses differentiation. Sporulation repression requires inactivation of entry into meiosis, thus Hac1^{i} production represses meiosis. In a previous study by my lab, results showed that bZIP transcription factor Hac1^{i} negatively regulates induction of early meiotic genes (EMGs) under nitrogen starvation. The aim of this thesis is to investigate the role of Hac1^{u} and Hac1^{i} bZIP conserved residues in regulating repression of EMGs. First, this introduction will discuss the ER. Then I will discuss ER stress with respect to the UPR and activation of the signalling pathway. The signalling pathway responsible for inducing pre-mRNA *HAC1* splicing will be explained, under stressed conditions. Next, I will highlight the significance of Hac1 bZIP features. I will look into the cell's response to nutrient environments, and the factors that control nutrient sensing which leads to the activation of integrated pathways. In addition, the response of diploid cells to nitrogen starvation is governed by the presence of fermentable or non-fermentable carbon sources, which decides cell differentiation fate. The cell response programs to nitrogen

starvation will also be discussed with reference to Hac1^{i} and its ability to negatively regulate differentiation. Finally, histone deacetylase complex (Rpd3-Sin3 HDAC) will be explored, because of Hac1^{i} role in regulating sporulation through this complex.

1.1 The endoplasmic reticulum and the unfolded protein response

1.1.1 The endoplasmic reticulum

In eukaryotes, most secreted proteins are initially targeted to the ER where they undergo synthesis, modification, and delivery to their target destinations. They are either inserted, or translocated into the ER lumen or lipid bilayer, depending on whether they are soluble or contain transmembrane domains, respectively. Furthermore, the ER is responsible for folding its own resident proteins along with one-third of all proteins. Due to high traffic of unfolded proteins moving through the ER, undesired flux through this organelle can be formidable. Fortunately, the ER is the optimal environment for adequate protein folding; this can be attributed to the compartment's oxidative nature, which promotes disulfide bond formation, and its possession of large number of proteins that boost folding. These molecular chaperones and foldases are present in all cellular compartments that support protein folding. Molecular chaperones assist nascent proteins to fold and prevent protein aggregation, through preventing interactions of hydrophobic residues (Ron and Walter, 2007, Hartl, 1996, Stevens and Argon, 1999, Walter and Ron, 2011). In yeast, ER resident folding-assisting proteins include calnexin (Cnx), chaperones of the Hsp70 and Hsp90 families (e.g., BiP/Kar2/Grp78, Grp94), the protein disulfide isomerases (Pdi) which catalyses the formation of disulfide bonds and the peptidyl-prolyl-isomerases (Gething and Sambrook, 1992).

Many post-translational modification take place in the ER, such as N-glycosylation and disulfide linkage formation (Walsh, 2010, Kukuruzinska and Lennon, 1998). N-linked glycosylation improves protein solubility, decreases aggregation, provides a binding site for CNX, facilitates PDI interaction, and can be a marker for ERAD (Aebi et al., 2010). After proteins translocate into the ER with the support of cytosolic chaperones (Ssa1-4,Ssb, Sse-1/2) (Shaner et al., 2005), nascent polypeptides are bound by BiP which mediates the folding of proteins, through an ATP-dependent cyclic process of release and binding to BiP (Normington et al., 1989). A cycle of Pdi and Ero1 activity mediate correct disulfide bond formation. Ero1, is an oxidative folding protein in the ER (Frand and Kaiser, 1998, Kim et al., 2012). Nascent glycoproteins are bound by Cnx, to prevent aggregation and degradation, and mediated the proper folding and processing of the N-

glycan. Properly folded proteins and processed glycoproteins are released to transport vesicles, having passed the ER quality control, vesicles are then transported to the Golgi network (Brodsky and Skach, 2011). Extended BiP binding indicates misfolding and leads to protein degradation through the ER- associated protein degradation (ERAD) mechanism (Molinari et al., 2005, Gietz and Schiestl, 2007). However, extended binding of BiP to partially misfolded proteins also lead to the activation of the unfolded protein response (UPR) (Welihinda et al., 1999, Mori et al., 1992) (Figure 1.1).

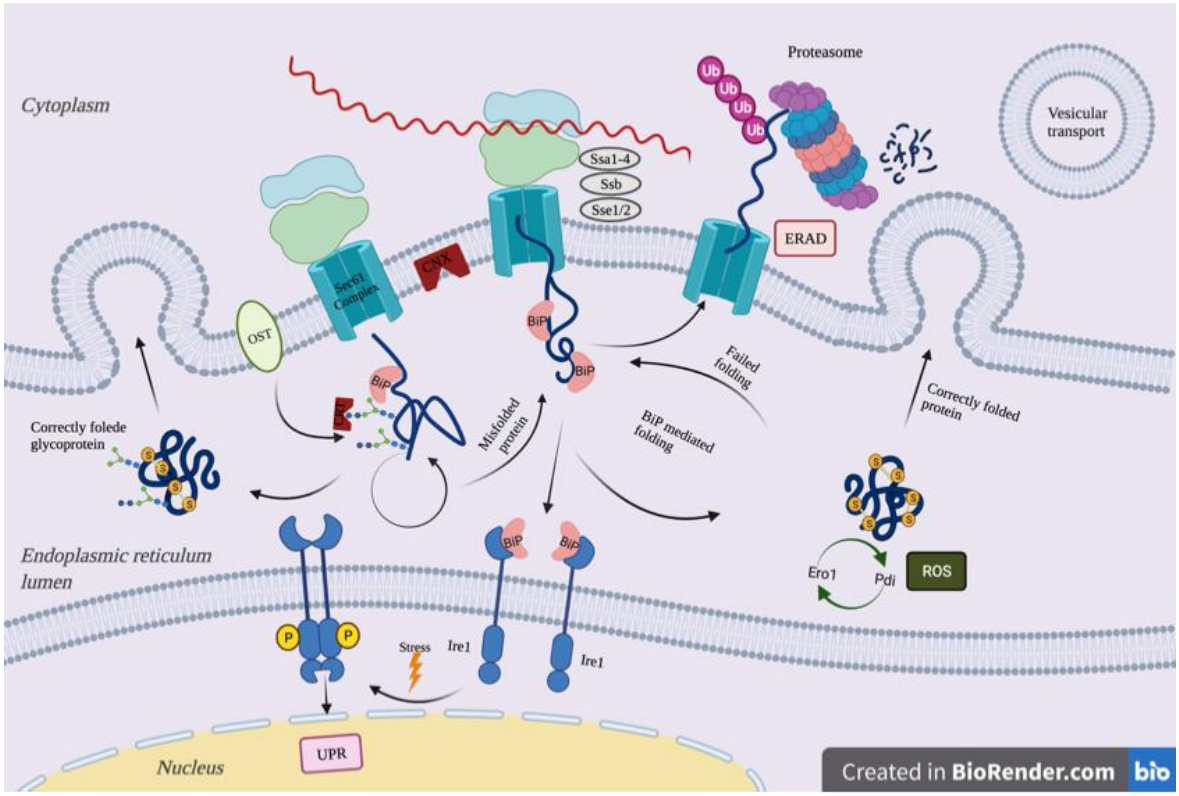

Figure 1-1 Protein folding and quality control in the endoplasmic reticulum in yeast.
A schematic illustration of protein folding, quality control, degradation, and secretion in the yeast *Saccharomyces cerevisiae*. Secretory proteins are transported into the ER through the Sec61 translocon complex of the ER membrane either co-translationally or post-translationally. In the latter case, cytosolic chaperones (Ssa1-4, Ssb, Sse1/2) support solubility and prevent aggregation of the polypeptide chains. After translocation to the ER, nascent polypeptides are bound by BiP.BiP mediates folding in an ATP-dependent cyclic process of release of and binding to BiP. The formation of correct disulfide bonds is mediated in a cycle of Pdi and Ero1 activity, which may lead to the formation of reactive oxygen species (ROS). Correctly folded proteins are released to transport vesicles, while prolonged BiP binding, indicating misfolding, leads to retrograde translocation to the cytosol and proteasomal degradation (ERAD). Nascent glycoproteins are bound by calnexin and mediated to correct folding and processing of the N-glycans. Failed folding leads to binding by the BiP complex and targeting to ERAD, while correctly folded and processed glycoproteins are released to transport vesicles. Prolonged binding of BiP to partially misfolded proteins lead to the induction of the unfolded protein response (UPR), mediated by Ire1.

1.1.2 The unfolded protein response

Accumulation of unfolded proteins in the ER lumen causes ER stress. Protein mis- or unfolding can be induced by environmental factors (e.g., low pH, temperature, oxidative stress), physiological (DNA-damage) or promoted by chemical agents (e.g., dithiothreitol (DTT), tunicamycin (Tm)). These drugs inhibit disulfide bond formation (DTT), or block protein glycosylation (Tm) (Hampton, 2000, Travers et al., 2000, Tkach et al., 2012). Under normal cellular conditions the rate of protein folding and the level of secreted proteins are balanced (Schröder and Kaufman, 2005) to maintain ER homeostasis. However, this homeostasis can be interrupted in response to programmes of cell differentiation, environmental conditions, and physiological state of the cell, causing ER stress or cellular damage (Smith et al., 2011, Özcan et al., 2004, Nishitoh et al., 2002). Accumulation of misfolded proteins can be lethal to the cell. In humans, several acute diseases are caused by such accumulation, for example Alzheimer's disease, Parkinson's disease, and type II diabetes (Chaudhuri and Paul, 2006). The unfolded protein response (UPR) is an ER signalling cascade, which upregulates the transcription of genes intended for maintaining ER homeostasis. This is done by transcribing genes to assist protein folding or protein degradation (ERAD) (Friedlander et al., 2000, Walter and Ron, 2011). In the yeast *Saccharomyces cerevisiae*, the UPR is activated to alleviate the ER stress arising from the accumulation of misfolded proteins. The UPR initiates a signal transduction pathway, in which the most upstream component of the pathway is Ire1 (Cox et al., 1993). Evidence has suggested that BiP/Kar2 plays a crucial role in regulating the UPR via interaction with Ire1. In that in an unstressed ER, the Ire1 luminal domain is associated with BiP/Kar2 as a chaperone substrate to inactivate the UPR (Figure 1.1). Therefore, identification of unfolded proteins is based on their competition with Ire1 for binding BiP/Kar2 (Figure 1.2) (Kimata et al., 2003, Pincus et al., 2010). There is also evidence that the luminal domain directly binds to unfolded proteins and that Ire1 is directly activated by unfolded proteins (Gardner et al., 2013, Adams et al., 2019).

1.1.3 IRE1

Ire1, is a transmembrane serine/threonine protein kinase with three functional domains. The N-terminal domain resides in the ER lumen and is believed to sense the extent of misfolded proteins in the ER (Cox et al., 1993). The C-terminal domain contains both protein kinase and site-specific endoribonuclease activities (RNase), this domain resides in the cytoplasm (Sidrauski and Walter, 1997, Cox et al., 1993, Mori, 2000). Upon ER stress

BiP/Kar2 is released from the Ire1 leading to Ire1 *trans*-autophosphorylation and aggregates, in the company of F-actin and type-II myosin (Ishiwata-Kimata et al., 2013), into discrete foci of Ire1 oligomers within the ER (Figure 1.2). The oligomerization of the activated Ire1 therefore promotes activity of its endoribonuclease, which is highly required for its splicing function. There is only one known substrate targeted by the Ire1 endoribonuclease activity (RNase), a precursor mRNA *HAC1 (HAC1^{u})*. The Ire1 ribonuclease is responsible for the cleavage step in the unconventional splicing of mRNA *HAC1^{u}* to generate mRNA *HAC1^{i}* encoding Hac1^{i} basic leucin zipper (bZIP) transcription factor, which in turn activates transcription of chaperone proteins in the UPR (Shamu and Walter, 1996, Welihinda and Kaufman, 1996, Sidrauski and Walter, 1997).

1.1.4 *HAC1* mRNA splicing by the Ire1 RNase domain

HAC1^{u} mRNA ("u" for uninduced) is constitutively transcribed but not translated in the cytosol. *Hac1^{u}* possesses a non-conventional intron near the 3′ end of the open reading frame, including the codons for the C-terminal 10 amino acids and the stop codon of the predicted protein (Cox and Walter, 1996). Stalling of *HAC1^{u}* translation is attributed to base pairing between the intron and the 5′ UTR forming a base-pair interaction (Rüegsegger et al., 2001, Uppala et al., 2022). The cis-acting bipartite element at *HAC1^{u}* 3′UTR (3′BE) allows for its selective recruitment to the oligomerized Ire1 clusters during ER stress to be spliced (Aragón et al., 2009, van Anken et al., 2014, Anshu et al., 2015). The resulting signalling cascade activates the UPR, and the intron is removed by two site-specific cleavages at the 5′and 3′ splice junctions. Thus, leading to the removal of a 252-nucleotide (nt) intron near the 3′ end of *HAC1 ^{u}* (Sidrauski and Walter, 1997). The two exons are subsequently joined by tRNA ligase (Rlg1) (Sidrauski et al., 1996), producing a new mRNA *HAC1^{i}* ("i" for induced). *HAC1^{i}* mRNA encodes a different protein, on which a new 18 amino acid tail is appended, containing the transactivation domain, in place of the previous C-terminal 10 amino acid tail. The newly generated mRNA can be efficiently translated to produce a functional transcription activator, Hac1^{i}, now that it is free from the inhibitory intron (Figure 1.2) (Cox and Walter, 1996, Welihinda et al., 2000). The translated Hac1^{i} contains a potent basic leucine zipper (bZIP) transcription factor (Gardner et al., 2013). *HAC1^{u}* may be translated due to experimental manipulation (mutating the nucleotides involved in base-pairing) of the transcriptional inhibitor, however, its encoded protein is unable to activate transcription as efficiently as Hac1^{i} (Chapman and Walter, 1997, Cox et al., 1997, Welihinda et al., 2000). The splicing of the translational attenuator from *HAC1^{u}* mRNA and the subsequent re-joining of the 5′ and 3′ parts is mechanistically

uncommon for mRNAs. The intron has a peculiar 5′ splice site (ss) (G|CCGUGAU, where "|" marks the exon|intron boundary) instead of the consensus of G|GUAUGU in yeast. It ends with a CG dinucleotide instead of the conventional AG dinucleotide. Moreover, it does not follow the conventional splicing machinery involving spliceosomes, which may allow for the stability of *HAC1*^{u} in unstressed cells. Indeed, production of *HAC1*^{i} mRNA only requires the two enzymes Ire1 and tRNA ligase in the UPR *in vitro* (Sidrauski et al., 1996, Cox and Walter, 1996, Sidrauski and Walter, 1997, Mori et al., 1996).

1.1.5 Hac1^{i} triggers the UPR

Once Ire1 has cleaved *HAC1*^{u} and *HAC1*^{i} has been successfully translated, Hac1^{i} is translocated into the nucleus (through its nuclear localization sequence 29-RKRAKTK-35, shared by both forms of Hac1) where it activates transcription of target genes (UPR-associated genes). *HAC1*^{u} encodes a 230 amino acid protein, while *HAC1*^{i} encodes a 238 amino acid protein (figure 1.3). UPR target genes are mediated by Hac1^{i} binding to one of two conserved unfolded protein response elements (UPRE): UPRE1 (GACAGCGTGTC) and UPRE2 (TACGTGT), which are the UPR-specific upstream activating sequences (Cox and Walter, 1996, Kawahara et al., 1997, Mori et al., 1996, Fordyce et al., 2012). Several UPR target genes carry the UPRE in their promoters, including elements of the ER resident chaperones *KAR2*, *PDI1*, *EUG1*, *FKB2*, and *LHS1* (Mori et al., 1998), and foldases, components of the protein secretory pathway, and genes involved in ERAD of misfolded proteins (Travers et al., 2000). The UPRE is both required and sufficient for transcriptional upregulation of genes by the UPR (Figure 1.2) (Kohno et al., 1993, Mori et al., 1992). Transcription of target genes involved in the UPR also involves the co-activator complex SAGA histone acetyltransferase (composed of Gcn5, Hfi1, Ada2, Ngg1, Ada5, Spt3, and Spt7). Gcn5/Ada5 complex subunits increases histone acetylation at chromatin encoding UPR-related genes (Welihinda et al., 2000, Welihinda et al., 1999). Histone acetylation reduces the positive charge in lysine residues in histone, which was tightly bound to the negatively charged DNA wrapped around it, to facilitate transcription. The protein subunit Gcn5 physically interacts with Ire1. Ada5 interacts with both Hac1 and Ire1, and is required for splicing *HAC1*^{u} mRNA in *vivo* (Welihinda et al., 2000).
The UPR displays a profound influence on *S. cerevisiae*, impacting the expression of genes involved in protein folding, cell surface architecture and secretion (Travers et al., 2000, Carrozza et al., 2005a). Nevertheless, the role of the UPR has been further recognised to be key in sensing and mediating nitrogen-regulating effects. *HAC1* mRNA activation takes place under nitrogen-rich conditions, and down-regulation of the UPR by nitrogen

starvation leads to cell differentiation in *S. cerevisiae* (Schröder et al., 2000). Moreover, the UPR is a versatile and sensitive regulatory mechanism involved in cellular development and environmental adaptation (Kaufman et al., 2002), confirming further complexity of this response (Schröder et al., 2003, Leber et al., 2004). Consequently, the transcriptional activation of nitrogen-sensitive genes involves the UPR-sensitive bZIP transcription factor $Hac1^{i}$ (Schröder et al., 2000, Schröder et al., 2004).

1.1.6 Hac1 half-life and the UPR

Both transcripts have the same transcription start site, so the proteins they encode differ only at their carboxyl termini. $Hac1^{u}$ and $Hac1^{i}$ have a similar half-life of 1.5-2.0 min, which leads to their rapid degradation using the ubiquitination pathway. Hac1's PEST degron interacts with SCF^{Cdc4} ubiquitin-ligase complex to mediate degradation; Hac1's accelerated degradation requires the functional nuclear localization sequence, basic residues (Chapman and Walter, 1997, Kawahara et al., 1997, Pal et al., 2007). Even more, $Hac1^{u}$ has a shorter half-life, due to the post-transcriptional silencing of $HAC1^{u}$ mRNA mediated by the 10 amino acid intron-encoded C-terminal tail (Di Santo et al., 2016). The short half-life of Hac1 dictates the importance of continuous generation of Hac1 to maintain UPR. For this reason the *HAC1* gene is autoregulated through its own UPRE promoter region (Ogawa and Mori, 2004). This interaction promotes positive feedback to produce Hac1 to sustain UPR; in other words, more elevated Hac1, the more transcription of *HAC1* and more Hac1. Once ER homeostasis is reached, the positive feedback loop is stopped by Ire1dephosphorylation by either Ptc2 or Dcr2 or both (Figure 1.2). Thus, decreasing the Ire1-mediated splicing of $HAC1^{u}$ (Welihinda et al., 1998, Guo and Polymenis, 2006) leading to rapid degradation of remaining Hac1 (Figure 1.3).

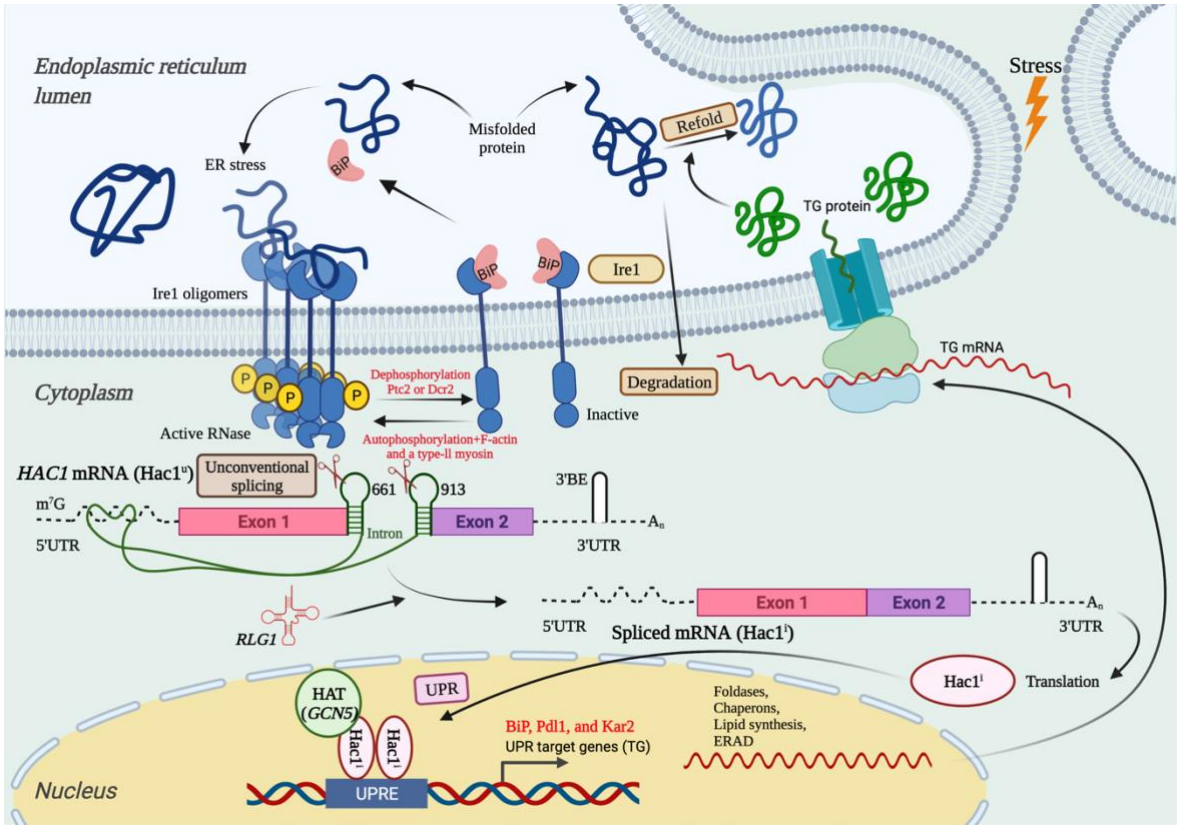

Figure 1-2 ER stress and the unfolded response signalling pathway.

A simplified view of IRE1+*HAC1* UPR signalling pathway in yeast. Accumulation of unfolded/misfolded proteins in the endoplasmic reticulum (ER) lumen triggers the autophosphorylation and oligomerization of Ire1p, which, together with Rlg1, removes the intron to release translation inhibition of *HAC1* mRNA. Pre-mRNA *HAC1* is constantly transcribed in the cytosol. Accumulation of mis- and un-folded proteins competes for BiP, which binds to Ire1 under non-stressed conditions to promote ER homeostasis and assist with folding. *Trans*- autophosphorylated Ire1 oligomers aggregate and cluster in the presence of F-actin and type-ll myosin to activate efficient RNase activity, it is at these foci that *HAC1* pre-mRNA is spliced. Translational fate of *HAC1* mRNA. The m^7G cap, 5′UTR (68 nt) and 3′UTR (416 nt), two exons (pink and purple, 661 and 56 nt, respectively), intron, and polyadenylated tail (A_n) of *HAC1* mRNA are shown. The intron interacts with the 5′UTR to form an RNA duplex. Under ER stress conditions, Ire1 cleaves two phosphodiester bonds at the nucleotide positions G 661 and G 913 (shown by scissors). Both positions are present in the two RNA hairpins. *HAC1* mRNA contains a 3′ *cis*-acting bipartite elements (3′BE) that signals to have the *HAC1* mRNA targeted to Ire1 foci for splicing. The single 252 nt *HAC1* intron is cleaved unconventionally by Ire1, where the 5′ and 3′ends are cleaved independently in random order. The two exons are then joined by the tRNA ligase Rlg1, which results in a translatable *HAC1* mRNA. Translated $Hac1^i$ enters the nucleus and transactivates target genes (TG) with a UPR element (UPRE), whose encoded proteins alleviate ER stress. The transcribed TG mRNAs are transported out of the nucleus for translation and enter the ER. The TG proteins (foldases, chaperones, and lipid synthesis) transported to the ER assist in the tolerance and recovery from ER stress. Proteins that fail to fold are directed to ER-associated degradation of unfolded/misfolded proteins (ERAD) for degradation. Created with BioRender.com

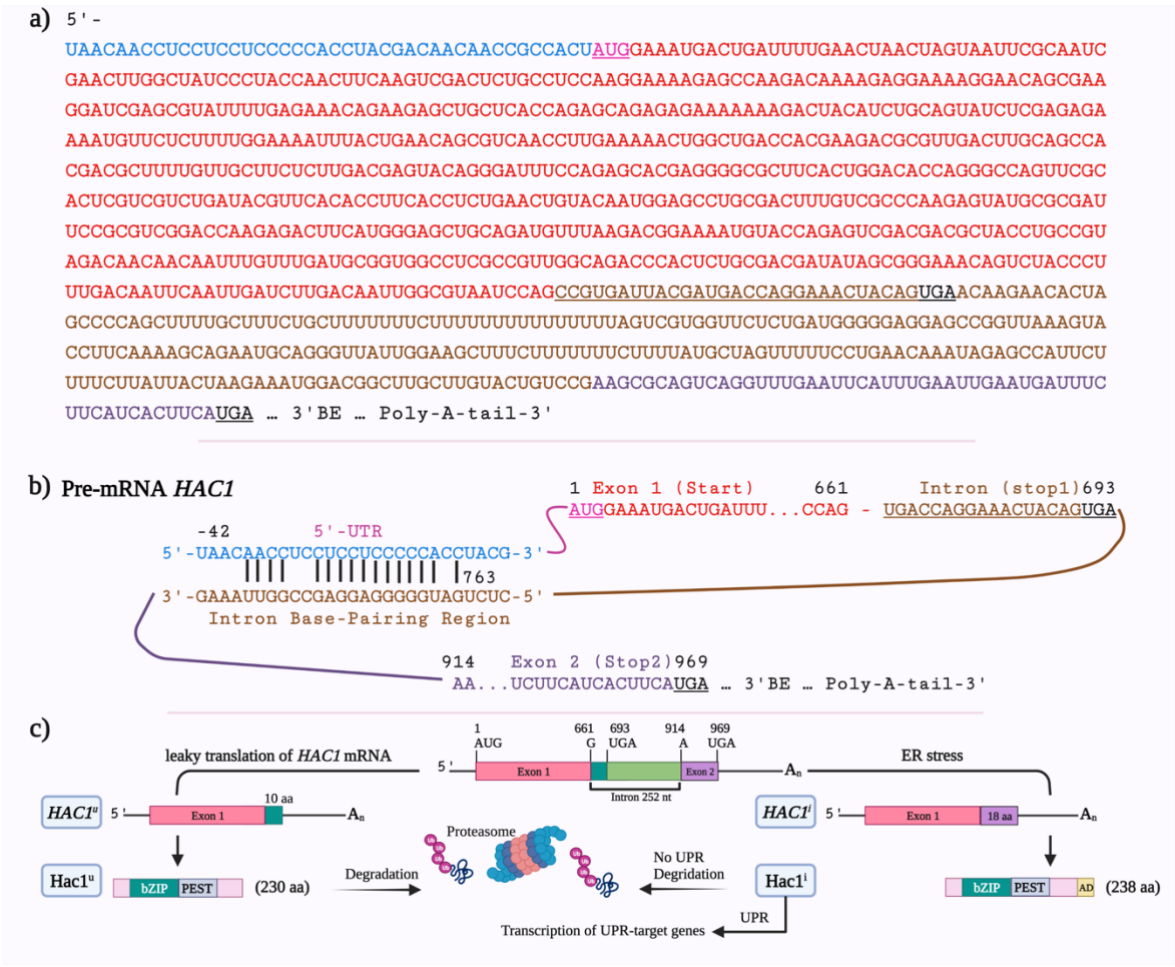

Figure 1-3 The *HAC1* gene is *Saccharomyces cerevisiae*.

(a) The annotated *HAC1*^{u} mRNA illustrating its sequence elements: 5′ untranslated region (5′ UTR) in blue, first exon in red, the 252 nt intron in brown, and the second exon in purple. The start (START) codon is pink and underlined, and the in-frame stop codons (UGA) in the intron (STOP1) and in the second exon (STOP2) are shown, respectively in black and underlined. The intronic sequence proposed to encode the C-terminal degron in Hac1^{u} is underlined in brown. The *HAC1*^{u} mRNA contains a 3′ bipartite element (3′ BE), for recognition and recruitment by Ire1 oligomers, in its 3′ untranslated region (3′ UTR). **(b)** An illustration presenting the base-pairs interaction between 5′ UTR and intron in *HAC1*^{u} to inhibit translation initiation of the pre-mRNA, with the same colour scheme as in (a). **(c)** A schematic representation of unspliced and spliced forms of *HAC1* mRNA and their protein coding regions. The two different forms of *HAC1* mRNA (*HAC1*^{u} and *HAC1*^{i}) are found in cells carrying out the unfolded protein response, which share the same transcription start site and differ in their carboxy termini. During ER stress, the 252 nt intron is cleaved and the two exons are joined producing Hac1^{i} protein (230 amino acid (aa)) with a unique 10 aa C-terminal tail, which proceeds to the nucleus to target the activation of UPR-target genes. The presence of identical clusters of PEST degron in both Hac1^{i} and Hac1^{u} C-terminals promote rapid degradation of undesired translated Hac1^{i} and Hac1^{u}, during ER homeostasis or as a result of *HAC1* mRNA bypassing the fail-safe mechanisms. Additionally, the Hac1^{u} (230 aa) 10 aa C-terminal tail contains a degron for further accelerated degradation. Put together, the half-life of both Hac1^{i} and Hac1^{u} are governed by the presence of the promoting degradation sites, which targets them to the proteasomes. Created with BioRender.com.

1.2 Hac1 domains

1.2.1 Hac1^{i} transactivation domain

In addition to the intron removal from *HAC1* mRNA facilitating translation of the functional Hac1^{i}, it also changes the sequence and properties of the encoded protein. Hac1^{i} and Hac1^{u} share the same amino-terminal sequence, not disrupted by the splicing event, containing a DNA-binding region (Kawahara et al., 1997). However, as mentioned, splicing replaces the Hac1^{u} carboxyl-terminal tail with a new carboxyl-terminal tail containing a transactivation domain. This transcriptional activation domain is key for the much higher transactivation activity of Hac1^{i} compared to Hac1^{u}. In a previous study to recognise the region(s) of Hac1 responsible for such a difference in transactivation by 230-aa Hac1 and 238-aa Hac1, they fused various Hac1 subregions immediately downstream of the DNA-binding domain of the yeast transcriptional activator Gal4. Transcriptional activation was determined by measuring the level of β-Galactosidase expressed from a UAS_{GAL}-*CYC1*- *lacZ* reporter gene integrated into the chromosome and UPRE-*lacZ* reporter. β-Galactosidase experiments revealed that the shorter protein Hac1^{u} (lacking the 18 amino acids) displayed reduced transactivation activity of Gal_4 activation domain and UPRE fused promoters, compared to Hac1^{i} (Figure 1.4). Further results from these experiments suggested that the 18 amino acid section plays a major role in transactivation activity of Hac1^{i} and that residue Ser-238 in the 18 amino acids encoded by the second exon are necessary for transactivation activity. Moreover, fusion of either C-terminal tail to an unrelated DNA-binding domain, the 18 amino acid tail served as an extremely active transcriptional activation domain, whereas the 10 amino acid tail was basically inactive (Mori et al., 2000, Kawahara et al., 1997, Chapman and Walter, 1997).Therefore, the intron effectually plays a role in separating the DNA-binding domain from the transcriptional activator, so in case the translational attenuation was bypassed, the translated product will be less active. Hence, the mechanism of Hac1^{i} activation is fitting to overcome undesired translation consequences such as, slow cell growth (Mori et al., 2000, Kawahara et al., 1997).

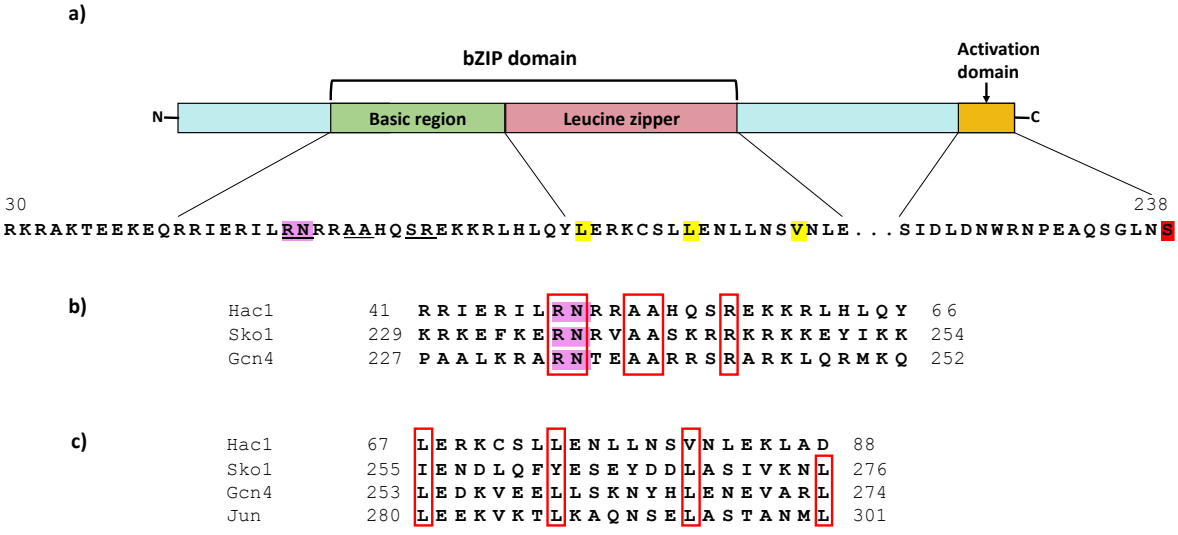

Figure 1-4 A schematic illustration showing the Hac1^{i} bZIP transcription factor's characteristic domains.

The sequences for Saccharomyces cerevisiae were obtained from Saccharomyces genome data base (a) The basic region of Hac1^{i} is in green, and the amino acid sequence showing the invariant asparagine (N) is highlighted in pink and the conserved amino acids are underlined. The leucine zipper region in pink, and the regions amino acids showing the heptad repeats are highlighted in yellow. The 18 amino acid C-terminal tail containing the activation domain is in orange, the serine-238, crucial for efficient transcriptional activity, is highlighted in red. (b) The sequence alignment of the bZIP domain basic region from selected yeast Saccharomyces cerevisiae proteins. Conserved amino acids in the basic region are enclosed within red boxes. (c) The sequence alignment of the bZIP domain leucine zipper region from selected proteins. Heptad repeat amino acids are enclosed within red boxes.

1.2.2 Hac1 bZIP transcription domain

Hac1 is a basic leucine zipper (bZIP) transcription factor. It is part of one of the largest and diverse families of transcription factors in eukaryotic cells. bZIP proteins are vastly involved in regulating different cellular processes such as the UPR and nutrient sensing (Asada et al., 2011, Nojima et al., 1994, Schröder et al., 2000). The Hac1 bZIP transcription factor is characterized by its highly conserved domain composed of two structural features (Nijhawan et al., 2008). The bZIP domain is between about 40 to 60 amino acids, and consistent of a conserved DNA-binding basic region and a diverse leucine zipper dimerization region (Figure 1.4) (Glover and Harrison, 1995, Alber, 1992). The N-terminus of the bZIP domain contains the DNA-binding basic region and consists of approximately 16 amino acid residues characterized by an invariant (NXAAXXCR) motif, which is responsible for nuclear localization and DNA binding. The leucine zipper includes a heptad repeat of leucine or other bulky hydrophobic amino acids (isoleucine,

valine, phenylalanine, or methionine) positioned 7 residues apart moving toward the C-terminus, which is involved in dimerization. Dimerization results in the correct protein structure for DNA binding by the adjacent highly basic region, which interacts directly with the acidic DNA (Alber, 1992, Ellenberger et al., 1992, Landschulz et al., 1988). In the Hac1 bZIP domain, the invariant asparagine corresponds to residue Asn-49; while the heptad repeats correspond to residues Leu-67, Leu-74, and Val-81 (Figure 1.4 a). Studies have shown that the leucine zipper sequence is in the form of coiled-coil, which mediates homo- and/or hetero-dimerization in bZIP proteins. The bZIP monomers form parallel α-helical dimers. Indeed, during bZIP DNA binding, the N-terminal region binds in the major groove to double-stranded DNA, while the C-terminal region facilitates dimerization to form a superimposed coiled-coil structure (leucine zipper). The stability of the dimer relies on the number of the heptad repeats (Landschulz et al., 1988, Ellenberger et al., 1992, Oas et al., 1990, O'Shea et al., 1989). Furthermore, the bZIP-DNA interaction structure has been proposed in two alike models, “scissors grip” and “induced helical fork” (Harrison, 1991, O'Neil et al., 1990). The two bZIP protein-DNA complex models suggest different roles for the invariant asparagine residue, found in the basic region of bZIP proteins. This highly conserved amino acid is proposed to form an N-cap structure that breaks the α-helix in the basic region, hence permitting it to bend sharply and to wrap around the DNA to execute the scissors grip model (Harrison, 1991). On the other hand, the invariant asparagine residue and other amino acids in the basic domain are proposed to make specific contacts with target genes through the highly conserved amino acids in the basic region according to the induced fork model (O'Neil et al., 1990).

In eukaryotes, Fos and Jun families are one of the best studied bZIP transcription factors (Johnson and McKnight, 1989), they contain the characteristic features of the bZIP domain, the basic region/leucin zipper (Landschulz et al., 1988). c-Fos and c-Jun are proto-oncogenes encoding proteins that form a complex which regulates transcription of promoters harbouring activation protein 1 (AP-1) element. An X-ray crystal structure shows the c-Fos and c-Jun bZIP region bound to DNA as a heterodimer. The distinct protein-DNA complexes shows that the coiled-coil is flexibly joined to the basic regions when comparing the two crystallographically complexes. Subsequently indicating that the c-Fos-c-Jun heterodimer does not recognize the asymmetric AP-1 (5′-TGACTCA-3′) DNA element in a unique way. Preferential formation of the c-Fos-cJun heterodimer over either of the homodimers is attributed to an extensive network of electrostatic interactions between subunits within the coiled-coil (Glover and Harrison, 1995, Halazonetis et al., 1988). The heterodimer binds with high affinity to the AP-1 transcription factor, thus regulating gene expression in response to different stimuli (e.g., cytokines, growth factors,

stress, and bacterial and viral infections) (Halazonetis et al., 1988, Hess et al., 2004). Also, AP-1 regulates numerus biological processes such as, differentiation, proliferation, and apoptosis (Ameyar et al., 2003). In yeast Gcn4 along with Sko1 share the conserved residues within the basic region with Hac1 (figure 1.4 b) and contain the heptad repeat residues (Figure 1.4 c) (Nehlin et al., 1992). Gcn4 is a well-studied bZIP transcription factor also known as a "master regulator" for gene expression. It is involved in transcribing the majority of the genes responsible for amino acid biosynthetic proteins; actively responsive during amino acid starvation (Hinnebusch and Natarajan, 2002). An X-ray crystal structure reveals that Gcn4 interacts with the DNA as a homodimer, each monomer of the Gcn4-DNA binding element forms a continuous α-helix with no apparent kinks or sharp bends; this interaction gives the form of a pair of tweezers (Figure 1.5). The intersecting angle between the monomers in the coiled-coil region resembles to Crick's knobs-into-holes packing scheme (O'Shea et al., 1989) for two α-helices. Stability of the homodimer is due to van der Waals interaction, the side-by-side packing conformation of leucine's in a zipper manner, and salt bridges taking place near the C-terminal residues in the bZIP domain. However, moving towards the basic region residues the protein subunits separate from the dimer axis in an effortlessly bending fork like manner, to house the DNA double helix further toward the N-terminal where the two helices open as tweezers. After clamping on opposite major grooves over the corresponding DNA half site, the first N-terminal turn of the helices do not wrap around the DNA but rather continues in a straight-line fashion outspreading the tweezer tips. It is important to note that the conserved asparagine in the bZIP families, Asn-235 makes connection with residues in the target element of the DNA binding site. Furthermore, the Gcn4-DNA complex is in agreement with the "induced fork" model (Ellenberger et al., 1992). The crystal structure revealed that bZIP Gcn4 bound to two different DNA duplexes, AP-1 (Ellenberger et al., 1992) and CRE (5′-TGACGTCA-3′) (König and Richmond, 1993) sites. Also, Gcn4 prefers and recognises the consensus sequence TGACTC, located upstream of several activated genes during amino acid starvation. Gnc4 binds to said DNA sequence and regulates transcription in response to environmental stress, and is rapidly degraded by the ubiquitin pathway (requires kinase Pho85 and SCF^{cdc4} ubiquitin-ligase complex, used in Hac1 degradation) under a rich amino acid condition (Arndt and Fink, 1986, Oliphant et al., 1989, Meimoun et al., 2000).

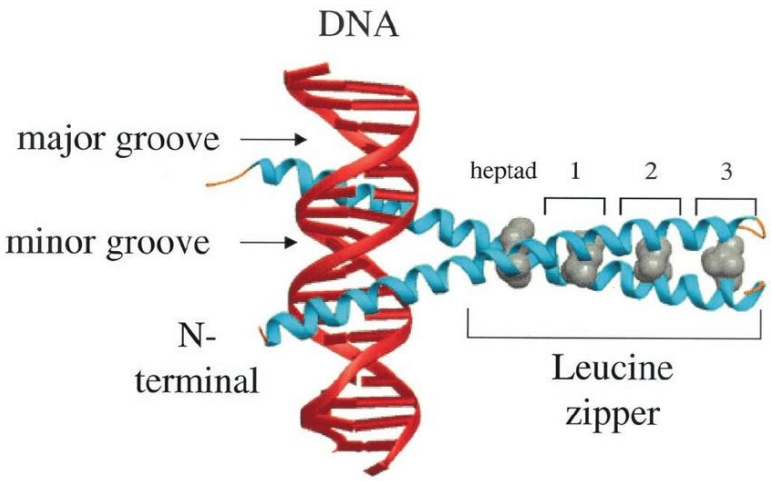

Figure 1-5 structure of the yeast bZIP homodimer, GCN4 (blue α -helices) bound to DNA (red helices).

The N-terminal DNA recognition helix lies in the major groove of the DNA. An almost invariant leucine presents every two turns of the C-terminal α -helix (at the d position) is shown in gray (Vinson et al., 2002).

1.2.3 Disruption in the bZIP domain

Since bZIP transcription factors are present and conserved in all eukaryotes, and they regulate target genes through a distinct structural motif that contains a basic region that directly contacts DNA, and an adjacent leucine zipper that mediates dimerization (Landschulz et al., 1988, Talanian et al., 1990, Ellenberger, 1994), it is safe to suggest that disruptions in the key residues will affect the proteins' function. The crystal structure of Gcn4 bound to DNA containing AP-1 and ATF/CREB revealed water-mediated interactions of both invariant basic domain residues, Asn-235 and R-243 with DNA, beyond their direct base contacts. The stability of the interaction required linkage of R-241/243/245 to main-chain carbonyl oxygen atoms through water molecules, this is made possible due to the slight bending of the basic domain α-helix around the DNA (Keller et al., 1995, König and Richmond, 1993). In the Fos-Jun X-ray structure, asparagine binds to the DNA palindrome CRE (5′-TGACGTCA-3′) through asparagine side-chain carbonyl oxygen interactions with hydrogen from the DNA (Glover and Harrison, 1995). Mutations or disruptions in eukaryotes bZIP conserved asparagine or arginine in the basic DNA-binding region, either abolishes or alters specific DNA binding or recognition, causing biological changes that can be lethal (Aukerman et al., 1991, Tzamarias et al., 1992, Lyon et al., 2003, Bowdish et al., 1995), more specifically mutation in the Gcn4 Asn-235 decreased the affinity with which it bound to DNA or even altered its specificity causing cell death (Tzamarias et al., 1992). Leucine zippers are rigid dimers of parallel extended helices. The hydrophobic heptad repeats along the C-terminal region interact to form a stable coiled-coil for each helix. The periodic repeat of leucine residues on the α-helix at every seventh position over a distance covers eight helical turns, when there are 4 leucine residues in each C-terminal. The polypeptide α-helical conformation allows the leucine side chain from one α-helix to interlock with those from the α-helix of the second polypeptide, promoting dimerization (O'Shea et al., 1989). In a study of the human immunodeficiency virus type 1 (HIV-1) gp41, substitutions in the leucine zipper-like heptad repeat renders the viruses non-infectious and envelope (Env) protein unable to mediate membrane fusion. They replaced each conserved leucine or isoleucine in the leucine zipper with proline residues, which affected the α-helical structure in a sever manner (Chen et al., 1998, Chen et al., 1993). The X-ray structure of the Gcn4 leucine zipper region, as mentioned before, displayed the importance of the leucine repeats interaction to form the coiled-coil structure (König and Richmond, 1993, Ellenberger et al., 1992). Genetic manipulation of single leucine residues in Gcn4 with other hydrophobic amino acids at the dimer interface, produced functionally variant Gcn4. However, when a

single leucine was substituted with either a polar or helix-breaking residue, the product variants were non-functional. Overall, the presence of a leucine in the dimer interface is required for efficient dimerization (Hu et al., 1990). Moreover, exchanging leucine zippers or DNA-binding regions between different bZIP proteins, had no effect on the dimerization efficiency but affected DNA- specificity (Hu et al., 1990). Given the evidence, the bZIP domain relies on conserved residues to facilitate its biological processes (Dwarki et al., 1990).

1.3 *HAC1* mRNA translational fail-safe

1.3.1 Leaky splicing of *HAC1^u* mRNA

In non-ER-stressed cells *HAC1* mRNA is stored as an unspliced isoform in the cytoplasm and no Hac1 protein is detectable (Cox and Walter, 1996, Chapman and Walter, 1997). Leaky splicing of *HAC1^u* is highly unfavourable, given it may cause activation of the UPR due to the accumulation of Hac1^i. There are two fail-safe mechanisms that help avoid leaky splicing. First, Kar2/BiP chaperone protein can handle residual Hac1^i weak signalling. As mentioned before, Kar2/Bip binds to Ire1 when it is not sequestered for protein folding and hinders Ire1 oligomerization and prevents its RNase splicing activity (Kimata et al., 2004, Pincus et al., 2010, Oikawa et al., 2007). Second, in the case of Ire1 dimer or oligomers clusters materialising, the 3′ BE in the 3′ UTR of *HAC1^u* is rapidly and efficiently removed. This prevents the translocation of *HAC1^u* to Ire1 foci (Aragón et al., 2009, Anshu et al., 2015), thus limiting Ire1-mediated splicing. As a result, *HAC1^i* mRNA are seldom detected in non-UPR cells (Bicknell et al., 2007), but leaky splicing of *HAC1^u* may still occur. To analyse this, a study utilizing the empirical measurement of splicing efficiency (SE) of introns based on the quantification of spliced (featuring exon-exon junctions) and unspliced (featuring exon-intron junctions) forms of individual genes or individual introns. The method of quantifying SE by using RNA-seq data was used (Xia, 2020). The results suggested there is weak splicing of *HAC1* in non-UPR cells, with ~ 2 % *HAC1^i* compared to ~ 69 % in UPR induced cell.

1.3.2 Leaky translation of *HAC1^u* mRNA

In non-ER-stressed cells *HAC1^u* mRNA is considered minimal given the well-established studies on the intron-mediated translation inhibition, and β-galactosidase reporter genes revealed Hac1^u as a weaker transcription factor than Hac1^i (Chapman and Walter, 1997, Kawahara et al., 1997, Mori et al., 2000). Together they don't suggest a risk of accidental UPR induction via Hac1^u. Even though, leaky translation of Hac1^u is rare, there is evidence of Hac1^u accumulation in the absence of efficient degradation in non-UPR cells (Di Santo et al., 2016). A fail-safe mechanism promoting rapid degradation is equally needed during Hac1^u production by leaky translation of *HAC1^u* mRNA, as in production of Hac1^i by leaky splicing and translation. This is made possible by the presence of a degron in the 10 amino acids encoded in the 5′ end of *HAC1^u* intron. Specifically, this degron is recognised by Duh1/Das1 (putative SCF ubiquitin ligase F-box protein), causing Hac1^u degradation in UPR induced cells (Di Santo et al., 2016).

1.4 Nutrient sensing pathways in *S. cerevisiae*

Diploid *S. cerevisiae* are capable of sensing nutrients or lack thereof in their surrounding environment, leading to alterations in their metabolic and transcriptional state to overcome nutritional changes. For example, cells growing in nitrogen-rich conditions are not limited anabolically, and protein synthesis exceeds protein folding in the ER leading to activating the UPR (Kaufman et al., 2002). Furthermore, in dealing with the change in conditions the yeast also decide on which of the various forms of developmental pathways it will pursue. There are many signalling pathways activated to trigger an effective adaptive response without inhibiting proliferation and without diminishing fermentative metabolism (Matallana and Aranda, 2017, Rødkær and Færgeman, 2014). Nutrient sensing and signalling pathways are well described with respect to adapting to changing environments (Rødkær and Færgeman, 2014, Conrad et al., 2014, Zhang et al., 2018). Different molecular systems respond to the presence or absence of nutrients, and most are cross regulated to attain a synchronised metabolic response. Here I will discuss the distinct cell sensing and signalling pathways involved in cell growth and proliferation in response to quality carbon and nitrogen sources in *S. cerevisiae*.

1.4.1 Carbon sensing pathway

S. cerevisiae can thrive on a variety of fermentable carbon sources, glucose being the favoured carbon source. Cells can modify their metabolism for optimal consumption of carbon sources. The use of glucose is executed through expression of genes encoding low affinity glucose transporters, such as hexose transporter 1-7 (Hxt1-7) and downregulation of genes involved in regulating growth on alternative carbon sources (gluconeogenesis, respiration and peroxisomal function) (Zhang et al., 2018, Ronne, 1995, Gancedo, 1998, Ozcan et al., 1996). Glucose sensing is mediated at the plasma membrane through the G-protein coupled receptor (GPCR) Gpr1. Once glucose is detected the G-protein α Gpa2 interacts with Gpr1 to initiates a signalling cascade (Figure 1.6) (Yun et al., 1998, Yun et al., 1997, Xue et al., 1998, Kraakman et al., 1999). Also, cells sense and transport glucose through hexose transporters (*HXT*) Rgt2/Snf3 transmembrane proteins, they also act as high/low affinity sensors, respectively (Ozcan et al., 1996). Glucose metabolism, furthermore, is regulated through cross-talk between two pathways, first the Rgt2/Snf3 glucose stimulation pathway responsible for glucose uptake (Kaniak et al., 2004, Johnston and Kim, 2005); second the Snf1/Mig1 glucose repression pathway that negatively regulates the genes involved in the glucose oxidation and the use of alternative sugars (Carlson, 1999). Its suggested that cells lock the signalling pathways in a cross-talking network to govern its sensitivity to environmental fluctuations in glucose (Broach, 2012, Santangelo, 2006), due to the need for glucose uptake and metabolism to induce the glucose repression pathway that inhibits Snf1 kinase (Özcan, 2002). The glucose uptake pathway is mediated by *HXT* via facilitated diffusion. *HXT* family members Hxt1-17 are expressed depending on glucose levels, the low affinity Hxt1 is expressed when glucose is abundant to fine tune glucose uptake (Özcan and Johnston, 1999, Diderich et al., 1999). Once glucose has been sensed hexose kinases Hxk1, Hxk2, and glucokinase Glk1 intracellular proteins bind and phosphorylate glucose at C_6 (Bianconi, 2003, Walsh et al., 1983). This results in glucose 6-phosphate leading to glycolysis (ROSE et al., 1991). Two signalling pathways respond to glucose sensing, 1) through PKA mediated monomeric Ras-GTPases, 2) via Gα homolog Gpa2 and a putative G-protein coupled respecter Gpr1 (Batlle et al., 2003, Broach and Deschenes, 1990, Harashima et al., 2006, Rolland et al., 2002). During glucose limitation Snf1 is required for the cell to adapt to the changing environment, and use alternate fermentable carbon sources such as sucrose and galactose or non-fermentable carbon sources such as ethanol and acetate, thus regulating the metabolic switch after glucose exhaustion (Gancedo, 1993, Palecek et al., 2002). Snf1is a serine/threonine protein kinase and is a member of the AMP-activated protein kinase

family that responds to AMP/ATP ratio (Carlson et al., 1981). When cells are subjected to non-fermentable carbon sources, Snf1 regulates activation of Cat8 and Sip4 and represses Mig1, thus regulating transcriptional derepression. Protein kinase A (PKA), Snf1, and the Rgt2p-Snf3p glucose sensors play redundant and overlapping roles in carbon source signalling (Rolland et al., 2002). Snf1 also has a role in different nutrient reactions and cellular developmental processes (including meiosis and sporulation, ageing, and diploid pseudohyphal growth) (Honigberg and Lee, 1998, Kuchin et al., 2002, Ashrafi et al., 2000).

1.4.2 Nitrogen sensing pathway

Nitrogen is a vital component of cellular metabolism because of its important role as a cellular building block (e.g., amino acids and nucleic acids). As a result, cells meticulously adapt to the accessibility and source of nitrogen in their surroundings, hence directing metabolic processes and influencing the developmental decisions of the cell (Johnston, 1977, Broach, 2012). Yeast cells prefer and metabolise ammonium and glutamine over other nitrogen sources like proline, urea, and allantoin; this leads to boosted growth rates. If cells are subjected to less favourable nitrogen sources, then transcriptional repression of numerous genes involved in nitrogen catabolism is initiated. Also known as, nitrogen discrimination pathway (NDP) or nitrogen catabolite repression (NCR) (Hofman-Bang, 1999). In the presence of desired nitrogen sources pseudohyphal growth or haploid invasive growth is prevented, and in the presence of any nitrogen source meiosis and sporulation is prevented (Lorenz and Heitman, 1998a, Schneper et al., 2004). Many of the regulatory events regulated by nitrogen availability are mediated via the target of rapamycin (TOR) signalling pathway (Broach, 2012, Rohde and Cardenas, 2004). The NCR pathway governs the utilization of different nitrogen sources, so during the presence of other nitrogen sources, genes needed for utilizing other sources are repressed (Cooper, 2002, Schneper et al., 2004). Cells sense nitrogen through ammonium transmembrane transporter Mep1, Mep2, and Mep3 involved in ammonium transport and nitrogen utilization (Figure 1.6) (Marini et al., 1994, Marini et al., 1997). In preferred nitrogen conditions and fermentable carbon source Mep1 and Mep2 are required for nitrogen sensing and activation of the cAMP-PKA pathway (Van Nuland et al., 2006). However, nitrogen starvation of diploid cells under a fermentable carbon source promotes a morphological switch from budding growth to pseudohyphal growth, both PKA and a mitogen-activated protein (MAP) kinase pathways are involved in the dimorphic switch (Gagiano et al., 2002). Mep2, but not Mep1 or Mep3 is essential for pseudohyphal growth (Lorenz and Heitman, 1998a). Furthermore, Gap1, a general amino acid permease, is

efficiently regulated in the presence of nitrogen, and during poor nitrogen circumstances, Gap1 is expressed in abundance with respect to the NCR pathway (Courchesne and Magasanik, 1983, Stanbrough and Magasanik, 1995). Gap1 interacts with the G-protein Gpa2 and regulates nitrogen sensing pseudohyphal differentiation (Kübler et al., 1997, Lorenz et al., 2000, Tamaki et al., 2000). The G-protein-coupled receptor system also senses glucose and mediates cAMP synthesis, which affects several targets of the PKA pathway including pseudohyphal, highlighting integration of glucose and nitrogen signals through Gpr1 in the pseudohyphal (Lorenz and Heitman, 1998a, Colombo et al., 1998, Xue et al., 1998, Lemaire et al., 2004, Versele et al., 1999).

1.4.3 The TOR signalling pathway

The Target of Rapamycin (TOR) is a highly conserved eukaryotic Ser/Thr-protein kinase functioning as a key integrator of signalling networks in response to nutrient sensing, specifically nitrogen and amino acids, thus, controlling cell growth and proliferation. Treatment of cells with rapamycin a macrolide from *Streptomyces hygroscopicus* bacteria living within the soil on the Rapa Nui or Easter Island (Sehgal, 2003), which is mediated through *Tor* genes together with FKBP12, results in physiological changes such as: G_1 cell cycle arrest, meiosis, protein synthesis inhibition, glycogen accumulation and autophagy by inhibiting the activity of Tor kinases. These responses mimic those seen in cells grown on poor media or starved for nutrients such as nitrogen and amino acids, NCR pathway. In mammalian cells, rapamycin inhibits Tor which then blocks cell proliferation and T cell maturation, thus accounting for the immunosuppressive and potential antioncogenic activity of the drug (Rohde et al., 2001). TOR kinases are found in two distinct protein complexes, named TOR complex1 (TORC1) and TOR complex 2 (TORC2) (Loewith et al., 2002, Barbet et al., 1996, Zheng and Schreiber, 1997, Aronova et al., 2007, Rohde and Cardenas, 2004, Wullschleger et al., 2006). TORC1 is composed of Tor1/Tor2, Kog1, Tco89, and Lst8, and is hypersensitive to rapamycin and is a regulator of cell growth in response to nutrient availability (Reinke et al., 2004, Chen et al., 2012). TORC2 is composed of Tor2, Lst8, Avo1, Avo2, Avo3, Bit61, and Bit2, and is insensitive to rapamycin and is involved in polarized cell growth, actin cytoskeletal organization and cell wall integrity (Loewith et al., 2002, Chen and Kaiser, 2003, Wedaman et al., 2003, Wullschleger et al., 2006). Interestingly, there is a suggested overlap between functions carried out by TORC1 and TORC2, seeing how treatment and/or inhibition of the Tap42/Sit4 phosphatase system influences actin polarization and cell integrity signalling (Torres et al., 2002, Wang and Jiang, 2003). Tap42 is essential to the TOR signalling

pathway and is physically associated with the protein phosphatase 2A (PP2A) and the Sit4 protein phosphatase catalytic subunits (Di Como and Arndt, 1996, Düvel et al., 2003). Association of Tap42 with Sit4 leads to inactivation of the phosphatase activity (Jiang and Broach, 1999). Tap42 interacts directly with TORC1 and controls transcriptional and translational programs that relate cell growth to amino acid availability, also regulates genes involved in NCR (Rohde et al., 2004, Hardwick et al., 1999). The presence of desirable nitrogen sources or high concentration of amino acids represses the general amino acid permease Gap1 (Magasanik and Kaiser, 2002). During nitrogen restriction Gap1 expression is stimulated by two GATA transcription factors Gln3 and Gat1 (Stanbrough and Magasanik, 1996, Stanbrough et al., 1995). Gap1 is also involved in activation of the PKA pathway that involves the protein Sch9 kinase on addition of amino acids to nitrogen starved cells (Donaton et al., 2003, Thevelein et al., 2005). Gln3 is a master regulator under alternative nitrogen sources along with Gat1 acting as transcriptional activators while Dal80 and Gzf3 act as transcriptional repressors of NCR sensitive genes (Scherens et al., 2006, Magasanik and Kaiser, 2002). Inhibition of the transcription factor Gln3 restricting induction of nitrogen catabolism repression genes and allowing for optimal nitrogen utilization. When nitrogen conditions are favourable, Gln3 is sequestered through Ure2 along with Gat1 into the cytoplasm. Limited nitrogen conditions and rapamycin treatment lead to dephosphorylation of Gln3/Gat1 and Ura2 by Sit4, resulting in complex dissociation and nuclear localization of the transcription factors, thus upregulation of NCR-sensitive genes (Figure 1.6) (Hardwick et al., 1999, Cardenas et al., 1999, Blinder and Magasanik, 1995, Beck and Hall, 1999). Therefore, Tor kinases phosphorylate Gln3 under good nitrogen conditions through Tap42/Sit4 deactivated phosphatase; there is also evidence that suggest Snf1 kinase as a regulator of Gln3 nuclear localization (Bertram et al., 2000, Bertram et al., 2002). In addition to the role of Tap42 and Sit4 in the TORC1 pathway, the Sch9 AGC kinase is another downstream regulator for TOR signals. Activation of Sch9 through TORC1-mediated phosphorylation induces ribosomal biogenesis and inhibits G_0 -arrest phase by avoiding nuclear localization of the protein kinase Rim15 under nitrogen-rich conditions. TORC1 or activated Sch9 phosphorylate Rim15 to prevent its nuclear localization. Cells treated with rapamycin, starved for glucose or nitrogen reverse TORC1-mediated phosphorylation in a manner independent of TORC1(Pedruzzi et al., 2003, Urban et al., 2007, Smets et al., 2008). In addition to Sch9 regulating core growth and stress genes in response to nitrogen source, it also directly suppresses signalling through the Gpr1 pathway. This TOR pathway and Gpa2-PKA pathway through Sch9 display a cross-talk between pathways; this may add to

the integration of multiple signalling pathways essential to the cell's decision to differentiate into pseudohyphal (Zaman et al., 2009).

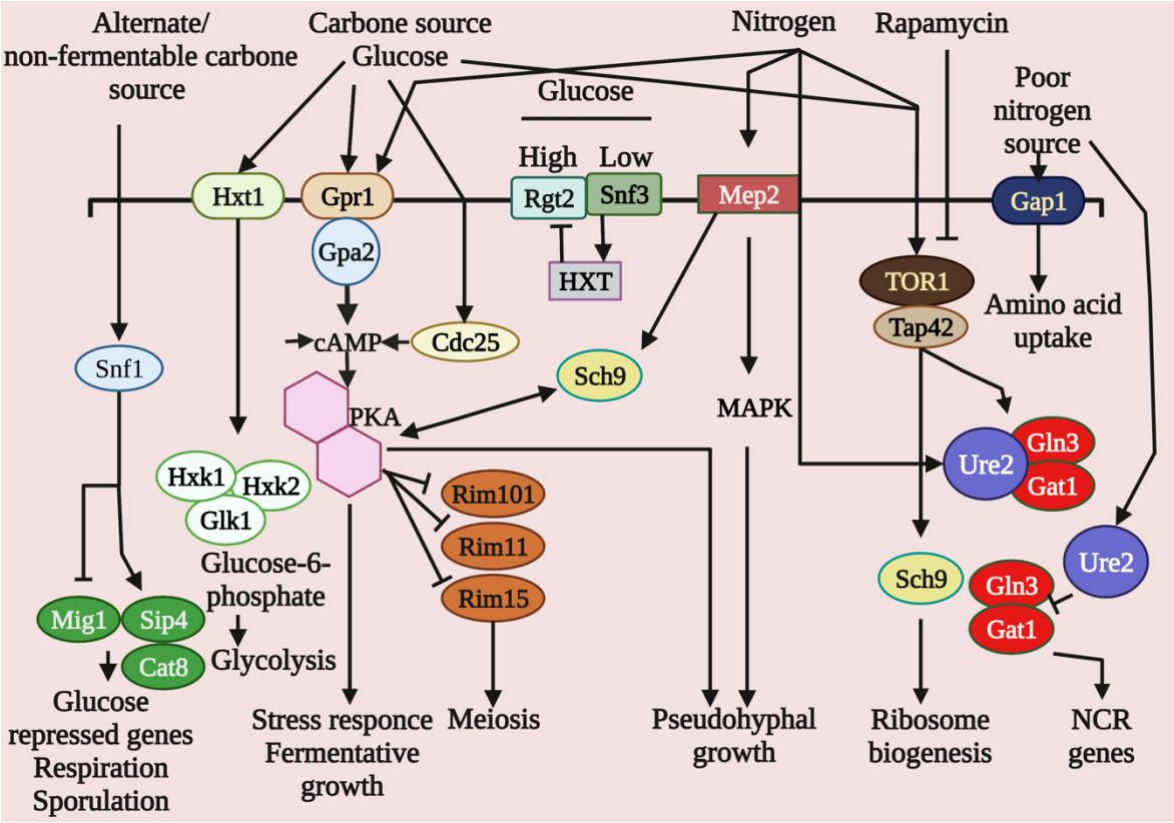

Figure 1-6 Nutrient sensing signalling pathways in *S. cerevisiae*.

Nutrients are sensed by *S. cerevisiae* through different sensors to activate signalling pathways that may function independently or converse with each other and may converge inducing a certain response. Carbon and nitrogen sources form major signalling pathways that regulate growth, metabolism, stress response and developmental pathways. Sensing and subsequent response to alterations in carbon sources are presented here. In the presence of glucose, plasma membrane sensing proteins Snf3, Rgt2, Gpr1 and Hxt1 lead to metabolic changes like glycolysis, induce differentiation pathways like meiosis or pseudohyphal growth. Glucose signals activate the production of cellular cAMP. This signalling pathway is called the cAMP-protein kinase A (PKA) pathway, which plays a major role in the regulation of cell growth, metabolism, and stress resistance. Snf1 is triggered in presence of alternate carbon source or non-fermentable carbon sources to induce expression of glucose repressed genes. Nitrogen sources are sensed through ammonium permease Mep2 and possibly through Gpa2-Gpr1. Growth on poor nitrogen sources also activates Gln3 and Gat1 through their dissociation from Ure2, through its dephosphorylation, to induce nitrogen catabolite repression (NCR) genes. Under nutrient-rich conditions, TORC1 inhibits the function of transcriptional activators that are involved in nitrogen catabolite-repression (Gat1, Gln3) by sequestering them to the cytoplasm by phosphorylated Ure2. Also, TORC1 activates ribosome biosynthesis through Sch9. Black arrows indicate transcriptional upregulation or downregulation. See text for further details.

1.5 *Saccharomyces cerevisiae* differentiation responses

Yeast *S. cerevisiae* can exist as a diploid or a haploid cell, diploid cells can undergo mitosis and grow via budding given sufficient nutrients, hence producing identical daughter cells (Hartwell, 1974). Haploid cells are able to mate (conjugate) with other haploid cells of the opposite mating type to produce **a**/α diploid cells (Herskowitz, 1988). When nutrients are limited, diploid cells can adopt one of many alternative differentiation fates in response to extracellular and intracellular nutrient environments. Cells can differentiate in the three following ways: 1) Cells can enter a stable non-proliferative state "quiescence" or "stationary phase" (cells age and undergo programmed death), 2) Cells can switch into pseudohyphal growth (grow as elongated chains of cells), 3) Cells can sporulate and form four haploid spores in ascus (These spores are formed as a way of packaging post meiotic nuclei, they signify the "gametic" stage of the yeast life cycle), which can then germinate when nutrient conditions improve. In addition, haploid cells show haploid invasive growth, which is similar, but not identical to pseudohyphal growth of diploid cells. The first two responses take place in the absence of nitrogen combined with a fermentable carbon source, the third response takes place in the absence of nitrogen along with the presence of a non-fermentable carbon source (Freese et al., 1982, Hartwell, 1974, Gimeno et al., 1992, Herman and Rine, 1997, Herskowitz, 1988). Stationary differentiation ceases cell growth and promotes genome-wide alterations in transcriptional expression and chromosome topography (Miles et al., 2013, Joshi et al., 2015), cytosolic fluidity (Munder et al., 2016), and cytoskeletal organization (Laporte et al., 2013). The key function of quiescence is to resist environmental stress, for example through induction of cell wall repair genes (Torres et al., 2002). As time progresses it has been proposed that cells may undergo programmed cell death to allow survival of potential viable cells, fatal cell do so by releasing their nutrients for the other more accommodating cell to utilize (Fabrizio et al., 2004). Pseudohyphal growth allows yeast colonies to expand and elongate to access remote nutrients with more efficiency. This foraging function takes place in two ways, first, foraging along the surface of the substrate by producing of filaments of elongated cell. Second, foraging by invasion of the filaments into the underlying substrate (Kron et al., 1994, Pitoniak et al., 2009). When faced with severe starvation, pseudohyphal cells may undergo sporulation. Sporulation or meiosis key function is to generate **a** or α haploid spores, they are more resistant to environmental stress (high temperature and prolonged starvation) than vegetative cells from which they arise (Muthukumar et al., 1993, Briza et al., 1990). Another function of sporulation is to increase genetic diversity through meiotic recombination paired with independent assortment of chromosomes

(Kupiec, 1997). In addition to mitosis, **a** or α haploid cells can undergo non-metabolic and quiescent stage when nutrients are limited. Haploid yeast cells can form morphological elongated filamentous cells known as invasive growth, thus altering the budding pattern and invasion of agar (Gimeno et al., 1992). From what was discussed above, cell fate depends on nutritional availability and cell type (Figure 1.7), also different fates lead to different cell functions. Even though differentiation choices are functionally distinct, they all respond to several of the same environmental cues, signalling pathways, and master regulators. I will discuss this next, for this thesis I will focus on pseudohyphal growth and meiotic differentiation.

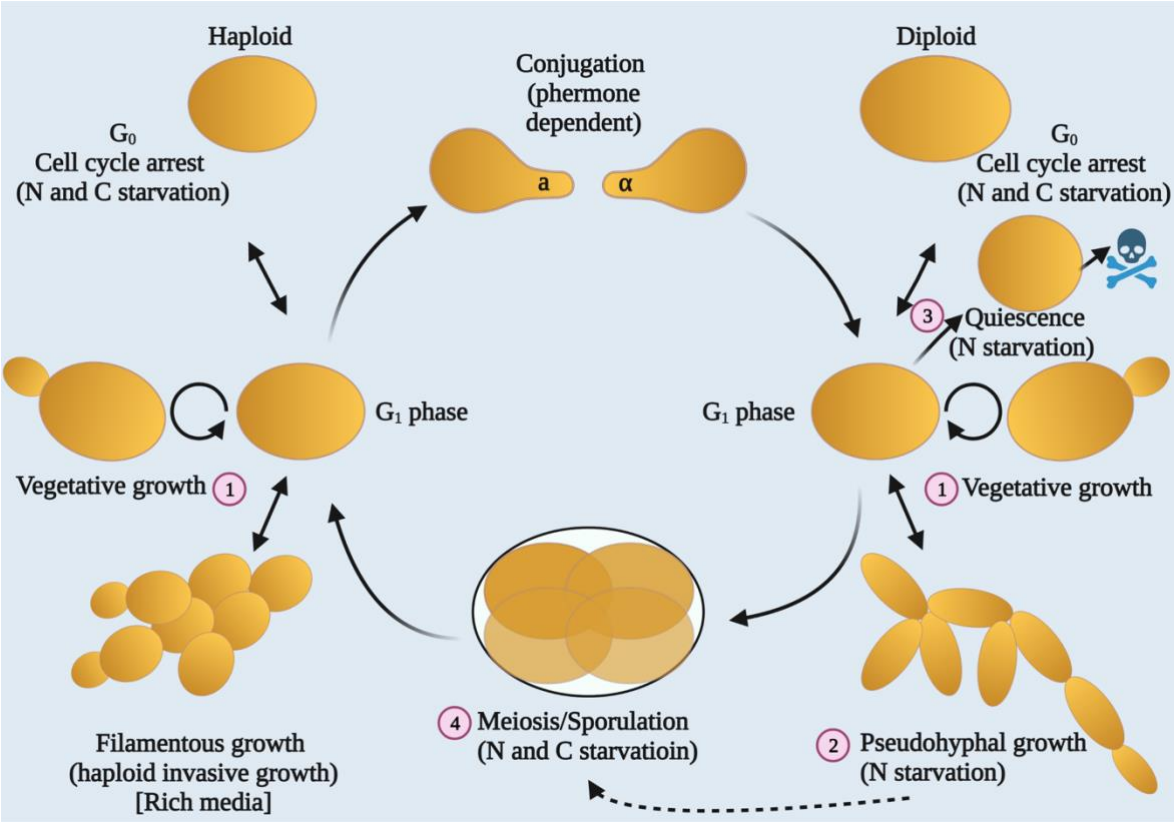

Figure 1-7 An illustration depicting the life cycle of *Saccharomyces cerevisiae* and alternative fates for haploid and diploid yeast.

Once every cycle, haploid and diploid cells must choose to enter into one of the four developmental pathways. All the developmental outcomes, except for mating pathway are regulated by nutrition and cell type. *S. cerevisiae* undergo vegetative growth under rich conditions (1), cells can differentiate to form chains of elongated pseudohyphal cells (2), rounded quiescent cells that subsequently age and succumb to programmed cell death (3), or tetrad asci, i.e., four haploid spores held together in an ascal sac, sporulation (4). Haploids can undergo invasive growth under rich conditions. Created with BioRender.com.

1.5.1 Master regulators of differentiation

Expression of master regulators define differentiation fate. They are required to initiate differentiation; furthermore, when expressed abnormally they are sufficient to activate differentiation in otherwise suppressed fates, making them true master regulators and important regulatory points in biological networks. Each differentiation pathway may require one or more master regulator and subsequent change in transcriptional regulation of downstream genes. Nevertheless, many of these master regulators induce more than one differentiation pathway, repress more than one pathway, or induce one pathway while repressing another. Pseudohyphal is regulated by Flo8, Ste12, Tec1, Sok2, Phd1, Mga1 and Nrg1 including other transcription factors, all lead to the activation of *FLO11* (Borneman et al., 2006, Cullen and Sprague Jr, 2012). Meiosis is activated by expression of the Ime4 RNA methylase, the Ime1 transcription factor and the Ime2 protein kinase (Neiman, 2011). Quiescence is induced by expression of Xbp1 transcription factor (Miles et al., 2013).

1.5.2 Pseudohyphal growth

Diploid cells of the budding yeast *S. cerevisiae* undertake a dimorphic transition under nitrogen deprivation coupled with a fermentable carbon source like glucose. Pseudohyphal growth is characterized by concerted changes in different cellular processes like the formation of multicellular chains or filaments of elongated cells extending from the colony, unipolar budding, adhesion of cells to one another after cell division and invasion of solid agar media (Gimeno et al., 1992, Kron et al., 1994). Pseudohyphal cells grow through symmetric cell division opposed to asymmetric cell division in budding (Kron and Gow, 1995). Also, poor nitrogen conditions activate an auto-signalling cue (fusel alcohols), which are natural metabolic products of the catabolism of certain amino acids, to stimulate formation of pseudohypthae (Chen and Fink, 2006, Dickinson, 1996). Pseudohyphal formation during nutrient restrictions is beneficial for the yeast, it allows for the cells to scavenge for available or scarce nutrients, or allow the cell time to deal with the stress source (Zaragoza and Gancedo, 2000). As for haploid cell when carbon sources are limited, they form invasive filamentous growth. The cells display an altered budding pattern when invading the agar medium, albeit having a less vigorous invasive growth when compared to diploid pseudohyphal (Gimeno et al., 1992, Kron and Gow, 1995, Gancedo, 2001).

1.5.2.1 Nutrient sensing and pseudohyphal growth

For optimal use of nutrients, a variety of sensing and signalling mechanisms are present in yeast. During nitrogen starvation coupled with a fermentable carbon source, pseudohyphal growth is induce through the Gpr1-Gpa2 system (Xue et al., 1998, Lorenz and Heitman, 1997). This GPCR system, containing the putative glucose receptor Gpr1 and the cognate Gα protein Gpa2, senses glucose and triggers the activation of a regulatory cascade. Indeed, activating the cAMP synthesis and thus activating cAMP-dependent protein kinase (PKA) via the GPCR system, inducing pseudohyphal growth (Figure 1.8) (Colombo et al., 1998, Kraakman et al., 1999). Also, a study showed that the Gpr1 signalling cascade acts as a dual sensor of carbon richness and nitrogen deficiency, in which the Gpr1 receptor is transcriptionally induced by nitrogen starvation and then senses the availability of fermentable carbon sources through its interaction with Gpa2 (Lorenz et al., 2000). Pseudohyphal differentiation can be triggered by maltose or maltotriose through a signalling pathway independent of Gpr1 receptor (Van de Velde and Thevelein, 2008). Snf3 and Rgt2 transmembrane receptors also sense but don't transport glucose, and regulate glucose signal transduction through their C-terminal tails to induce catabolic pathways (Bukau and Horwich, 1998, Özcan et al., 1998). Glucose phosphorylating enzymes Glk1, Hxk1, Hxk2 are involved in the uptake of glucose leading to the regulation of several genes (Rolland et al., 2001, BIsSON and Fraenkel, 1983).
Pseudohyphal growth primarily respond to nitrogen starvation or unfavourable nitrogen sources such as proline (Gimeno et al., 1992, Lorenz and Heitman, 1998b). The conserved family of MEP (methylamine permease) proteins are ammonium channels, in yeast three MEP proteins (Mep1, Mep2, Mep3) play a role in the uptake of extracellular ammonium ions into cells; of the three, Mep2 has the highest affinity and hence can detect low nitrogen concentration in the environment, making it the most divergent MEP of the three (Siewe et al., 1996, Marini et al., 1997). Because of the dual role of Mep2, when ammonium is low or absent, as a sensor Mep2 controls induction of pseudohyphal differentiation (Lorenz and Heitman, 1998a). Furthermore, Mep2 function is proposed to be linked to the MAP kinase pathway in inducing pseudohyphal in response to nitrogen starvation (Figure 1.8) (Rutherford et al., 2008). Overall suggesting that regulation of pseudohyphal growth is complex, due to the cell integrating various signals through many pathways to control differentiation (Lorenz and Heitman, 1998b).

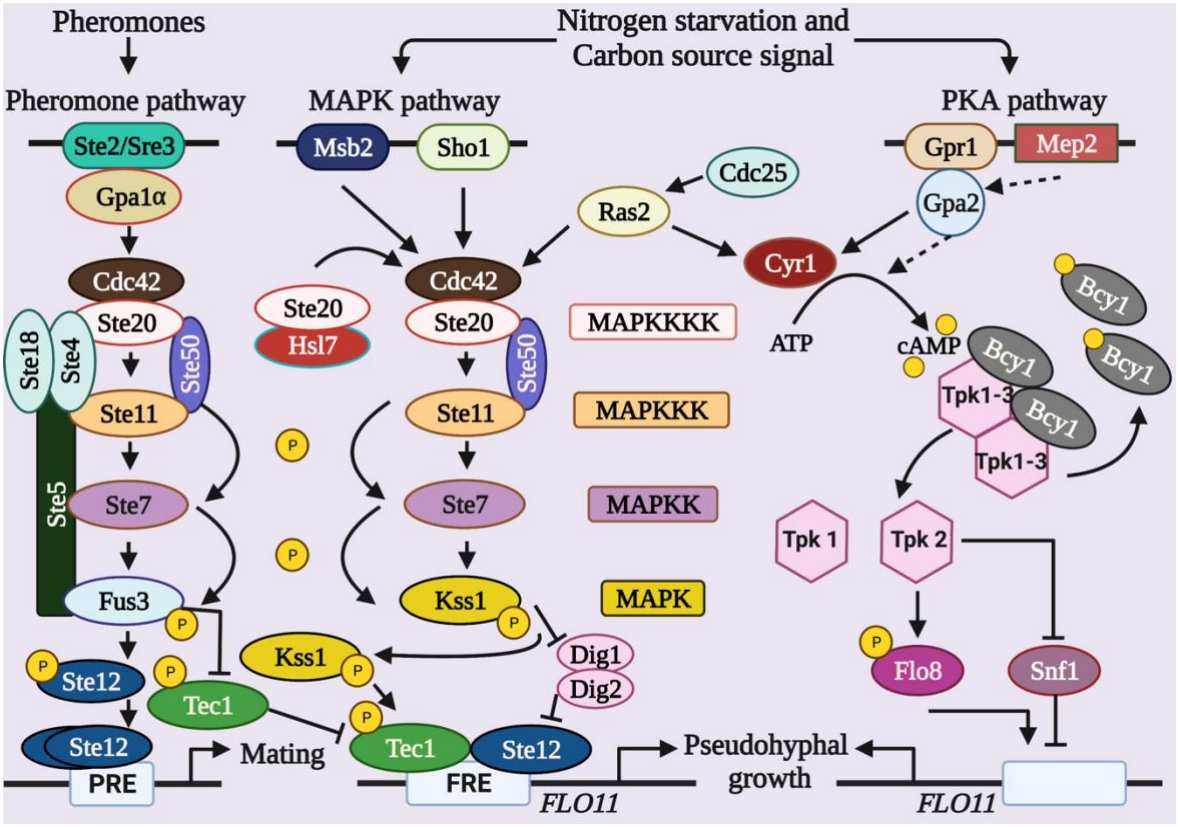

Figure 1-8 The MAPK and PKA signalling pathway involved in pseudohyphal growth.
Nitrogen starvation is sensed by Ras2 which activates Cdc42 and Cyr1, respectively. Gpa2 is also suggested to activate Cyr1. Which then controls the expression of the cell surface flocculin Flo11 via two distinct pathways, the cAMP-dependent PKA pathway and the MAPK pathway. In the PKA pathway Cyr1 catalyses the synthesis of cAMP from ATP. This second messenger is able to bind to the regulatory subunit of PKA, Bcy1, thereby dissociating it from the catalytic subunits, Tpk1, Tpk2, and Tpk3. These are then able to phosphorylate downstream targets and regulate in this way protein activity and gene expression. PKA activates the transcriptional activator Flo8 and inactivates the transcriptional repressor Sfl1, both of which contribute to the increased expression of Flo11. Ras2 activates Cdc42, which activates the MAPK cascade via its effector, Ste20. The MAP kinase Kss1 inactivates the repressors Dig1 and Dig2, thereby allowing Ste12 and Tec1 to activate the expression of Flo11 as well as of other proteins involved in cell elongation. MAPK can induce Kss1 transcription of filamentation genes in response to nitrogen limitation, which requires a heterodimer of Ste12 with Tec1. Separately, MAPK can induce transcription of mating genes in response to mating pheromones, which requires the scaffold protein Ste5 and the downstream transcription factor Ste12 independent of Tec1. In each pathway, the MAPK promotes transcription by phosphorylating and displacing the repressor proteins Dig1 and Dig2 from the transcription factor. Pheromone sensing depends on the Ste2 and Ste3 receptors that respectively bind α-and **a**-factor and that transmit the signal to the heterotrimeric G-protein consisting of the Gα protein Gpa1 and the βγ subunit Ste4 and Ste18. Ste4 recruits both the scaffolding protein Ste5 and Ste20 (which can also be stimulated by Cdc42) to the membrane resulting in activation of the mating MAP kinase cascade (Ste11, Ste7 and Fus3). Activation of the MAP kinase pathway results in growth arrest and conjugation. FRE, filamentation response element; PRE, pheromone response element. Created with BioRender.com.

1.5.2.2 Pathways regulating pseudohyphal growth

Two distinct, but interconnected, signalling pathways are involved in regulating pseudohyphal differentiation. The first involves the pheromone responsive mitogen-activated protein (MAP) kinase pathway, which regulates mating between two opposite type haploid cells (Liu et al., 1993, Roberts and Fink, 1994, Cook et al., 1997, Madhani et al., 1997) and yeast filamentous growth. The second signalling pathway, as mentioned before, is the nutrient sensing cAMP dependent protein kinase A (PKA) pathway. Both pathways function in parallel to regulate pseudohyphal differentiation (Lorenz and Heitman, 1997, Kübler et al., 1997, Lorenz et al., 2000).

1.5.2.3 The MAP kinase (MAPK) pathway regulates filamentous growth

The MAP kinase cascade components required for filamentous growth comprise of the Ste7, Ste11, Ste20 and Kss1 kinases. When Kss1 is unphosphorylated, it associates with Ste12 transcription factor and the negative cofactor regulators Dig1 and Dig2, thus inhibiting transcription of genes involved in filamentous and invasive growth. This pathway allows the dissociation of Ste12 from Kss1 to form a heterodimer with the transcription factor Tec1, by derepressing Dig1 and Dig2. The Ste12-Tec1 heterodimer then regulates expression of Tec1 itself and other targets, including the master regulator for pseudohyphal and haploid invasive growth, Flo11. The promoters of these target genes contain filamentous response elements (FREs) (Gavrias et al., 1996, Cook et al., 1996, Lo and Dranginis, 1998, Madhani and Fink, 1997, Bardwell et al., 1998). Flo11 is a glycosylphosphatidylinositol-anchored cell-surface protein required for calcium-dependent cell–cell adhesion (GPI-anchored cell surface glycoprotein) also known as flocculin (Lo and Dranginis, 1996, Lo and Dranginis, 1998). During pseudohyphal differentiation the upstream components that induce the MAP kinase pathway comprise Cdc42 plasma-membrane tethered protein, Ras2 GTP-binding protein and 14-3-3 proteins Bmh1 and Bmh2 (Mösch et al., 1996, Roberts et al., 1997), which is activated by the Sho1 osmosensing receptor (O'Rourke and Herskowitz, 1998, Davenport et al., 1999).
Ras2 causes enhanced pseudohyphal growth during nitrogen starvation (Gimeno et al., 1992). Msb2 signalling mucin recruits the upstream signalling proteins, Cdc42, Ste20 and Sho1, to mediate activation of MAPK cascade (Cullen et al., 2004). Cdc42 interacts with Ste20 (Cdc42-activated signal transduction kinase) to displace the negative regulator Hsl7 (Fujita et al., 1999). Also, Ste20 interacts with Sho1 in response to nitrogen depletion to activate MAPK pathway (O'Rourke and Herskowitz, 1998). The p21-activated kinase

Ste20 phosphorylates Ste11, activating its kinase function, subsequently phosphorylating Ste7; then active Ste7 phosphorylates Kss1, regulating activation of the MAPK regulatory pathway (Figure 1.8) (Chol et al., 1994, Wu et al., 1995).
In contrast, the upstream components of the mating pathway are not required for diploid filamentous growth, the components include pheromones and their receptors Ste2 or Ste3, the G-protein βγ subunit Ste4-Ste18 and the scaffold protein Ste5 (Figure 1.8) (Liu et al., 1993).
Furthermore, it is important to note like diploid cells pseudohyphal growth, haploid cells form filaments and invade the growth media during prolonged growth in a rich carbon and mitogen environment. Haploid cells exhibit elongated cells, shift to a unipolar instead of an axial pattern of budding and form filaments of chains of cells (Roberts and Fink, 1994). The MAPK pathway components that regulate diploid pseudohyphal differentiation also control haploid invasive growth (Roberts and Fink, 1994).

1.5.2.4 Other yeast MAPK pathways

In *S. cerevisiae* five signalling pathways are known to involve an MAPK cascade, of which as many as three of them use a common MAPKKK, Ste11. The MAPK cascades have distinct inputs and outputs, albeit using overlapping sets of signalling components. These pathways respond to pheromones (PH), high osmolarity (HOG), filaments and invasive growth (FG), cell wall integrity (CWI), and spore wall assembly. The crosstalk takes place between PH, HOG, and FG (Dohlman and Thorner, 2001, Schwartz and Madhani, 2004, Hohmann et al., 2007, Gustin et al., 1998).

1.5.2.5 The cAMP- protein kinase A (PKA) pathway regulates filamentous growth

Three GPCRs have been identified in *S. cerevisiae*. Two are mating-pheromone receptors (Ste2 and Ste3) that mediate cellular response through MAPK cascade during mating (Sprague Jr, 1992). In response to nitrogen limitation, the cAMP cascade comprises the G-protein coupled receptor (GPCR), Gpr1, the G-protein α subunit Gpa2, cAMP-dependent protein kinase, the transcription factors Flo8 and Sfl1, and the cell-surface flocculin Flo11 (Lorenz and Heitman, 1997, Kübler et al., 1997, Lorenz et al., 2000, Pan and Heitman, 1999, Rupp et al., 1999, Robertson and Fink, 1998). As I have mentioned before, the coupling of the Gpr1 receptor to the Gα protein , Gpa2, regulates cAMP production in response to glucose, hence promoting pseudohyphal growth (Lorenz and Heitman, 1997, Kübler et al., 1997, Lorenz et al., 2000, Xue et al., 1998, Colombo et al., 1998, Yun et al.,

1998, Kraakman et al., 1999). Also, nitrogen starvation induces expression of the Gpr1 receptor, may be mediated by upstream Mep2 ammonium permease (Xue et al., 1998, Lorenz and Heitman, 1998a). It has been suggested that Gpr1 and Gpa2 might function as a dual sensor of rich carbon source and nitrogen deprivation. Mutations in the elements involved in the cAMP-PKA cascade; for example, *RAS2*, *GPA2*, and *GPR1* leads to defects in pseudohphal development and invasive growth. The Ras2-GTP binding protein is required for pseudohyphal growth, overexpression of constitutively active RAS^{val19} decreased GTPase activity and promoted pseudohyphal development in diploid cells (Gimeno et al., 1992). Activated Ras2 regulates the downstream target adenylate cyclase (Cyr1) to produce cellular cAMP (Toda et al., 1985, Kataoka et al., 1985). The increased cAMP activates PKA, which in negatively regulated by Bcy1 subunit during cell growth. Mutation of Bcy1 activates PKA and promotes filamentous growth. PKA catalytic subunits are encoded by three genes *TPK1*, *TPK2*, and *TPK3*; which play a redundant role in vegetative growth (Toda et al., 1987, Pan and Heitman, 1999). However, in pseudohyphal differentiation Tpk2 subunit induces the differentiation fate, while Tpk1 and Tpk3 repress filamentation (Pan and Heitman, 1999, Robertson and Fink, 1998). Tpk2 catalytic subunit regulates the transcriptional activator Flo8 to enhance filamentous growth, which then regulates expression of Flo11, the cell surface flocculin to regulate pseudohyphal and invasive growth (Pan and Heitman, 1999, Rupp et al., 1999). Sfl1 is a transcriptional repressor and activator, which inhibits regulatory transcription of *FLO11* preventing filamentation, and displaying an antagonistic function to that of Flo8 in response to nutritional signals (Figure 1.8) (Robertson and Fink, 1998). Pde2 a cAMP phosphodiesterase protects the cell from extracellular cAMP and inhibits pseudohyphal growth when overexpressed in the cell, while exogenous cAMP enhances pseudohyphal growth during nitrogen starvation (Ward et al., 1995).

Overall, *FLO11* master regulator is transcriptionally regulated through Ste12-Tec1 heterodimer in the MAPK pathway, while the transcriptional activator Flo8 regulates the expression of *FLO11* in the cAMP-PKA signalling pathway independent of Ste12-Tec1. Gpa1 is a negative regulator of MAPK pathway in response to pheromone stimuli in concert with two GPCR receptors (Ste2: α-factor receptor, and Ste3: a-factor receptor) (Dietzel and Kurjan, 1987).

1.5.2.6 Crosstalk between MAP kinase and cAMP signalling

There are many links between the MAP kinase and cAMP-PKA signalling pathways, to regulate the complex regulation of yeast pseudohyphal differentiation. In addition to converging of MAP kinase and cAMP-PKA to regulate transcription of *FLO11* promoters (Sengupta et al., 2007, Rupp et al., 1999), required for pseudohyphal growth in diploids and invasive growth in haploids , they also meet at other points. First, the small G-protein Ras2 functions upstream as a branchpoint and regulates activation of both MAP kinase and the cAMP-PKA (through adenylyl cyclase) signalling cascade (Roberts et al., 1997, Lorenz and Heitman, 1997, Pan and Heitman, 1999, Rupp et al., 1999, Mosch et al., 1999). Second, a suggested division of labour between both pathways coordinates the regulation of invasive growth and the adhesion of mother and daughter cells, in which the PKA cascade induces the switch in budding patterns and the MAP kinase cascade induces cell elongation. Evident from the filaments growth largely composed of round, rather than elongated cells when activation of PKA is robust, by exogenous cAMP or the *bcy1* mutation,indicating that the PKA pathway does not play a role in cell elongation during Pseudohyphal growth. In concurrence with this hypothesis, Tpk2 catalytic subunit is not required for cell elongation, but for invasive growth and the switch to unipolar budding. On the other hand, Ste12 a component of the MAP kinase pathway is required for cell elongation and media invasion (Pan and Heitman, 1999).

1.5.3 Meiosis (sporulation)

Meiosis is a biological cellular development and survival mechanism, in which an **a**/α diploid cell gives rise to four haploid progenies (**a** or α) in an ascus. The ascus is the anucleate but still intact mother cell encasing the four spores of the tetrad (Kupiec, 1997, Neiman, 2005). The meiosis differentiation program is triggered during nitrogen starvation coupled with a non-fermentable carbon source, acetate or ethanol (Herskowitz, 1988, Kupiec, 1997). Approximately 400 genes are required to modulate meiosis (Enyenihi and Saunders, 2003, Neiman, 2005), and over 1,000 genes are known to alter expression during meiosis (Chu et al., 1998, Primig et al., 2000). The physiological and morphological changes basic to meiosis and spore formation are orchestrated by a highly regulated gene expression cascade, and organized into temporal classes involving early, middle, and late expressing genes (Chu et al., 1998, Primig et al., 2000, Mitchell, 1994). When undergoing meiosis and sporulation these genes are specialized for the process, while otherwise repressed during vegetative growth (Folco et al., 2017). Meiosis occurs in three major phases. First, the early phase, here is when cells decide their fate to differentiate, in response to the absence of nitrogen and glucose and mating type (Mitchell, 1994); cells exit the mitotic growth at the G1 phase and enters premeiotic S phase. Second, induction of early meiotic gene (EMGs), prophase, the cells undergo DNA duplication and homologous recombination. Finally, the major cytological events of meiosis take place, where two meiotic divisions causing chromosome segregation, give rise to four haploid nuclei that are then packaged into spores. In meiotic prophase, homologous chromosomes pairs come together to form a synapse. The chromosomes are in perfect alignment and bound tightly together via a protein lattice called a synaptonemal complex; subsequently, influencing interhomolog crossover recombination (Page and Hawley, 2004, Voelkel-Meiman et al., 2012, Chu et al., 1998). The process of meiosis and spore formation together is referred to as sporulation.

The meiosis differentiation process is triggered by the expression of Ime1 transcription factor (Initiator of Meiosis 1). Ime1 is a master regulator of the sporulation development; abnormal expression of Ime1 is sufficient to activate sporulation of vegetative diploid cells (Smith et al., 1990, Kassir et al., 1988). Expression of *IME1* is induced by different cues including, nitrogen source, carbon source, mating type, and extracellular pH (Kassir et al., 1988, Smith et al., 1990, Su and Mitchell, 1993). Initiation of meiosis relies on two signals: nutrient starvation and the presence of *MAT***a** and *MAT*α gene products (Kassir and Simchen, 1989). *IME1* is not transcribed in the presence of glucose in the vegetative growth media, while a low basal level of *IME1* can be detected in vegetative acetate media

(Kassir et al., 1988). Upon nitrogen depletion and the presence of acetate in the media, *IME1* mRNA levels are highly induced in *MAT***a**/*MAT*α diploid cells, but not detected in cells harbouring a single active *MAT* allele (MAT-insufficient cells), subsequently ~ 6 to 8 h later levels start to decline (Kassir et al., 1988, Smith and Mitchell, 1989). The *IME1* transcription in response to nutritional cues and cell type, is regulated by distinct positive and negative regulatory elements (Sagee et al., 1998, Smith et al., 1990, Sherman et al., 1993, Granot et al., 1989). Thus, *IME1* is mediated by a positive and negative feedback loop (Shefer-Vaida et al., 1995).

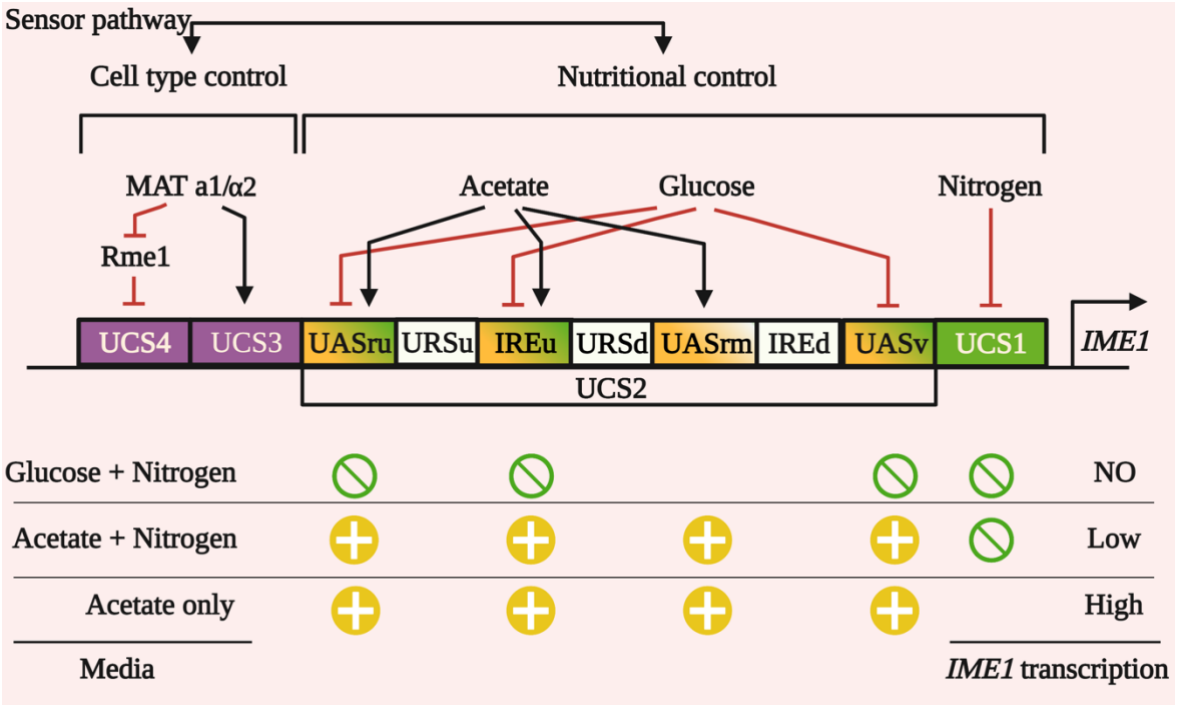

Figure 1-9 Schematic structure of the IME1 5′ untranslated region showing IME1 promoter regulation by different stimuli.

The *IME1* promoter is divided into four Upstream Control Regions, UCS1-4. UCS3 and UCS4 respond to a cell type control pathway, which inhibits sporulation in haploid yeasts. UCS1 responds to nitrogen richness and has a repressive effect on *IME1* transcription. UCS2 responds to the type of carbon source. Glucose represses *IME1* transcription through the DNA elements UASv, IREu and UASru, whereas acetate activates *IME1* transcription through UASrm, IREu and UASru. In media containing nitrogen and glucose, *IME1* is repressed. The balance between UCS2 and UCS1 regions permits a minimal expression of *IME1* in media containing acetate and nitrogen. In these conditions, the depletion of nitrogen suppresses UCS1 repressive action: sporulation is induced by the overexpression of *IME1*. Green or yellow elements have respectively repressive or positive effects on *IME1* transcription. Created with BioRender.com.

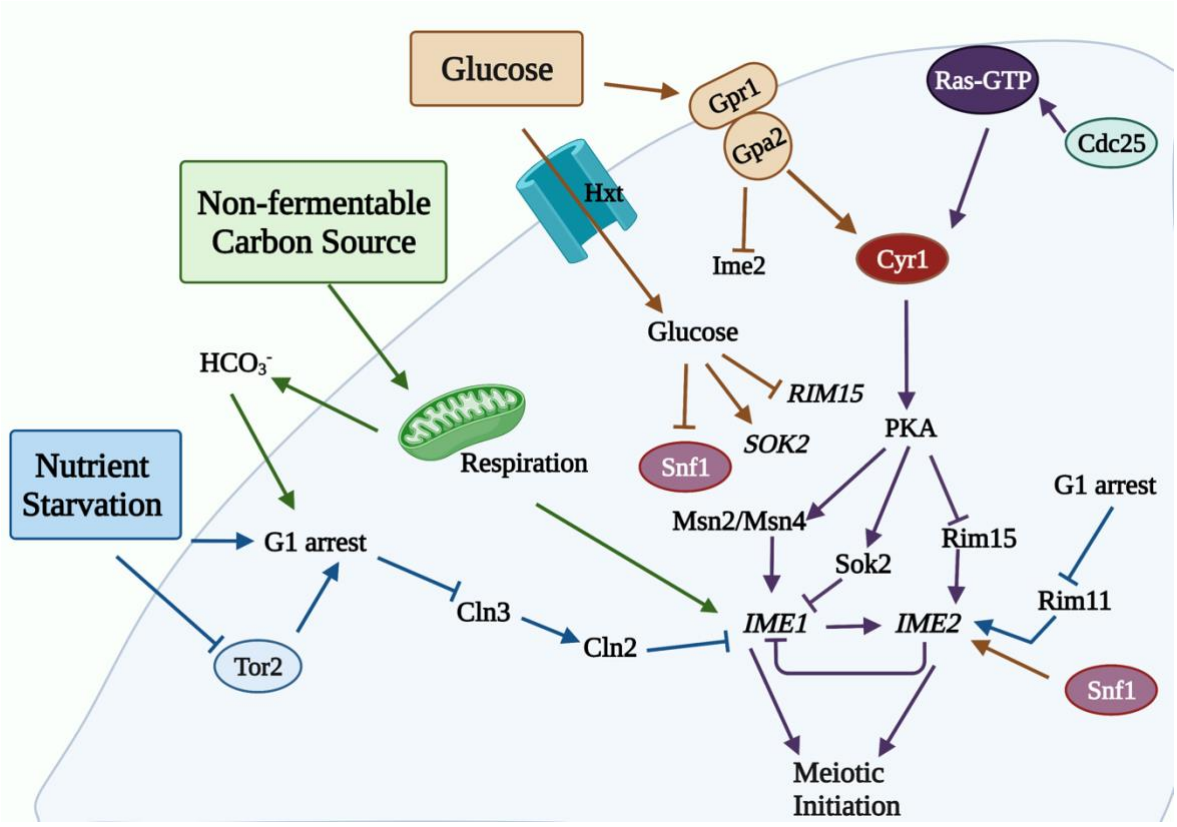

Figure 1-10 Model for the signal network that controls meiotic initiation in *S. cerevisiae*.
The three principal nutritional signals required to initiate meiosis are shown in boxes. The diagram shows some of the signal transduction pathways that control meiotic induction and examples of where these pathways are connected. Each pathway follows through in identical arrow or inhibiter line colours (Brown, Green, Blue, and purple). Created with BioRender.com.

1.5.3.1 Nutritional cues regulating *IME1* and meiotic induction

In the budding yeast *S. cerevisiae*, the decision to pursue meiosis/sporulation as the differentiation fate over other developmental programs (e.g., mitotic cycle, pseudohyphae growth, or stationary phase- G_1 arrest) depends on the induction and function of the master regulator, *IME1*, by sensing nutritional cues and mating type. Nitrogen starvation leads to G_1 arrest in the mitotic cycle. Glucose absence is essential, because the sheer presence of glucose can inhibit entry into meiosis and promote pesudohyphal growth instead (Kassir and Simchen, 1989, Smith and Mitchell, 1989, Gimeno et al., 1992). Acetate as the non-fermentable carbon source results in respiratory metabolism, hence inducing entry into meiosis (Treinin and Simchen, 1993). Also, the mating type *MAT* signal is essential for *IME1* transcription and efficient meiosis (Kassir et al., 1988, Sherman et al., 1993). Cell mating type is fundamental in meiosis initiation; while diploid cells can undergo meiosis, haploids are inhibited from interring this differentiation fate. The nutrient signal is necessary at numerus stages: *IME1* transcription (Kassir et al., 1988), *IME1* mRNA

translation (Sherman et al., 1993), Ime1 interaction with its meiotic target, Ume6 (Rubin-Bejerano et al., 1996), and is required for entry into the first meiotic division (Lee and Honigberg, 1996). Therefore, upon nitrogen starvation in the presence of a non-fermentable carbon source, *IME1* is transcribed to induce a set of early meiotic genes (EMGs) that proceeds the sporulation program (Su and Mitchell, 1993).
An uncommonly large 5′ promoter region in *IME1* senses the levels of stimuli and subjects *IME1* to positive and negative regulation. The 2.4 kb promoter region consist of activation and repression elements, at which nutritional cues and cell type converge to regulate induction of meiosis (Granot et al., 1989, Sagee et al., 1998). The promoter is divided into four contiguous regions, upstream control regions (UCS1-4), and other regulatory elements within this region, such as upstream activating region (UAS) (Figure 1.10) (Sagee et al., 1998). Furthermore, several conserved signalling pathway sense and control sporulation, PKA, TORC1, and UPR.

1.5.3.2 Nitrogen sensing and signalling pathways

IME1 senses nitrogen signal through the UCS1 promoter element. β-Galactosidase studies of *ime1-lacZ* chimeric gene present on a single-copy vector reporter, in which various portions of the 5′ upstream region of *IME1* were fused, confirmed that the four UCS (UCS1 to UCS4) mediate the regulation of *IME1* transcription. To confirm the negative role of UCS1, results from comparing β-galactosidase activity between *UAS-his4-lacZ* in the presence of glucose, acetate, or nitrogen starvation revealed an increase in *HIS4* induction. While expressing *UAS-his4-UCS1-lacZ* prevents the transcriptional activation function of *HIS4* UAS in vegetative culture with either glucose or acetate as the sole carbon source but has no effect upon nitrogen depletion. Together these results have shown that deletion of UCS1 results in increase expression of *IME1* in vegetative growth media containing glucose, expression is even higher in vegetative growth media containing acetate (Sagee et al., 1998). These results indicated that UCS1 is negatively regulated in the presence of glucose and nitrogen. Also, glucose has a partial effect compared to nitrogen on the repression of UCS1, suggesting that nitrogen is the key signal regulating the function of UCS1 (Figure 1.10) (Sagee et al., 1998). UCS1 alone lacks UAS activity and cannot induce expression of reporter genes (Nadjar-Boger, 2000).
The cAMP-PKA pathway is also involved in meiosis. The nitrogen signal can be transmitted via this pathway to *IME1* to induce meiosis (Matsuura et al., 1990, Matsumoto et al., 1983). PKA activators, such as Cdc25, a Ras GDP/GTP exchange factor, Cyr1, and Ras2 are suggested to negatively regulate sporulation (Figure 1.9). This was seen as a

result of mutation in the *cdc25*, *cyr1*, and *ras2* causing poor PKA activity leading to expression of *IME1* and spore formation in the presence of nitrogen (Matsuura et al., 1990, Matsumoto et al., 1983, Smith and Mitchell, 1989, Shilo et al., 1978). In addition, the constitutive active PKA, as a result of $RAS2^{val19}$ or *bcy1* mutations results in sporulation defective cells, that can be rescued by overexpressing *IME1* (Matsuura et al., 1990). The nitrogen signal is proposed to be transmitted via Cdc25 to UCS1, where Cdc25 is a known as a positive regulator of cAMP-PKA (Broek et al., 1987). Thus, cAMP-PKA both promotes growth and inhibits *IME1* transcription.

It is not clear if nitrogen directly represses entry into meiosis or if nitrogen starvation induces meiosis indirectly by causing a G_1 arrest. Given some evidence, the latter hypothesis is favoured due to meiosis being active in the presence of nitrogen and lack of other required nutrients (Freese et al., 1984, Freese et al., 1982). TORC1 and UPR pathways are indicative of the unclear direct, or indirect, role of nitrogen sensing in entry into meiosis. The Tor2, a subunit of TORC1, mediates many nutritional signalling pathways including the NDP (Raught et al., 2001). Inhibition of TORC1 is enough to induce *IME1* transcription and allow sporulation, even in efficient nutrient conditions, mimicking a nitrogen starvation environment (Loewith and Hall, 2011). Therefore, under nitrogen-rich condition, TORC1 is active and inhibits *IME1* transcription (Nakazawa et al., 2012, Jambhekar and Amon, 2008). The nitrogen discrimination pathway is activated under poor nitrogen condition. TORC1 pathway can be inhibited by treatment with rapamycin drug, allowing for the activation of the TORC1 pathway and induction of *IME1* resulting in meiosis and sporulation when nutrients are available. However, because the active TORC1 pathway regulates several metabolic transcriptional events required for growth, the pathway activated by the drug does not directly interact and induce sporulation genes (Hardwick et al., 1999). Thus, it is suggested that TORC1 pathway promotes entry into meiosis by causing alterations in the metabolism that results in G_1 arrest. Also, distinct cooperation between PKA and TORC1 signalling induce *IME1* and allow entry into meiosis (Nakazawa et al., 2016).

Another pathway that senses nitrogen and may contribute to the switch from G_1 to meiosis, involves *HAC1*. Spliced *HAC1* is required to activate the UPR, and regulates entry into meiosis during nitrogen starvation coupled with a non-fermentable carbon source (Schröder et al., 2000, Patil and Walter, 2001). I will discuss the pathway further later.

1.5.3.3 Induction of *IME1* by non-fermentable carbon sources

When a non-fermentable carbon source is present alone, *IME1* transcription is detected at basal levels. This observation is a result of the antagonistic repressive action of UCS1, URSu, URSd, and IREd and positive action of UASru, IREu, UASrm and UASv (USA activity in vegetative growth) of the *IME1* promoter (Figure 1.9). Once nitrogen has been depleted, derepression of UCS1 promotes higher transcriptional induction of *IME1* (Kassir et al., 2003).

Transcriptional initiation of *IME1* requires respiratory metabolism of a non-fermentable carbon source. Overexpression of *IME1* bypasses the need for non-fermentable carbon respiration to activate meiosis. Alkalization of the media, due to the CO_2 product of respiration, may contribute to meiotic induction (Ohkuni and Yamashita, 2000). This is deduced given the role of Rim101 in both accommodation to extracellular alkalization and *IME1* transcription (Lamb et al., 2001, Su and Mitchell, 1993). And the activation of the Srb10-Srb11 cyclin-kinase complex in an alkalized media, is required to activate *IME2*, an early meiotic gene, efficiently and induce meiosis (Ohkuni and Yamashita, 2000, Cooper and Strich, 2002).

1.5.3.4 Glucose sensing and signalling pathways regulating *IME1*

The slightest concentration of glucose in media inhibits meiotic development. The UCS2 element within the promoter of *IME1*, is the site of glucose sensing. The UCS2 region contains the UAS activity of *IME1*, and harbours alternate positive and negative elements. In the presence of glucose UASru, IREu, and UASrm elements are repressed, but active when glucose is absent and/or presence of acetate (Kassir et al., 2003). Glucose inhibits induction of *IME1* through several integrated signalling pathways, which repress transcriptional activation of *IME1* through its promoter elements UCS1, UASru, IREu and UASv (Figure 1.10). Thus, glucose suppresses meiotic initiation through several various signalling cascades. Many cellular processes that react to glucose are mediated through the glucose repression pathway (Johnston, 1992). The key component of this cascade is Snf1 protein kinase, which is repressed by glucose. Snf1 is required for the transcription of Ime1 and Ime2, and for spore formation (Honigberg and Lee, 1998). Rgt2 and Snf3 glucose sensors, which function upstream of Snf1, play a role in maintaining *IME1* suppression during late stage of growth in the presence of glucose (Özcan and Johnston, 1999). In addition, glucose is sensed by Gpr1-Gpa2 which then activate the cAMP-PKA pathway and allow pseudohyphal development (Lorenz et al., 2000), the coupled sensor also

controls meiosis. In the presence of glucose and nitrogen PKA inhibits *IME1* and *IME2* transcription, Gpa2 binds to Ime2 and represses its kinase activity, thus inhibiting undesired entry into meiosis. Overexpression of Ime2, in the presence of glucose or nitrogen, inhibits pseudohyphal growth and promotes sporulation (Donzeau and Bandlow, 1999). Suggesting that Gpa2 and Ime2 functions as a switch mediating entry into meiosis or pseudohyphal (Pan et al., 2000). The RAS pathway is transiently activated by glucose and is suggested to have a role in meiosis initiation (Thevelein and De Winde, 1999). In *S. cerevisiae* there are two RAS genes, *RAS1*, is activated by glucose, and *RAS2* regulates nitrogen starvation response. As I discussed before, the Ras proteins induce both Cdc42/Ste20 MAP kinase pathway and cAMP-PKA pathway to control pseudohyphal growth (Mosch et al., 1999, Pan and Heitman, 1999). Interestingly, only the PKA pathway regulates meiotic differentiation. Thus, activation of the PKA pathway is suggested to indirectly inhibit entry into meiosis. Glucose also inhibits expression of *RIM15* a serine/threonine protein kinase, while PKA and TORC1 pathways directly phosphorylate Rim15 and inhibit its activity (Figure 1.10) (Reinders et al., 1998, Swinnen et al., 2006). Rim15 kinase is required to allow the association of Ime1 to Ume6 (a transcriptional activator of EMGs) to activate the early meiotic genes, consistent with the presence of increased levels of *RIM15* in acetate growth media (Vidan and Mitchell, 1997). Nutrient starvation inhibits signalling through the PKA and TORC1 pathways, leading to dephosphorylation of Rim15. Active Rim15 phosphorylates endosulfine (a protein belonging to the highly conserved cAMP-regulated phosphoprotein family). Phosphorylated endosulfine acts as an inhibitor of $PP2A^{Cdc55}$ and there by leading to entry into meiosis, $PP2A^{Cdc55}$ is a protein phosphatase (Sarkar et al., 2014, Plank, 2022). The PKA pathway may also suppress *IME1* through the Msn2-Msn4 transcription complex. PKA hyperphosphorylates Msn2-Msn4 protein complex and inhibits its transcriptional activating function (Garreau et al., 2000). In contrast, transcriptional activators Msn2-Msn4 promote *IME1* expression in the presence of acetate (Sagee et al., 1998). Inactivation of PKA under meiotic conditions leads to enhanced activity of Rim11, a kinase that phosphorylates Ime1 and Ume6 (Malathi et al., 1997, Xiao and Mitchell, 2000). Msn2-Msn4 induces transcription of several stress-response genes through binding to the stress response element (STRE) located in the promoters of these genes (Smith et al., 1998). One such stress-response gene, *TPS1*, is required to induce *IME1*. More specifically, *IME1* promoters contain an STRE which may regulate *IME1* transcription (Sagee et al., 1998). Deletion of *TPS1* sporulation defect phenotype can be rescued by overexpressing Mck1, which is a protein kinase also required for efficient transcription of *IME1* and expression of *IME2* (De Silva-Udawatta and Cannon, 2001). However, Mck1 regulates *IME1*

independent of the PKA pathway (Rayner et al., 2002). PKA may also regulate the Msn2-Msn4 protein complex through phosphorylating Sok2 (a DNA-binding protein) (Ward and Garrett, 1994), which is suggested to bind Msn2-Msn4 and switch it to a transcriptional repressor. Thus, Sok2 functions as a transcriptional suppresser of the PKA target *IME1* (Shenhar and Kassir, 2001). Put together *IME1* transcriptional regulation is vital and complex, as it is evident by the positive and negative regulation of the highly unusual promoter region.

1.5.3.5 Meiosis activation through G1 arrest and *CLN3*

Budding yeast cell make developmental decisions during the G_1 phase of the cycle (Pringle and Hartwell, 1981). Both haploid and diploid cell arrest at the G_1 phase under nutrient starvation, in which haploid cells undergo several metabolic adaptations to survive and become quiescent by entering G_0 phase, while diploid cell enter the meiotic cycle and proceed to sporulate (Herskowitz, 1995, Hirschberg and Simchen, 1977). In the late G_1 phase the commitment to divide takes place also known as the S phase. The most upstream activator of S seems to be Cln3 cyclin, which activates Cdc28 kinase to promote the transition from G_1 to S phase (Dirick et al., 1995). Several signalling pathways that mediate entry into G_1 arrest converge to mediate expression of *CLN3*, which encodes a G_1 cyclin (Honigberg and Purnapatre, 2003). During the cell cycle Cln3 is present at constant levels, but its fundamental function is to promote the transition from G_1 to S phase. *CLN3* inhibits *IME1* expression and Ime1 localization to the nucleus, thus it makes sense that Cln3 level decrease rapidly when G_1 arrest occurs. The Cln3 decline is required for meiotic initiation (Gallego et al., 1997, Parviz and Heideman, 1998, Colomina et al., 1999). During G_1 phase, Cln3 activates the Swi4-Swi6 complex, which is required for transcription of two other G1 cyclins, *CLN1* and *CLN2* (Levine et al., 1996). Both SWI6 and *CLN2* are required for *IME1* repression (Figure 1.10) (Purnapatre et al., 2002)

1.5.3.6 Commitment to meiosis (return-to-growth)

Commitment to meiosis is accomplished when meiotic cells cannot return to the mitotic cell cycle, even if the induction stimuli (nutrient starvation) are alleviated. Therefore, maintaining diploid cells in a nutrient deprived medium (acetate and absent nitrogen) is crucial to execute sporulation, given that returning cells to a rich media can allow cells to re-enter the mitotic cell cycle (Esposito and Esposito, 1974, AT, 1958, Sherman and Roman, 1963, Blinder and Magasanik, 1995, Honigberg et al., 1992). Cells that initiated

meiosis and completed meiotic DNA replication, meiotic recombination, and synaptonemal complex formation can efficiently return to growth. However, when the cells exit the meiotic prophase and enter the first meiotic division (M1), the ability to return to vegetative growth decreases dramatically. When cells complete meiosis and sporulate, even if moved to a rich medium, then they have reached the meiotic commitment point (Nachman et al., 2007, Winter, 2012). Studies proposed a model where cells transit through a series of steps: first "readiness," then "partial commitment," and finally "full commitment" (Simchen, 2009). When cells overexpress *IME1* in stationary-phase cultures containing limited glucose, cells can execute the early meiotic events, including DNA replication, commitment to recombination, and synaptonemal complex formation and dissolution. But later meiotic events like chromosome segregation, commitment to meiosis, and sporulation do not transpire. Returning the cells into sporulation media will allow cell to resume meiotic development even if *IME1* levels are high, Ime1 is regulated by a negative feedback loop mechanism that limits its synthesis to a transient period during induction of meiosis, suggesting that nutritional cues can control early and late stages of differentiation through an *IME1*-independent pathway (Lee and Honigberg, 1996, Bertram et al., 2002). Furthermore, genes involved in meiotic commitment have been scarcely identified until recently. Spo14, was previously suggested to be involved in coordinating induction of late meiotic events, and NDT80 encoding protein was implicated in ensuring commitment to meiosis (Honigberg et al., 1992, Tsuchiya et al., 2014). In a recent study, Bcy1, Ime2, Bmh1, Bmh2, Cdc5, and Pes4, have been identified as novel factors required for meiotic commitment (Gavade et al., 2022). The results suggested that commitment is actively maintained throughout meiosis; in which, Ime2, Bmh1, Bmh2, and Cdc5 established meiotic commitment; Bmh1, Bmh2, and Pes4 maintained meiotic processes for commitment; or Bcy1blocked the mitosis-inducing signal (Gavade et al., 2022).

1.5.3.7 The *MAT* signal transmits to *IME1* and meiosis

Along with nutritional signals required to control meiosis, cell type signals are also key to promote meiosis. Cell type controls and ensures that *IME1* is not transcribed in haploid cells under any nutritional environments. The *MAT* signal is transmitted via two distinct elements in the *IME1* promoter (UCS3 and UCS4), which do not overlap with elements required for nutritional regulation (UCS1 and UCS2) (Covitz and Mitchell, 1993, Sagee et al., 1998). *RME1* (**r**epressor of **me**iosis) encodes a zinc-finger DNA-binding protein (Figure 1.9) (Covitz et al., 1991, Shimizu et al., 1997), which is expressed abundantly in haploids compared to diploids and represses *IME1* through at least two diverse

mechanisms. First, Rme1 binds to RRE1 site within the UCS4 of *IME1* promoter to suppress *IME1* transcription. Second, Rme1 binds to a similar site in the promoter of *CLN2*, which encodes a G1 cyclin, to activate its transcription, activate expression of Cln2 inhibits *IME1* transcription (Covitz et al., 1991, Covitz and Mitchell, 1993, Purnapatre et al., 2002, Frenz et al., 2001). Meiotic development is restricted to *MAT**a**/MATα* diploids, in these cells the homeodomain proteins, **a1** and α2 form a heterodimeric regulator, that binds to an operator site in the *RME1* promoter inhibiting its induction (Covitz and Mitchell, 1993, Herskowitz, 1992). In addition to inhibiting *RME1*, **a1**-α2 heterodimers also induce expression of *IME1* through expressing *IME4*. *RME1* and *IME4* mediated signal transduction in two different signal pathways independent of one another, given that Rme1 does not transmit the *MAT* signal to *IME4* (Shah and Clancy, 1992). *IME4* positively mediates activation of sporulation and is only detected in diploid cells. *IME4* is repressed in haploids through production of antisense *IME4* transcripts, whereas in diploids antisense transcription is repressed by binding of the **a1**-α2 heterodimer (Hongay et al., 2006). However, *IME4*, and its N^6-adenosine methyltransferase function, is only essential for meiosis in S288C but dispensable for meiosis in SK1 yeast strain (Agarwala et al., 2012). There is a difference in meiotic efficiency between the two strains of *S. cerevisiae*, SK1 has high sporulation efficiency while S288C has low sporulation efficiency (Ben-Ari et al., 2006, Deutschbauer and Davis, 2005). Evidence have shown that *IME4* functions upstream of *RME1*, by methylating a site in the 3′ UTR of the *RME1* mRNA and reducing its expression in S288C strains. In contrast, in the SK1 strain, the presence of a natural polymorphism in the *RME1* mRNA promoter reduces *RME1* transcription, thus eliminating the need for methylation (Bushkin et al., 2019). Moreover, diploids that are *rme1Δ*, *ime4Δ*, *ucs3Δ*, or *ucs4Δ* induce meiosis only under nitrogen starvation (Sagee et al., 1998, Shah and Clancy, 1992, Kassir and Simchen, 1976). In this thesis. I utilized SK1 haploid yeast strain deleted for *RME1* to allow for the meiotic mechanism to respond in the presence of acetate (non-fermentable carbon) and nitrogen starvation.

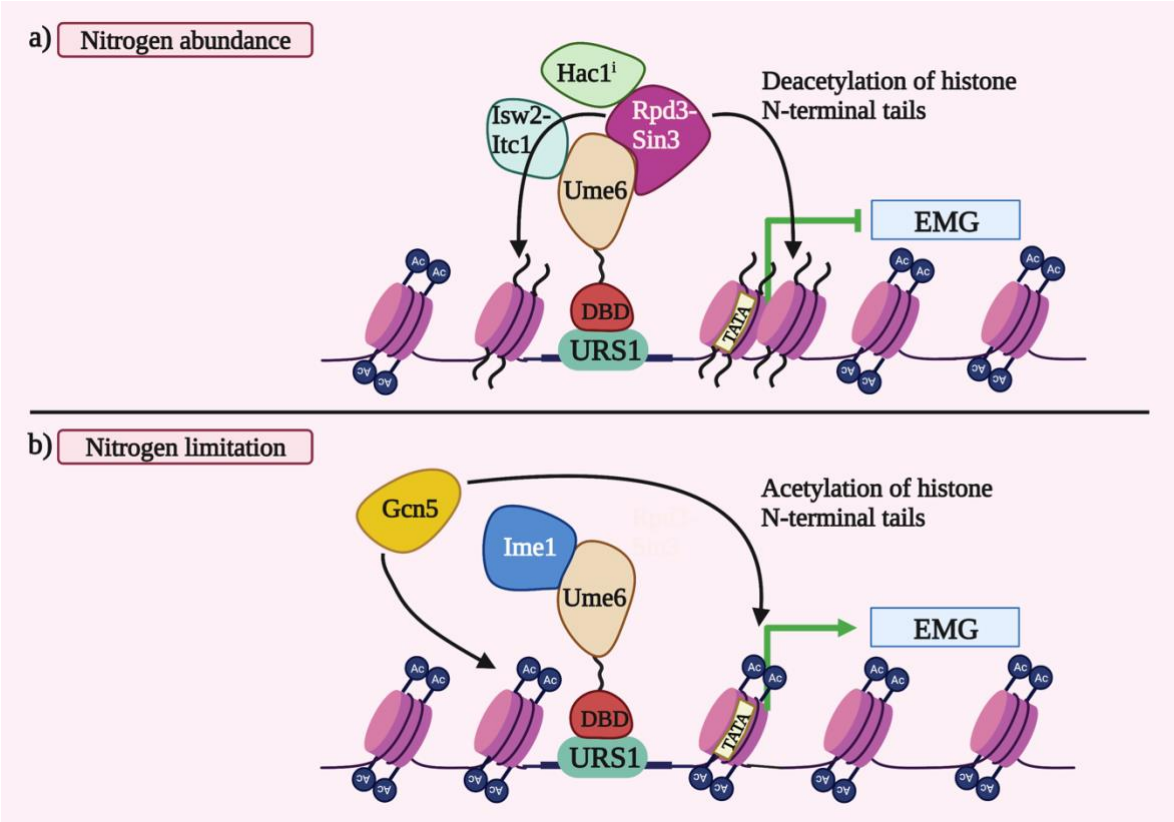

Figure 1-11 Interaction of transcriptional regulators, histone-modifying enzymes, and chromatin remodelling complexes in regulation of early meiotic genes.

(a) Under nitrogen-rich conditions, Ume6 negatively regulates transcription of EMGs by recruitment of Sin3-Rpd3 histone deacetylase (HDAC) which lead to histone deacetylation. Repressor-directed deacetylation of histone N-terminal tails deacetylation of histone N-terminus on nucleosomes in the vicinity of the Ume6-binding site inhibits binding of general transcription factors at the TATA box, thereby repressing transcription. Rpd3 is the catalytic subunit of the histone deacetylase complex (HDAC). **(b)** Under nitrogen starvation, Ime1 associates with Ume6 and Gcn5 acetylates histone to induce early meiotic genes (EMGs). Activator-directed hyperacetylation of histone N-terminal tails Hyperacetylation of histones in the vicinity of the Ume6-binding site facilitates access of general transcription factors required for initiation. Gcn5 is the catalytic subunit of the histone acetyltransferase (HAT) complex. Created with BioRender.com.

1.5.3.8 Regulation of meiosis in yeast

1.5.3.8.1 Ime1-Ume6

Exposure of cells to altering nutritional environments provides central signals that promote dramatic changes in transcription, metabolism, and cell division. The *IME1* gene is a master regulator and encodes a transcriptional activator required for transcription of early meiotic genes (EMGs) (Smith et al., 1993, Mandel et al., 1994, Kassir et al., 2003). Diploid cells carrying an *IME1* null mutation leads loss of expression of all meiotic genes excluding *IME4* (Kassir et al., 2003, Kupiec, 1997). Overexpression of Ime1 bypasses the need for **a1** and α2 gene products for sporulation (Kassir et al., 1988). Ime1 associates with Ume6, a key transcriptional regulator of EMGs, for example *IME2, HOP1* and *SPO13*. Ume6 is required for the EMGs repression during vegetative growth and for EMGs activation during meiosis inducing conditions (Malathi et al., 1997, Vershon and Pierce, 2000, Rubin-Bejerano et al., 1996). During meiosis, Ime1 and Ume6 are phosphorylated by protein kinases, Rim11 and Mck1, to promote and ensure stability of the Ime1-Ume6 association (Xiao and Mitchell, 2000, Malathi et al., 1997, Malathi et al., 1999). In the presence of glucose, this association can be destabilised due to glucose inhibition of Rim15, which is required for EMG transcription, suggesting that glucose suppression of Rim15 may be accountable for glucose suppression of Ime1-Ume6 interaction (Vidan and Mitchell, 1997). Also, Ume6 is a C6-zinc cluster DNA-binding protein that binds to the upstream repressing site 1 (URS1) consensus sequence (5′-TCGGCGGCT-3′) in promoters of EMGs and non-meiotic genes (Strich et al., 1994, Anderson et al., 1995). Rim15 is required for efficient interaction between Ime1 and Ume6; in *rim15Δ* cells a reduction in their interaction is detected (Vidan and Mitchell, 1997). Deletion of *UME6* results is derepression of EMGs, and the non-meiotic genes harbouring the URS1 element, in vegetative growth (Bowdish and Mitchell, 1993, Strich et al., 1994, Lopes et al., 1993). *ume6Δ* cells arrest early in meiosis, during prophase, and reveal a delay in induction and transcription reduction of mid and late genes (Steber and Esposito, 1995), suggesting that Ume6 plays a role in meiotic progression, in addition to its function in vegetative repression. Also, because *ume6* mutant strains showed no association between Ime1 and promoters of EMGs, it is suggested that Ume6 recruits the Ime1 transactivator to induce EMGs during meiosis (Bowdish et al., 1995, Pnueli et al., 2004). Furthermore, a study showed that Ume6 is abolished early in meiosis by Cdc20, an activator of the anaphase-promoting complex/cyclosome (APC/C) ubiquitin ligase. Cdc20 interacts with Ume6 *in vivo* indicating that the regulation control is direct. Ume6

association with Ime1 results in a more efficient destruction of Ume6 and allows entry into meiosis by inducing EMGs. Also, stabilizing the Ime1-Ume6 complex by inactivating or mutating, Cdc20, prevented meiotic genes transcription and meiotic development. During vegetative growth, PKA phosphorylates Cdc20, thus Ume6 is safe from destruction. These findings suggest that Ume6 must be degraded for meiotic gene induction and meiotic progression (Mallory et al., 2007). Under mitotic growth conditions Ume6 is not degraded as Cdc20 is inactive due to its phosphorylation by PKA. Early meiotic genes are transcribed following histone acetylation by Gcn5 histone acetyl transferase (Figure 1.11 b) (Burgess et al., 1999). The switch of URS1 from an inhibiting to an activating element requires the function of histone acetyltransferases. Ime1 is a positive activator of Ime2 an EMG, Ime2 is transcribed during meiosis and displays a high level of bound acetylated histone H3, which is mediated by Gcn5 histone H3 acetyltransferase and is required for induction of *IME2* transcription during meiosis, but not Ime1 (Burgess et al., 1999). Gcn5, is the catalytic subunit of SAGA histone acetyltransferase complex (Grant et al., 1997). In addition, its suggested that Gcn5 acetylates Ume6 to induce Ume6 degradation (Mallory et al., 2012). However, the proposed hypothesis that activation of EMGs by destruction of Ume6 through APC-Cdc20 or Gcn5 is incompatible with the need for Ume6 to recruit Ime1 to promoters. Also, the inability of *ume6Δ* cells to efficiently promote EMGs and proceed through the sporulation differentiation is incompatible with the distinct suppressive function for Ume6 (Steber and Esposito, 1995). In contrast to Gcn5, the Rpd3 histone H4 deacetylation has a distinct and opposite effect on *IME2*; *RPD3* mediates histone H4 deacetylation distinctly at the *IME2* promoter during vegetative growth but not during meiosis (Burgess et al., 1999).

1.5.3.8.2 URS1 regulation via Rpd3-Sin3

The majority of the EMGs are held silent during mitotic development; a key component of the regulation of these genes is enforced by the conserved URS1 element located upstream of the open reading frame of all the EMGs (Williams et al., 2002). During mitotic progression, Ume6 bound to URS1 recruits Rpd3, corepressor Sin3, and chromatin remodelling factor Isw2 (Kadosh and Struhl, 1997, Goldmark et al., 2000). The complex may repress EMGs through preventing access to SAGA histone acetyltransferase complex to the promoters of *IME2* (Figure 1.11a) (Raithatha et al., 2021). These components suppress EMGs in part via deacetylation of the surrounding histones (preferentially lysines 5 and 12 in H3 and H4), and development of a modified inaccessible chromatin structure (Goldmark et al., 2000, Kadosh and Struhl, 1997, Kadosh and Struhl, 1998b). The Rpd3

deacetylase histone tails associate with up to two nucleosomes from the binding region, through removing acetyl group from N-terminal lysine residues of H2A, H2B, H3, and H4 and promotes suppression (Figure 1.11a) (Kadosh and Struhl, 1998b, Rundlett et al., 1998, Suka et al., 2001). Inactivation of Rpd3 or Sin3 through mutations leads to derepression of EMGs, promoting their expression during vegetative growth (Bowdish and Mitchell, 1993). The examination that LexA-Ume6 fusion protein confers Ime1-dependent activation on a LexA operator-regulated reporter gene is compatible with the notion that Ume6 inhibits EMGs by recruitment of Rpd3-Sin3 suppressers, and that the complex is converted into an activator when binding Ime1 (Bowdish et al., 1995, Rubin-Bejerano et al., 1996). In addition, observation of EMGs regulation propose that Ume6 stays stable and bound to the promoters of EMGs during the early steps of the meiosis program, where it forms a stage for the recruitment of both transcriptional repressor Rpd3 and activator Ime1 (Raithatha et al., 2021). Rpd3 functions as a co-repressor protein complex, regulates transcription and other progressions through influencing chromatin remodelling; Rpd3 in *S. cerevisiae* forms both a large and small complexes referred to as Rpd3L (1.2 MDa) and Rpd3S (0.6 MDa) (Carrozza et al., 2005a). Rpd3L consists of Rpd3, Ume1, Sds3, Sap30, Cti6, Rxt2, Rxt3, Dep1, Ume6, Ash1 and Pho23 subunits. Rpd3S complex also consists of Rpd3, Ume1, and Sin3, in addition to Eaf3 and Rco1. Even though both complexes share a three-subunit core, they each execute diverse functions. Rpd3L binds to promoter elements and inhibits transcription. Rpd3S functions in a signalling pathway from elongating RNA polymerase II by the Set2 histone methyltransferase. Set2 methylated histones are recognized by the chromodomain of Eaf3, a subunit of the Rpd3S, which results in recruitment of Rpd3S to the coding regions of transcribed sequences. The recruited Rpd3 deacetylates the histones and represses intragenic transcription initiation (Joshi and Struhl, 2005, Carrozza et al., 2005b, Keogh et al., 2005). The Rpd3-Sin3 histone deacetylase (HDAC) complex is conserved, and functions as a transcriptional silencer in all eukaryotes (Ng and Bird, 2000, Pazin and Kadonaga, 1997). The *RPD3-SIN3* histone deacetylase complex mediates the transcriptional regulation of several genes involved in meiosis, osmotic stress, metabolism, heat stress response, telomere boundary regulation, and anaerobic growth (Rundlett et al., 1998, Kadosh and Struhl, 1997, Ehrentraut et al., 2010, De Nadal et al., 2004, Ruiz-Roig et al., 2010, Vidal and Gaber, 1991). Rpd3-Sin3 also positively regulates *IME1* transcription early in meiosis and negatively by inhibiting *IME1* transcription during late meiosis. The influence is direct, due to Rpd3 and Sin3 being recruited through Ime1 to the IREu element in its promoters (Rubinstein et al., 2007). Ime1 here is recruited by the transcription factor Msn2-Msn4 (Kahana et al., 2010). Deletion of Rpd3 increases histone acetylation *in vivo*, extends life span, and increases telomeric suppression of transcription (Rundlett et al.,

1996, Kim et al., 1999). Mutations of *RPD3* in diploids results in a defect in mitotic recombination and sporulation (Dora et al., 1999). So, during vegetative growth in the presence of glucose, Ume6 bound to URS1 in promoters of EMGs, such as *IME2*, recruits the Rpd3-Sin3 HDAC and causes deacetylation of lysines in histone H4, along with Isw2 a component of the ATP-dependent chromatin remodelling complex Isw2-Itc1(Figure 1.11a) (Goldmark et al., 2000, Fazzio et al., 2001).

1.5.3.8.3 Isw2-Itc1

The Isw2-Itc1 complex is associated as a heterodimer, and related to the switch/sucrose non-fermentable (Swi/Snf) family of ATP-dependent chromatin remodelling enzymes (Tsukiyama et al., 1999, Fitzgerald et al., 2004); both Isw2 and Itc1 are involved in the chromatin remodelling activity of the complex (Gelbart et al., 2001), which inhibits gene transcription by repositioning the promoter nucleosomes into transcriptionally inactive chromatin (Kent et al., 2001, Längst and Becker, 2001). An *in vivo* study identified two novel subunits of the Isw2 chromatin remodelling complex, Dls1 and Dpd4, which contain histone fold motifs. Depending on the Isw2 target, the subunits seem to be required for normal repressive chromatin structure; hence, the subunits are required to a certain degree in Isw2 function, and are required for Isw2 functions at stages subsequent to its interaction with chromatin, Dpd4 subunit anchors Isw2 to extranucleosomal DNA (McConnell et al., 2004, Dang et al., 2007). Including the SWI/SNF subfamily there are three other subfamilies of the chromatin remodelling ATPases (ISW1, CHD1, and INO80) which have different domain organization and catalytic activity (Clapier and Cairns, 2009, Hota and Bartholomew, 2011). ISW, imitation switch, remodelers (Isw1a/b and Isw2) and CHD1, chromodomain helicase DNA-binding, function in maturation and spacing to create nucleosomal arrays with specific spaces (Boeger et al., 2004). Isw1/Chd1 maintain chromatin structure during transcription via avoiding histone exchange (Smolle et al., 2012), also Chd1 is a component of SAGA (Pray-Grant et al., 2005). Swr1/Ino80 are involved in nucleosome editing via exchanging histone variants (Bash et al., 2006, Jungblut et al., 2020), Isw2/Ino80 promotes replication fork progression (Vincent et al., 2008). It has been proposed that Isw2 executes its function by modifying the spacing of sequential mono-nucleosomes along short, contiguous stretches of chromatin via nucleosome sliding (Tsukiyama et al., 1999, Kagalwala et al., 2004). Isw2-Itc1 is readily associated with linker DNA through Itc1, leading in spacing nucleosomes every 200 base pairs (bp). Thus, its suggested that nucleosomes retains adequate spacing as a function of the extensive and length of Itc1 binding with linker DNA (Kagalwala et al., 2004). The

previous data shows that repression of EMGs relies on histone deacetylation and chromatin remodelling functions. Rpd3-Sin3 HDAC and Isw2 chromatin remodelling complex are recruited by Ume6 to exert repression of EMGs, which deacetylates histones in the target promoters, and promote the formation of a nuclease-inaccessible chromatin structure proximal to the target URS1 site, respectively. Hens, agreeing with the notion that nucleosome modification and position together direct promoter function; additionally, a TATA box is included within the inaccessible structure (Figure 1.11 a,b), which may result in inhibiting the TATA box binding protein (TBP) at specific target promoters of EMGs, including *HOP1* and inducing repression (Shimizu et al., 2003).

1.5.3.8.4 Ime2

Ime2, Ndt80, and Rim4 are early and early-late genes required for high-level transcription of EMG. *IME2,* is a meiosis-specific serine/threonine protein kinase, which is required for several functions in inducing proper meiotic progression (Smith and Mitchell, 1989, Benjamin et al., 2003). Activation of Ime1 transcription factor induces activation of *IME2*, resulting in optimum upregulation of several known meiosis -specific genes during meiotic inducing condition (Smith and Mitchell, 1989, Mitchell et al., 1990). Again, derepression of *IME2* through mediated conversion of Ume6, bound to its URS1 promoter, to an activator has been discussed. Early genes are induced throughout meiotic S phase and prophase (Primig et al., 2000, Chu et al., 1998). Also, proceed onto the end of prophase and during preparation for the first meiotic division (Allers and Lichten, 2001, Padmore et al., 1991, Byers, 1981, Xu et al., 1995). Exiting pachytene, entry into the meiotic division, and spore formation requires the activation of middle genes (Chu and Herskowitz, 1998). Ime2 has been proposed to function in two mechanisms to mediate induction of middle meiotic genes by targeting specific genes. During vegetative growth, Sum1, a DNA-binding protein, represses middle gene promoters (Xie et al., 1999). During meiotic development, Ime2 is suggested to compete with Hst1, for the interaction with Sum1, relieving inhibition of middle genes expression. Hst1 is NAD (+)-dependent histone deacetylase. This Ime2-Sum1 negative regulation results in upregulation of Ndt80, a transcription factor required for adequate middle gene expression (Pak and Segall, 2002, Hepworth et al., 1998, Chu and Herskowitz, 1998, Ahmed, 2010). It has been proposed that Ime2 negative regulation is achieved by catalysing Sum1 phosphorylation, in contrast the positive regulation is mediated by Ime2-dependent phosphorylation of Ndt80, activated Ndt80 can induce transcription of its own gene and middle sporulation genes (Benjamin et al., 2003, Sopko et al., 2002). For example, Ndt80 transcribes *CLB2*, which harbours a

middle sporulation element, and encodes a B-type cyclin that promotes meiotic chromosome division and spore formation (Sopko et al., 2002). The high-level transcription of Ndt80 due to Ime2 activation, leads to a positive feedback which ensures irreversible meiotic commitment (Tsuchiya et al., 2014). Another role for Ime2 is as a meiosis-specific cyclin-dependent kinase (CDK)-like kinase to mediate several steps in meiotic progression (Honigberg, 2004). Cdc28, is a key cyclin-dependent kinase necessary for both cell cycle and meiosis (Mendenhall and Hodge, 1998, Benjamin et al., 2003). Ime2 targets Sic1, an inhibitor of the Clb-Cdc28 kinase (Dirick et al., 1998, Stuart and Wittenberg, 1998). Ime2 functions as a Cln/Cdc28 replacement during meiosis, allowing for the degradation of Sic1 through its phosphorylation by Ime2. This results in the activation of Clb-Cdc28 kinase to induce meiotic DNA replication. However, when cells are undergoing mitosis, Sic1 is phosphorylated by Cln-Cdc28 rather than Ime2; Sic1 is phosphorylated at many sites to ensure its degradation and cell entry into S phase (Nash et al., 2001). Another target of Ime2 is replication protein A (RPA), the cellular single-stranded DNA-binding protein that is crucial for functions during DNA replication, repair, and recombination. Ime2 direct phosphorylation of the RPA middle subunit Rfa2 early in meiosis (Clifford et al., 2004, Iftode et al., 1999).
During late stages of meiosis, expression of Ime2 leads to repression of *IME1* (Shefer-Vaida et al., 1995, Smith and Mitchell, 1989). Also, Ime2 protein kinase is proposed to phosphorylate Ime1 and target it for degradation (Guttmann-Raviv et al., 2002). These two negative-feedback loops on *IME1* induction ensures that Ime1 is expressed in a limited window relative to Ime2. In addition, the prolonged expression of Ime2 correlates with other results showing Ime2 continued role during meiosis progression (Foiani et al., 1996, Sia and Mitchell, 1995). These results propose that following *IME2* initial induction by Ime1, extended *IME2* expression does not involve Ime1 during later stages of meiosis.

1.5.3.8.5 Rim4

Rim4, is a putative RNA-binding protein, its induced early in meiosis and is involved in regulation of early and middle sporulation genes. Rim4 is required for both *IME1*- and *IME2*- dependent activation pathways, deletion of Rim4 leads to significantly decreased expression of *IME2*, but not *IME1*. Rim4 is also required for meiotic division and recombination (Deng and Saunders, 2001, Soushko and Mitchell, 2000).

1.5.3.9 RPD3-SIN3

In the yeast *S. cerevisiae*, histone acetylation and deacetylation happen through both targeted and global mechanisms. In the targeted mechanism, histone acetyltransferase (HAT) and deacetylase (HDAC) enzymes are recruited to promoter elements by certain transcriptional activators and suppressers, respectively. In the global mechanism, HATs and HDACs enzymatically alter histones across large chromatin domains, including coding sequences, without any clear DNA-sequence preference. Additionally, exact acetylatable lysines can act as binding sites for regulatory components. Also, histone deacetylation can be involved in gene activity, albeit being known for its repressive function. HDACs are transcriptional suppressers that decrease histone acetylation levels to generate localized regions of suppressed chromatin. Specific sets of genes and regions of the genome are deacetylated by one of five related HDACs in yeast (Rpd3, Hda1, Hos1, Hos2, and Hos3), suggesting "division of labour" approach (Kurdistani and Grunstein, 2003). HDACs maintain reduced levels of acetylation at repressed genes, by catalysing the removal of acetate groups from the acetylated lysine residues in the histone N-terminal domains (Kadosh and Struhl, 1998a, Rundlett et al., 1996). The HDAC Rpd3 plays a role in the modulation of several distinct genes. Albeit being principally known for being associated with transcription repression; it has been seen to have a role in transcriptional activation. For example, activation of osmoregulated genes rely on Rpd3 histone deacetylase, through its recruitment by MAPK, Hog1 (Kadosh and Struhl, 1998a, Vidal and Gaber, 1991, Kadosh and Struhl, 1997, Puig et al., 2004, De Nadal et al., 2004). *In vitro*, Rpd3 functions as part of corepressors protein complex, it does not bind directly to DNA but regulates chromatin architecture through DNA-binding transcription factors (like Ume6 and Hog1) (Kadosh and Struhl, 1997) .

1.5.3.9.1 Large Rpd3 complex and small Rpd3 complex

As mentioned before, there are two known Rpd3 complexes, the large Rpd3L complex (Rpd3, Ume1, Sds3, Sap30, Cti6, Rxt2, Rxt3, Dep1, Ume6, Ash1 and Pho23), and the small Rpd3S complex (Rpd3, Ume1, Sin3, Eaf3 and Rco1) (Kadosh and Struhl, 1997, Puig et al., 2004, Lechner et al., 2000, Loewith et al., 2001, Kurdistani et al., 2002). Their differing positioning on chromatin are likely mediated by the additional components whom characterise each complex (Carrozza et al., 2005a). Mutation of Rpd3L in diploid cells, leads to defects in mitotic recombination and sporulation, highlighting its role in meiotic progression; Rpd3L also controls the transcriptional program of haploid cells entering quiescence (Dora et al., 1999, Lardenois et al., 2015, McKnight et al., 2015). The Rpd3L-

Sin3 complex is recruited to promoters in association with specific transcription components like Ume6, Ash1, Ime1, Whi5, and Stb1 (Carrozza et al., 2005a, Rubinstein et al., 2007, Takahata et al., 2009). At the promoter region, Rpd3 deacetylates specific lysine residues on histone H3 and H4 (preferably at lysine 5 and 12) in a localized region covering around two nucleosomes (Kadosh and Struhl, 1998b). Whereas, Rpd3S negatively regulates transcriptional elongation, by recruiting it to the open reading frame via RNA polymerase II after its phosphorylation by Cdk7/Kin28 on Ser5 within the C-terminal domain (Govind et al., 2010). The stability of these complexes or their performance of distinct catalytic function such as histone methylation, might be owed to their specific subunits (Carrozza et al., 2005b, Keogh et al., 2005, Silverstein and Ekwall, 2005). Ume1 and Sin3 are core components of both complexes. Sin3 is found in both complexes, and functions as a scaffold to compile and organize different components and is involved in targeting the complex to certain promoters through its linking with specific DNA-binding proteins (Gray and Ekström, 2001, Ng and Bird, 2000, Knoepfler and Eisenman, 1999). For example, Sin3 associates with Ume6 in a Rpd3-Sin3-dependent manner to repress or activate promoters (Kadosh and Struhl, 1998b).

1.5.3.9.2 Rpd3 in meiotic development

Induction of meiosis relies on nitrogen starvation coupled with a non-fermentable carbon source. A transcriptional cascade is then activated to transcribe genes generally categorised into three stages early (EMGs), middle (MMGs), and late (LMGs) times during meiotic development, which are all regulated by Ime1 master regulator. Histone deacetylase Rpd3 functions dynamically in the transcriptional inhibition and induction of IME1, EMGs, MMGs, and LMGs. Such as, Rpd3s functions as a positive activator and negative inhibiter to regulate *IME1* transcription early- and late- meiosis, respectively. The influence is direct, due to Rpd3-Sin3 being recruited via Ime1 promoter element, IREu (Rubinstein et al., 2007). Rpd3 functions as a negative regulator of EMGs, *IME2*, after the Ume6 platform recruits Rpd3-Sin3 to the URS1 promoter element (Kadosh and Struhl, 1998b). Rpd3 functions as a positive regulator, vital regulator of MMGs, LMGs, and the early-middle gene *NDT80* transcription. The *NDT80* encodes key transcriptional inducer of MMGs (Hepworth et al., 1998). But it is not yet clear if Rpd3 binds directly to promoters of these genes. The dual and opposing functions of Rpd3 is proposed to result from its existence in two different complexes that target certain genes. Deletion of *SDS3* and *DEP1* from Rpd3L and *ROC1* from Rpd3S, which disrupts the integrity and function of the complexes, revealed distinct effects of the catalytic subunit, Rpd3, on three key positive

regulators of meiosis. Depending on the target gene and growth environments, the control of *IME1*, *IME2*, and *NDT80* by Rpd3 in the mutant strains showed the following: 1) reporter assays revealed that the integrity of Rpd3L and Rpd3S is indispensable for repression by Rpd3, 2) the catalytic activity of Rpd3 functions only as a positive regulator in Rpd3S possibly due to the role of Eaf3 subunit in the transcriptional activator NuA4-HAT, but only activates *NDT80* during vegetative growth, 3) Rpd3's catalytic activity alternates from a negative to a positive regulator depending on nitrogen starvation, 4) Rpd3's noncatalytic activity, which is independent of the complexes integrity, inhibits transcription. Furthermore, the transcription induction does not associate with histone H4 deacetylation, proposing an influence on a nonhistone protein (Yeheskely-Hayon et al., 2013, Rundlett et al., 1996, Kurdistani et al., 2002). In contrast, recruitment of Rpd3 by Ume6 to *IME2* promoters induced deacetylation of histones H3 and H4, subsequently repressing transcription in vegetative growth (Kadosh and Struhl, 1997, Kadosh and Struhl, 1998a).

1.5.3.9.3 Rpd3 role in various biological processes

Rpd3 can also maintain global levels of histone deacetylation, evident from elevated levels of histone acetylation in both coding and intergenic regions of the genome (Vogelauer et al., 2000). In strains deleted for *SDS3*, the integrity of Rpd3L complex is compromised and Sin3 can be chromatographically separated from Rpd3. Also, the remaining subunits in Rpd3L in *sds3Δ* cells showed minor or no histone deacetylase activity. These data supports the crucial role of Sds3 in the integrity and catalytic activity of Rpd3-Sin3 HDAC (Lechner et al., 2000). Rpd3-Sin3 HDAC is also involved in iron homeostatic regulation, specifically through its Cti6 subunit. Also, Cti6 and several components (Sin3, Sds3, Sap30, and Pho23) of the Rpd3L complex are required for both growth under iron limitations and telomeric, rDNA, and mating type silencing regulation; *RPD3* deletion increases telomeric silencing. Cti6, a PHD finger containing protein, is not an essential component of Rpd3-Sin3 HDAC and mediates promoter repression through Rpd3. Also, *cti6Δ* strains have no effect on *IME2* expression (Puig et al., 2004, Loewith et al., 2001, Lechner et al., 2000).

1.6 Unfolded protein response pathway's involvement in nutrient sensing and developmental programs

As discussed before, accumulation of unfolded proteins in the ER triggers the UPR to alleviate ER stress. A signal transduction pathway relays the signal of unfolded or misfolded proteins from the ER lumen to the nucleus in response to the stress, in which Ire1 activates $Hac1^{i}$ to coordinate the transcription of several genes to relieve ER stress. This response upregulates transcription of chaperones within the ER, components of the ER-associated degradation (ERAD) pathway, and genes required for ER expansion (Schröder and Kaufman, 2005, Cox and Walter, 1996, Travers et al., 2000). In this section I will discuss the UPR pathways involvement in nutrient sensing and developmental programs.

1.6.1 The UPR pathway's role in nutrient sensing and differentiation

In yeast, the UPR is complex and involved in regulating several cellular developments and environmental adaptation (Kaufman et al., 2002). A whole-genome expression profiling, utilizing microarrays, showed that the induced UPR regulates activation of 381 open reading frames (ORFs) out of 6300 in response to ER stress. About half of the ORFs have shown to be involved in the secretory pathway, however around 100 ORFs which are regulated by the UPR have no function in the secretory pathway, denoting the possibility for their functions in other biological processes (Travers et al., 2000). The UPR is not only triggered by stress, but also by glucose limitation, altered redox status, or altered protein synthesis rates (Rutkowski and Hegde, 2010). The UPR also plays a role in sensing and responding to nitrogen starvation, the morphological adaptation depends on the type of carbon source (fermentable or non-fermentable). In diploid cells, activation of the UPR inhibits two distinct nitrogen starvation responses, pseudohyphal growth and sporulation. Moreover, the UPR itself is activated during vegetative growth in the presence of nitrogen-rich conditions, this may be due to accumulation of unfolded proteins as a result of rapid translation in a nitrogen-rich environment (Schröder et al., 2000). On the other hand, when cells are starved for nitrogen, they synthesise proteins at a lower rate reducing the ER load, which results in Ire1 deactivation subsequently inhibiting $Hac1^{i}$ synthesis. The UPR pathway senses nitrogen starvation, in the presence of a fermentable carbon source or non-fermentable carbon source and regulates cell fate. In nitrogen-rich conditions, *HAC1* mRNA splicing is detected (Figure 1.12), in contrast during nitrogen starvation the splicing activity is repressed (Schröder et al., 2000). In nitrogen starved cells, overexpression of

Hac1^{i} reduced induction of EMGs, while in nitrogen-rich environments, *hac1Δ* upregulated mRNA transcription of EMGs. Also, subjecting cells to tunicamycin, an inhibiter of N-linked glycosylation of nascent polypeptides in the ER (Hubbard and Ivatt, 1981), repressed ascospore formation (Weinstock and Ballou, 1987) and transcriptional induction of EMGs in an *IRE1*-dependent manner (Schröder et al., 2000). It is important to note that Ime1 expression levels were not affected in either condition. EMGs negatively regulated by Hac1^{i} include *IME2*, *HOP1*, and *SPO13*; within the promoters of these genes, I find the URS1 (activation and repression) element. URS1, is also found in non-meiotic genes like *CAR1*, arginase (Gailus-Durner et al., 1996, Messenguy et al., 2000). In addition, there are two other regulatory elements common to the promoters of EMGs, an enhancer on non-fermentable carbon sources, known as T_4C (Bowdish and Mitchell, 1993), and UAS_H, the binding site for Abf1 transcription factor (Gailus-Durner et al., 1996). Negative regulation of EMGs through Hac1^{i} under nitrogen-rich condition, requires inactivation of Ume6 bound to URS1 (Raithatha et al., 2021). Ume6 recruits both the Rpd3-Sin3 HDAC and the *ISW2* chromatin remodelling complex to URS1, however *ISW2* is dispensable for repression of transcription by Hac1^{i} (Schröder et al., 2004). Also, Rpd3-Sin3 catalytic activity is involved in transcriptional repression by Hac1^{i}. Furthermore, overexpression of Hac1^{i} inhibited pseudohyphal development, while *ire1Δ* and *hac1Δ* derepressed pseudohyphal development. Subjecting cells to tunicamycin and 2-deoxyglucose, which activates UPR, suppressed pseudohyphal development in wild-type cells but not in cells deleted for *HAC1* or *IRE1* (Schröder et al., 2000). Together, the findings suggest that Hac1^{i} is synthesised in response to nitrogen-rich conditions and displays a negative effect on nitrogen starvation response. Schroder et al, 2000 suggested a model of UPR-signalling pathway sensing the nutritional state of the cell and regulating the nitrogen starvation induced differentiation responses (Figure 1.12); also, Schroder et al, 2004 suggested a model for regulating growth and differentiation by the UPR-signalling cascade through Hac1^{i}. Indeed, these findings show a novel function for the Hac1^{i} transcription factor to negatively regulate EMGs. The apparent overlap between a nitrogen starvation response and the UPR is a first, as there may be a functional overlap between Hac1^{i} and Ume6 in the regulation of EMGs. Also, repression of EMG through Hac1^{i} is not direct, since Hac1^{i} does not bind directly to the DNA but depends on Ume6, which is constitutively bound to URS1, the platform for the negative regulation. The Schroder et al, 2004 study proposed a novel framework for negative transcriptional regulation by a bZIP transcription factor, Hac1^{i}. Therefore, the UPR pathway is directly involved in nutrient sensing and orchestrating cell fate decisions in yeast.

1.6.2 Basal activity of the UPR during vegetative growth

Under normal nutrient rich condition, *S. cerevisiae* shows basal UPR activity proposed to deal with the presence of unfolded proteins in the ER expressed during vegetative growth. Hence, the UPR is always active in accommodation to the cells changing environment. Subsequently, degrading unfolded proteins through ERAD to maintain homeostasis if need be (Travers et al., 2000). Wild-type cells in nutrient-rich environments also undergo basal UPR activity; this is evident from the UPR role in repressing pseudohyphal growth under nitrogen-rich conditions. In this case, transcription of $Hac1^{i}$ in unstressed, vegetatively growing cells occurs. In the presence of different carbon sources *HAC1* mRNA splicing was detected. In the presence of glucose about 1 % to 3 % of $HAC1^{i}$ mRNA is detected; interestingly, during growth in acetate media the amount of $HAC1^{i}$ mRNA was at least 10-folds more. Cell type has no bearing on the basal low-level UPR activity in unstressed cells. Therefore, the small amounts of *HAC1* splicing in wild-type cells grown on glucose are sufficient for repression of pseudohyphal growth, as cells deleted for *HAC1* or *IRE1* constitutively grew as pseudohyphal. Thus, the basal UPR activity inhibits Pseudohyphal development in a nitrogen-rich environment in vegetatively developing cells (Schröder et al., 2000).

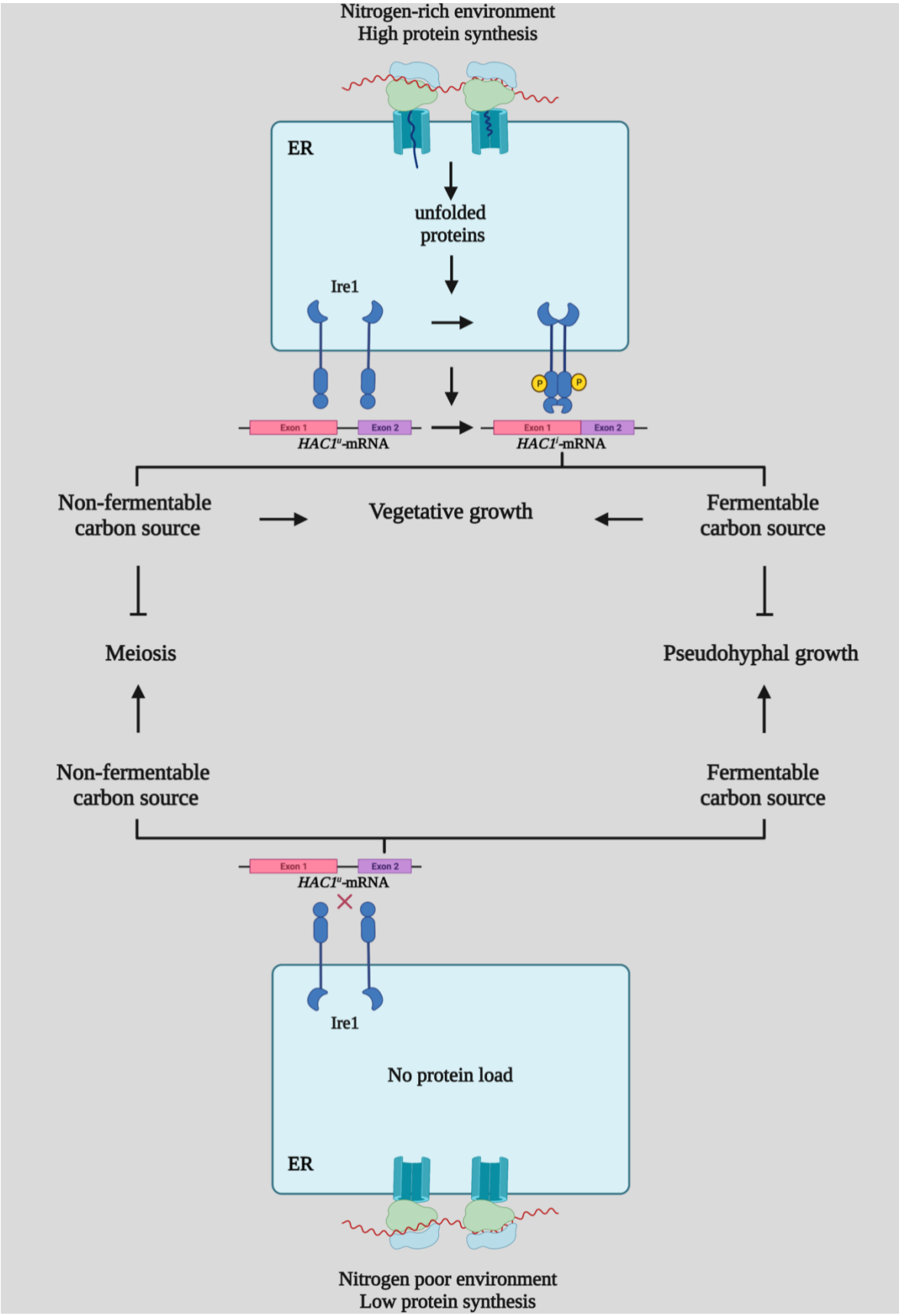

Figure 1-12 A model showing of a nitrogen-sensing pathway.

UPR as a nutrient sensor regulating differentiation events in yeast. In nitrogen-rich environment, *HAC1* mRNA is spliced due to high protein synthesis, which represses pseudohyphal growth and meiosis. When nitrogen is limited, the Hac1^{i} splicing and synthesis are shut off and depending on the carbon source cells undergo meiosis or pseudohyphal growth.

1.7 Aims

Aims:

Characterise conserved residues in the Hac1 bZIP transcription factor domains in regulating EMGs. Observe the consequence of manipulating these Hac1 residues, located within the bZIP domain and the transactivation domain, on negatively regulating EMGs.

1) *HAC1* manipulation, by constructing functional $Hac1^{u}$, through overlap PCR deletion approach. And constructing three classes of point mutations in the different domains of $Hac1^{i}$ bZIP transcription factor using a genetic approach.

2) Characterisation of which structural elements of Hac1, i.e., its DNA-binding region, leucine zipper region, or transcriptional activation domain, are required for activation of UPRE regulated genes by Hac1. The mutants will be expressed in *S. cerevisiae* cells and compare their effect to wild type Hac1 on induction of UPRE. Activation of UPRE will be monitored by using plasmids encoding a β-galactosidase reporter in which the β-galactosidase (lacZ) gene of Escherichia coli is under control of known promoter elements of genes activated by the unfolded protein response, UPRE.

3) Characterisation of which structural elements of Hac1, i.e., its DNA-binding region, leucine zipper region, or transcriptional activation domain, are required for repression of EMGs by Hac1. The mutants will be expressed in *S. cerevisiae* cells and compare their effect to wild type Hac1 on expression of EMGs. Expression of EMGs will be monitored by using plasmids encoding series of β-galactosidase reporter plasmids in which the β-galactosidase (lacZ) gene of *Escherichia coli* is under control of known promoter elements of early meiotic genes, such as URS1 and T_4C elements. In addition, expression of several early meiotic genes (*IME1*, *IME2*, and *HOP1*, *SPO13*) will be monitored by Northern blotting.

4) Observe and detect comparable steady levels of Hac1 and Hac1 mutant proteins, by developing an optimised protocol to enrich and precipitate Hac1 expressed from the single copy plasmid (pRS314). Choose which optimised techniques will enrich and precipitate Hac1 due to it being a low abundant protein in *S. cerevisiae*.
A) Ammonium sulfate precipitation-Western blotting technique.
B) Immunoprecipitation-Western blotting technique

5) Identify potential targets of Hac1^{i} transcriptional repression involved in the meiotic pathway. Expression of Hac1^{i} in *S. cerevisiae* cells and observe expression or lack thereof known components of the Rpd3-Sin3 histone deacetylase complex histone deacetylase complex (Dep1, Cti6, Rxt2, Rxt3, Pho23, Sds3, Sap30). mRNA expression of the subunits (*DEP1*, *CTI6*, *RXT2*, *RXT3*, *PHO23*, *SDS3*, *SAP30*) will be monitored by Northern blotting.

2 MATERIALS AND METHODS

2.1 Materials

2.1.1 Reagents

2.1.1.1 Yeast and Bacterial medium Reagents

Here I show reagents used to prepare the different liquid and solid medium used for cell growth.

Media reagents

Table 2-1 Media reagents

Name	Supplier	Product number
YPD Broth	Formedium, Norfolk	CCM0210
YPD Agar	Formedium, Norfolk	CCM0105
Yeast Nitrogen Base without Amino acids	Formedium, Norfolk	CYN0410
Yeast Extract Powder	Formedium, Norfolk	YEA02
Peptone	Formedium, Norfolk	PEP03
Acetic acid, potassium salt 99+%, pure anhydrous (KOAc)	Acros Organics, Leicestershire	220150010
Agar	Formedium, Norfolk	AGA03
D-(+)-Galactose	Apollo Scientific, Cheshire	BIG1724
Potassium hydrogen phthalate (K- phthalate)	VDR Chemicals (BDH), Leicestershire	26948.260
myo-Inositol	Fluka Chemical Corp, Dorset	57570
L- Tyr	Formedium, Norfolk	DOC0192
Uracil	Formedium, Norfolk	DOC0213

L- Arg	Sigma-Aldrich, Dorset	W381918
L- His	Formedium, Norfolk	DOC0144
L- Met	Formedium, Norfolk	DOC168
L – Trp	Formedium, Norfolk	DOC0188
L – Iie	Formedium, Norfolk	DOC0152
L – Lys	Formedium, Norfolk	DOC0161
L – Val	Formedium, Norfolk	DOC0197
L – Ser	Formedium, Norfolk	DOC0181
Adenine sulphate	Formedium, Norfolk	DOC0229
L – Phe	Formedium, Norfolk	DOC0173
L – Glu	Formedium, Norfolk	DOC0132
L – Leu	Formedium, Norfolk	DOC0157
L – Asp	Formedium, Norfolk	DOC0121
L – Thr	Formedium, Norfolk	DOC0185
LB Broth (Lennox)	Formedium, Norfolk	LBX0102
LB-Agar Lennox	Formedium, Norfolk	LBX0202
Ampicillin	Apollo Scientific, Cheshire	BIA0104

2.1.1.2 Chemical reagents

In this table I present the reagents used throughout the experiments in this thesis.

Table 2-2 Chemical reagents

Name	Supplier	Product number
Acetic acid (HOAc)	Thermo Fisher Scientific, Leicestershire	A/0360/PB17
4-(2-Aminoethyl)benzenesulphonyl fluoride hydrochloride (AEBSF)	Apollo Scientific, Cheshire	BIMB2003
Agarose	Fisher Scientific, Leicestershire	BP 1356-500
Ammonium Persulphate 98 %	Sigma Aldrich, Dorset	A3678
Acrylamide	Fisher Scientific, Leicestershire	164855000
β-Mercaptoethanol	Alfa Aesar, Leicestershire	A15890
Bovine serum albumin (BSA)	Fisher Scientific, Leicestershire	BP 1600-100
Benzamidine hydrochloride hydrate	Apollo Scientific, Cheshire	OR11123
1-Butanol	VWR Chemicals (BDH), Leicestershire	100616J
Chymostatin	Melford Laboratories, Ipswich	C1104
Dithiothreitol (DTT)	Apollo Scientific, Cheshire	BIMB1015
Dowex® MR-3 LCNG hydrogen and hydroxide form	Supelco (a Sigma Aldrich Brand), Dorset	13684-U
Dimethyle sulfoxide	Sigma-Aldrich, Dorset	D8418
Ethanol	Fisher Scientific, Leicestershire	E/0500/17

Ethylenediaminetetraacetic acid (EDTA)	Fisher Scientific, Leicestershire	BPE119-500
Ethidium bromide	Sigma-Aldrich, Dorset	E1510-10ML
Formamide	Fisher Scientific, Leicestershire	181090025
Ficoll® PM 400	Amersham, Dorset	17-0300-10
Glycerol	Thermo Fisher Scientific, Leicestershire	G/0600/17
Glycine	Fluka Chemical Corp, Dorset	50046
Glyoxal	Sigma-Aldrich, Dorset	G5754
Glass Beads 0.5 mm diameter	Biospec Products, Neots	11079105
21-Hydroxyprogesterone (Deoxycorticosterone (DOC))	Sigma-Aldrich, Dorset	D6875
Hydrochloric acid	Thermo Fisher Scientific, Leicestershire	H/1100/PB17
Iodoacetamide	Sigma-Aldrich, Dorset	I-6125
Leupeptin hydrochloride	Apollo Scientific, Cheshire	BIMI2442
Methanol (MeOH)	Thermo Fisher Scientific, Leicestershire	M/4000/PC17
Methylenebisacrylamide	Merck Life Science, Dorset	M7279
Potassium hydroxide pellets	Thermo Fisher Scientific, Leicestershire	P/5600/53
Propan-2-ol	Thermo Fisher Scientific, Leicestershire	P/7490/17

Potassium phthalate monobasic	Sigma-Aldrich, Dorset	P6758
Potassium acetate	Fisher Scientific, Leicestershire	P3760153
Phenol/Chloroform/Isoamyl Alcohol (25:24:1 Mixture)	Fisher Scientific, Leicestershire	BPE1752P-400
Protein A Sepharose, preserved in 25 % (w/v) slurry in PBS + 0.01 % NaN_3	Santa Cruz Biotechnology, Heidelberg	SC-2001
Phenylmethanesulfonyl fluoride (PMSF)	Apollo Scientific, Cheshire	BIP0329
Pepstatin A	Fluka Chemical Corp, Dorset	77170
Reporter lysis 5 x buffer	Promega, Hampshire	E397A
Salmon sperm DNA solution (10 mg/ ml)	Thermo Fisher Scientific, Leicestershire	15632011
Sodium dodecyl sulphate (SDS)	Thermo Fisher Scientific, Leicestershire	BPE116-500
Tris(2-carboxyethyl)phosphine hydrochloride. TCEP	Apollo Scientific, Cheshire	BIT0122
Thermo Scientific Pierce Anti-HA Magnetic beads	Fisher Scientific, Leicestershire	13474229
Tris(hydroxymethyl)aminomethane	Apollo Scientific, Cheshire	BI2888
Tetramethylethylenediamine	Sigma-Aldrich, Dorset	T9281
Triton X-100	Fisher Scientific, Leicestershire	T/3751/08
Tween 20	Fisher Scientific, Leicestershire	10485733

2.1.2 Buffers and Solutions

Tables 2.1 and 2.2 outline the protocol of the buffers and solutions used in this thesis. All solutions are prepared in type I laboratory H_2O (resistivity 18 MΩ cm, total organic carbon < 1 ppb, microorganisms < 1 cfu/ml, particles < 0.05 µm diameter) generated by the NANO pure Diamond UV/UF TOC water purification system and sterilized by autoclaving (121°C, 20 – 30 min). If this is not possible, solutions are prepared in autoclaved type I laboratory H_2O and then filter sterilized by filtration over a 0.22 µm filter.

Table 2-3 Commonly used buffers and solutions and their protocol

Solution	Quantity	Protocol
Ethylenediaminetetraacetic acid (EDTA), 0.5 M	500 ml	1. Dissolve 93.1 g $Na_2EDTA \cdot 2H_2O$ in ~350 ml H_2O. 2. Adjust pH to 8.0 with 10 M NaOH (~25 ml) 3. Add H_2O to 500 ml. 4. Autoclave.
Tris(hydroxymethyl)aminomethane (Tris)-acetate-EDTA 50 x TAE	1 l	242 g Tris base 57.1 ml HOAc 37.2 g $Na_2EDTA \cdot 2H_2O$ Add H_2O to 1 l
1 x TAE	1 l	20 ml 50 x TAE Add H_2O to 1 l
10 x TE (8.0)	4 l	400 ml 1 M Tris·HCl (pH 8.0) 80 ml 0.5 M EDTA Add H_2O to 4 l Autoclave
Tris(hydroxymethyl)aminomethane (Tris)·HCl (pH 8.0), 1 M	1 l	1. Dissolve 121.14 g Tris in ~800 ml H_2O. 2. Adjust pH to 8.0 with conc. HCl (~ 42 ml). 3. Add H_2O to 1 l. 4. Autoclave.
Tris·HCl (pH 6.8), 1 M	1 l	1. Dissolve 121.14 g Tris in ~800 ml H_2O.

		2. Adjust pH to 8.0 with conc. HCl (~ 42 ml). 3. Add H_2O to 1 l. 4. Autoclave.
Tris·HCl (pH 8.9), 1 M	1 l	1. Dissolve 121.14 g Tris in ~800 ml H_2O. 2. Adjust pH to 8.0 with conc. HCl. 3. Add H_2O to 1 l. 4. Autoclave.
Tris·HCl (pH 8.5), 1 M	1 l	1. Dissolve 121.14 g Tris in ~800 ml H_2O. 2. Adjust pH to 8.0 with conc. HCl. 3. Add H_2O to 1 l. 4. Autoclave.
Magnesium Chloride $MgCl_2$, 1 M	100 ml	1. Dissolve 20.33 g $MgCl_2 \cdot 6\ H_2O$ in ~ 80 ml H_2O. 2. Add H_2O to 100 ml. 3. Autoclave.
Sodium chloride NaCl, 1 M	500 ml	1. Dissolve 29.22 g of NaCl in ~ 400 ml H_2O, stir. 2. Add H_2O to 500 ml. 3. Autoclave.
Potassium chloride KCl, 1M	500 ml	1. Dissolve 37.27 g of KCl in ~ 400 ml H_2O, stir. 2. Add H_2O to 500 ml. 3. Autoclave.
(4-(2-hydroxyethyl)-1-piperazineethanesulfonic acid) HEPES (pH 7.9), 0.5 M	500 ml	1. Dissolve 59.57 g of HEPES in ~ 400 ml H_2O, stir. 2. Add H_2O to 500 ml. 3. Autoclave.
NaH_2PO_4, 0.4 M	500 ml	1. Dissolve 24 g NaH_2PO_4 in ~400 ml H_2O. 2. Add H_2O to 500 ml. 3. Autoclave.

Na_2HPO_4, 0.4 M	500ml	1. Dissolve 28.4 g Na_2HPO_4 in ~400 ml H_2O. 2. Add H_2O to 500 ml. 3. Autoclave.
Sodium dodecyl sulphate 10% (w/v) (SDS)	500 ml	1. Dissolve 50 g SDS in ~450 ml H_2O. 2. Add H_2O to 500 ml. 3. Do NOT autoclave.
10 % (v/v) Tween 20	50 ml	1. Dissolve 5.55 g Tween 20 in ~ 40 ml autoclaved H_2O. 2. Add H_2O to 50 ml. 3. Filter sterilise.
10 % (v/v) Triton X-100	50 ml	1. Dissolve 5.55 g Tween 20 in ~ 40 ml autoclaved H_2O. 2. Add H_2O to 50 ml. 3. Filter sterilise.
10 x TBST	1 l	24.2 g Tris base 80g NaCl 10.6 g Tween 20 Dissolve in ~800 ml Adjust pH ~ 7.6 with HCl Add H_2O to 1 l Note: this was diluted with deionised H_2O to 1 x for use in blocking solution and washing of PVDF membranes.
Glycine·HCl (pH 2.5), 1 M	500 ml	Dissolve 37.535 g glycine in 400 ml H_2O Adjust the pH to 2.5 with HCl. Add H_2O to 500 ml Autoclave.
10 x SDS-PAGE running buffer	1 l	144.13 g glycine 30.03 g Tris 10.00 g SDS

		Add H_2O to ~ 900 ml, stir until completely dissolved, then add H_2O to 1 l.
10 x Semi-Dry Transfer Buffer	500 ml	73.19 g Glycine 60.6 g Tris-Base Dissolve in ~350 ml H_2O Add H_2O to 500 ml
1 x Semi-Dry Transfer Buffer + 5 % Methanol	1 l	100 ml 10 x semi-Dry transfer buffer 50 ml Methanol Adjust with H_2O to 1 l
6 x SDS-PAGE + β-mercaptoethanol sample buffer	10 ml	3.50 ml 1 M Tris·HCl 3.78 g glycerol 1.00 g SDS 500 µl 10 g/l bromophenol blue 200 µl β-mercaptoethanol Add H_2O to 10 ml
30% (w/v) acrylamide, 0.8% (w/v) methylene bisacrylamide	100 ml	30 g acrylamide 0.8 g methylene bisacrylamide Dissolve in ~90 ml H_2O, adjust H_2O to 100 ml. Add 5 g Dowex MR-3 mixed bead ion exchanger, and stir for 1 h at RT. Filter over a 0.22 µm filter and store at 4ºC in the dark.
1 x TBST + 5% (w/v) skimmed milk powder		5 g milk powder dissolve in 90 ml 1 x TBST Adjust to 100 ml with 1 x TBST

Table 2-4 Specialist used buffers and solutions and their protocol

Solution	Quantity	Protocol
2 mM dNTPs	1 ml	910 µl H_2O 10 µl 100 mM Tris·HCl (pH 8.0) 20 µl 100 mM dATP 20 µl 100 mM dCTP 20 µl 100 mM dGTP 20 µl 100 mM dTTP
Stop buffer (Alkaline Phosphatase, Calf Intestinal (CIAP))	1 ml	Mix 10 µl 1 M Tris·HCl (pH 7.5), 200 µl 1 M NaCl, 2 µl 0.5 M EDTA, 50 µl 10 % SDS
100 mM deoxycorticosterone (DOC)	100 ml	Add 3.725 g deoxycorticosterone to 100 ml of ethanol Filter sterilise, store at 4°C
50 mg/ml ampicillin	50 ml	2.5 g ampicillin, sodium salt. Dissolve in ~ 40 ml H_2O add H_2O to 50 ml, and filter sterilise. Store in 1 ml aliquots at -20°C.
2 x assay buffer	400 ml	177 ml 0.4 M Na_2HPO_4 23 ml 0.4 M NaH_2PO_4 0.8 ml 1 M $MgCl_2$ 2.8 ml β-mercaptoethanol 532 mg 2-nitrophenyl- β -Dgalactopyranoside Add H_2O to 400 ml and mix. Store in 50 ml aliquots at -20°C.
10 mU/ µl β-galactosidase	100 µl	Add 1 µl 1 U/µl β-galactosidase to 99 µl ice-cold 1 x RLB and mix well, put on ice. Note: make fresh for assay
0.1 mU/ µl β-galactosidase	1 ml	Add 10 µl of 10 mU/ µl β-galactosidase (1:100 dilution) to 990 µl ice-cold 1 x RLB and mix well, and place on ice.
1 x reporter lysis buffer (RLB)	50 ml	Add 10 ml of 5 x Reporter lysis buffer to 40 ml ice-cold autoclave H_2O

Na_2CO_3, 1 M	500 ml	1. Dissolve 53.0 g Na_2CO_3 in ~ 400 ml H_2O. 2. Adjust H_2O to 500 ml.
0.1 M iodoacetamide + 0.1 M Tris·HCl (pH 8.0)	10 ml	Add 184.96 mg iodoacetamide to 1 ml 1 M Tris·HCl (pH 8.0), then add H_2O to 9 ml and mix. Bring solution to 10 ml by adding H_2O
1 M dithiothreitol (DTT)	10 ml	1.54 g dithiothreitol Dissolve in ~ 9 ml H_2O. Add H_2O to 10 ml. Filter sterilise. Store at -20°C.
(tris(2-carboxyethyl)phosphine) (TCEP), 0.5 M	40 ml	5.73 g of TCEP dissolve in ~35 H_2O. Adjust to 40 ml with H_2O Store in 1 ml aliquots at -20°C.
10 mg/ml ethidium bromide	25 ml	Dissolve 250 mg ethidium bromide in ~ 20 ml sterile H_2O. Add sterile H_2O to 25 ml. Store at 4°C protected from light.
30% (v/v) glycerol	500 ml	189 g glycerol Add H_2O to ~400 ml, mix well by stirring. Add H_2O to 500 ml and autoclave
Lithium acetate (LiOAc), 1 M	250 ml	25.50 g $LiOAc·2H_2O$ Dissolve in ~200 ml H_2O. Add H_2O to 250 ml. Filter sterilise.
50% (w/v) PEG 4000	500 ml	Add 250 g PEG 4000. Add ~200 ml H_2O Stir for a few minutes, add H_2O to ~ 450 ml, stir until PEG 4000 is nearly completely dissolved. Add H_2O to 500 ml and mix. Filter sterilise.
One- step buffer (0.2 M LiOAc + 40 % (w/v) PEG 4000)	10 ml	Add 2 ml of 1 M LiOAc to 8 ml 50% (w/v) PEG 4000 and mix solution well
Lysis buffer 1	500 ml	7.2 ml 0.4 M NaH_2PO_4

		24 ml 0.4 M Na_2HPO_4 4.38 g NaCl 5.5 g (v/v) Triton X-100 63 g glycerol 1 ml 0.5 M EDTA (pH 8.0) Add H_2O to ~ 400 ml, and dissolve. Add H_2O to 500 ml. Store at 4°C.
Lysis buffer 3	50 ml	24 g Urea 12 ml 10 % SDS 2.5 ml 1 M Tris-HCl, pH 7.5 at 4°C 1 ml 0.5 M EDTA, pH 8.0 Mix overnight at room temperature (RT) Next day add H_2O to 50 ml and keep buffer at RT
Ammonium sulphate ($[NH_4]_2SO_4$), 4 M	250 ml	1. Dissolve 132.14 g $(NH_4)_2SO_4$ in ~200 ml H_2O. 2. Mix until dissolved. 3. Add H_2O to 250 ml. 4. autoclave.
Dialysis buffer	1 l	1. 20 ml 0.5 M HEPES, pH 7.9 2. 50 ml 1 M KCl 3. 1 ml 0.5 M EDTA, pH 8.0 4. 1 ml 1 M DTT Stir, and store at 4°C
Bicinchoninic acid protein assay working solution (BCA).	15 ml	Reagent A: 10 g/l bicinchoninic acid disodium salt, 20 g/l $Na_2CO_3 \cdot H_2O$, 1.6 g/l disodium tartrate, 4.0 g/l NaOH, 9.5 g/l $NaHCO_3$. Adjusted to pH 11.25 with 10 M NaOH. Reagent B: 40 g/l $CuSO_4 \cdot 5H_2O$ Mix 50 parts of reagent A with 1 part of reagent B. Note: when mixing reagents A and B a white precipitate

		may form [$Cu(OH)_2$] this will dissolve upon further mixing of the reagents.
Chemiluminescence detection with luminol	15 ml	15 ml 100 mM Tris·HCl (pH 8.5) + 0.1 % (v/v) Tween 20 75 µl 250 mM luminol 33.3 µl 90 mM *p*-coumaric acid 4.35 µl 30 % (w/w) H_2O_2 Mix well and keep protected from light

2.1.3 RNA Buffers and Solutions

Table 2.3 outlines the protocol of the buffers and solutions used in this thesis for RNA experiments. All solutions are prepared in type I laboratory H_2O treated with 0.1 % diethylpyrocarbonate (DEPC) then autoclaved. If this is not possible, solutions are prepared in autoclaved type I laboratory DEPC-H_2O.

Table 2-5 Buffers and solutions used for RNA work and their protocol

Solution	Quantity	Protocol
DEPC-H_2O	1 l	1 mL DEPC 1 l sterile H_2O, stir for 30 min Autoclave.
EDTA (pH 8.0), 0.5 M	500 ml	1. Dissolve 93.1 g $Na_2EDTA·2H_2O$ in ~350 ml in DEPC-H_2O. 2. Add DEPC-H_2O to 500 ml. 3. Add 0.5 mL DEPC, stir 30 min 4. Autoclave.
1 M Tris·HCl (pH 7.5)	500 ml	1. Dissolve 60.57 g Tris in ~ 400 ml DEPC-H_2O. 2. Adjust pH w/conc HCl. 3. Add DEPC-H_2O to 500 ml. 4. Autoclave.
1 M Tris·HCl (pH 8.0)	500 ml	1. Dissolve 60.57 g Tris in ~ 400 ml DEPC-H_2O. 2. Adjust pH w/conc HCl. 3. Add DEPC-H_2O to 500 ml. 4. Autoclave.

20 mM Tris·HCl (pH 8.0)	500 ml	Add 10 ml 1 M Tris·HCl (pH 8.0), add DEPC-H_2O to 500 ml.
RNA buffer	500 ml	1. Dissolve 14.61 NaCl in 390 ml DEPC-H_2O. 2. Add 390 µl DEPC and stir for 30 min at RT. 3. Autoclave. 4. Add 100 ml 1 M Tris·HCl (pH 7.5) and 10 ml 0.5 M EDTA (pH 8.0)
Phenol: $CHCl_3$: isoamylalcohol (25:24:1 (v/v/v)), saturated with RNA buffer	50 ml	1. Add 25 ml Phenol: $CHCl_3$: isoamylalcohol (25:24:1 (v/v/v)), buffered w/0.1 M Tris·HCl (pH 8.0) to 50 ml tube and mix vigorously with 25 ml RNA buffer. 2. Centrifuge for 2 min at 3,000 rpm to separate phases and discard the upper phase (use the hood). 3. Repeat steps 1 and 2 once, this time leave ~ 5 ml of upper phase solution to prevent oxidation on top of the phenol: $CHCl_3$: isoamylalcohol (25:24:1 (v/v/v)) saturated with RNA buffer. 4. Store in 50 ml tube protected from light at 4°C.
6 M Glyoxal, deionized	50 µl	Mix 50 ml 6 M glyoxal with 5 g Dowex MR-3 mix bed ion exchanger for 1 h at RT. Remove ion exchanger by filtration and store 6 M glyoxal at −80°C in single use 0.5 ml aliquots.
200 mM NaH_2PO_4	500 ml	1. Dissolve 12.21 g NaH_2PO_4 in ~450 ml DEPC- H_2O, add DEPC- H_2O to 500 ml. 2. Add 0.5 ml DEPC and stir for 30 min at RT.

		3. Autoclave.
200 mM Na_2HPO_4	500 ml	1. Dissolve 14.21 g Na_2HPO_4 (35.83 g Na2HPO4·12 H_2O) in ~450 ml DEPC-H_2O, add DEPC- H_2O to 500 ml. 2. Add 0.5 ml DEPC and stir for 30 min at RT. 3. Autoclave.
100 mM $Na_xH_{3-x}PO_4$, (pH 7.0)	1 l	195 ml 200 mM NaH_2PO_4, 305 ml 200 mM Na_2HPO_4. Add DEPC- H_2O to 1. Add 1 ml DEPC, stir 30 min at RT and autoclave.
10 mM $Na_xH_{3-x}PO_4$, (pH 7.0)	1 l	100 ml 100 mM $Na_xH_{3-x}PO_4$, (pH 7.0). Add DEPC- H_2O to 1 l.
6 x RNA sample loading buffer	100 ml	1.To 63 g glycerol and 250 mg bromophenol blue add 10 ml 100 mM $Na_xH_{3-x}PO_4$ (pH 7.0) and DEPC- H_2O to ~ 90 ml. 2.Stir until bromophenol blue is dissolved. 3.Add DEPC- H_2O to 100 ml. 4. Add 100 µl DEPC and stir for 30 min at RT. 5.Autoclave.
RNA denaturation solution	38.44 µl (1 sample)	8.44 µl glyoxal 25 µl DMSO 5 µl 100 mM $Na_xH_{3-x}PO_4$, (pH 7.0)
2 x SSC + 0.1 % (w/v) SDS	500 ml	50 ml 20 x SCC 5 ml 10 % (w/v) SDS Add DEPC- H_2O to 500 ml.
0.2 x SSC + 0.1 % (w/v) SDS	500 ml	5 ml 20 x SCC 5 ml 10 % (w/v) SDS Add DEPC- H_2O to 500 ml.
20 x SSC + 20 % (w/v) dextran sulfate	100 ml	17.53 g NaCl 8.82 g Na_2-citrate

		20 g dextran sulfate, dissolve in ~ 80 ml DEPC- H_2O. Adjust to 100 ml with DEPC- H_2O. Add 100 µl DEPC and stir at RT for 30 min. Autoclave
20 x SSC	1 l	175.3 g NaCl 88.2 g Na_2-citrate dissolve in ~ 800 ml DEPC- H_2O. Adjust to 1 l with DEPC- H_2O. Add l ml DEPC and stir at RT for 30 min. Autoclave
2 x SSC	1 l	50 ml 20 x SSC Add DEPC- H_2O to 500 ml.
10 % (w/v) SDS	500 ml	1. Dissolve 50 g SDS in ~450 ml DEPC- H_2O. 2. Add H_2O to 500 ml. 3.Add 0.5 ml DEPC and stir 30 min at RT 4. Leave overnight in oven at 50-60°C 5. Do NOT autoclave.
100 x Denhardt's solution	500 ml	10 g Ficoll 400 10 g Polyvinylpyrrolidone 10 g BSA (fraction V) Dissolve in 400 ml DEPC- H_2O. Adjust to 500 ml with DEPC- H_2O and filter sterilize. Aliquot into 50 ml tubes and store at 4°C.
Pre-Hybridization buffer	20 ml	5 ml 20 x SSC, 2 ml 10% (w/v) SDS, 1 ml 100 x Denhardt's solution and prewarm to 42°C. Add 0.2 ml salmon sperm DNA (2 mg) to 1.8 ml DEPC- H_2O for final concentration of 1 mg / ml Denature DNA by boiling for 5 min, and chill on an ice-water bath. Add

		denatured salmon sperm DNA to the prewarmed mixture of 20 x SSC, SDS, Denhardt's solution and DEPC-H_2O. mix, add 10 ml formamide prewarmed to 42°C, and mix
Hybridization buffer	5 ml	1.25 ml 20 x SSC/1.25 ml dextran sulphate, 0.5 ml 10% (w/v) SDS, 250 µl 100 x Denhardt's solution and prewarm to 42°C. Add 50 µl 1 mg/ml salmon sperm DNA to 450 µl DEPC-H_2O in a 1.5 ml microcentrifuge tube. Denature DNA by boiling for 5 min, and chill on an ice-water bath. Add denatured salmon sperm DNA to the prewarmed mixture of 20 x SSC, SDS, Denhardt's solution and DEPC-H_2O. mix, add labelled DNA prob and salmon sperm mix, then add 2.5 ml formamide prewarmed to 42°C, and mix
4 M NH_4OAc	100 ml	1.Dissolve 54.43 g $NaOAc \cdot 3\ H_2O$ in DEPC-H_2O, then add DEPC-H_2O to 100 ml. 2. add 100 µl DEPC, stir for 30 min at RT, and autoclave

2.1.3.1 List of Enzymes

Table 2-6 List of Enzymes

Name	Product Number	Company
Alkaline Phosphatase, Calf Intestinal (CIAP) 1 U/µl	M1821	Promega
β-Galactosidase Enzyme Assay System with Reporter Lysis Buffer	E2000	Promega
Go*Taq* G2 flexi polymerase 5 U/µl	M7805	Promega
Go*Taq* flexi Polymerase 5 U/µl	M890A	Promega
Pfu DNA Polymerase 2-3 U/µl	M774A	Promega
T4 DNA Ligase	M1801	Promega
RNase A, 10-20 mg/ml, DNase-free	EN0531	Fermentas

2.1.3.2 Commercially Available Kits

Table 2-7 List of Kits

Name	Product Number	Company
Random primed labelling kit RediPrime II	RPN 1633	GE Healthcare
Buffer Used with Calf Intestinal Alkaline Phosphatase	M1833	Promega
DC™ Protein assay reagent A	500-0113	BIORAD
DC™ Protein assay reagent B	500-0114	BIORAD
Gel filtration on a Microspin S-200 HR column	27-5120-01	GE Healthcare
GeneRuler 1 kb DNA ladder	SM0311	Thermo Fisher Scientific
GeneRuler DNA ladder mix	SM0331	Thermo Fisher Scientific
Mini dialysis kit, up to 250 µl for 50 samples, 8 kDa cut-off	80-6484-13	GE Healthcare
PageRuler™ Prestained Protein Ladder, 10 to 180 kDa	26616	Thermo Fisher Scientific
PureYield™ Plasmid Miniprep System	A1223	Promega
Pierce ECL Plus Western Blotting Substrate	32132	Thermo Fisher Scientific

Pierce™ ECL 2 Western Blotting Substrate	11517371	Thermo Fisher Scientific
Wizard SV Gel and PCR Clean-Up System	A9282	Promega
QIAGEN Plasmid *Plus* Midi Kit (25)	12943	Qiagen
QuikChange II XL Site-Directed Mutagenesis	200521	Agilent

2.1.4 Yeast, Bacterial Strains and Plasmids

2.1.4.1 Yeast Strains

The yeast *Saccharomyces cerevisiae* was used as the model organism for the work in this thesis. All yeast strains were in the SK-1 genetic background (Kane and Roth, 1974). Specific strains were used with different genotypes which are outline in Table 7.
MSY 134-36 was the strain used for and for β-galactosidase, western blot, and northern blot experiments. PWY 260 was the strain used to generate template by PCR for producing probes complementary to sequence of interest.

Table 2-8 Yeast Strain

Strain	**Genotype**	**Source**
MSY 134-36	SK-1 MAT**a** *arg6 rme1Δ5::LEU2 ura3 leu2::hisG trp1::hisG lys2 ho::LYS2*	(Schröder et al., 2000, Schröder et al., 2004)
PWY 260	W303 MAT**a** *ire1Δ::TRP1 ade2-1 can1-100 his3-11, - 15::HIS3+ UPRE-lacZ leu2-3,-112::LEU2+UPRE-lacZ trp1-1 ura3-1*	(Papa et al., 2003)
MSY 742-03	SK-1 MAT**a** *arg6 rme1Δ5::LEU2 ura3 leu2::hisG trp1::hisG lys2 ho::LYS2 pho23Δ::kanMX2*	Martin Schröder Lab2
MSY 744-01	SK-1 MAT**a** *arg6 rme1Δ5::LEU2 ura3 leu2::hisG trp1::hisG lys2 ho::LYS2 cti6Δ::kanMX2*	Martin Schröder Lab2
MSY 740-01	SK-1 MAT**a** *arg6 rme1Δ5::LEU2 ura3 leu2::hisG trp1::hisG lys2 ho::LYS2 dep1Δ::kanMX2*	Martin Schröder Lab2
MSY 736-01	SK-1 MAT**a** *arg6 rme1Δ5::LEU2 ura3 leu2::hisG trp1::hisG lys2 ho::LYS2 sap30Δ::kanMX2*	Martin Schröder Lab2

MSY 738-01	SK-1 MAT**a** *arg6 rme1Δ5::LEU2 ura3 leu2::hisG trp1::hisG lys2 ho::LYS2 rxt2Δ::kanMX2*	Martin Schröder Lab2
MSY 756-01	SK-1 MAT**a** *arg6 rme1Δ5::LEU2 ura3 leu2::hisG trp1::hisG lys2 ho::LYS2 rxt3Δ::kanMX2*	Martin Schröder Lab2

2.1.4.2 Bacterial Strains

Escherichia coli was used for all cloning purposes. The different strains used are outlined in table 2.9.

Table 2-9 **Bacterial Strains**

Strain	Genotype	Source
XL2-blue MRF' Ultracompetent Cells	Δ(*mcr*A)183 Δ(*mcr*CB-*hsd*SMR-*mrr*)173 *end*A1 supE44 thi-1 recA1 *gyr*A96 relA1 *lac* [F' *pro*AB *lac*I^{q} Z ΔM15 Tn*10* (Tet^{r}) Amy Cam^{r}]	Agilent
XL-10 Gold Ultracompetent cells	Tet^{r} Δ(*mcr*A)183 Δ(*mcr*CB*hsd*SMR-*mrr*)173 *end*A1 *sup*E44 *thi*-1 *rec*A1 *gyr*A96 *rel*A1 *lac* Hte [F'*pro*AB *lac*I ^{q} Z ΔM15 Tn*10* (Tet^{r}) Amy Cam^{r}]	Agilent
DH5α	F^{-} φ80*lacZ*ΔM15 Δ(*lac*ZYA*arg*F)$_{U169}$ *rec*A1 *end*A1 *hsd*R17(r_k^-, m_k^+) *pho*A *sup*E44 *thi*-1 *gyr*A96 *rel*A1 λ	M. Schröder lab

2.1.4.3 Plasmids

Reporter plasmids contain a *CYC1* promoter, from which all known upstream activating sites were removed, drive the expression of the *lacZ* gene in pLGΔ312SΔSS and its derivatives (Bowdish and Mitchell, 1993). Also, expression of Hac1 and its derivatives (constructed for this study) are driven from their own promoters in pRS314-HA-*HAC1* plasmids. *HAC1* was tagged with a single HA-tag that was inserted into the *Spe*I site in the *HAC1* ORF (Chapman and Walter, 1997, Schröder et al., 2004). Table 2.10 displays the

plasmids used in this study. Plasmids were sustained in *E. coli* (DH5α or XL10-GOLD) strains with ampicillin as selection marker. *E. coli* cells were selected by antibiotic ampicillin. Plasmids in *S. cerevisiae* were selected by metabolic marker as indicated below.

Table 2-10 Plasmid List

Plasmid	Description	Source
pKB144	Reporter plasmids T_4C-*CYC1-lacZ URA3*- 2 µ	(Bowdish et al., 1995)
pKB148	Reporter plasmids URS1-*CYC1-lacZ URA3*- 2 µ	(Bowdish et al., 1995)
pKB150	Reporter plasmids URS1-URS1-*CYC1-lacZ URA3*- 2 µ	(Bowdish et al., 1995)
pKB160	Reporter plasmids T_4C-URS1-*CYC1-lacZ URA3* 2 µ	(Bowdish et al., 1995)
pLGΔ312SΔSS	Reporter plasmids *CYC1-lacZ URA3*- 2 µ	(Bowdish and Mitchell, 1993)
pRS314	Yeast, single copy (*CEN6 ARS4*) shuttle vector carrying the *TRP1* marker	(Sikorski and Hieter, 1989)
pRS314-HA-*HAC1^i*	HA-*HAC1^i TRP1-CEN*	(Schröder et al., 2004)
pRS314-HA-*HAC1^u*	HA-*HAC1^u TRP1-CEN*	This study
pRS316-g*HAC1*	*HAC1 URA3-CEN*	(Back et al., 2005)
pRS303	*HIS3* Marker	(Sikorski and Hieter, 1989)
Z691	UPRE-*lacZ* in pSEY102c (*CEN4 ARS1 URA3 amp^R*)	(Morl et al., 1993)
pRS303-Hac1^i	*HIS3* Marker	This study
pRS314-HA-Hac1^i (Δ *Bss*HII)	1138 bp removed from pRS314-HA-Hac1^i with *Bss*H2	This study
pRS314-HA-HAC1^i-N49L	HA-HAC1^i *TRP1 CEN*	This study
pRS314-HA-HAC1^i-L67P/L74P/V81P	HA-HAC1^i *TRP1 CEN*	This study

pRS314- HA-HAC1^{i}-S238A	HA-HAC1^{i} *TRP1 CEN*	This study
pRS246	Yeast, high copy plasmid (*REP3 FRT URA3)* 2 µ	(Christianson et al., 1992)
pRS246-HA-HAC1^{i}	HA-HAC1^{i} in pRS246, (*REP3 FRT URA3)* 2 µ	This study
p2UG	GRE3-*CYC1*-URA3-2µ	(Schena et al., 1991)
pG-N795	GPD-N795-TRP1-2µ	(Schena et al., 1991)
p2UG-HA-HAC1^{i}	GRE3-*CYC1*-HA-HAC1^{i} -URA3-2µ	(Schröder et al., 2004)

2.1.5 Primers

2.1.5.1 Oligodeoxynucleotides for plasmid cloning experiments

Table 2.11. List of primers and oligonucleotides. Oligonucleotides were synthesized by Eurogentec Ltd. Mutagenic base substitutions in oligodeoxynucleotides used for site-directed mutagenesis of targeted mutations are shown in bold. Silent restriction site and their mutagenic base substitutions are bold and underlined.

Table 2-11 Oligonucleotides for cloning

Name	Purpose	Sequence
H9333	Fusion PCR Hac1^{u}, F primer 1st ORF (a)	CTGCCTCCAAGGAAAAGAGCCAAG
H9334	Fusion PCR Hac1^{u}, R primer 1st ORF (b)	ATACCCTCTTGCGATTGTCTTCACTGTAGTTTCCTGGTC
H9335	Fusion PCR Hac1^{u}, F primer 3'UTR (c)	GACCAGGAAACTACAGTGAAGACAATCGCAAGAGGGTAT
H9336	Fusion PCR Hac1^{u}, R primer 3'UTR (d)	GATAGAAAAAAAGCAGAGCGTGGC

H9343	FP Hac1^{i} V81P+ EcoR1 silent restriction site	AAAATGTTCTCTTTTGGAAAATTTACTGAA**TTC**C**CC**CAACCTTGAAAAAC TGGCTGACCACGAAG
H9344	RCP Hac1^{i} V81P+ EcoR1 silent restriction site	**CTTCGTGGTCAGCCAGTTTTTCAAGGTTGGGGGAATTCAGTAAAT** **TTTCC** **AAAAGAGAACATTTT**
H9345	FP Hac1^{i} L74P+ Hpy8 I silent restriction site	**TACATCTGCAGTATCTCGAGAGAAAATGTAGTCTACCGGAAAATT** **TACTG** **AACAGCGTCAACCTTG**
H9346	RCP Hac1^{i} L74P+ Hpy8 I silent restriction site	CAAGGTTGACGCTGTTCAGTAAATTTTCC**GGT**AGA**CT**ACATTTTCTCTCG AGATACTGCAGATGTA
H9347	FP Hac1^{i} N49L+ EciI silent restriction site	GAAGGATCGAGCGTATTTTGAGA**CT**C**C**G**CC**GAGCTGCTCACCAGAGCAGA GAG
H9348	RCP Hac1^{i} N49L+ EciI silent restriction site	CTCTCTGCTCTGGTGAGCAGCTC**GG**C**G**G**AG**TCTCAAAATACGCTCGATCC TTC
H9396	FP Hac1^{i} L74P+ Hpy8 I silent restriction	TACATCTGCAGTATCTCGAGAGAAAATGT**AG**TCT**ACC**GGAAAATTTACTG AA**TTC**C**CC**CAACCTTG

	site+ V81P mutation	
H9397	RCP Hac1^{i} L74P+ Hpy8 I silent restriction site+ V81P mutation	CAAGGTTG**GG**G**GAA**TTCAGTAAATTTTCC**GGT**AGA**CT**ACATTTTCTCTCG AGATACTGCAGATGTA
H9451	FP Hac1^{i} L67P	AAGACTACATCTGCAGTATC**C**CGAGAGAAAATGTAGTCTAC
H9452	RP Hac1^{i} L67P	GTAGACTACATTTTCTCTCG**G**GATACTGCAGATGTAGTCTT
H9341	FP Hac1^{i} S238A	TTGAATGATTTCTTCATCACT**G**CATGAAGACAATCGCAAGAGG
H9342	RCP Hac1^{i} S238A	CCTCTTGCGATTGTCTTCATG**C**AGTGATGAAGAAATCATTCAA
59959 H04	Confirm mutations	CTCGACGTCGACGGTATCG
7793k	Confirm *HAC1^{u}* fusion	TTACTGAACAGCGTCAACC

2.1.5.2 Oligodeoxynucleotides to amplify DNA template for Northern blot experiments.

Primers were used to generate template from yeast strain PWY 260 by PCR for making templates complementary to sequence of interest used in RNA experiments are shown in Table 2.12.

Table 2-12 Oligodeoxynucleotides to amplify DNA template for target RNA

Name	Purpose	Sequence
H9523	Hop1 forward	CGTAAAACACTACACGGCATC
H9524	Hop1 reverse	TCCTGTAACCACGACTCGAC

H9525	Ime2 forward	CGCCGAGTTTTTTCGATTCC
H9526	Ime2 reverse	GCATCATCCCAAAATCCACC
H9527	Spo13 forward	ATAGAGCGCCCCTCATTTG
H9528	Spo13 reverse	CCACTAGACTCATAATCGGAAC
H9530	Hop1 forward	GTTGCGAATGTGGATTGGAAGT
H9531	Hop1 reverse	GGCTTTAGGGGAACTGGTGG
H9532	Ime2 forward	TATTTGGGCATTCGGGTGCG
H9533	Ime2 reverse	TTTCTGCGGGCAATTTTGTTGA
H9534	Spo13 forward	ATGCTCAACAGTACTCAAAGGCT
H9535	Spo13 reverse	CTCTTGGCCAACAAAATCTCCG
H9538	Ctl6 forward	ACGGCGGCGATTGGAAGTGTA
H9539	Ctl6 reverse	CTCGTGTTGCCGTCCTTGGCT
H9540	Dep1 forward	CGCTCCCAAGCTATCCAGCCT
H9541	Dep1 reverse	TGTAGTCACGGATCGCGGCA
H9542	Rxt3 forward	AAAGGTGTGCCTTCCAGTAGGGG
H9543	Rxt3 reverse	AGAAATTCGGCCTACGACCTGCC
H9544	Pho23 forward	GTTGGTGTGTGCTGGCGGAG
H9545	Pho23 reverse	CGACATAACTGACGTGCTGGAGGA
H9548	Sap30 forward	GGCTAGGCCAGTTAATACAAACGCT
H9549	Sap30 reverse	TTCTCACCACGTTGGCCAGGTC
H9550	Rxt2 forward	TGATAGGTCGTCATCGTCTTCTTCG
H9551	Rxt2 reverse	ATCTCAGCTGTTGCTTCTTGTTGA

2.1.6 Antibodies

The antibodies utilized to detect the various derivatives of Hac1 tagged with HA epitope. And immunoprecipitation of $Hac1^{i}$ protein tagged with HA when using the free antibodies approach method.

Table 2-13 Antibodies

Antibody	Clonality	Species	Dilution Factor	Supplies	Product Number
Anti-HA (α-HA)	Polyclonal	Rabbit	1000	Sigma Aldrich, Dorset	H6908
anti-rabbit IgG (H+L)- peroxidase HRP linked	Polyclonal	Goat	2000	Cell Signalling, London	7074S

2.2 Methods

2.2.1 Microbiology

2.2.1.1 Growth and Maintenance of *Saccharomyces cerevisiae*

S. cerevisiae were revived, grown, and maintained on, rich dextrose YP (1 % (w/v) Bacto-yeast extract, 2 % (w/v) Bacto-peptone) supplemented with 2 % (w/v) glucose (YPD), and 2 % (w/v) agar for solid media (Table 14 and 15). Plasmids in yeast were selected and maintained on synthetic media (0.675 % (w/v) yeast nitrogen base (without amino acids)) containing the required supplements and supplemented with 2 % (w/v) glucose, and 2 % (w/v) agar for solid selective media, also pre-culture were prepared in selective liquid media (SD, SD -Ura, SD -Trp, SD - Ura -Trp) (Table 14 and 15). To isolate cells and test for growth on non-fermentable carbon source, I used rich acetate media YP (1 % (w/v) Bacto-yeast extract, 2 % (w/v) Bacto-peptone) supplemented with 2 % (w/v) KOAc (YPAc). For plasmid selection I used synthetic acetate media (0.675 % (w/v) yeast nitrogen base (without amino acids)) containing the required supplements, (0.1 % (w/v) Bacto-yeast extract and supplemented with 1 % (w/v) KOAc, 1 % K-phthalate (adjusted with KOH pellets to pH 5.0) (PSP2, PSP2 -Ura, PSP2 -Trp, PSP2 -Ura -Trp). Nitrogen starvation media to sporulate cells was composed of 2 % (w/v) KOAc, 0.05 % (v/v) myo-inositol, containing the required amino acid supplements (C-SPO, C-SPO- Ura, C-SPO- Trp, C-SPO- Ura -Trp) (Table 14) (Sherman, 1991).
Glycerol stocks of *S. cerevisiae* transformed with plasmids from this study were prepared for long term, storage. Cultures were grown to late log-phase in YPD and glycerol was added to the culture to a final concentration of 1 Vol. of culture 1 Vol. of 30% (v/v) glycerol. Cultures were snap frozen in liquid nitrogen and stored at -80°C.

Table 2-14 Liquid media for *Saccharomyces cerevisiae*

Medium	Composition	Quantity	Recipe
SD medium	0.67% (w/v) yeast nitrogen base w/o amino acids	600 ml	4 g yeast nitrogen base w/o amino acids
	2% (w/v) D-glucose		12 g D-glucose
	30 mg/l L-Tyr		18 mg L-Tyr
	20 mg/l uracil[2]		5 ml 2.4 g/l uracil
	20 mg/l L-Arg·HCl		5 ml 2.4 g/l L-Arg·HCl
	20 mg/l L-His·HCl		5 ml 2.4 g/l L-His·HCl[1,2]
	20 mg/l L-Met		5 ml 2.4 g/l L-Met
	20 mg/l L-Trp[3]		5 ml 2.4 g/l L-Trp[1,2]
	30 mg/l L-Ile		5 ml 3.6 g/l L-Ile
	30 mg/l L-Lys·HCl		5 ml 3.6 g/l L-Lys·HCl
	150 mg/l L-Val		5 ml 18 g/l L-Val
	375 mg/l L-Ser		5 ml 45 g/l L-Ser
	20 mg/l adenine sulfate		10 ml 1.2 g/l adenine sulfate
	50 mg/l L-Phe		10 ml 3.0 g/l L-Phe
	100 mg/l L-Glu		10 ml 6.0 g/l L-Glu
	100 mg/l L-Leu		16.7 ml 3.6 g/l L-Leu
			Added H_2O to 580 ml, stirred until all solid had dissolved, dispensed into bottles and autoclaved. After the medium cooled down to ~ 55°C added:
	100 mg/l L-Asp		15 ml 4.0 g/l L-Asp[2]
	200 mg/l L-Thr		5 ml 24 g/l L-Thr[2]

Medium	Composition	Quantity	Recipe
PSP2 medium	0.67% (w/v) yeast nitrogen base w/o amino acids	600 ml	4 g yeast nitrogen base w/o amino acids
	0.10% (w/v) bacto-yeast extract		0.6 g bacto-yeast extract
	1% (w/v) KOAc		6 g KOAc
	30 mg/l L-Tyr		18 mg L-Tyr
	50 mM K-phthalate (pH 5.0)		Dissolve 6.13 g K-phthalate in ~ 400 ml H_2O, adjusted pH to 5.0 with KOH pellets
	20 mg/l uracil[2]		5 ml 2.4 g/l uracil
	20 mg/l L-Arg·HCl		5 ml 2.4 g/l L-Arg·HCl
	20 mg/l L-His·HCl		5 ml 2.4 g/l L-His·HCl[1]
	20 mg/l L-Met		5 ml 2.4 g/l L-Met
	20 mg/l L-Trp[3]		5 ml 2.4 g/l L-Trp[1]
	30 mg/l L-Ile		5 ml 3.6 g/l L-Ile
	30 mg/l L-Lys·HCl		5 ml 3.6 g/l L-Lys·HCl
	150 mgl/ L-Val		5 ml 18 g/l L-Val
	375 mg/l L-Ser		5 ml 45 g/l L-Ser
	20 mg/l adenine sulfate		10 ml 1.2 g/l adenine sulfate
	50 mg/l L-Phe		10 ml 3.0 g/l L-Phe
	100 mg/l L-Glu		10 ml 6.0 g/l L-Glu
	100 mg/l L-Leu		16.7 ml 3.6 g/l L-Leu Added H_2O to 580 ml, stirred until all solid had dissolved, dispensed into bottles and autoclaved. After the medium cooled down to ~ 55°C added:
	100 mg/l L-Asp		15 ml 4.0 g/l L-Asp
	200 mg/l L-Thr		5 ml 24 g/l L-Thr

Medium	Composition	Quantity	Recipe
C-SPO medium	2% (w/v) KOAc	600 ml	12 g KOAc
	30 mg/l L-Tyr		18 mg L-Tyr
	20 mg/l adenine sulfate		10 ml 1.2 g/l adenine sulfate
	20 mg/l uracil[2]		5 ml 2.4 g/l uracil
	20 mg/l L-His·HCl		5 ml 2.4 g/l L-His·HCl[1]
	20 mg/l L-Arg·HCl		5 ml 2.4 g/l L-Arg·HCl
	20 mg/l L-Met		5 ml 2.4 g/l L-Met
	40 mg/l L-Trp[3]		10 ml 2.4 g/l L-Trp[1]
	30 mg/l L-Lys·HCl		5 ml 3.6 g/l L-Lys·HCl
	100 mg/l L-Leu		10 ml 3.6 g/l L-Leu
	50 mg/l L-Phe		10 ml 3.0 g/l L-Phe
	5 mg/l myo-inositol		500 µl 10 g/l myo-inositol
			Added H_2O to 580 ml, stirred until all solid dissolved, dispensed into bottles and autoclaved. After the medium cooled down to ~55°C added:
	210 mg/l L-Thr		5.25 ml 24 g/l L-Thr

All stock solutions were sterilized by autoclaving except for L-Thr, L-Asp, L-His, and L-Trp. These named stock solutions were filter sterilized.

1) Stored stock solution at 4°C.

2) SD, SPS2, and C-SPO dropout medium were made excluding the concerned amino acid stock or in combination with (note 3)

3) SD, SPS2, and C-SPO dropout medium were made excluding the concerned amino acid stock or in combination with (note 2)

Table 2-15 Solidified media for *Saccharomyces cerevisiae*

Medium	Composition	Quantity	Recipe
SD agar	0.67% (w/v) yeast nitrogen base w/o amino acids	600 ml	4 g yeast nitrogen base w/o amino acids
	2% (w/v) D-glucose		12 g D-glucose
	2% (w/v) agar		12 g agar
	30 mg/l L-Tyr		18 mg L-Tyr
	20 mg/l uracil[2]		5 ml 2.4 g/l uracil
	20 mg/l L-Arg·HCl		5 ml 2.4 g/l L-Arg·HCl
	20 mg/l L-His·HCl		5 ml 2.4 g/l L-His·HCl[1,2]
	20 mg/l L-Met		5 ml 2.4 g/l L-Met
	20 mg/l L-Trp[3]		5 ml 2.4 g/l L-Trp[1,2]
	30 mg/l L-Ile		5 ml 3.6 g/l L-Ile
	30 mg/l L-Lys·HCl		5 ml 3.6 g/l L-Lys·HCl
	150 mg/l L-Val		5 ml 18 g/l L-Val
	375 mg/l L-Ser		5 ml 45 g/l L-Ser
	20 mg/l adenine sulfate		10 ml 1.2 g/l adenine sulfate
	50 mg/l L-Phe		10 ml 3.0 g/l L-Phe
	100 mg/l L-Glu		10 ml 6.0 g/l L-Glu
	100 mg/l L-Leu[3]		16.7 ml 3.6 g/l L-Leu
			Added 488 ml H_2O in a 1 l Erlenmeyer flask, stirred until the suspension is homogenous, and autoclaved. After the medium did cool down to ~55°C added:
	100 mg/l L-Asp		15 ml 4.0 g/l L-Asp[2]
	200 mg/l L-Thr		5 ml 24 g/l L-Thr[2]
			Poured ~25 ml into one 90 mm petri dish.

Medium	Composition	Quantity	Recipe
PSP2 agar	0.67% (w/v) yeast nitrogen base w/o amino acids	600 ml	4 g yeast nitrogen base w/o amino acids
	0.10% (w/v) bacto-yeast extract		0.6 g bacto-yeast extract
	1% (w/v) KOAc		6 g KOAc
	2% (w/v) agar		12 g agar
	30 mg/l L-Tyr		18 mg L-Tyr
	50 mM K-phthalate (pH 5.0)		Dissolve 6.13 g K-phthalate in ~ 400 ml H_2O, adjusted pH to 5.0 with KOH pellets
	20 mg/l uracil[2]		5 ml 2.4 g/l uracil
	20 mg/l L-Arg·HCl		5 ml 2.4 g/l L-Arg·HCl
	20 mg/l L-His·HCl		5 ml 2.4 g/l L-His·HCl[1]
	20 mg/l L-Met		5 ml 2.4 g/l L-Met
	20 mg/l L-Trp[3]		5 ml 2.4 g/l L-Trp[1]
	30 mg/l L-Ile		5 ml 3.6 g/l L-Ile
	30 mg/l L-Lys·HCl		5 ml 3.6 g/l L-Lys·HCl
	150 mgl/ L-Val		5 ml 18 g/l L-Val
	375 mg/l L-Ser		5 ml 45 g/l L-Ser
	20 mg/l adenine sulfate		10 ml 1.2 g/l adenine sulfate
	50 mg/l L-Phe		10 ml 3.0 g/l L-Phe
	100 mg/l L-Glu		10 ml 6.0 g/l L-Glu
	100 mg/l L-Leu		16.7 ml 3.6 g/l L-Leu
			Added H_2O to 488 ml, mix all components by stirring until the suspension is homogenous and autoclaved. After the medium cooled down to ~55°C added:
	100 mg/l L-Asp		15 ml 4.0 g/l L-Asp
	200 mg/l L-Thr		5 ml 24 g/l L-Thr
			Poured ~25 ml into one 90 mm petri dish.

2.2.1.2 *S. cerevisiae* Cell Culture, Sporulation

A pair of forceps was dipped in ethanol and passed briefly through Bunsen burner. A single isolated *S. cerevisiae* colony was picked up with tip of the toothpick using forceps from an appropriate agar plate and was aseptically inoculated to 14 ml sterile tube containing 2-4 ml appropriate medium. The tubes were then incubated in incubator shaker at 30ºC until saturation (generally 2-3 d) (preculture). These precultures A_{600} were measured, 100 µl cell suspension and 900 µl of medium used to grow the overnight cultures were added to semi-micro cuvette and mixed. This is 1:10 dilution of original grown culture. Using 1000 µl of medium as blank for spectrophotometer, the absorbance at A_{600} of 1:10 diluted culture was determined. Appropriate medium was added to sterile Erlenmeyer flasks at the appropriate volumes. The amount of inoculum to be added was calculated as the amount required to yield A_{600} ~ 0.02. From 14ml culture tubes with yeast culture, the calculated culture was added to flasks. The flasks were placed into a shaker incubator with shaking at 225 – 250 rpm at 30ºC overnight. The growth of the culture was monitored at regular intervals once visible growth was seen after 12- 24 h by removing 1000 µl and pipetting into a disposable semi-micro cuvette and determining the A_{600} of the sample. Cultures grown in YPD were monitored at intervals of 1.5-2 h and PSP2-dropout or SD-dropout grown cultures were monitored every 2-4 h. When the yeast culture achieved A_{600} of 0.3 – 0.8, this was considered as exponential growth phase.
Once within this range, a 10 ml (β-galactosidase reporter assay), 20 ml (Northern blot), 200 ml (Western blot) sample from each culture were taken for 0 h time point, spun at 3,500 rpm for 2 min at 4°C, the supernatant was discarded, and the pellet flash frozen in liquid nitrogen and stored at – 20°C. The remaining culture was spun at 3,500 rpm for 2 min at 4°C, the supernatant was discarded. The pellet was then washed with ice-cold sterile H_2O then spun at 3,500 rpm for 2 min at 4°C, the supernatant was discarded. The pellet was resuspended in 20 ml (β-galactosidase reporter assay), 40 ml (Northern blot), 200- 400 ml (Western blot) C-SPO-dropout (to induce cell sporulation) the flasks were placed into a shaker incubator with shaking at 225 – 250 rpm at 30ºC for 4-8 h (10 ml β-galactosidase reporter assay), 20 ml (Northern blot), 200 ml (Western blot) sample from each culture were taken for each 4 and 8 h time point). The collected samples were spun at 3,500 rpm for 2 min at 4°C, the supernatant was discarded, and the pellets were flash frozen in liquid nitrogen and stored at – 20°C.

2.2.1.3 Induction of Expression from Glucocorticoid Response Elements in *S. cerevisiae*

Yeast strains, MSY 134-36 containing p2UG or p2UG-HA-Hac1^{i} were grown overnight in 4 ml SD-Ura-Trp to saturation. The preculture was then used to inoculate 55 ml of PSP2-Ura-Trp at an A_{600} of 0.03 in sterile Erlenmeyer flask. The flasks were placed into a shaker incubator with shaking at 225 – 250 rpm at 30ºC overnight. When the yeast culture achieved A_{600} of 0.3 - 0.8, this was considered as exponential growth phase. The flask with the exponentially growing yeast culture was place on a bench, working close to the flame of a Bunsen burner 50 µM 21-Hydroxyprogesterone (Deoxycorticosterone) (DOC) was added to the cultures to induce expression. The flasks were returned into the shaker and the cultures were incubated at 30°C, 225-250 rpm for 1 h. Samples were collected as described

2.2.1.4 Growth and Maintenance of *Escherichia coli*

E. coli cells were grown in Luria-Bertani (LB) medium (1% (w/v) Bacto tryptone, 0.5% (w/v) Bacto yeast extract, 1% (w/v) NaCl, pH 7.5) which was supplemented with 100 µg/ml ampicillin. Solid media was supplemented with 2% (w/v) agar.
Glycerol stocks of *E. coli* transformed with plasmids from this study were prepared for long term, storage. Cultures were grown to late log-phase and glycerol was added to the culture to a final concentration of 1 Vol. of culture 1 Vol. of 30% (v/v) glycerol were added. Cultures were snap frozen in liquid nitrogen and stored at -80°C.

2.2.2 Molecular Biology

2.2.2.1 Plasmid Extraction from *E. coli*

Plasmids were extracted from *E. coli* using different commercially available kits, depending on the required concentration and purpose of the plasmid. Methodology for each kit is outlined below. Also, for plasmid diagnostic purposes I used plasmid DNA miniprep from *E. coli* (**2.2.2.2 and 2.2.2.3)**.

2.2.2.2 Plasmid DNA miniprep from *E. coli*

1.5 ml of a saturated overnight *E. coli* culture were transferred into a 1.5 ml microcentrifuge tube. The remaining culture was stored at 4°C. The cells were collected by centrifugation for 1 min at 14,000 x g, RT and the supernatant was aspirated. The tubes were centrifuged again for 1 min at 14,000 x g, RT and supernatant was aspirated. 100 µl 50 mM D-Glc, 25 mM Tris·HCl (pH 8.0), 10 mM EDTA were added, and the cells were

resuspended by vertexing or pipetting up and down. The tubes were incubated for 5 min at RT. Then added 200 µl 0.2 N NaOH, 1% (w/v) SDS and mixed by inverting tubes 4-6 times and incubated on ice for 5 min. 150 µl ice-cold 5 M KOAc (pH 4.8) were added and mixed by inverting tubes 4 - 6 times and incubated for 5 min on ice. This was followed by centrifugation for 3 min at 14,000 x g, 4°C and transferred the supernatant into a new 1.5 ml microcentrifuge tube. 0.8 ml ethanol were added and mixed by inverting the tubes 2-3 times. The tubes were then incubated at RT for 2 min or stored at - 20°C. The tubes were then centrifuged for 1 min at 14,000 x g, RT and the supernatant was discarded. 1 ml 70% ethanol, was added to the tubes and centrifuged for 1 min at 14,000 x g, RT. The supernatant was discarded by aspiration or inverting the tube and centrifuged again briefly to collect the remaining liquid at the bottom. The residual 70% ethanol was pipetted out and the pellets were dried in air for 5 min at RT. The pellets were resuspended in 30 µl 1 x TE (pH 8.0), 0.3 mg/ml RNase A and incubated at 4°C until pellets are dissolved (~ 0.5 - 1 h).

2.2.2.3 PureYield Plasmid Miniprep System

This system was also used to extract plasmid for diagnostic purposes in addition to extracting plasmids for use in this thesis. The protocol takes place at room temperature (RT).

E. coli cultures were grown overnight at 37 ˚C at ~ 230 rpm to saturation in 2 ml of LB broth containing 100 µg/ml ampicillin. 1 ml culture was transferred to 1.5 ml microcentrifuge tube and centrifuged at maximum speed 14,000 x g in a tabletop microcentrifuge for 1 min and remove supernatant. Add 200 µl of resuspension solution and mixed with the pellet by pipetting up and down. 100 µl of cell lysis buffer were added and mixed by resuspending the pellet in the lysis buffer. The solution should change to blue, indicating complete lysis. Do not exceed 2 min of lysing the cells as this might result in plasmid DNA denaturation. 350 µl of neutralization solution were then added and mix thoroughly by inverting the tube 6 times. A cloudy white precipitate formed then the tube was centrifuge at maximum speed for 10 min. A PureYield Minicolumn was placed into a PureYield Collection Tube and the supernatant was transfered into the PureYield Minicolumn, do not disturb the cell debris pellet. The setup was centrifuge at maximum speed for 1 min and the flowthrough was discarded, then the PureYield Minicolumn was placed back into the PureYield Collection Tube. 750 µl wash buffer with ethanol were added and centrifuged for 1 min and the flowthrough was discarded, then the PureYield Minicolumn was placed back into the PureYield Collection Tube. 500 µl of wash buffer

with ethanol was added and centrifuged for 5 min at maximum speed. Then re-centrifuged for 1 min to remove excess wash buffer. Transfered the PureYield Minicolumn into a clean 1.5 ml microcentrifuge tube, then 30 µl of elution buffer was directly added to the minicolumn matrix. Left to stand for 1 to 2 min at RT. Finally centrifuged at maximum speed in a microcentrifuge for 1 min to elute the plasmid DNA. Samples were then stored at - 20°C.

2.2.2.4 QIAGEN Plasmid *Plus* Midi Kit (25)

E. coli pre-cultures were grown to saturation overnight in 2 ml of LB broth supplemented with 100 µg/ml of ampicillin at 37 ˚C, ~ 230 rpm. 200 ml of LB broth were prepared with 100 µg/ml of ampicillin and inoculated with 1 ml of precultures and allowed to grow overnight to an A_{600} of between 1.5 - 2.0. Cells were then spun at 4,750 x g for 15 min at 4°C. The bacterial pellet was resuspended in 4 ml of buffer P1 containing the RNase A (cold buffer), for complete resuspension the resuspended pellet was pipetted up and down until no cell clumps remained and then transferred in to a 50 ml centrifuge tube (polypropylene). 4 ml of buffer P2 were added and vigorously mixed by inverting the sealed tube 4-6 times, and incubated at RT for 3 min. Then 4 ml buffer S3 were added and mixed immediately and thoroughly by inverting 4-6 times, also a fluffy white material was formed. Next, the tubes were centrifuged at ≥ 20,000 x g for 15 min at 4°C. Afterwards the supernatant containing plasmid DNA was transferred promptly into a clean 50 ml centrifuge tube (polypropylene) and centrifuged at ≥ 20,000 x g for 5 min at 4°C again to remove any suspended material and avoid clogging the QIAfilter cartridge. The lysate was then transferred into the QIAfilter cartridge and left to incubate for 10 min. During incubation, the vacuum manifold and the QIAGEN Plasmid *Plus* Midi spin columns were prepared. Then the plunger was gently inserted into the QIAfilter cartridge to filter the cell lysate into a new tube. Next, 2 ml buffer BB were added to the clear lysate and mixed by inverting the tube 4-6 times. The lysate was then transferred to the QIAGEN Plasmid *Plus* Midi spin column with a tube extender attached on the QIAvac 24 plus. The vacuum source was switched on to draw the solution through the QIAGEN Plasmid Plus Midi spin column. After the liquid was drawn through the column, the vacuum source was switched off. To wash the plasmid DNA, 7 ml buffer ETR were added to the QIAGEN Plasmid *Plus* Midi spin column and drawn out with the vacuum like before. Another wash with 7 ml PE buffer with 70 % (v/v) ethanol was done the same way as the wash before. The QIAGEN Plasmid Plus Midi spin column was transferred into a clean 1.5 ml microcentrifuge tube. Finally, to elute the plasmid DNA, 200 µl of Buffer EB (10 mM Tris·Cl, pH 8.5) were

added to the centre of the QIAGEN Plasmid *Plus* Midi spin column, and left to stand for at least 1 min, and then centrifuged for 1 min. Samples were then quantified and stored at -20°C.

2.2.3 Plasmid DNA, and RNA Quantification

The most common technique to determine DNA and RNA yield and purity is measurement of absorbance. Absorbance readings are performed at 260 nm (A_{260}) where DNA absorbs light most strongly, and the number generated allows for estimation of the concentration of the solution. To ensure the numbers are useful, the A_{260} reading should be within the instrument's linear range (generally 0.1–1.0). DNA concentration is estimated by measuring the absorbance at 260 nm, adjusting the A_{260} measurement for turbidity (measured by absorbance at 320 nm), multiplying by the dilution factor, and using the relationship that an A_{260} of 1.0 = 50 µg/ml pure dsDNA.

Concentration (µg/ml) = (A_{260} reading – A_{320} reading) × dilution factor × 50µg/ml

Total yield is obtained by multiplying the DNA concentration by the final total purified sample volume.

DNA yield (µg) = DNA concentration × total sample volume (ml)

However, DNA is not the only molecule that can absorb UV light at 260nm. Since RNA also has a great absorbance at 260nm, and the aromatic amino acids present in protein absorb at 280nm, both contaminants, if present in the DNA solution, will contribute to the total measurement at 260nm. To evaluate DNA purity, measure absorbance from 230nm to 320nm to detect other possible contaminants. The most common purity calculation is the ratio of the absorbance at 260nm divided by the reading at 280nm. Good-quality DNA will have an A_{260}/A_{280} ratio of 1.8-2.0. A reading of 1.6 does not render the DNA unsuitable for any application, but lower ratios indicate more contaminants are present. The ratio can be calculated after correcting for turbidity (absorbance at 320nm).

DNA purity (A_{260}/A_{280}) = (A_{260} reading – A_{320} reading) ÷ (A_{280} reading – A_{320} reading)

To quantify the concentration of plasmid DNA and RNA from extractions, two absorbance methods were used.

2.2.3.1 Molecular Devices SpectraMAX 190 Plate Reader

Plasmid DNA was diluted 1:10 using sterile H_2O to a total volume of 100 µl. A 100 µl blank (H_2O) and the samples were loaded onto a Greiner 96 well UV transparent plate

(Sigma-Aldrich, # M3812-40EA) and read on the Molecular Devices SpectraMAX 190 plate reader (Molecular Devices, Sunnyvale, USA, model no. 190) at 260, 280 and 320 nm. I also used this method to quantify RNA samples.

2.2.3.2 NanoDrop 1000 UV

1 µl of plasmid DNA was placed onto the fiber optic cable of the NanoDrop 1000 UV Visible Spectrophotometer and measured with high accuracy by the spectrophotometer at the spectrum 260, 280 and 320 nm. Before measuring the required sample, the fiber optic cable is whipped gently and 1µl of H_2O is measured to create a blank, which the samples are then measured against.

2.2.4 *In vitro* DNA Manipulation

2.2.4.1 Overlap Extension PCR

Overlap extension PCR was performed to delete a fragment from the plasmid DNA pRS316-gHAC1, also used as the template in the PCR reaction. Here I used the *GoTaq* Flexi DNA Polymerase protocol (Promega).

The first step of PCR (two separate PCR reaction) was to generate two flanking fragments from the HAC1 gene, the open reading frame (ORF) and the 3′ untranslated region (3′-UTR). The pair of primers indicated in (Table 2.11) were used. The resulting PCR product ORF and 3′-UTR contain a "tail" of nt that are derived from the fragment that will be recombined. Both PCR reactions were carried out with 10 ng of template DNA, 1 µM of both forward and reverse primers, 20 µl of 5 x colourless Go*Taq* Flexi buffer, 200 µM of dNTP mix, 8 µl 25 mM $MgCl_2$, 2.5 U Go*Taq* Flexi DNA Polymerase and bring final volume with sterile H_2O to 100 µl in a PCR tube.

For amplification by PCR, the following PCR setup was used. Denaturation at 95°C for 2 min.

Table 2-16 PCR (Overlap extension)

Segment	Cycle	Temperature	Time
Initial Denaturation	1	95°C	2 min
Denaturation	30	95°C	30 sec
Annealing		70-74°C	30 sec
Extension		74°C	1 min / 30 sec
Final Extension	1	72°C	5 min
Refrigeration	Hold	4°C	∞

The resulting two PCR fragments were cleaned up using Wizard SV Gel and PCR Clean-Up System. Following the clean-up, the two PCR products were treated with *Hind* III restriction enzyme at 37°C for 1 h to digest the template plasmid at the desired deletion region. The resulting products were then cleaned-up again and used as template for the second step of PCR.

The second step of the overlap extension PCR also known as the fusion step, was done to recombine or ligate the previously two PCR products prepared from the first step. In this fusion PCR reaction, because of the terminal complementarity, the two PCR products from step one form an extended PCR product. Which then during the overlap extension, the recombined product is amplified with the two outermost primers. For this PCR reaction 40 – 80 ng PCR fragment (ORF) and 50 – 100 ng PCR fragment (3′-UTR), 1 µM of both forward and reverse primers, 20 µl of 5 x colourless Go*Taq* Flexi buffer, 200 µM of dNTP mix, 8 µl 25 mM $MgCl_2$, 2.5 U Go*Taq* Flexi DNA Polymerase and bring final volume with sterile H_2O to 100 µl in a PCR tube. Then to amplify by PCR the exact setup as the first two PCR was used (Table 2.16), but the extension time was changed to 1 min and 35 sec. The final fusion PCR product was then tested on an agarose gel to confirm successful amplification reaction. Now the amplified fragment is ready to be digested and subcloned into the desired plasmid.

2.2.4.2 Site Directed Mutagenesis

Site directed mutagenesis was performed using the PCR based QuikChange II XL Site-Directed Mutagenesis protocol (Agilent). Primers (Table 2.11) were designed to mutate either a single or several point mutations in the plasmid DNA template (pRS303-HA-HAC1[i], constructions described in Results). The reaction was carried out with 45 ng of template DNA, 125 ng of both forward and reverse mutagenic primers, 5 µl of 10 x reaction buffer, 200 µM of dNTP mix, 3 µl of QuikSolution, 1 µl of *pfuUltra* HF DNA polymerase (2.5 U/µl) and adjusted with sterile H_2O to a final volume of 50 µl in a PCR reaction tube.

Each PCR reaction used the cycling parameters outlined in Table 2.17.

Table 2-17 Cycling parameters for the QuikChange II XL method

Segment	Cycle	Temperature	Time
Initial Denaturation	1	95°C	1 min
Denaturation	18	95°C	50 sec
Annealing		55°C	50 sec
Extension		68°C	4 min and 40 sec
Final Extension	1	72°C	7 min
Refrigeration	Hold	4°C	∞

Following the PCR reaction, 12 µl of each sample was tested on an agarose gel to confirm successful amplification reaction before treating the PCR sample with 10 U *Dpn* I restriction enzyme at 37°C for 1 h. This is done to digest the methylated, non-mutated, parental DNA. Now the PCR product is ready to be transformed into *E. coli* by electroporation.

2.2.4.3 Restriction Endonuclease Digestion of Plasmid DNA

Plasmid DNA was digested using commercially available enzymes with the buffers supplied. Digests were performed in 10-20 µl volumes containing 1-10 µg of plasmid DNA and 10 U of enzyme. Digests were incubated at the recommended temperature for 2 to 16 hours.

2.2.4.4 Dephosphorylation of DNA 5′ termini with Calf Intestinal Alkaline Phosphatase (CIAP)

After the restriction digest (pRS314-HA-HAC1[i]) to subclone digested fusion PCR fragment from the overlap extension PCR (2.2.4.1), the digested plasmid DNA sample ends were calculated (in picomoles). For immediate use, sufficient CIAP was diluted in 1 x CIAP reaction buffer to a final concentration of 0.01 U/µl. Each picomole of DNA ends will require 0.01 U CIAP. In a 1.5 microcentrifuge tube the following combination was added, 3.87 pmol ends (10 µg), 4 µl 0.01 U CIAP, 5 µl 10 x CIAP reaction buffer then adjusted to a final volume of 50 µl using H_2O. The sample was mixed by flipping then centrifuged briefly to collect all the liquid to the bottom of the tube. The sample was then incubated at 37°C for 30 min. Following this step 4 µl 0.01 U CIAP was added to the sample and incubated at 37°C for another 30 min. To stop the reaction 300 µl of stop buffer was added. DNA was isolated using phenol/$CHCl_3$ extraction.

2.2.4.5 Phenol/$CHCl_3$ Extraction of DNA

All steps were performed in the hood. 1 Vol. of phenol/chloroform/isoamylalcohol (25/24/1 v/v/v), saturated with 1 M Tris·HCl (pH 8.0) was added to the sample. After vigorous mixing of the aqueous and phenolic phase, the sample was spun at 12,000 x g, RT for 1 min to separate both phases. The upper aqueous layer was then transferred to a clean 1.5 ml microcentrifuge tube. The sample was then extracted again with phenol /chloroform/isoamylalcohol (25/24/1 v/v/v), saturated with 1 M Tris·HCl (pH 8.0) then mixed, spun, and moved to a new 1.5 ml microcentrifuge tube. The two phenolic phases were then pooled together in a 1.5 ml microcentrifuge tube and extracted with ¼ Vol. 1 x TE buffer (pH 8.0). After a vigorous mixing of the aqueous and phenolic phase, the sample was spun at 12,000 x g, RT for 1 min to separate both phases. The upper aqueous layer was then transferred into a clean 1.5 ml microcentrifuge tube. Again, TE buffer was added to the pooled phenolic phase and treated as before, the resulting aqueous phases were pooled together. 1 Vol. $CHCl_3$/isoamylalcohol (24/1 v/v) was then added to the pooled aqueous phase and repeat it at least once. Note: One $CHCl_3$/isoamylalcohol (24/1 v/v) extraction is not sufficient to remove all traces of phenol. Four extractions are, but the minimal number of extractions requires to complete remove the phenol, is somewhere between two and four. The tube was vortexed briefly to mix the aqueous and organic phase, then centrifuged at 12,000 x g, RT for 1 min to separate both phases. Finally, the upper aqueous phase was transferred to a new 1.5 ml microcentrifuge tube and prepared for ligation.

2.2.4.6 Agarose Gel Electrophoresis of DNA

To analyse, diagnose, and separate plasmid DNA or fragments, a 1 % (w/v) gel was cast by dissolving the desired amount of electrophoresis-grade agarose powder into the appropriate volume of 1 x TAE buffer in an Erlenmeyer flask using a microwave. The agarose was melted in a microwave oven at the highest power setting for 1 – 5 min, swirling every ~30 to 60 s to ensure even mixing and to avoid boiling over of the agarose solution. The flask was allowed to cool down to ~ 55 ˚C at RT, then 0.5 µg/ml of ethidium bromide was added the contents were mixed by swirling. The melted agarose was poured into the casting platform and the gel comb was inserted making sure that no bubbles are trapped underneath the combs and all bubbles on the surface of the agarose are removed before the gel sets. After the gel had solidified the casting platform was removed to open the sealed ends and the gel comb was removed taking care not to tear the sample wells. The gel was

placed into a tank filled with 1 x TAE buffer with 0.5 µg/ml ethidium bromide, enough to cover the gel.

The DNA samples were prepared in a 1.5 ml microcentrifuge tube, x µl DNA sample, 1 x DNA sample loading buffer, and the sample was brought to a desired final volume with H_2O. Samples are loaded into the lanes with the first lane containing 5 µl of Gene Ruler DNA ladder 1 kb. The gel tank was assembled so that DNA will migrate toward the anode. The voltage was then set depending on the size of the gel and time required to run the gel, typically 1 to 5 V/cm of gel, to begin electrophoresis. Once the blue dye has migrated far enough in the gel, the power supply was turned off and the gel was exposed to a UV light source ($\lambda = 254$ nm) to visualise the DNA and a picture was taken, or plasmid DNA fragments were excised.

2.2.4.7 DNA Gel Extraction, Gel and PCR Clean-Up

Digested plasmid DNA was run on an agarose gel to separate the fragments based on size. Then using a UV transilluminator, the UV light ($\lambda = 312$ nm) was used to visualise and cut out the desired fragments, the UV source was switched off during DNA fragment excising to avoid damaging the DNA, using a clean scalpel. Fragment were then put into clean 1.5 ml microcentrifuge tube.

After weighing an empty 1.5 ml microcentrifuge tube, each gel fragment in the tubes were weighed. The weight of the empty 1.5 ml microcentrifuge tube was subtracted from the total weight (gel fragment + 1.5 ml tube) to obtain the weight of the gel slices.

For gel and PCR clean-up I used Wizard SV Gel and PCR Clean-Up System kit. Membrane binding solution was added to the gels at a ratio of 10 µl of solution per 10 mg of agarose gel slice. The Mixture was then vortexed, and the tubes were incubated in a water bath at 65°C for 10 min or until the gel is completely melted. It is important to note that the maximum capacity of the column is 350 mg of agarose for one pass through the column. Up to 3.5 g of agarose can be passed through a column.

To purify DNA from the dissolved gel or PCR product the following protocol was followed using a kit (Wizard SV Gel and PCR Clean-Up System). An SV Minicolumn was placed in a Collection Tube for each dissolved gel or PCR product, then the dissolved gel mixture or prepared PCR product was transferred to the SV Minicolumn assembly and incubated for 1 min at RT. The SV Minicolumn assembly was centrifuged in a microcentrifuge at 16,000 × g for 1 min. The SV Minicolumn was removed from the Spin Column assembly, and the liquid in the Collection Tube was discarded. Then the SV Minicolumn was returned to the Collection Tube. The assembly was then centrifuge for 1

min at 16,000 x g after adding 700 µl of wash solution diluted with 95 % ethanol (EtOH). Then 500 µl wash solution was added to the assembly and centrifuged for 5 min at 16,000 x g, in both wash steps the flowthrough solution is emptied out. Then a final 1 min centrifugation of the SV Minicolumn assembly was done to remove any residual EtOH. The SV Minicolumn was then carefully removed and added to a clean 1.5 ml microcentrifuge tube. 30 - 50 µl of Nuclease-Free Water was applied directly to the centre of the column without touching the membrane with the pipette tip. After a 1 min incubation at RT the tube with the column was centrifuged for 1 min at 16,000 x g to collect the sample DNA fragments or PCR product in the 1.5 ml microcentrifuge tube, the SV Minicolumn was removed, the sample was then prepared for further experiments. The clean-up method was also used to clean up enzyme digested DNA plasmids.

2.2.4.8 Ligations of DNA fragments

DNA ligations were performed with an insert to vector ratio ranging from 1:3 to 1:7, vector was routinely added at 100 ng. Reactions were performed in 10 µl volumes and each reaction contained X ng DNA fragments, 1 U of T4 DNA ligase, and 1 µl of 10 x ligation buffer supplied with the enzyme (Promega). The reactions were incubated at 15°C overnight. The samples were then used to transform *E. coli* by chemical transformation.

2.2.4.9 DNA sequencing

Sequencing DNA plasmid samples were prepared at 100 ng/µl in 5µl and sequencing specific primers at 3.2 µM/µl. Plasmids were then sequenced by DBS Genomics (Durham University, Durham, UK). Sequences were then aligned using BioEdit (Ibis Biosciences, Carlsbad, California).

2.2.5 Chemical Transformation of *E. coli*

Competent *E.coli* cells, (L2-blue MRF' Ultracompetent Cells, XL10-Gold Ultracompetent cells, or DH5α), were thawed-out gently on ice, and 45 - 50 µl were aliquoted into a chilled 14 ml BD falcon polypropylene round-bottom tube. 2 µl of β-mercaptoethanol provided with the kit were added to each aliquot of cells but not when transforming DH5α. Aliquots with β-mercaptoethanol were swirled gently for 10 min, placing back on ice every 2 min. 2-3 µl solution containing the plasmid of interest or ligation reaction product were added to the competent cells. Cells were incubated on ice for 30 min. Cells were then heat-shocked for 42 s at 42°C in a water bath. Once the tubes were pulled-out of the water bath they were placed on ice for 2 min. 0.9 - 1 ml of either preheated S.O.C, NZY^{+}, or LB

medium was added to the tube containing L2-blue MRF' Ultracompetent Cells, XL10-Gold Ultracompetent cells, or DH5α, respectively. The cultures were then incubated for 1 h at 37°C with shaking at ~ 250 rpm. After incubation, 200 µl of cell suspension was plated onto one LB agar plate containing 100 µg/ml ampicillin. Cells were harvested from the remaining ~ 700 µl by centrifugation at 12,000 x g at RT for 30 s in a benchtop microcentrifuge, and the supernatant was aspirated. The cell pellet was then resuspended in ~ 100 µl appropriate medium and plated onto one LB agar plate containing 100 µg/ml ampicillin. Plates were incubated in a 37ºC incubator for 16 h. 5 µl 1 x TE (pH 8.0) was used as a negative control to determine if contamination of materials gives rise to undesired colonies during the chemical transformation.
Note: S.O.C Medium composition: 2 % (w/v) tryptone, 0.5 % (w/v) yeast extract, 10 mM NaCl, 2.5 mM KCl, 10 mM $MgCl_2$, 10 mM $MgSO_4$, and 20 mM glucose.
NZY^+ Medium composition: 1 % (w/v) NZ amine (casein hydrolysate), 0.5 % (w/v) yeast extract, 0.5 % (w/v) NaCl.

2.2.6 Transformation of *Saccharomyces cerevisiae*

Here the lithium acetate/single-stranded carrier DNA/PEG method (Gietz and Schiestl, 2007) was used. The cells were grown by inoculating 2 ml YPD broth with a single colony and incubated until saturation (A_{600} > 3.0). This was the preculture. For each transformation 5 ml YPD broth was inoculated (e.g., for 10 transformations 55 ml of media would be inoculated) with an A_{600} = 0.001 using the preculture and incubated at 30°C with shaking at 250 rpm. The absorbance was measured the next day to observe an A_{600} of ~ 0.8-1.0 has been reached. The culture was transferred to a sterile 50 ml tube and spun at 3,500 rpm for 2 min at 4°C after which the supernatant was discarded, and the cell pellet was placed on ice. The pellet was resuspended in 8 ml of one-step buffer (1 part 0.2 M LiOAc and 4 parts 40% (w/v) PEG 4000). The cell suspension was centrifuged again at 3,500 rpm for 2 min at 4°C, after which again the supernatant was discarded, and the pellet was placed back on ice and left for 1 - 2 min to allow for the remaining one-step buffer to collect at the bottom of the tube and be removed. 88 µl of one-step buffer were added for each transformation required and an additional 88 µl to ensure sufficient cell suspension was available. The pellet was resuspended by vortexing until no clumps remained. 88 µl of suspension were added to a sterile 1.5 ml tube containing 10 µl 10 mg/ml of sheared salmon sperm DNA (Clontech/Takara # 630440) (pre-boiled for 5 min in a heat block then put on ice), and 1 µg (for single plasmid transformation) or 200 ng and 1µg (for 2 plasmids transformation). The tube was then vortexed at maximum speed for 15 s. The tube was

incubated at 42°C in a water bath for 30 min, then placed on ice before being briefly spun at max speed (~ 13,000 x g for 10 s at RT) to collect the pellet and the supernatant was aspirated. The cell pellet was resuspended in 200 µl of sterile H_2O and the full suspension was spread on a SD agar plate with an appropriate amino acid dropout (dictated by the marker used in the plasmid). The plate was incubated at 30°C for ~ 5-7 days to allow for single colonies to grow.

2.2.6.1 Replica Plating and Acetate Testing

To ensure that cells could grow on media containing only non-fermentable carbon source, and avoiding cells containing a mutation preventing their growth, known as petite cells, replica plating from the SD-dropout plates to synthetic acetate plates (PSP2- dropout) was utilised. This was achieved by placing the SD-dropout plate onto a sterile piece of velvet and applying gentle pressure. A PSP2-dropout plate was then placed onto the velvet and again gentle pressure was applied allowing for the transferring of colonies. The PSP2-dropout plate was then incubated at 30°C for 2 d to allow for single colonies to grow. These colonies were then matched to the SD-dropout plates to confirm which cells were not petites. It was these non-petite cells that were streaked onto a fresh SD-dropout plate and incubated again at 30 ˚C for 3-5 days to allow for single colonies to grow for use in future experiments. The chosen colonies able to grow on non-fermentable carbon source were prepared for cryo-storage and stored at - 80 ˚C.

2.2.7 Protein Biochemistry

2.2.7.1 Protein Extraction for β-Galactosidase Assays

The frozen yeast culture samples were thawed on ice. Once fully thawed, the pellet was resuspended in 1 ml ice-cold sterile H_2O. The cell suspension was transferred into a 1.5 ml microcentrifuge tube and centrifuged at 12,000 x g for 1 min at RT and the supernatant was aspirated. 100 µl of ice-cold 1 x Reporter Lysis Buffer (RLB) were added to each cell pellet sample and resuspended by pipetting up and down. All of the suspension was then transferred to a 2 ml flat-bottom screw cap tub (previously prepared with ~ 150 mg acid-washed glass beads). The tubes were homogenised in the Precellys 24 instrument (Bertin Technologies, Montigny-le-Bretonneux, France) at 6,500 rpm for 3 cycles of 10 s, a 5 min break was taken between each cycle during which time the samples were placed on ice. Following homogenisation 100 µl of ice-cold 1 x RLB buffer were added to each sample and each tube was briefly vortexed. Samples were centrifuged at 12,000 x g for 2 min at

4°C to separate the supernatant which contained the protein from the cell debris. The supernatant was transferred into a clean 1.5 ml microcentrifuge tube. Protein lysate samples were flash frozen in liquid nitrogen and stored at - 80°C. All tube were labelled appropriately in advance.

2.2.7.2 DC Protein Assay

To quantify the total amount of protein in the lysate a DC assay (Bio-Rad, Hemel Hempstead, UK, cat. no. #500-0113 and #500-0114) was run. A BSA protein standard was prepared in H_2O or RLB (Protein extraction with RLB) with concentrations of 62.5, 125, 250, 500, 1000 and 2000 µg/ml, and 5 µl was added to a U-bottomed well (two replica well per standard). A 1:10 dilution (diluted in H_2O or 1 x RLB) of lysate was prepared of which 5 µl was added per well (in duplicate/triplicate). 25 µl reagent A and 200 µl reagent B were added into each well. The plate was placed at RT on an orbital shaker at 50 rpm for 15 min after which the absorbance was read at 750 nm using the Spectramax 190 plate reader.

2.2.7.3 β-galactosidase Assay

For this assay the method described in (Miller, 1972, Schenborn and Goiffon, 1993) was used. To test the levels of β-galactosidase activity and therefore the expression of reporter genes the b-galactosidase reporter assay kit (Promega) was used. 1 µl of 1 U/µl of β-galactosidase was added to 99 µl of ice cold 1 x RLB (Table 2.4), mixed and placed on ice to create the 1:100 dilution. 10 µl of this 1:100 dilution was added to 990 µl of ice-cold 1 x RLB (Table 2.4) to make a 1:10000 dilution. A standard range was created of 0, 0.5, 1.0, 1.5, 2.0 mU/50µl of β-galactosidase. Standards were diluted in RLB. The appropriate volume of RLB was added to each well, followed by the required volume of sample to a total volume of 50 µl. 50 µl of 2 x assay buffer (200 mM $Na_xH_{3-x}PO_4$ (pH 7.3), 2 mM $MgCl_2$, 100 mM b-mercaptoethanol, 1.33 mg/ml 12-nitrophenyl-β-D-galactopyranoside) (Table 2.2) were added to each well and the plate covered with parafilm and incubated at 37°C for 30 min. Following incubation, 150 µl of 1 M Na_2CO_3 were added to each well to stop the reaction. The plate was then read on the Spectramax 190 plate reader at 419 nm.

2.2.7.4 Extraction of Whole Yeast Cell Protein Extract for Western Blots

Once the pellets were thawed, they were resuspended with cold sterile H_2O and transferred to a 1.5 ml microcentrifuge tube. After spinning down at 12,000 x g for 1 min at 4°C and

removing the supernatant from the sample, the pellet was resuspended in 2 Vol. of the appropriate lysis buffer (mentioned in RESULTS). All of the suspension was then transferred to a 2 ml flat-bottom screw cap tub (previously prepared with ~ 200-400 mg acid-washed glass beads). The tubes were homogenised in the Precellys 24 instrument at 6,500 rpm for 4-6 cycles of 10 s, a 5 min break was taken between each cycle during which time the samples were placed on ice. Samples were centrifuged at 12,000 x g for 2 min at 4°C to separate the supernatant which contained the protein. This supernatant was removed and placed in a clean 1.5 ml microcentrifuge tube. Protein lysate samples were ready for western blot.

2.2.7.5 Bicinchoninic Acid (BCA) protein assay

To quantify how much protein was extracted from samples lysed with urea-based lysis buffers, a bicinichonic acid (BCA) assay was used (Smith et al., 1985). Protein lysates were diluted 1:10 with 0.1 M 2-iodacetamide in 0.1 M Tris-HCl (pH 8.0) and incubated in a 37°C water bath for 15 min, this is to destroy the β-mercaptoethanol present in the lysate. 10 µl of BSA standards (0, 62.5, 125, 250, 500, 1000 and 2000 µg/ml), blank, and sample were added to the bottom of a U-bottom 96 well plate. 200 µl of working solution (Table 2.2) were added to each well, the plate was covered and incubated at 60°C for 30 min. Absorbance was then be read at 562 nm using the Molecular Devices SpectraMAX 190 (Molecular Devices LLC, Sunnyvale, California). These values allowed for the required dilutions for equal loading on the SDS-PAGE gel to be calculated.

2.2.7.6 $(NH_4)_2SO_4$ Precipitation

The lysate sample was centrifuged at 10,000 x g for 10 min at 4°C. The supernatant was transferred into a 0.7 ml polycarbonate centrifuge tube (depending on the experiment, the supernatant might contain 10 % 4 M $(NH_4)_2SO_4$). Into the supernatant, saturated 4 M $(NH_4)_2SO_4$ was added to a final concentration of 2.6 M and centrifuged at 100,000 x g for 1 h, at 4°C. The precipitated proteins were used as whole cell extracts (0 % - 70 % or 10 % - 70 % $(NH_4)_2SO_4$ fraction). In specific experiments, the proteins in this extract were further fractionated by differential additions of saturated 4 M $(NH_4)_2SO_4$ (1, 1.5, and 2 M). The proteins precipitated were collected separately by centrifugation at 100,000 x g for 1 h, at 4°C. The precipitates were dissolved in 200 µl of dialysis buffer. The polycarbonate centrifuge tube was centrifuged using TLA-120-1 rotor.

2.2.7.7 Protein Purification by Dialysis

Ammonium sulphate $(NH_4)_2SO_4$ precipitated protein samples are dialyzed to remove salts that may interfere with protein quantification and migration in SDS-PAGE. The dialysis membrane incorporated into the cap was pre-wet in the dialysis buffer (20 mM HEPES (pH 7.9), 50 mM KCl, 0.25 mM EDTA (pH 8.0), 0.5 mM DTT). The buffer was prepared earlier and stored at 4°C. Samples were cautiously pipetted into the conical bottom of the tube and adjusted to ~ 200 µl, then capped with the previously pre-wet membrane incorporated cap. The capped tube was inserted into a float, then with the cap and membrane side-down placed in a stirred beaker containing 1 l dialysis buffer at 4°C overnight. Following dialysis, the tube was centrifuged briefly. This brings the entire content of the tube back to the conical bottom for maximum recovery. The dialysed sample can be stored in the same tube by simply replacing the dialysis cap with a standard cap. Samples were then prepared for quantification and SDS-PAGE. The protein concentrations were determined by Bio-Rad *DC* protein assay.

2.2.8 Immunoprecipitation (IP)

2.2.8.1 Immunoprecipitation (IP) With Protein A Agarose

All steps in this protocol were performed on ice or at 4°C, if not indicated otherwise. Pre-loading step, 10 µl of Protein A Agarose (sc-2001 Santa Cruz Biotechnology, Heidelberg), for each IP sample were transferred into a 1.5 ml snap-cap centrifuge tub using a large orifice tip (e.g., for 10 IPs 105 µg of Protein A Agarose were added) to be washed with the appropriate lysis buffer (0.5 % Triton X-100, 01 % NP-40). After the beads were washed, they were gently spun at 500 x g for 1 min at 4°C. The supernatant was then discarded using a gel loading tip. The wash step was repeated two more times, then 1 Vol. lysis buffer was added to the beads resulting in the solution being 50 % slurry (beads).

10 -20 µl and 50 µl of whole protein extracts containing either p2UG-HA-Hac1^{i} or pRS314-HA-Hac1^{i}, respectively were added to a 1.5 ml microcentrifuge tube. 10 µl of beads were added to the lysate and adjusted to 200 µl with lysis buffer. The tube was incubated with overhead rotation, overnight at 4°C. The tube was then collected and spun at 500 x g for 1 min at 4°C and the supernatant was transferred to a new 1.5 ml microcentrifuge tube. The beads were saved to test as a pre-immunoprecipitation control in a Western blot. 0.5 µl (unless indicated otherwise) of anti-HA antibody were added to the supernatant then incubated with overhead rotation, overnight at 4°C. 10 µl of beads

(previously prepared) was added to the immunoprecipitation and incubated with overhead rotation for 1-2 h, at 4°C, then spun at 500 x g for 1 min at 4°C. The supernatant was then removed carefully with a gel loading tip not to remove any of the beads. The beads were then washed 3 x with 500 µl lysis buffer, then spun at 500 x g for 1 min at 4°C after each wash. A final wash of the beads with 500 µl H_2O was spun and the supernatant was removed without disturbing the beads. Then 20 µl 6 x SDS-PAGE sample buffer with β-mercaptoethanol were added to the beads and boiled in a heat block for 5 min at 100°C. The tube was left on a rack on the bench for 1 min to cool down then the eluate was collected by spinning the tubes at 12,000 x g for 2 min, at RT. The sample was then loaded onto an SDS-PAGE.

2.2.8.2 Immunoprecipitation (IP) With Anti-HA Magnetic Beads

After cells were lysed with the appropriate lysis buffer and quantified, Thermo Scientific Pierce Anti-HA Magnetic Beads with affinity particles for immunoprecipitation of recombinant HA-tagged proteins expressed *in vitro* systems, were used to immunoprecipitated HA-Hac1^{i}.

Pre-loading step, 10 µl (10 µg) of Anti-HA Magnetic Beads for each IP sample were transferred into a 1.5 ml snap-cap centrifuge tube using a large orifice tip (e.g., for 10 IPs 105 µg of Anti-HA Magnetic Beads were added) to be washed with the appropriate lysis buffer (Used in whole lysate extraction). 300 µl of ice-cold lysis buffer were added to the beads. The tube was gently mixed by inverting then placed into a magnetic stand to collect the beads against the side of the tube. The supernatant was aspirated and discarded; this wash step was repeated one more time. 10 -20 µl and 18 – 20 mg of whole protein extracts containing either p2UG-HA-Hac1^{i} or pRS314-HA-Hac1^{i}, respectively were added to a 1.5 ml microcentrifuge tube. 10 µl of pre-washed magnetic beads were added to the tube. The sample was adjusted to the proper volume (as indicated in RESULTS) and incubated overnight with overhead rotation at 4°C. The sample was collected on ice and then spun at 500 x g for 1 min at 4°C to collect all the solution to the bottom of the tube. The tube was placed into the magnetic stand to collect the beads against the side of the tube, and the unbound sample was removed and saved for analysis. The beads were then washed 3 x with 300 µl ice-cold lysis buffer, then the tube was placed into the magnetic stand to collect the beads and readily remove the supernatant after each wash. A final wash with 300 µl H_2O was spun and the supernatant aspirated without disturbing the beads same as before. Then ~ 38 µl 6 x SDS-PAGE sample buffer without β-mercaptoethanol was added to the beads and boiled for 5 min at 100°C. The sample was allowed to cool down on the

bench then spun at 12,000 x g for 10 s at RT. The tube was placed into the magnetic stand to collect the beads on the side to transfer the elute, using a gel loading tip, to a clean 1.5 ml microcentrifuge tube. ~ 2-3 % (v/v) β- Mercaptoethanol was added to the sample then boiled for 5 min at 100°C. The sample was allowed to cool down on the bench then spun at 12,000 x g for 1 min at RT. The sample was then loaded onto an SDS-PAGE.

2.2.8.3 SDS-PAGE With TV100

Protein lysates were run on 12 % SDS-PAGE gel with a 1 mm/ 1.5 mm spacing between the glass plates (Depending on the final volume of the loading lysate sample). The gel was made of a stacking gel and a separating gel. The composition of the stacking gel buffer (for a 12 % SDS-PAGE gel with a 1 mm comb insert) was 3 ml 30% (w/v) acrylamide, 0.8% (w/v) bisacrylamide, 1.875 ml 1 M Tris·HCl, pH 8.9, 2.52 ml H_2O, 75 µl 10% SDS, 22.5 µl 10% ammonium persulphate (APS), and 5 µl tetramethylethylenediamine (TEMED). Butanol was then added to obtain a stacking gel with a straight line, and the casted gel was washed with deionized H_2O after 40 min at RT. The separating gel buffer composition was 340 µl 30% (w/v) acrylamide, 0.8% (w/v) bisacrylamide, 625 µl 1M Tris·HCl, pH 6.8, 1.549 ml H_2O, 25 µl 10% SDS, 11.25 µl 10% APS, and 3.75 µl TEMED. These volumes were to cast one gel (for 12 % SDS-PAGE gel with a 1 mm comb insert). After the addition of H_2O, the solution was degassed for 5 min.
Once polymerised, lysate samples were diluted using H_2O to the desired concentration. Prior to loading, 6 x SDS-PAGE + β- Mercaptoethanol loading buffer was added to the sample, unless mentioned otherwise. The sample was then boiled at 100°C for 5 min, left to cool to at RT and sample was loaded into the well. A molecular weight marker was loaded into the first lane of the gel. The gel was run for 2 h at 120 V in a Fisherbrand TV100 gel system. Gels were always run until the bromophenol blue dye front had run off the bottom of the gel.

2.2.8.4 Coomassie Staining of Polyacrylamide Gels

Gels were soaked in a tray containing 20 % (w/v) trichloroacetic acid + 0.1 % (w/v) Coomassie Brilliant Blue R250 for 30 min at RT with shaking at 15 rpm. The solution in the tray was decanted, and the gel background staining was removed with 8 % (v/v) HOAc + 7 % (v/v) MeOH.

2.2.8.5 Western blotting

The gel was removed from the electrophoresis unit and the stacking gel was carefully removed. The separating gel was transferred into a tray filled with semi-dry buffer for 15 min at 50 rpm at RT. A PVDF membrane (Amersham HyBond^{TM}- P, pore size 0.45 µm, GE Healthcare, Little Chalfont, UK, cat. No. RPN303F) was cut to the size of the gel and soaked in 100% methanol for 5 min then moved to a tray with semi-dry buffer. 8 pieces of Whatman 3 MM paper were cut to the size of the gel and soaked in semi-dry buffer. Once all the components were prepared, they were stacked onto the semi-dry horizon blot system (Atto, East Sussex, UK, Model #AE-6675L). The stacking of the components first involved the wetting of the blot transfer apparatus with semi-dry buffer, only where the stack will reside. 4 pieces of Whatman paper were stacked with air bubbles removed from between each piece by rolling a glass tube over the stack with gentle pressure. The pre-wetted PVDF membrane was then placed over the Whatman paper followed by the SDS-PAGE gel. Again, any air bubbles were removed as above. The final 4 pieces of Whatman paper were stacked on top of the gel and again air bubbles were removed. The blot apparatus was then closed to allow for transfer. The transfer was performed with a constant current of 2 mA/cm ^{2} of membrane for 1 h and 15 min. Once transferred, the membrane was stored in 5% milk-TBST at 4°C (cold room) on a shaker at 35 rpm for a minimum of 1 hour, ideally overnight.

2.2.8.6 Antibody staining

The HA-tagged proteins were detected using anti-HA (α-HA) antibodies. Antibody information can be found in Table 12. The membrane was incubated on a roller mixer at 4°C (cold room) in 2 ml of 5% milk in TBST containing α-HA antibody at an appropriate dilution overnight. After incubation, the membrane was washed 4 times in 50 ml TBST at 50 rpm for 5 min for each wash. The membrane was incubated on a roller mixer at RT for 2 h with anti-rabbit IgG (H+L)- peroxidase HRP linked secondary antibody with appropriate dilution, again the membrane was washed in TBST as above.

Detection

Two detection reagents were used to detect the tagged proteins on the membrane. To detect low amounts of expressed protein ECL2 was used. For higher amounts of expressed protein a detection reagent of 5 ml Tris·HCl pH 8.5 + 0.1 % (v/v) Tween 20, 25 µl 250 mM luminol 11.1 µl 90 mM *p*-coumaric acid and 1.45 µl 30 % H_2O_2 was used (Schneppenheim et al., 1991). 2 ml of the selected detection reagent was applied to the

membrane and allowed to develop at room temperature for 5 min. Films were exposed to Thermo-Scientific CL – X-Posure X-ray film (Thermo Fisher Scientific, Cramlington, UK, cat. No. 34091.) for varying exposure times, from 1 s to 10 min, this was completed in a dark room. Films were developed using the Xograph Compact X4 (Xograph imaging systems, Stonehouse, UK).

2.2.9 RNA Methods

When working with RNA, substantial care was taken to prevent degradation of the RNA sample through contamination of samples with ubiquitous, environmental RNases and to efficiently inhibit and separate cellular RNases. All materials used for RNA work were RNase free if possible (e.g., tips, tubes, solutions).

2.2.9.1 DNA Templates to be Used as Probes

The DNA templates which were probed and used to detect the presence of complementary nucleic acid sequences (target sequences) by hybridization in the Northern blot assay were amplified from 50 µg genomic DNA (PWY 260) or 10 ng of plasmid DNA. The PCR used 1 µM primes, 2.5 U Go*Taq* G2 flexi polymerase in a final volumen of 10 µl. To obtain large amounts of DNA template, I prepared 100 µl for each sample. Fragments were gel purified.

Table 2-18 DNA Template Amplification

Segment	Cycle	Temperature	Time
Initial Denaturation	1	95°C	30 sec
Denaturation	30	95°C	30 sec
Annealing		72°C	60 sec
Extension		68°C	30 sec
Final Extension	1	72°C	5 min
Refrigeration	Hold	4°C	∞

2.2.9.2 RNA Isolation from *Saccharomyces cerevisiae*

The cell pellet was resuspended in 1 ml ice-cold DEPC-H_2O, transferred to a 1.5 ml microcentrifuge tube (RNase free), and cells collected by centrifugation at 12,000*g*, RT, for 15 s. Then cells were resuspended in 300 µl RNA buffer and transferred to a 2 ml screw-cap microcentrifuge tube. ~ 200 mg glass beads (equivalent to ~200 µl) (glass beads acid-washed, diameter 0.45–0.55 mm, sterilized by baking at 200°C for ⩾ 4 h) have

been previously added to the screw-cap tube, then 300 µl of phenol/$CHCl_3$/isoamylalcohol RNA buffered (25/24/1 v/v/v) was added. The tube was well mixed by flipping. Cells were lysed in the Precellys instrument at 4°C using 2 cycles of 30 sec at 6,500 rpm with a break of 30 sec between both cycles. After 1 min centrifugation at 12,000 x g at 4°C the upper phase was transferred into a new 1.5 microcentrifuge tube. 300 µl phenol/$CHCl_3$/isoamylalcohol, RNA buffered (25/24/1 v/v/v) was added to the 1.5 microcentrifuge tube and briefly vortexed and centrifuged for 1 min at 12,000 x g at 4°C. The upper phase was transferred into a new 1.5 microcentrifuge tube. 900 µl EtOH (ice-cold) was added to the sample which was then incubated at - 80°C overnight. After centrifugation at 12,000 x g for 2 min at 4°C (repeated once for 10 sec) the supernatant was aspirated. The pellet was resuspended in 70 % (v/v) EtOH as a wash step, then centrifuged at 12,000 x g for 2 min at 4°C (repeated once for 10 sec). The supernatant was aspirated, and the pellet was allowed to dry on air for 5 -10 min. ~50 – 100 µl of formamide was added to the pellet to dissolve the RNA by incubation at RT for 1 – 2 h, the sample was mixed if required. After centrifuging at RT for 5 min at 12,000 x g, the supernatant was transferred to a clean 1.5 ml microcentrifuge tube and the RNA sample was quantified and stored at - 80°C.

2.2.9.3 RNA Denaturating Agarose Gel Electrophoresis

The electrophoresis apparatus was prepared by thoroughly washing with 2 % (w/v) SDS. The electrophoresis apparatus was then thoroughly rinsed with ultrapure H_2O to remove traces of SDS.
1.4 % (w/v) gel was prepared by melting agarose in 10 mM $Na_xH_{3-x}PO_4$ (pH 7.0) and allowed to cool to 55°C by placing the flask into a 55°C oven. The gel was then cast, comb inserted, and allowed gel to solidify. During the denaturation of RNA samples for 1 h, the agarose gel was immersed in 10 mM $Na_xH_{3-x}PO_4$ running buffer, and a buffer pump to recirculate the buffer during electrophoresis was installed (the tubbing of the pump was rinsed by running DEPC-H_2O through it). In a RNase-free 1.5 ml microcentrifuge tube the appropriate amount of RNA (10 µg RNA/lane) and the RNA denaturation solution (Table 2.3) were added. The sample was mixed, and the RNA was denatured by incubating the mixture in a heat block at 50°C for 1 h. The sample was cooled at RT and centrifuged at RT for 10 sec at 12,000 x g to collect the sample at the bottom of the tube.10 µl 6 x RNA sample loading buffer was added, and the tube was vortexed. Immediately after centrifugation for 10 s at 12,000 x g the sample was loaded onto the gel. 10 µg DNA size marker, denatured like the RNA sample, was added to the first lane and one blank lane was

left between the lane containing the size marker and the sample. Gel was run at 3 V/cm of electrode distance with constant buffer recirculation until the bromophenol blue tracking dye migrated about 80 % along the length of the gel. The size marker lane was cut-off and stain in 0.5 M NH_4OAc + 0.5 μg/ml ethidium bromide overnight. The size marker lane gel was destained with frequent changes with H_2O and photographed the marker under UV (λ = 254 nm) light.

2.2.9.4 Capillary Transfer of RNA

A positively charged Nylon membrane and 8 Whatman 3 MM paper were cut to the size of the cut-out agarose gel, a large piece of Whatman 3 MM papers, a stack of paper towels ~ 10 cm high, 2 glass trays (sterilized by baking at 200°C for ⩾ 4 h), 2 x 10 ml pipets, and 20 x SSC buffer were prepared for the capillary Transfer of RNA. The gel was cut-out using a clean scalpel and a ruler to guid the cutting lines.

1 dry Whatman 3 MM paper was taped to the top of the paper towels stack, then 3 Whatman 3 MM papers were wetted in 20 x SSC buffer and added to the stack while rolling the pipet on top of each paper to remove bubbles. The positively charged Nylon membrane was wetted in DEPC-H_2O then transferred to 20 x SSC. The membrane was then placed on the stack, and the bubbles were removed. 20 x SSC was then pipetted onto the membrane till there was liquid standing over a large area of the membrane, without delay the gel was placed onto the membrane by aligning the gel with the membrane on one of the two shorter sides. The gel was then let down steady and slowly while checking that the liquid front between the gel and the membrane was running along to ensure that no air bubbles were being trapped. The last 4 Whatman 3 MM papers were soaked in 20 x SSC and placed on the gel; bubbles were removed by rolling the pipet over the surface of the paper. The large piece of Whatman 3 MM papers was soaked in 20 x SSC and placed on top of the stack; the piece was long enough to connect both trays filled with 20 x SSC when placing the ends in the trays. Using cling film, the trays and the stack were covered, and a glass plate was placed on top of the stack. The setup was left at RT overnight then disassembled using forceps. The membrane with the nucleic acid side-up was then placed onto a piece of Whatman 3 MM paper and immediately covalently crosslinked the RNA to nylon membrane by UV irradiation (λ = 254 nm, 120 mJ/cm^2). The membrane was wrapped in Saran wrap and stored indefinitely at −20°C.

2.2.9.5 Hybridization

Membranes were incubated with ≥ 50 ml 20 mM Tris–HCl (pH 8.0) for 15 min at 65°C. This step strips covalently bound glyoxal from RNA and was only done once for every membrane. Using the prehybridization solution described in Table 2.3, the membranes were prehybridised with ~125 µl/cm^2 (~ 20 ml/membrane) prehybridization solution at 42°C for ⩾ 3 h. Denatured salmon sperm and formamide are added just before adding the solutions to the hybridization bottle. DNA template was diluted to a concentration of 10 – 25 ng in 45.0 – 47.5 µl of 1 x TE buffer, pH 8.0. The DNA template was denatured by heating for 5 min at 95 – 100°C. The sample was placed for cooling in an ice-water bath for 5 min and centrifuged for 10 s. The denatured DNA was added to the reaction tube and the blue pellet was dissolved by repeatedly flicking the tube, then centrifuged for 10 s at RT to collect the whole solution at the bottom of the tube. 2.5 µl [α-^{32}P] dCTP were added to the sample tube and mixed by flicking. The sample was incubated at 37°C for 10 min. The reaction was then stopped by adding 5 µl of 0.2 M EDTA. The DNA probe encoding the target sequence was labelled with [α-^{32}P] dCTP by random priming using a commercially available kit (e.g., RediPrime II from GE Healthcare). Labelled DNA was separated from unincorporated nucleotides by gel filtration on a Microspin S-200 HR column (GE Healthcare). In which the resin was resuspended in a Microspin S300 column by vortexing. The cap was loosened one-fourth of a turn and the bottom closure was snapped off. The column was placed in a 1.5 ml screw-cap microcentrifuge tube for support. The column was pre-spun at 3,000 rpm for 1 min. The column was placed into a new 1.5 ml tube, the cap was removed, but retained, and the sample was applied to the top-centre of the resin, being careful not to disturb the bed. The tube was closed with the cap, but not tightly. The column was spun at 3,000 rpm for 2 min, and the purified sample was collected at the bottom of the support tube. After this step, the labelled DNA probe and 0.5 ml of 1 mg/ml salmon sperm sample were denatured by heating to 95 – 100°C for 5 min, then immediately placed into an ice-water bath for 5 min. The tubes were centrifuged briefly and placed back into the ice-water bath. The labelled probe and denatured salmon sperm were then added to the hybridization solution. The probe was used at a concentration of 10 ng DNA probe/5 ml hybridization solution. Membranes were hybridized overnight.

Membranes were transferred to large trays and washed with a large volume of 2 x SSC, 0.1 % (w/v) SDS three times for 5 min at RT, and once with 0.2 x SSC, 0.1 % (w/v) SDS for 5 min at RT, trays were covered with a glass top while shaking. Membranes were transferred back into the hybridization bottle (washed with deionized water) and incubated

with a large volume of prewarmed 0.2 x SSC, 0.1 % (w/v) SDS for 15 min at 42°C. Membranes were rinsed briefly in 2 x SSC and blot off for excess liquid. The damp membranes were wrapped in Saran wrap and placed in a cassette; all edges were taped. The wrapped blots were exposed to PhosphorImager screen in a cassette for different time points. Using a Typhoon 9400 system (GE Healthcare, Little Chalfont, UK) and image is captured from the PhosphorImager screen. Before returning the screen to the cassette, it is erased by exposing it to light for 20 min. All mRNA bands were quantified by phosphorimaging on the Typhoon 9400 system. Volumetric measurements were normalised to the loading control pC4/2.

2.2.9.6 Stripping and Rehybridization

Membranes were incubated in ≥ 50 ml 50 % (v/v) formamide, 1 % (w/v) SDS, and 0.1 x SSC at 65°C for 30 min. The solution was discarded, and incubation with the solution was repeated once again. Then the membranes were incubated with ≥ 50 ml 1 % (w/v) SDS, and 0.1 x SSC at 65°C for 10 min. Once the membranes were stripped, they were either re-prehybridize as described before (**2.2.9.5**) for further testing, or wrapped in Saran wrap and stored indefinitely at −20°C.

2.2.10 Statistical Analysis

Data from repeats of experiments (protein assays, β-galactosidase assays, and Northern blots) were compiled and averages were calculated in Microsoft Excel. Errors were propagated using the law of error propagation for random, independent errors (Ku, 1966). For all data where statistical analysis has been completed, the error bars are representative of SEM. Prism 8 software by GraphPad Software, Inc. (La Jolla, California) was used to determine statistical difference ($p < 0.05$) between means of data sets in β-galactosidase assays using 2-way ANOVA test. The parameters of the test included the use of Tukey's test to correct for multiple comparison. A multiplicity adjusted p value was reported for each comparison, the adjustment was to account for multiple comparisons.

3 Production of *HAC1* Mutants to Investigate *HAC1* Domains Key Residue Functions

3.1 Rationale

It is widely known that *HAC1* belongs to the bZIP family (Mori et al., 1996, Cox and Walter, 1996, Nikawa et al., 1996). Interestingly, *HAC1* mRNA is constitutively expressed at a high level in the yeast cytoplasm but not translated due to an intron which inhibits mRNA translation (Chapman and Walter, 1997). The expression and activity of the Hac1 transcription factor is mediated by an unconventional post-transcriptional mechanism (Mori, 2003). The transcriptionally functional Hac1 ($Hac1^{i}$) is only produced when the intron block at the 3′ end of its mRNA is removed through an unconventional splicing event (Sidrauski and Walter, 1997). *HAC1* pre-mRNA encodes a protein of 230 aa, whereas mature mRNA encodes protein of 238 aa; both proteins share an identical N-terminal 220 aa carrying the bZIP domain, which is unaffected by splicing (Cox and Walter, 1996). It is well documented that the splicing event causes replacement of the C-terminal tail region of Hac1 from 10 aa to the second exon-encoded 18 aa. Both products of the unspliced $HAC1^{u}$ and spliced $HAC1^{i}$ are synthesized and detected in yeast cells (Kawahara et al., 1997, Chapman and Walter, 1997). The notion that synthesised product of $HAC1^{u}$ is immediately degraded is rebutted, given that $Hac1^{u}$ can be generated in yeast cell from constructs without introns and has a half-life similar to functional $Hac1^{i}$ ($t_{1/2} \cong 2$ min) (Kawahara et al., 1997, Chapman and Walter, 1997). Recently, a study showed a protocol measuring the stability and intracellular targeting and recruitment of $HAC1^{u}$ mRNA during the UPR. The method allowed the quantification of $HAC1^{u}$ by co-expressing fluorescent-labelled $HAC1^{u}$ and Ire1, followed by estimating their co-localization using FACS (Fluorescence Activated Cell Sorter) analysis. Results from this method further supports the stability of $HAC1^{u}$ mRNA with a half-life of approximately 2 min during UPR (Paira and Das, 2022).

In many studies it is strongly mentioned that bZIP transcription factors share highly conserved residues in the basic region and leucine zipper domain, allowing for informed point mutations (Landschulz et al., 1988, Agre et al., 1989). These highly conserved residues give the bZIP transcriptional factors their characteristic function. In which the DNA-binding sites is important in target gene regulation, and leucine zipper is required for protein dimerization (Fujii et al., 2000, Lyon et al., 2003). In addition to the bZIP regions, $Hac1^{i}$ harbours a potent transactivation domain within its C-terminal tail, specifically serine-238 was suggested to be responsible for $Hac1^{i}$ high transcriptional regulation (Mori et al., 2000).

To examine functional changes of the Hac1 protein activity, various mutant derivatives of the protein construct were constructed. The design and manufacture of these constructs is detailed in this chapter.

3.2 Construction of *HAC1^u*, an Intron-less Form of *HAC1* mRNA

HAC1^u was constructed using a PCR-based method by overlap extension. The strategy for deletion overlap extension PCR is a two-step process, and involves two PCR fragments (Figure 3.1 a). The first step (primary PCR) includes two independent PCRs to generate two PCR fragments that are used as template for the second step of PCR (Ligation PCR). The two PCR fragments from the first step correspond to the flanking regions of a deletion area. In other words, deletion is essentially a ligation or recombination of two separate DNA fragments (Lee et al., 2010).

Because a long-range base pairing interaction between the *HAC1* mRNA intron and 5′ UTR is key for the attenuation of *HAC1^u* translation, disruption of the interaction leads to Hac1^u being synthesized with approximately the same stability as Hac1^i (Rüegsegger et al., 2001). In order to express 230 aa-Hac1 (Hac1^u), a previous study constructed a functional *HAC1^u* gene by removing the region of nucleotides 691-966 containing the first stop codon, most of the intron, and the 18-aa segment from the *HAC1* gene (Kawahara et al., 1997).To construct Hac1^u to be examined in this study I used a PCR-based method by overlap extension (Figure 3.1 a). I designed two primers that span the fusion region. First set of primers (a and b) were designed (Table 2.11) to amplify the first ORF in *HAC1* subsequently, removing most of the intron from the *HAC1* gene and the second exon (Figure 1.3). Specifically, pRS316-g*HAC1* plasmid was used as the template for the PCR amplification reaction. 1st PCR reaction (which will start 100 bp upstream of the *Mlu*I site and end after the stop codon of the first ORF, and lead over directly into the 3′-UTR sequences (AGACAATCGCAAG……)) which essentially amplifies parts of the 1st ORF with an overhang over the 3′ UTR (AB) (Figure 3.1 a). Hence, I removed the sequence of nucleotides from 663 (which does not include the first stop codon), resulting in a 618 bp fragment (ORF) (Figure 3.1 b). The 2nd PCR reaction (which overlaps with the sequences before the stop codon of the first ORF) amplifies the 3′UTR along with 150 bp past an *Asc*I site. The other set of primers (c and d) were designed to amplify the 3′UTR, starting after the second stop codon at nucleotide 970 (Figure 3.1 a and c), and ends past an *Asc*I site. This results in a 313 bp amplified 3′UTR fragment (CD). Both PCR fragments were confirmed by agarose gel and combined for one final PCR fusion reaction. In the second step of ligation PCR, the final PCR reaction fuses both resulting PCR products by mixing

the fragments, the recombinant product is then PCR-amplified using the two outermost primers (a and d) that anneal up and down stream of *Mlu*I and *Asc*I, respectively while allowing the overlapping regions to combine. I confirmed the size of the final fusion product of 931 bp by agarose gel (Figure 3.1 b). The final recombinant product was then subcloned into pRS14-HA-*HAC1*^{i}, which will replace the *HAC1*^{i} cDNA gene with the *HAC1*^{u} construct (Figure 3.1 d) and at the same time retain the single HA-tag in the *Spe*I site at the 5′ end of the *HAC1* ORF. The fusion product was cut with *Mlu*I and *Asc*I and cloned into pRS314-HA-*HAC1*^{i} that has itself been cut with *Mlu*I and *Asc*I and treated with calf intestinal alkaline phosphatase (CIAP) to dephosphorylate the DNA 5′ termini. The upstream of the *MluI* site and downstream of the *AscI* site are already present in the *HAC1* locus. The final plasmid construct pRS314-HA-*HAC1*^{u} was then sequenced to confirm product fusion (Figure 3.1 d) and transformed into MSY-134-36 yeast strain.

This PCR-based approach avoids introduction of restriction endonuclease sites at the ends of a PCR product for the following reasons: a) Such sites are sometimes poor substrates for restriction endonucleases. b) Cutting close to the ends of a linear piece of DNA cannot be monitored (except by ligation and transformation), because the few bp cut off do not significantly change the migration of the piece of DNA in agarose gels. The long overhangs on the fusion PCR product allow for exactly this – assessing whether the two enzymes have cut, because of size differences of 100-200 (total 2x of this) for DNA pieces of the size of the fusion product.

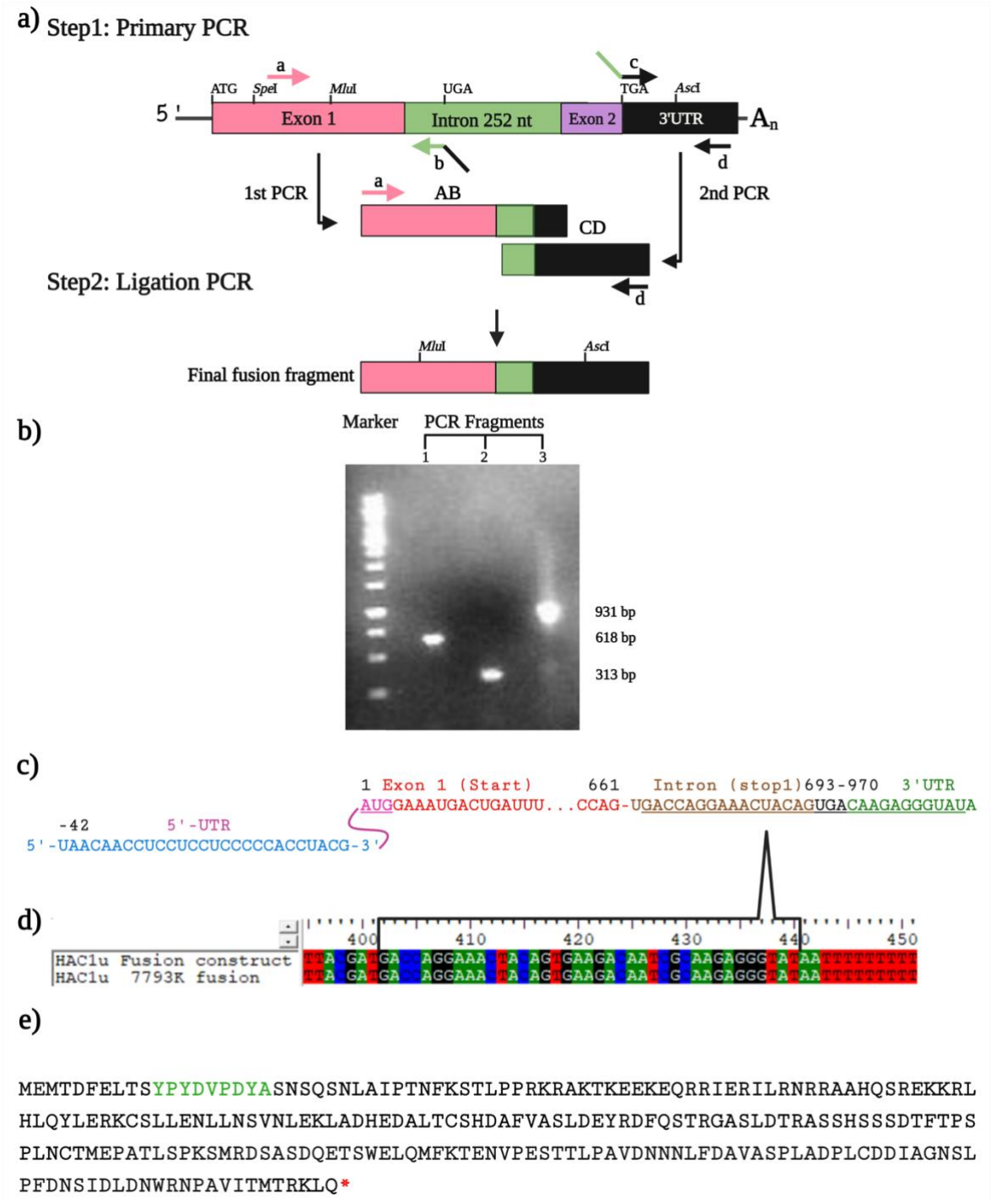

Figure 3-1 *HAC1*^{u} intron deletion strategy.

(a) Schematic overlap extension PCR protocol for deletion mutagenesis. Two PCR products representing the flanking regions of the sequence to be deleted are prepared by using one nonchimeric and one chimeric primer. Primary step: Two parallel PCR reactions are run to isolate the pieces of DNA surrounding the deletion site. Each reaction has two primers: a normal set (a & d) and a chimeric set (c & d) that include an extra ~19 bases that will control reassembly. (Chimeric primers = ~19 normal bases + ~19 overlapping bases). In the second step, two PCR products are used as the template for a ligation PCR that contains the outermost primer pair. Ligation PCR: The two "overlapping pieces" from the "Primary PCR" are combined with the "normal set" of primers (a & d) for the final PCR step. First, ligation occurs as the "overlapping pieces" template synthesis of the final product; Second, primers A & D amplify the synthesis of the final product. The recombined PCR product (final fusion fragment) is re-cloned by making use of the appropriate restriction sites in two flanking regions (*Mlu*I & *Asc*I). **(b)** Agarose gel UV image of products amplified

using primers a and b (lane 1, ORF), primers c and d (lane 2, 3′UTR), and primers a and d (lane 3, fusion). Red arrows indicate the PCR amplified fragments size. **(c)** An illustration presenting the *HAC1*^{u} construct sequence as a result of removing the intron and second exon and fusing the first exon with the 3′UTR. The ORF starts at the start codon (ATG), pink, in the first exon and end at the stop codon within the intron (TGA), black, the green colour sequence is the 3′UTR. The underlined sequence is the overhang used as the template to fuse both AB & CD fragments. **(d)** Plasmid DNA sequencing analysis confirmed proper fusion and recombination of the product PCR (pRS314-HA-*HAC1*^{u}), here I used primer 7793K to confirm the fusion sequence of the two fragments. **(e)** Hac1^{u} translated amino acid sequence including the HA-tag (green) and stop codon (*). Created with BioRender.com.

3.3 Construction of pRS303-HA-*HAC1*^{i}

To introduce the point mutations needed for this study, I used site-directed mutagenesis as described previously. This PCR-based procedure requires the design of short primers (Table 2.11) and a plasmid template. Here I first used pRS314-HA-Hac1^{i} or pRS316-gHac1^{i} plasmids as the template for the PCR reaction (8440 bp,7312 bp, respectively). However, running the resulting PCR reaction on an agarose gel (electrophoresis) did not show any amplification of the target DNA. Furthermore, transformation of *E. coli* cells (L2-blue MRF' Ultracompetent Cells) with these PCR products did not give any colonies. This may be due to the large size of the template plasmids, and so using them as templates in the single-site mutagenesis reaction was unsuccessful.

This led me to sub-clone HA-*HAC1*^{i} fragment (897 bp) from pRS314-HA-Hac1^{i} into pRS303 (4443 bp). Restriction digests for both the donor and recipient plasmids were set up using *Bss*HII and *Spe*I, the desired fragments were isolated by excising them from an agarose gel and then conducting gel purification. To fuse the insert into the vector, a DNA ligation reaction was set up at 3:1 ratio and left overnight at 15°C to construct and produce pRS303-HAC1^{i} (5340 bp) recombinant plasmid. In addition to setting up the desired ligation reaction a negative control was set up in parallel, a ligation of the recipient plasmid DNA without any insert to accommodate for the possible amount of background from uncut or self-ligating recipient plasmid backbone. The ligation reactions were transformed into *E. coli* competent cells, resulting in a significant number of colonies 2 x 10^{2} in the insert + recipient plasmid plate. The negative control plate did not yield many colonies, 10 colonies were counted. The finished plasmid was isolated from the bacterial colonies and digested using either *Hind*III or *Sal*I to confirm successful insert + plasmid ligation. The resulting plasmid construct pRS303-HA-HAC1^{i} was now ready to be used as a shorter plasmid template in the site-directed mutagenesis PCR based reaction.

3.4 Mutation of the Conserved Asparagine Residue in the Basic Region of Hac1^{i}

The DNA binding basic region is highly conserved in many members of the bZIP transcription factor family (Figure 1.4 b). Mutation of several conserved residues in the basic region, including the invariant asparagine and arginine, previously was shown to eliminate the functional role of these bZIP proteins (Pu and Struhl, 1991a). Because Hac1^{i} and Gcn4 share a conserved basic region, I surmised that, Hac1^{i} will have similar crucial functional characteristics by the conserved residues. Like Gcn4 transcription factor, Hac1^{i} contains an invariant asparagine and arginine residue within the basic DNA binding region (NXAAXXCR). These conserved residues have a direct functional role in protein-DNA binding specificity (Pu and Struhl, 1991a, Fujii et al., 2000, Miller, 2009).

As a result of Hac1^{i} alignment with Gcn4, the basic region showed the invariant asparagine at position 49 in the amino acid sequence (Figure 1.4 b). Asparagine mutation to leucine was determined based on Gcn4 Asn-235 to Leu-235 alteration, which generated a mutant protein defective as a DNA-binding protein (Pu and Struhl, 1991a). Here I asked the question, what role does this highly conserved asparagine play in the function of Hac1^{i}. However, I first needed to introduce the desired mutation within the DNA- binding site of Hac1^{i}.

In order to mutate the desired target amino acid in the basic site, I used site-directed mutagenesis to alter Asn-49 to Leu-49 (Figure 3.2 a) using the primer pair indicated in (Table 2.11), and the pRS303-HA-HAC1^{i} as the PCR template. The resulting PCR product was sequenced to confirm the desired mutation and to ensure no other undesired changes in the sequence. The HA-HAC1^{i}-N49L was then sub-cloned into the pRS314-HA-HAC1^{i} plasmid from pRS303- HA-HAC1^{i}-N49L using restriction enzymes *BssH*II and *Spe*I for both plasmids, thus excising compatible fragments (vector, 6405 bp and insert, 897 bp) for ligation. The resulting pRS314-HA-HAC1^{i}-N49L plasmid construct (7302 bp) was then confirmed by diagnostic restriction enzyme (*Sal*I) and transformed into MSY-134-36 yeast strain to be further analysed. In addition, to add an exclusive diagnostic measure to the newly generated plasmid, a silent restriction site was introduced near the mutant sequence using the same primers that introduced the Asn-49 mutation, *Eci*I. This alters the target nucleotides in the ORF without changing the amino acid sequence or function. The desired mutation and the inflicted silent restriction site were confirmed by sequencing (Figure 3.2 a).

3.4.1 Multiple Mutations in the Leucine Zipper Region

The bZIP transcription factor Hac1^{i} also contains the leucine zipper structural motif found in many eukaryotic transcription factors. This structural motif leucine zipper mediates dimerization which stabilises the transcription factors DNA-binding efficiency, and consists of α-helices with 4 or 5 leucine residues 7 amino acids apart (Landschulz et al., 1988). Mutations in the well-studied Gcn4 transcription factor leucine zipper, proposed that some mutated derivatives of Gcn4 carrying two leucine substitution display functional impairment (Van Heeckeren et al., 1992). Alignment of Hac1^{i} and Gcn4 show the conserved residues in the leucine zipper required for α-helix formation. I then asked the question, if mutating the heptad repeats in the Hac1^{i} bZIP domain required for its function in this study. Again, I first needed to construct a disrupted leucine zipper mutant derivative of Hac1^{i}. To construct a possible leucine zipper compromised Hac1^{i} mutant, three conserved residues in the leucine zipper were substituted. Leu-67, Leu-74, and Val-81 were subjected to mutation (Figure 3.2 b), and all residues were substituted with proline through site-directed mutagenesis as mentioned in the Methods. The residues were substituted with proline due to it being predicted to seriously disrupt the α-helix nature of the leucine zipper (MacArthur and Thornton, 1991). The mutations were done subsequently after confirming each mutation by sequencing (Figure 3.2 b). The final HA-HAC1^{i}-L67P/L74P/V81P product was then sub-cloned into pRS314-HA-HAC1^{i} from pRS303-HA-HAC1^{i}-L67P/L74P/V81P. the final recombinant product was transformed into *E-coli*, extracted and proper ligation confirmed by digestion. Here I also used the same restriction enzymes as described in the previous basic region mutation result. The plasmid carrying the triple leucine zipper mutations pRS314-HA-HAC1^{i}- L67P/L74P/V81P, was transferred into MSY 134-36 yeast strain for further analysis. Also, I introduced two silent restriction sites through the same primers used for the L74 and V81 targeted mutations, *Hpy*8I and *Eco*RI, respectively (Figure 3.2 b).

3.4.2 Mutation of the Hac1^{i} S238 Residue Located in the Transactivation Domain

Previous studies have shown that replacement of the *HAC1* mRNA C-terminus, which replaces 10 aa with 18 aa by splicing, synthesizes a mature Hac1 with high transactivation properties. Specifically, the molecular basis of the difference in their transactivation potential relies on a single serine residue in the Hac1^{i}. This crucial residue Ser-238 displayed diminished activating potential when mutated to Ala (Kawahara et al., 1997, Chapman and Walter, 1997, Mori et al., 2000). I asked if this mutation, of Ser to Ala, in

the transactivation domain would influence Hac1^{i} function in this study. To subject *HAC1^{i}* to this mutation, I also used pRS303-HA-HAC1^{i} plasmid as the template for the site-directed mutagenesis PCR reaction. The primer pair used to implement these mutations are mentioned in (Table 2.11). Afterwards, the resulting product pRS303-HA-HAC1^{i}-S238A was sequenced to confirm the point mutation (Figure 3.2 c), and like pRS303-HA-*HAC1^{i}-L67P/L74P/V81P*, was digested with *Bss*HII and *Spe*I and the HA-*HAC1^{i}-S238A* fragment was subcloned into pRS314-HA-HAC1^{i}. The resulting construct pRS314-HA-HAC1^{i}-S238A was confirmed by digestion with *Sal*I, then transformed to yeast strain MSY-134-36.

3.5 Discussion

To characterise different mutants of the Hac1 bZIP transcription factor in regulating transcription within both the UPR and meiosis pathways, I needed to generate different informed Hac1 mutant constructs. The *HAC1* pre-mRNA form has been previously produced by intron-less constructs or by disrupting the interaction between the *HAC1* 5′UTR and intron (Kawahara et al., 1997, Rüegsegger et al., 2001). The overlap extension PCR protocol for deletion mutagenesis generated an intron-less translatable form of *HAC1^{u}* mRNA, which was used in this study (Figure 3.1 a). Since previous studies of bZIP transcription factors showed that point mutations within key domains of the proteins interrupt their functions, domain which share consensus sequences and residues with other well studied bZIP transcription factors, its highly likely that introducing similar point mutations will yield functionally disrupted Hac1^{i} bZIP transcription factors. Specific mutations in the Gcn4 DNA-binding region (invariant asparagine) and leucine zipper region (leucine heptad repeats) abolished the Gcn4 bZIP domain function in *vivo* and *vitro* (Pu and Struhl, 1991a, Van Heeckeren et al., 1992), these disruptive alterations guided the protein substitutions within Hac1^{i} for my study. Using site-directed mutagenesis, the target amino acids were altered to study their importance within the bZIP domain. The mutant Hac1^{i} constructs produced either carried a mutation in the invariant asparagine within the DNA-binding region (pRS314-HA-*HAC1^{i}-N49L*) (Figure 3.2 a), or mutations of the three heptad repeats within the leucine zipper region (HA-*HAC1^{i}-L67P/L74P/V81P*) (Figure 3.2 b). Also, mRNA splicing-mediated C-terminal replacement of transcription factor Hac1 introduces 18 amino acids, within these 18-aa a serine at residue 238 is required for effective transactivation activity of Hac1^{i} in the UPR (Mori et al., 2000). Also, using site-directed mutagenesis, a Hac1^{i} mutant construct was generated to alter the Ser-238 with an Ala-238 (pRS314- HA-*HAC1^{i}-S238A*) (Figure 3.2 c). As a result of the *HAC1* mutations

the different constructs were sequenced, confirmed, and ready to be characterised in regulating transcription through UPRE and URS1. It is important to note that *HAC1* in this study was subjected to novel manipulations. Hac1^{u} construct as a result of the overlap PCR manipulation allowed the protein to maintain the 3′UTR, which consists of the 3′ cis-acting bipartite elements (3′BE) that signals to have the *HAC1* mRNA targeted to Ire1 foci for splicing (Anshu et al., 2015). Also, mutating the conserved asparagine or heptad repeats in *HAC1* allowed for the original study of the specific residues roles in regulating transcription via Hac1^{i} bZIP transcription factor, in UPR and meiosis. Results from the experiments would further support the importance of the conserved residues highlighted in the bZIP transcription factors, and aid in specifying mutation targets for bZIP transcriptional function studies (Dwarki et al., 1990, Ellenberger, 1994) .

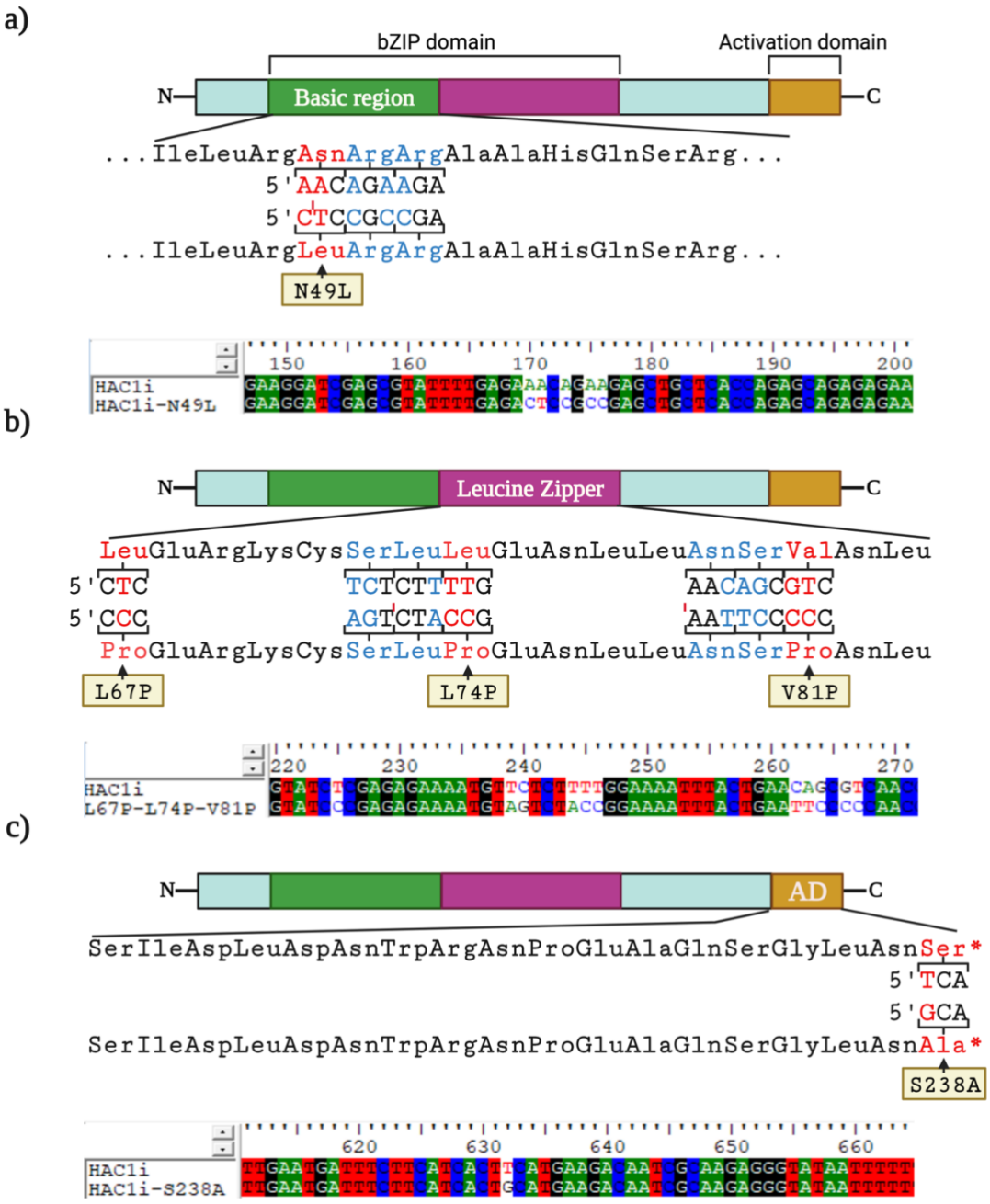

Figure 3-2 Structure of Hac1^{i} bZIP domain, composed of the DNA-binding region and leucine zipper dimerization region, in addition to the transactivation domain at the C-terminus.

The site-directed mutagenesis strategies of the *HAC1^{i}* target sequence in the conserved and activation domains are shown. Red colour indicates the alteration for the desired mutations, blue colour indicates alterations to introduce silent restriction sites, and the red (|) indicates the restriction sites. **(a)** Point mutations in the DNA-binding domain and plasmid DNA sequencing analysis confirming point mutations **(b)** Point mutations in the dimerization domain and plasmid DNA sequencing analysis confirming point mutations **(c)** Point mutation in the activation domain and plasmid DNA sequencing analysis confirming the point mutation. Created with BioRender.com

4 Hac1 Mutant Derivatives in Regulation of UPRE-Controlled Genes

4.1 Rationale

When the ER is stressed due to accumulation of unfolded proteins, it is well known that Hac1 is the bZIP transcription factor involved in regulation of the unfolded protein response (UPR) (Mori et al., 1996, Cox and Walter, 1996). Mature Hac1 ($Hac1^{i}$) binds to UPRE, a conserved promoter present in chaperone genes, e.g., *KAR2* and promotes transcription of those target genes (Mori et al., 1998). Studies have also shown that *hac1Δ* strains are defective in activation of the UPR thorough UPRE promoters of target genes (Cox and Walter, 1996, Nikawa et al., 1996).

In yeast cells, $Hac1^{u}$ and $Hac1^{i}$ expressed from plasmids are stable and can bind UPRE; however, the transactivating activity of the $Hac1^{u}$ is lower than that of $Hac1^{i}$ (Kawahara et al., 1997). Transactivation activity of different fragments derived from 230 aa and 238 aa Hac1 have been analysed; however, fragment variants carrying alterations within the bZIP domain have not been examined, with regards to UPRE induction (Mori et al., 2000). The Mori et al., 2000 experiment demonstrated a difference in transcriptional activation, when fusing different Hac1 subregions directly downstream of the DNA-binding domain of the yeast transcriptional activator Gal4. Transcriptional activation was determined by measuring the level of β-galactosidase expressed from a UAS_{GAL}-*CYC1-LacZ* reporter gene. The results showed when missing the leucine zipper domain of Hac1, which was replaced with the leucine zipper from Gcn4, that the 230 aa type construct had a low effect on induction of β-galactosidase compared to the 238 aa type. Suggesting that the C-terminal tail replacement by splicing is responsible for the difference in transactivation, but not the leucine zipper region, thus revealing that the 18 aa tail is important in transactivation activity of Hac1 and that Ser-238 in the 18 aa exon is crucial for transactivation (Mori et al., 2000). As mentioned before, the basic DNA-binding region of bZIP proteins carry an invariant asparagine residue, this residue makes direct contact with DNA bases within the major groove and drives binding specificity (Fujii et al., 2000, Miller, 2009). Furthermore, dimerization of the leucine zipper domain in bZIP transcription factors dictate protein-DNA binding under control of the conserved leucine residues (Landschulz et al., 1988, Yamamoto et al., 1988). In this chapter I will examine the effect of the previously constructed Hac1 mutant variants on regulating the UPRE promoter region, through analysing induction levels measured from UPRE-*lacZ* reporter plasmid.

4.2 Hac1^{i} is Required to Efficiently Activate UPRE-controlled genes

It has been previously shown that β-galactosidase activity measured from unstressed cells expressing 238 aa Hac1^{i} was about 12-fold higher than that in cells expressing 230 aa Hac1^{u}, when the β-galactosidase *lacZ* reporter gene was under the control of UPRE (UPRE-*lacZ*). It was further concluded that replacement of the C-terminus generates a transcription factor with higher activity, probably through phosphorylation of its S238 (Kawahara et al., 1997, Mori et al., 2000).

To analyse the effect of Hac1^{u} and Hac1^{i}-S238A constructs from this study on the UPRE promoter region and compare it to existing results, I used the β-galactosidase assay. I grew cells to mid-log phase in media lacking the appropriate amino acids (SD -Ura-Trp). Induction of the UPRE in strains carrying wild-type (EV meaning vector alone) and the mutant Hac1^{i} were assayed using an UPRE-*lacZ* reporter gene. Cells were prepared and harvested as described in Material and Methods. The strains were assayed under conditions at which they grew continuously under normal carbon and nitrogen conditions. As expected, EV (strains with vector pRS314 alone) cells exhibited diminished levels of UPRE expression, in contrast to Hac1^{i} ~ 19- fold higher induction of β-galactosidase levels through UPRE activation (Figure 4.1 a). As shown in Figure 4.1 a, the strain expressing the 230 aa Hac1^{u}, induced β-galactosidase activity ~ 11-fold compared to EV. I then compared UPRE induction levels of Hac1^{i} to Hac1^{u}, which is lacking the 18 aa, as expected there was about a 1.6- fold increase in induction. This can be related to the C-terminal domain transactivation activity (Mori et al., 2000).

The Hac1^{i}-S238A mutant defective in transactivation activity activated the UPRE at lower levels compared to Hac1^{i}, the single mutant strain showed approximately 1.8-fold reduction in UPRE-controlled β-galactosidase induction compared to the unmutated Hac1^{i} (figure 4.1 a). In addition, both 230 aa Hac1^{u} and Hac1^{i}-(S238A) induce comparable levels of β-galactosidase from the UPRE-*lacZ* reporter gene.

These results correlate with the previously observed study in that the 18-aa segment plays a major role in transactivation activity of Hac1 and that S238 within the 18-aa is crucial for transactivation. The data also shows Hac1^{u} UPRE activation potential to be less potent than Hac1^{i} (Mori et al., 2000, Kawahara et al., 1997, Chapman and Walter, 1997). The constitutive expression of Hac1^{i} from pRS314-Hac1^{i} has been shown by Schröder et al, 2004.

4.3 Hac1^{i} Requires Specific Residues in the bZIP Domain to Activate the UPRE-controlled plasmid

To characterize Hac1^{i} conserved residue's role in regulating the UPRE-controlled genes, I analysed β-galactosidase expression from reporter genes driven by two of the Hac1^{i} mutants. In strains expressing Hac1^{i}-(N49L), induction of UPRE from UPRE-*lacZ* reporter gene was abolished compared to Hac1^{i} (figure 4.1 b). The strain carrying the mutation in the invariant asparagine within the DNA-binding domain showed similar basal activity shown by the EV strain, where no Hac1 is being expressed. Thus, the results showed about a significant 25-fold decrease in β-galactosidase induction from the UPRE reporter gene regulated by the Hac1^{i}-N49L compared to Hac1^{i} (Figure 4.1 b).

Also, since mutations in the conserved heptad residues abolish dimerization, I examined the Hac1^{i} leucine zipper region residues requirement in activating the UPRE-controlled gene. I observed a significant decrease in the expression of β-galactosidase from the UPRE-*lacZ* construct after expressing the Hac1^{i}-L67P/L74P/V81P mutant, compared to high activation when expressing Hac1^{i}. Also, there was no significant difference between EV and Hac1^{i}- L67P/L74P/V81P in induction of β-galactosidase activity. Data analysis showed ~ 15-fold β-galactosidase induction from the Hac1^{i} regulated UPRE reporter when compared to Hac1^{i}-(S238A). EV induced basal amounts of β-galactosidase activity of about 3-folds less than the Hac1^{i}- L67P/L74P/V81P mutant (Figure 4.1 b). The results also showed that the EV strains inability to induce UPRE is comparable to the strain expressing the Hac1^{i} triple mutant in the leucine zipper domain. Thus, the conserved residues in the bZIP regions appear to have a role in regulating expression of reporter genes through UPRE. When comparing reporter gene induction of both Hac1^{i}-N49L and Hac1^{i}-L67P/L74P/V81P, results show compatible levels of low induction. Both mutants seem to similarly abolish Hac1^{i} functional ability to induce genes via UPRE.

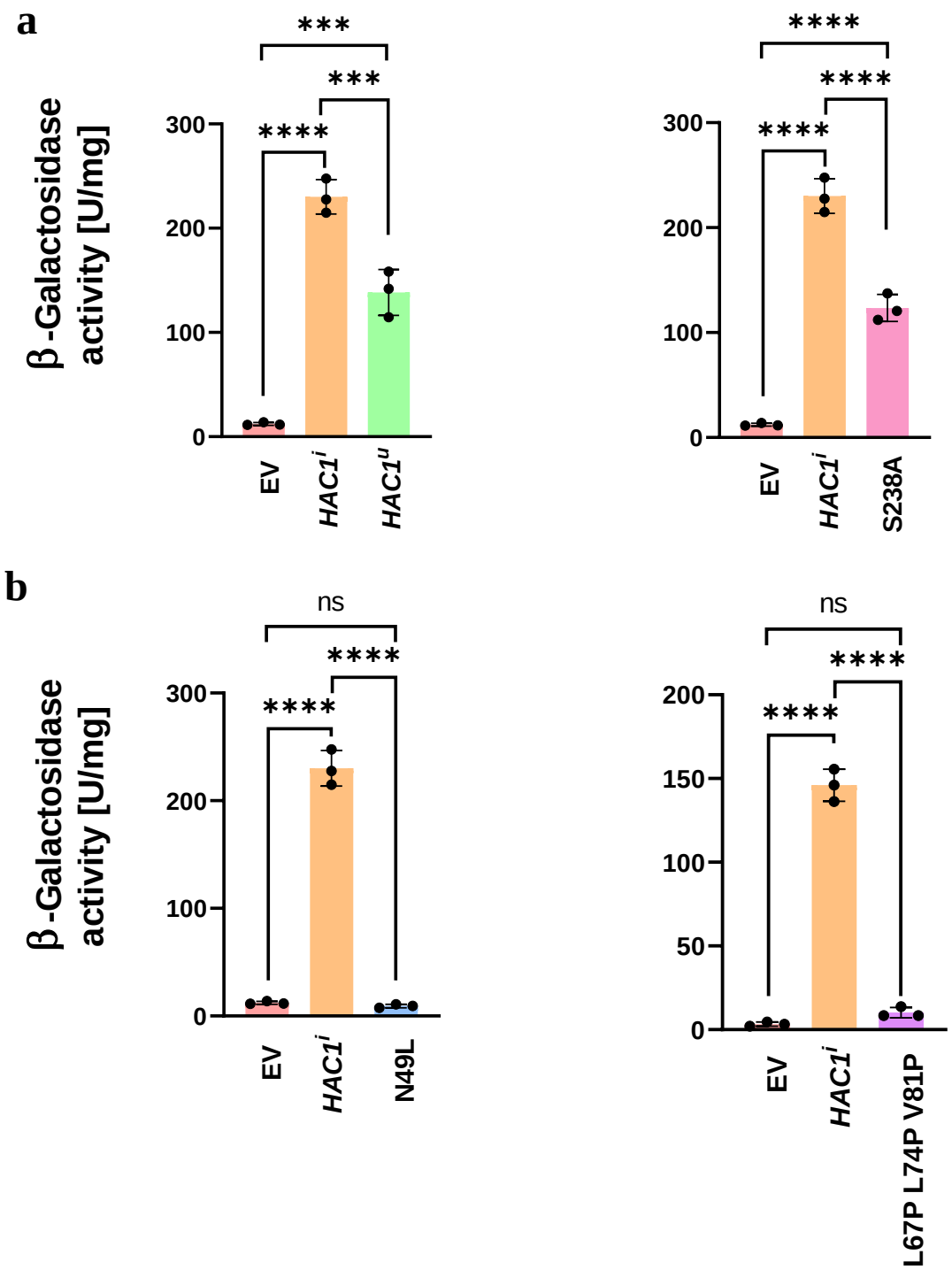

Figure 4-1 Hac1 mutant derivatives in regulation of UPRE-*lacZ*.

Quantification of collected data from three biological repeats of the β-galactosidase reporter assays show the Hac1 mutants activation potency on induction of UPRE-*lacZ* reporter gene. Data collected and plotted for the EV and Hac1^{i} are the same across all the three first graphs, showing (HAC1^{u}, S238A, and N49L). Bars represent standard errors. These data were subjected to a one-way ANOVA test to determine statistical differences ($p < 0.05$) using all data. *, $P \leq 0.05$; **, $P \leq 0.01$; ***, $P \leq 0.001$; ****, $P \leq 0.0001$. **(a)** The 238-aa (Hac1^{i}) is a more potent activator of the UPRE-associated reporter expression compared to the 230-aa (Hac1^{u}), indicated by reporter activity. The S238A mutant shows comparable levels of reporter activity to Hac1^{u}, when compared to EV (pRS314). **(b)** Point mutations in the conserved bZIP regions (DNA-binding and leucine regions) displayed a disruption in the Hac1^{i} ability to induce activation of UPRE-*lacZ* reporter gene. The significant difference between the Hac1^{i} and its mutants suggest an imperative role for the disrupted residue to maintain Hac1^{i} regulation via UPRE.

4.4 Discussion

To observe and characterise the transcriptional activation by Hac1^{i} and its mutants in the UPR, I examined the expression of UPRE-*lacZ* reporters in vegetative growth. Hac1^{i} and the Hac1 derivatives were constitutively expressed from pRS314 plasmids. It has been demonstrated that Hac1^{i} and mutant *HAC1* (Hac1^{u} and Hac1^{i}-S238A) display different transactivation activity, observed by the transcriptional activator Gal4 and measuring β-galactosidase expressed from UAS$_{GAL}$-*CYC1-lacZ* reporter plasmids (Mori et al., 2000). EV and Hac1^{i} control data is reproduced in several graphs, where the Hac1^{u}, S238A, and N49L mutants are depicted (Figure 4.1). However, EV and Hac1^{i} data in the graph depicting L67P/L74P/V81P represents data collected on a separate day form three independent transformants (Figure 4.1). Samples taken after 0, 4, and 8 h were used for β-galactosidase assays, and the activities are presented as the mean ± SD, based on duplicate determinations with three independent transformants. Expression of β-galactosidase from UPRE-*lacZ* regulated by Hac1^{i} showed high levels of expression, when compared to Hac1^{u} and Hac1^{i}-S238A mutants lower induction regulation (Figure 4.1 a). These results agree with the previously suggested (Mori et al., 2000) crucial role of the 18-aa C-terminal segment in transactivation potential of Hac1and that Ser-238 in the 18-aa is required for transactivation. Since Hac1^{i} is a bZIP transcription factor, it contains a DNA-binding region and leucine zipper region. I tested the requirement of key residues within these regions for regulating β-galactosidase expression through induction of UPRE-*lacZ*. Mutation of the invariant asparagine in Hac1^{i} (Hac1^{i}-N49L) to a leucine disrupted the Hac1^{i} function to positively regulate induction of β-galactosidase through UPRE promoter (Figure 4.1 b). Triple mutation in the leucine zipper region of the heptad repeats to proline, suggest disruption of the coiled-coil formation and subsequently preventing Hac1^{i} dimerization was also observed. The levels of β-galactosidase measured as a result of UPRE induction via Hac1^{i}- L67P/L74P/V81P was indistinguishable to basal activity levels measured by EV (empty vector) (Figure 4.2 b). Together these results suggest a crucial role for the invariant asparagine and leucine zipper of the bZIP domain in binding UPRE to activate the Hac1^{i} target genes in the UPR pathway. The findings may also be a result of the mutant constructs not being expressed in the cells. Further expression analysis will need to be done to address this possibility.

A previous study proposed that Hac1^{i} bound DNA of target genes with Gcn4 as a heterodimer. This Gcn4/Hac1^{i} heterodimer complex hence promotes induction of transcription by mediating UPRE activation and promoting UPR (Patil et al., 2004). Mutation of the leucine zipper region of Hac1^{i} will disrupt the heterodimer complex

formation, and this will result in loss of UPRE induction. This may explain the lack of UPRE-*lacZ* activation when expressing the Hac1^{i}- L67P/L74P/V81P mutant. Therefore, the leucine zipper region is required to promote Gcn4/Hac1^{i} heterodimer complex formation to mediate UPR as proposed by Patil et al., 2004.

5 Hac1 bZIP Conserved Residues Play a Role in Transcription Regulation of EMGs by Hac1^{i}

5.1 Rationale

A previous study has shown that the UPR is functionally involved in nitrogen sensing. This process is displayed by the UPR-pathway in regulating the developmental programs (differentiation) in response to nitrogen in the budding yeast. The study proposed that in nitrogen-rich conditions there are high polypeptide translation levels along with limited protein unfolding in the ER, thus indicating an activated UPR. The activation of the UPR-pathway supresses the ability of cells to differentiate. In contrast, nitrogen starvation reduces translation levels, this enables nascent polypeptide chains to fold more efficiently, and thus down regulate the UPR, and consequent derepression of differentiation pathways (Schröder et al., 2000). In yeast *Saccharomyces cerevisiae* these differentiation programs are pseudohyphal growth and meiosis (Kron et al., 1994, Herskowitz, 1988, Kupiec, 1997). Furthermore, the unconventional splicing of *HAC1* by *IRE1* in the UPR is required to sufficiently repress the differentiation programs by synthesising Hac1^{i} (Schröder et al., 2000). It has been established that overexpression of spliced Hac1^{i} negatively regulates differentiation in response to nitrogen starvation.

Therefore, entry into meiosis is negatively regulated by Hac1^{i}. Hac1^{i} regulates repression of EMGs responsible for meiosis, such as *IME2*, *HOP1*, *SPO13*. Repression is regulated through the EMGs upstream promoter site URS1 (consensus sequence TCGGCGGCT). Also, the Rpd3-Sin3 histone deacetylase complex (HDAC) recruitment to the URS1 site by Ume6 is required for Hac1^{i} to negatively regulate EMGs efficiently in response to nitrogen starvation, and the catalytic activity of Rpd3 is required for this negative regulation (Schröder et al., 2004). The study also revealed that Hac1^{i} is a peripheral component of the HDAC (Schröder et al., 2000, Schröder et al., 2004). Expression of Hac1^{i} during nitrogen starvation interferes with sporulation, hence overexpression of Hac1^{i} is sufficient to simulate a nitrogen-rich environment and interfere with spore formation (Schröder et al., 2004).

Repression of EMGs transcription through a bZIP transcription factor is a novel mechanism with not much known about it. Here I investigate if the 230 aa construct Hac1^{u} can repress EMGs transcription through the URS1 site like Hac1^{i}. In addition, I examined the involvement of crucial residues within the Hac1 bZIP domain in negative regulation of EMGs by Hac1^{i} under nitrogen starvation. Also, I tested the strains carrying the S238A mutant in repressing transcription of EMGs.

5.2 238 aa Hac1 represses URS1 activation significantly stronger than 230 aa Hac1

Under nitrogen–rich conditions synthesis of Hac1^{i} in part represses the EMGs; in contrast, synthesis of the protein from the endogenous genomic locus is shut-off in nitrogen starved cells (Schröder et al., 2000). Therefore, to allow for expression of Hac1^{i} in nitrogen starved cells, a plasmid carrying a copy of *HAC1^{i}* under the control of its own constitutive promoter was introduced through transformation into yeast, hence, overexpression of Hac1^{i} represses meiotic genes mirroring a rich state condition while activating the starvation response. Furthermore, all strains here were grown in PSP2 media with a non-fermentable carbon source (acetate) and collected in mid-log phase (designated '0 h'), and subjected to nitrogen starvation for 4 h and 8 h in complete sporulation (C-SPO) medium (Schröder et al., 2000, Schröder et al., 2004).

To investigate the role of 230-aa Hac1 (Hac1^{u}) in repressing the EMGs promoter element URS1, I evaluated the expression levels of β-galactosidase from URS1-*CYC1-lacZ* reporters in response to nitrogen starvation. I hypothesised that Hac1^{u} can mediate negative regulation of transcription through URS1 in response to nitrogen starvation. To test this hypothesis, the effect of Hac1^{u} was studied on the activation of a minimal *CYC1* promoter fused to a T_4C enhancer, URS1 elements, or a combination of both by nitrogen starvation. To express Hac1^{u} in conditions of nitrogen starvation, where endogenous *HAC1* transcription is turned-off, like Hac1^{i} Hac1^{u} was overexpressed from a single-copy plasmid (pRS314-HA-*HAC1^{u})* carrying Hac1^{u} under the control of its own constitutive promoter in yeast.

In Figure 5.1 a, reporter plasmids carrying *CYC1-lacZ* gene alone with no promoter elements (T_4C and URS1) were no induced for expression of β-galactosidase activity, when expressing EV, Hac1^{i} or Hac1^{u}. These results are comparable to expression of reporter plasmids harbouring URS1 alone (Figure 5.1 c). Induction of high levels of β-galactosidase ~ 30-folds from promoters carrying the T_4C enhancer (Figure 5.1 b) compared to URS1 and *lacZ* alone (Figure 5.1 a and c), specifically at Hac1^{i} 4 and 8 h starvation, reveals the crucial role of URS1 in regulating reporter repression via Hac1^{i} (Schröder et al., 2004). These reporter plasmid expression levels act as controls for the experiment (Figure 5.1 a, b, and c), in that induction of quantitative β-galactosidase during nitrogen starvation via Hac1^{i} requires both T_4C and URS1. The results showed, as previously reported (Schröder et al., 2004, Bowdish and Mitchell, 1993), that nitrogen starvation induced β-galactosidase expression from reporter plasmids harbouring URS1, but not the T_4C enhancer alone when regulated by Hac1^{i} (Figure 5.1 b and c). When

expressing Hac1^{u}, activation of reporters harbouring URS1 element alone by nitrogen starvation was noticeably blunted as when expressing Hac1^{i} (Schröder et al., 2004). In contrast, Hac1^{u} had no negative affect on the T_4C enhancer alone as in the presence of Hac1^{i} (figure 5.1 b) (Schröder et al., 2004). Furthermore, to validate the assay system, I observed URS1 mediated suppression of *lacZ* reporters in nitrogen-rich conditions at 0 h in T_4C-URS1 compared to no repression in T_4C (Figure 5.1 b and d) and β-galactosidase activation during nitrogen starvation (Figure 5.1 b and d) (Schröder et al., 2004).
As expected, (Figure 5.1 d) in EV cells 4 h of nitrogen starvation caused a 6-fold (0 h ≈ 8 U/mg vs 4 h ≈ 48 U/mg) increase in the URS1 mediated induction of β-galactosidase, indicating the induction of early meiotic genes. By 8 h starvation URS1 activation was further increased by more than 2.5-fold relative to 4 h (8 h ≈ 140 U/mg). In cells expressing Hac1^{i}, nitrogen starvation did not induce URS1-controlled genes as indicated by the absence of increased β-galactosidase activity at both 4 and 8 h, which were significantly lower compared to EV cells not expressing the Hac1^{i} construct. This is consistent with previous reports on Hac1^{i}'s role in repressing early meiotic genes via URS1 (Schröder et al., 2000, Schröder et al., 2004). Interestingly, the presence of the Hac1^{u} construct also resulted in a significant reduction in β-galactosidase reporter activity compared to EV at 8 h of nitrogen starvation, seen as an approximately two-fold reduction, suggesting that Hac1^{u} is also able to repress early meiotic genes through URS1. However, Hac1^{u} was not as potent at repressing early meiotic genes regulating promoter element URS1 as Hac1^{i}, which is evident by the statistically significant 10-fold increase in reporter activity in Hac1^{u} mediated β-galactosidase induction compared to Hac1^{i} cells at 8 h of nitrogen starvation (8 h ≈ 6 U/mg in Hac1^{i} vs 8 h ≈ 63 U/mg in Hac1^{u}). The observation that Hac1^{u} is a less effective regulator of gene activity than Hac1^{i} is consistent with the study demonstrating that Hac1^{i} is a more effective transcription factor compared to Hac1^{u} (Mori et al., 2000). Furthermore, the Hac1^{i} regulation potency correlates with results seen from the last chapter in regulating UPRE promoter sites compared to Hac1^{u}.
Conclusion, it is expected that there is a difference in transcription activation between Hac1^{i} and Hac1^{u} proteins and this potentially has two meanings: either the Hac1 protein needs the C-terminal of the Hac1^{i} version to interact with something in the histone deacetylase or the C-terminus activates transcription of a gene, and that protein is part of the repression activity of RPD3. Hac1^{i} is required to repress entry into meiosis (Schröder et al., 2000; Schröder et al., 2004). To further address the importance of the C-terminus in transcription repression by Hac1, mutation in the proposed activation domain (S238A) is in play.

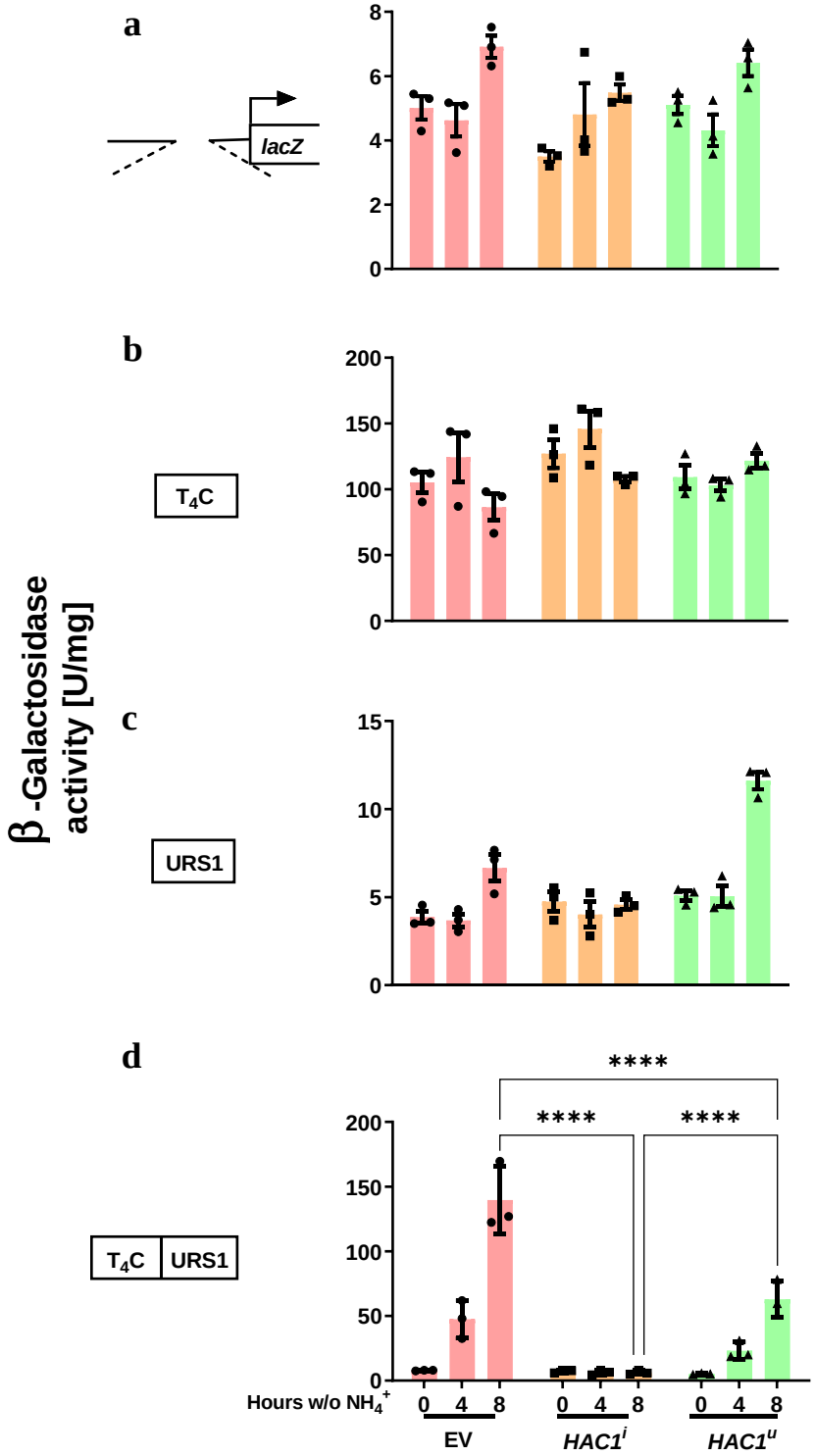

Figure 5-1 Hac1 bZIP conserved residues play a role in mediating transcription of URS1-*CYC1-lacZ*. The C-terminal in the spliced form Hac1^{i} is required to negatively regulate transcription of EMGs. Expression of *lacZ* reporter plasmids harbouring the inserts shown on the left in an UAS-less *CYC1* promoter before, 4 and 8 h after induction of nitrogen starvation in yeast strains transformed with pRS314, pRS314-HA-Hac1^{i} or pRS314-HA-Hac1^{u}, continuously overexpressing Hac1^{i} and Hac1^{u}. The average and standard error from three independent biological repeats were calculated and quantified. These data were subject to a two-way ANOVA test to determine statistical difference ($p < 0.05$) using all data. *, $P \leq 0.05$; **, $P \leq 0.01$; ***, $P \leq 0.001$; ****, $P \leq 0.0001$.This analysis showed that there were statistical differences between Hac1^{i} and Hac1^{u}.The error bars represent the standard deviation. Data from strains transformed with empty vector (EV) were used in both figures 5.1 and 5.4 for all graphs.

5.3 N49 Invariant Asparagine within the DNA-Binding Region is Required to Repress Transcription of EMGs by Hac1^{i}

As mentioned before the Hac1^{i} DNA-binding domain features an asparagine that is functionally conserved in yeast bZIP transcription factors (Figure 1.4 b) (Landschulz et al., 1988, Pu and Struhl, 1991b). The basic region is necessary and sufficient for DNA-binding specificity (O'Neil et al., 1990, Talanian et al., 1990, Agre et al., 1989), and as in other bZIP proteins Hac1^{i} contains the invariant asparagine residue at position N49. Mutations in the well-studied Gcn4 invariant asparagine altered the DNA-binding specificity (Tzamarias et al., 1992).

Expected induction or lack thereof β-galactosidase from reporters harbouring T_4C, URS1, or none of them, is compatible with results from Figure 5.1 a, b, and c; the same is true for Figure 5.3, 5.4 a, b, and c.

To evaluate the contribution of the invariant asparagine (Asn-49) within the Hac1^{i} DNA-binding domain to repress EMGs via URS1, I characterized the nitrogen starvation response of Hac1^{i} invariant Asn-49 residue, within the DNA-binding domain, on induction of the URS1-*lacZ* reporter plasmid. I hypothesised that mutating the conserved invariant asparagine will abolish Hac1^{i} ability to repress EMGs through URS1.

To test this hypothesis, I assayed the effect of Hac1^{i}-N49L on URS1-controlled transcription under nitrogen starvation, using the previous assay system. As expected, at 0 h in vegetative cell growth (Figure 5.2 d) EV, Hac1^{i}, and Hac1^{i}-N49L show no induction of β-galactosidase at comparable levels (Figure 5.2 c and d, compare 0 h URS1 to T_4C-URS1) but activated induction of the T_4C-URS1-*lacZ* reporter when expressing EV and Hac1^{i}-N49L during nitrogen starvation (Figure 5.2 d). Negative regulation of URS1-controlled transcription by Hac1^{i}-N49L was nearly completely abolished. However, the mutant retained some ability to repress induction of β-galactosidase compared to EV (Figure 5.2 d). Hac1^{i}-N49L loss of negative regulation is evident from the nonsignificant deference to EV derepression of *lacZ* reporter plasmid at 8 h nitrogen starvation. In addition, I observed after 4 h nitrogen starvation both EV and Hac1^{i}-N49L exhibited different but significant loss of URS1 mediated repression (figure 5.2 d, 4 h ≈ 90 U/mg in Hac1^{i}- N49L vs 4 h ≈ 150 U/mg in EV). Furthermore, at 8 h nitrogen starvation the strains expressing the mutant Hac1^{i} partially derepressed URS1-controlled transcription compared to EV, which has no repression ability (Figure 5.2 d, 8 h ≈ 25-fold in Hac1^{i}- N49L vs 8 h ≈ 32-fold in EV compared to 8 h Hac1^{i}). The significance of the point mutation in the DNA-binding domain in disrupting the Hac1^{i} ability to efficiently repress URS1 mediated transcription is clear from these data.

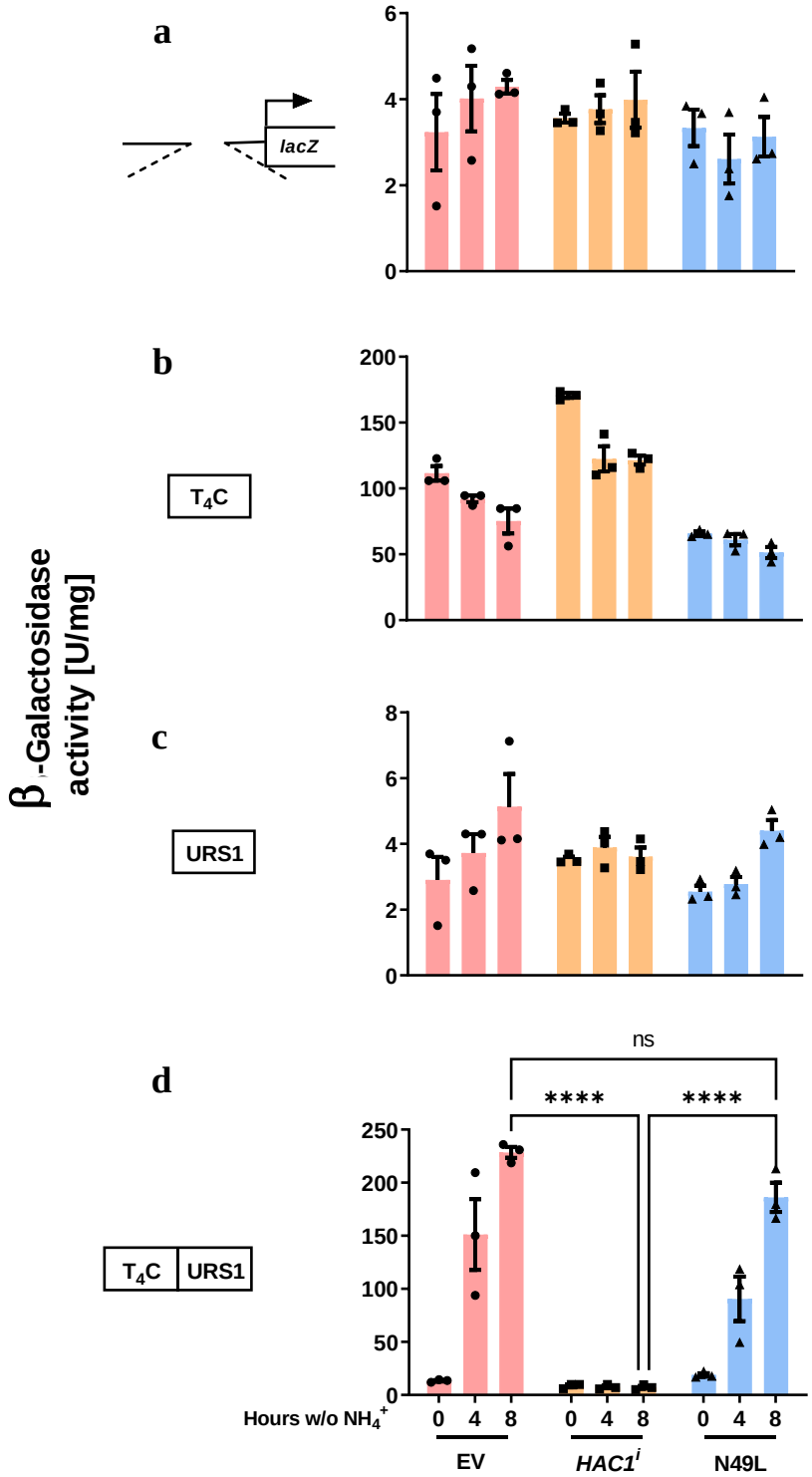

Figure 5-2 The invariant asparagine within the DNA-binding region is required to negatively regulate transcription of URS1-*CYC1-lacZ*.

The conserved invariant asparagine is required to efficiently negatively regulated repression of genes regulated by the URS1 promoter element. Expression of *lacZ* reporter plasmids harbouring the inserts shown on the left in an UAS-less *CYC1* promoter before, 4 and 8 h after induction of nitrogen starvation in yeast strains transformed with pRS314, pRS314-HA-HAC1^{i} or pRS314-HA-HAC1^{i}-N49L, continuously overexpressing Hac1^{i} and Hac1^{i}-N49L. The average and standard error from three independent biological repeats were calculated and quantified. These data were subject to a two-way ANOVA test to determine statistical difference ($p < 0.05$) using all data. *, $P \leq 0.05$; **, $P \leq 0.01$; ***, $P \leq 0.001$; ****, $P \leq 0.0001$. This analysis showed that there were significant statistical differences between Hac1^{i} and Hac1^{i}-N49L.The error bars represent the standard deviation.

5.4 Point Mutations in the Leucine Zipper Domain Mitigate Transcriptional Repression on URS1 by Hac1^{i}

Given that Hac1^{i} is a bZIP transcription factor naturally its prone to dimerize (Gentz et al., 1989, Kouzarides and Ziff, 1988, Turner and Tjian, 1989). The C-terminus forms a coiled-coil structure that provides productive DNA-binding (Landschulz et al., 1988, O'Shea et al., 1989, Saudek et al., 1991). The 7-unique amino acid position in the leucine zipper that support the C-terminal α-helical structure (Hodges et al., 1973) is also present in Hac1^{i} (Figure 1.4 c). This conserved motif in this domain consists of the leucine repeats.
To investigate whether mutation in the leucine repeat residues affect repression of transcription controlled by URS1 via Hac1^{i}, I assayed the repression mediated by the Hac1^{i}-L67P/L74P/V81P triple mutant in repressing transcription of EMGs promotor URS1. I hypothesised that several point mutations in the Hac1^{i} leucine zipper will abolish Hac1^{i} ability to negatively regulate transcription of genes controlled by the URS1 element. As expected at 0 h in nitrogen rich conditions basal levels of induction by EV, Hac1^{i}, and Hac1^{i}-L67P/L74P/V81P were detected from reporters harbouring T_4C-URS1, due to repression mediated by endogenous Hac1^{i}, compared to high β-galactosidase activity levels from T_4C alone (Figure 5.3 b and d). The data also showed a difference when comparing β-galactosidase induction levels regulated by EV, Hac1^{i}, and Hac1^{i}-L67P/L74P/V81P on T_4C-URS1 promoters at 4 h nitrogen starvation. At 8 h nitrogen starvation a significant partial increase in β-galactosidase induction was observed from strains expressing Hac1^{i}-L67P/L74P/V81P, compared to high induction levels assayed from EV strain, while Hac1^{i} maintained efficient repression of β-galactosidase activity (Figure 5.3 d, compare 8 h ≈ 90 U/mg in Hac1^{i}-L67P/L74P/V81P VS 8 h ≈ 190 U/mg in EV). Therefore, overexpression of Hac1^{i}-L67P/L74P/V81P resulted in partial derepression of URS1-controlled *lacZ* expression. Moreover, the mutant Hac1^{i} construct shows to maintain significant repression on β-galactosidase activity (Figure 5.3 d). A further mutation in the region may have a more tangible effect on eliminating suppression of the reporter plasmid. This data shows that the three mutated leucine zipper residues are required for Hac1^{i} to negatively regulate EMGs transcription governed by URS1 element. Furthermore, both mutants Hac1^{i}-N49L and Hac1^{i}-L67P/L74P/V81P regulate URS1-controlled *lacZ* expression differently. The Hac1^{i}-N49L mutant nearly completely abolishes Hac1^{i} negative regulation of URS1 mediated expression compared to Hac1^{i}-L67P/L74P/V81P (Figure 5.2 d and 5.3 d).

The behaviour of the Hac1^{i}-N49L mutant in regulating URS1-controlled *lacZ* expression agrees with its regulation of UPRE-controlled *lacZ* expression, in that in both cases the Hac1^{i} mutant has no regulation potential (Figure 4.1 b and 5.2 d). However, Hac1^{i}-L67P/L74P/V81P mutant behaves with potency in regulating some repression of URS1 mediated genes, compared to its lack of regulating potency of the UPRE mediated gene (Figure 4.1 b and 5.3 d). These observations suggests that the different parts of the protein may play additional roles in the different pathways.

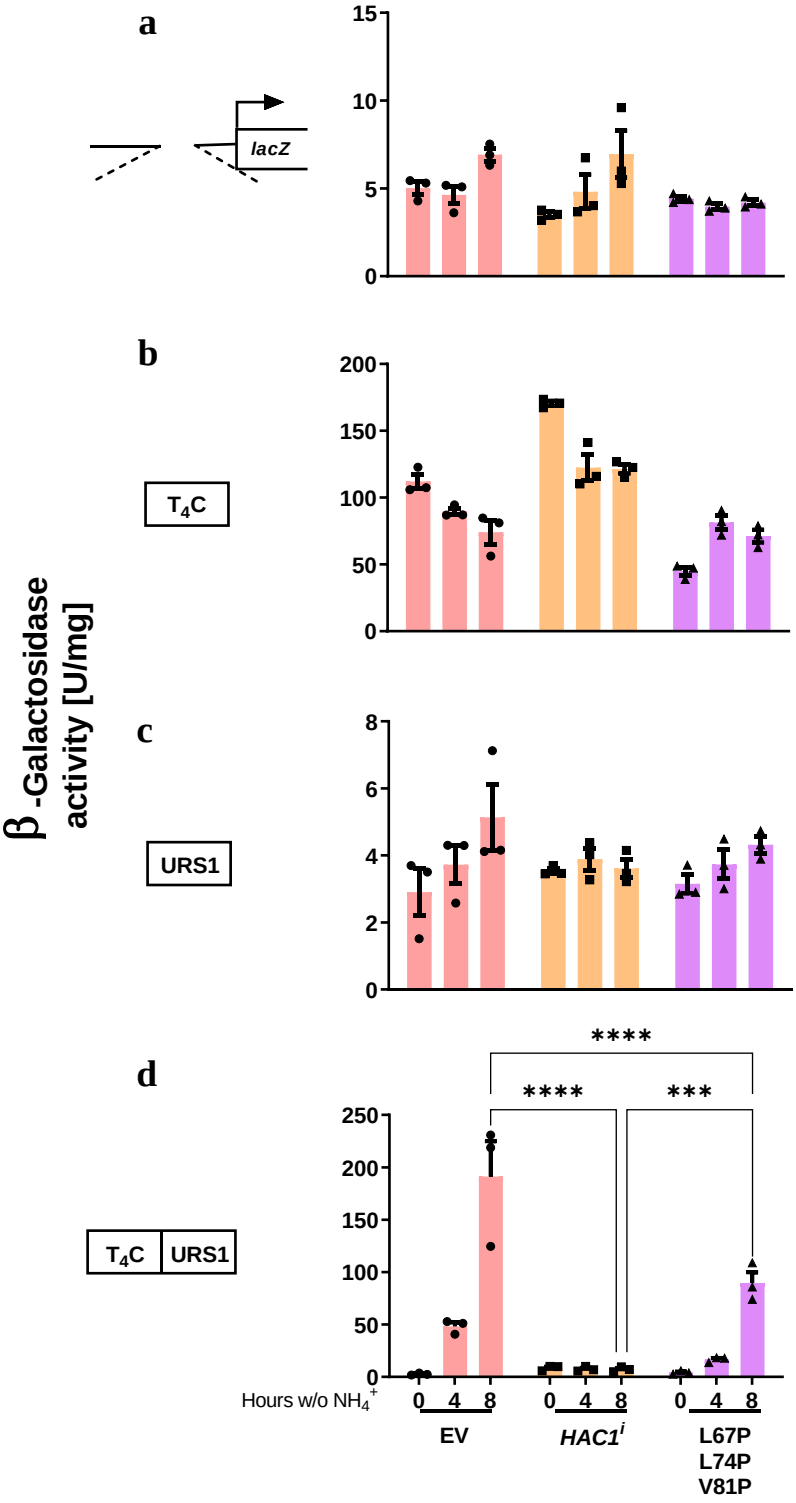

Figure 5-3 The leucine zipper mutant has a role in regulating repression of URS1-*CYC1-lacZ*.

The conserved leucine zipper residues play a role in repressing transcription of genes regulated by the URS1 promoter element. Expression of *lacZ* reporter plasmids harbouring the inserts shown on the left in an UAS-less *CYC1* promoter before, 4 and 8 h after induction of nitrogen starvation in yeast strains transformed with pRS314, pRS314-HA-HAC1^{i} or pRS314-HA-HAC1^{i}-L67P-L74P-V81P, continuously overexpressing Hac1^{i} and Hac1^{i}- L67P-L74P-V81P. The average and standard error from three independent biological repeats were calculated and quantified. These data were subject to a two-way ANOVA test to determine statistical difference ($p < 0.05$) using all data. *, $P \leq 0.05$; **, $P \leq 0.01$; ***, $P \leq 0.001$; ****, $P \leq 0.0001$. This analysis showed that there were significant statistical differences between Hac1^{i} and Hac1^{i}- L67P-L74P-V81P.The error bars represent the standard deviation.

5.5 S238 is Required for Efficient URS1 Element Transcription Repression Mediated by Hac1^{i}

The activation domain of Hac1^{i} features a serine that has been functionally proven to increase the Hac1^{i} transactivation activity (Mori et al., 2000) as mentioned before. The serine is only present in the spliced Hac1 due to the 10 aa replacement with the 18 aa as a result of splicing (Cox and Walter, 1996, Kawahara et al., 1997). In addition, 238 aa Hac1 has significantly higher transactivation activity than 230 aa Hac1 in regulating the UPR (Mori et al., 2000), and as evident in chapter 4. A point mutation of Ser to Ala in Hac1^{i} was responsible to inhibit the Hac1^{i} transactivation potential. For these reasons, I suggested a role for the serine residue in regulating repression of genes controlled by URS1. To analyse the role of the serine, within the transactivation domain, I investigated if the negative regulation of transcription by Hac1^{i} is mediated by Ser-238 during nitrogen starvation. I analysed the resulting β-galactosidase activity mediated by transcription of *lacZ* reporter plasmid governed by URS1.The data from reports carrying T_4C-URS1 promoters display a slight increase in β-galactosidase activity after 4 h nitrogen starvation from reporter genes regulated by EV and Hac1^{i}-S238A; however, Hac1^{i} retained the ability to repress any elevation in β-galactosidase activity (Figure 5.4 d). At 8 h nitrogen starvation, overexpression of Hac1^{i}-S238A displayed significant derepression of URS1-controlled *lacZ* reporters approximately nine folds higher than Hac1^{i} (Figure 5.4 d). However, the negative effected of the mutant Hac1^{i} on URS1 suppression was still ~ 2.5-folds less than EV at 8 h, while Hac1^{i} efficiently suppressed expression of the reporter plasmid (figure 5.4 d). This suggest that the mutant still retains some form of negative regulation on URS1 mediated transcription in response to nitrogen starvation. Furthermore, comparison between Hac1^{u} (Figure 5.1 d) and Hac1^{i}-S238A (Figure 5.4 d) ability to negatively regulate URS1 mediated repression revealed comparable results. At 8 h nitrogen starvation both Hac1 mutant constructs induced β-galactosidase activity at comparable levels (Figure 5.1 d and 5.4 d, compare 8 h ≈ 63 U/mg in *HAC1^{u}* VS 8 h ≈ 54 U/mg in Hac1^{i}-S238A) while still retaining the ability to partially repress indicational transcription through T_4C-URS1. Both Hac1^{u} and Hac1^{i}-S238A β-galactosidase assay were done on the same day using the same EV and Hac1^{i} colonies.

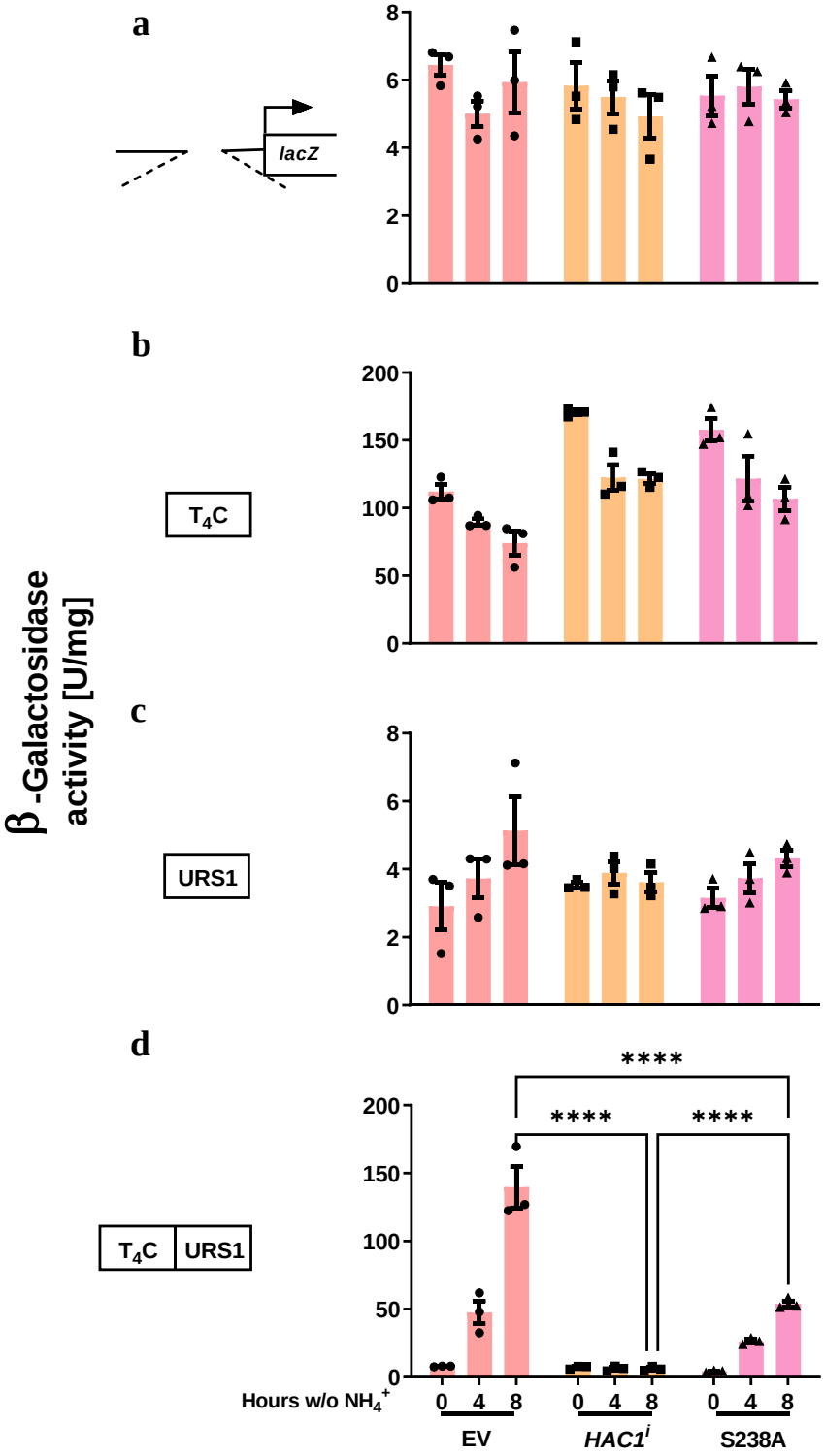

Figure 5-4 The transactivation domain residue Ser-238 plays a role in repressing URS1-*CYC1-lacZ*.
The transactivation domain residue Ser-238 plays a role in repressing transcription of genes regulated by the URS1 promoter element. Expression of *lacZ* reporter plasmids harbouring the inserts shown on the left in an UAS-less *CYC1* promoter before, 4 and 8 h after induction of nitrogen starvation in yeast strains transformed with pRS314, pRS314-HA-HAC1^{i} or pRS314-HA-HAC1^{i}-S238A, continuously overexpressing Hac1^{i} and Hac1^{i}-S238A. The average and standard error from three independent biological repeats were calculated and quantified. These data were subject to a two-way ANOVA test to determine statistical difference ($p < 0.05$) using all data. *, $P \leq 0.05$; **, $P \leq 0.01$; ***, $P \leq 0.001$; ****, $P \leq 0.0001$.This analysis showed that there were significant statistical differences between Hac1^{i} and Hac1^{i}-S238A.The error bars represent the standard deviation.

5.6 Repression of EMGs Requires Specific Residues Within the Domains of the bZIP Transcription Factor Hac1

To further test and confirm Hac1 variant mutant constructs effect on induction of early meiotic genes (EMGs) such as *IME2*, *HOP1*, and *SPO13*, I assayed the transcription induction levels of the EMGs mRNA by northern assays. I suggest that since the Hac1 variant mutant derivatives display a significant effect on β-galactosidase induction levels through URS1 repression or de-repression, then transcriptional levels from endogenous EMGs mRNA will show comparable results under similar conditions. Induction of EMGs by Hac1 is mainly controlled at the transcriptional level and involves activation of Ume6 by binding it to Ime1(Rubin-Bejerano et al., 1996, Malathi et al., 1997). Nitrogen starvation induces *IME1* and activates transcription of EMGs by the Ume6-Ime1 complex, however repression of EMGs by $Hac1^{i}$ is independent of *IME1*(Kupiec, 1997, Schröder et al., 2000). Thus, northern analysis (Figure 5.5) to detect *IME1* mRNA expression levels were examined in EV cells and cells overexpressing $Hac1^{u}$, $Hac1^{i}$ and its mutants. Overexpression of $Hac1^{i}$ at 0 h in nitrogen-rich and 2 h after induction of nitrogen starvation had no significant effect on transcription of *IME1* compared to EV, as observed from previous studies (Schröder et al., 2000). Moreover, at 4 h overexpression $Hac1^{u}$ and the $Hac1^{i}$ mutants N49L, L67P/L74P/V81P, and S238A expression of *IME1* mRNA levels were significantly affected compared to EV and $Hac1^{i}$ regulated expression (Figure 5.5). 4 h expression of mutant S238A is compatible to *IME1* mRNA expression levels regulated by $Hac1^{i}$ (Figure 5.5). While 4 h *IME1* levels induced by EV, N49L and L67P/L74P/V81P show no significant deference (Figure 5.5). Overall, *IME1* mRNA expression levels as an effect of expressing $Hac1^{i}$ and its mutants were insignificant at 0 h, 2 h, but significant at 4 h nitrogen starvation.

Furthermore, in a previous study expression of EMGs *IME2*, *HOP1*, and *SPO13* from cells expressing $Hac1^{i}$ were repressed four- to five-fold (Schröder et al., 2000), analytical results from this study also showed a four- to five-fold repression of EMGs in response to nitrogen starvation at 4 h when comparing EV to $Hac1^{i}$ inducing cells. I then compared expression of EMGs in cells expressing the different mutants and unspliced form of *HAC1* mRNA, to confirm results from β-galactosidase experiments. As expected, samples collected at 0 h under nitrogen-rich and vegetative growth conditions overexpressing Hac1 derivatives exhibited no induction of EMGs transcription resembling EV cells expression (Figure 5.5). In EV cells at 2 to 4 h

nitrogen starvation EMGs were exponentially expressed, while mRNA levels at 2 h nitrogen starvation was statistically nonsignificant compared to significant expression at 4 h starvation. These results corelate with the data collected from the previous β-galactosidase assays, where no exogenous Hac1 is present to repress expression of EMGs. Moreover, consistent with β-galactosidase assays induction of the 230 aa $Hac1^{u}$ showed a partial loss of repression on EMGs expression, approximately two- to three-fold at 4 h nitrogen starvation compared to $Hac1^{i}$ repression (figure 5.5). Excitingly, both key bZIP domain mutants N49L and L67P/L74P/V81P significantly alleviated EMGs repression and exhibited ~ 3.2 -3.6 expression compared to $Hac1^{i}$ detected repression levels at 4 h nitrogen deprivation (Figure 5.5). The Asn-49 point mutant $Hac1^{i}$ nearly completely abolished the proteins transcriptional repression function, which is compatible to the previous β-galactosidase experiment (Figure 5.2 d). However, the triple leucine zipper mutant $Hac1^{i}$ relieved EMGs repression at a slightly higher level, when compared to the mutant's function in the β-galactosidase assays (5.3 d). This may be due to the regulation of URS1 promoter bound to EMGs being more sensitive to the triple mutant $Hac1^{i}$ compared to regulation of *lacZ* reporters harbouring URS1.

After 4 h nitrogen starvation in cells inducing $Hac1^{i}$-S238A there was a 1.5- to 1.8-fold increase in *IME2*, *HOP1*, and *SPO13* expression, indicating that the mutant $Hac1^{i}$-S238A is marginally derepressing EMGs, but was not statistically significant (Figure 5.5). These results again agree with the analysis from the β-galactosidase assays (Figure 5.4 d), which indicates the requirement of the serine within the activation domain to efficiently repress transcription of EMGs. Furthermore, all Hac1 designed constructs retained to some extent the ability to repress expression of EMGs during nitrogen starvation.

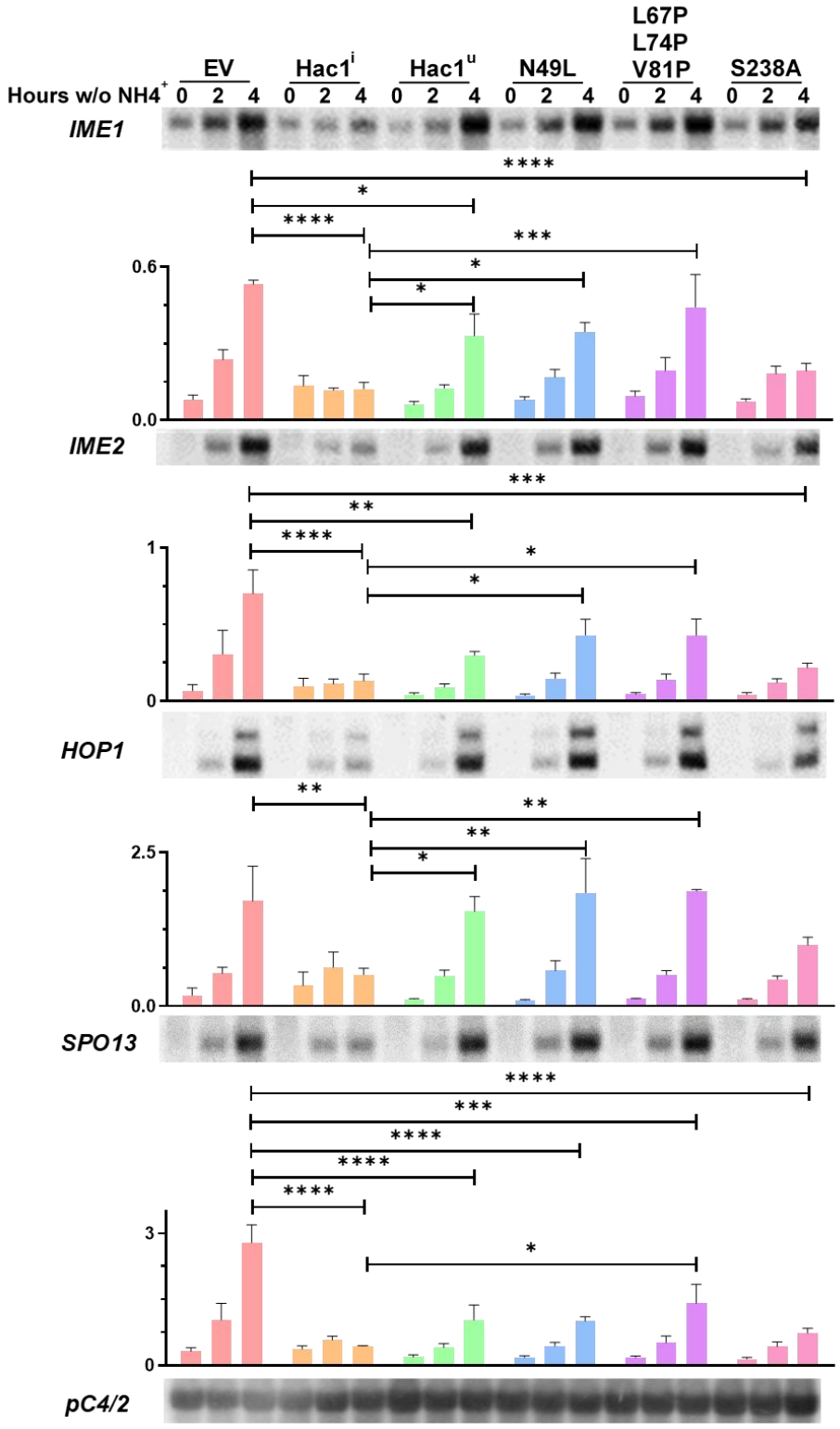

Figure 5-5 Hac1 conserved residues are required for negative regulation of EMGs during nitrogen starvation.

Northern blots analysis for *IME1*, *IME2*, *HOP1*, *SPO13*, and the loading control pC4/2 on RNA extracted from *rme1*Δ strains carrying and expressing the indicated Hac1 mutant or empty vector (EV). Mid-exponential growth phase cells were starved for nitrogen for the indicated time. The average and standard error from three independent biological repeats were calculated and quantified. Analysis was obtained from an ordinary two-way ANOVA with Tukey's correction for multiple comparisons on the ln-transformed data. Bars represent standard errors, ($p < 0.05$) using all data. *, $P \leq 0.05$; **, $P \leq 0.01$; ***, $P \leq 0.001$; ****, $P \leq$ 0. 0001. Nonsignificant P-values are not shown to allow for better view of the significant P-values.

5.3 Discussion

To observe and characterise the transcriptional repression by Hac1^{i} and its mutants in meiosis, I looked at the repression of URS1-*CYC1-lacZ* reporter expression in nitrogen-rich and nitrogen starvation conditions. Hac1^{i} bZIP transcription factor has been shown to effectively regulate transcriptional repression of URS1-controlled reporter plasmids in response to nitrogen sensing (Schröder et al., 2004). In this study expression of the mutant Hac1^{u} partially repressed induction of β-galactosidase from reporter plasmids under the control of URS1 (Figure 5.1 d). The lack of the Hac1^{u} ability to completely repress URS1 activation, as seen from Hac1^{i}, suggest the importance and requirement of the highly potent Hac1^{i} to negatively regulate induction of meiosis under nitrogen-rich conditions. The Hac1^{u} is missing the 18 aa present in the Hac1^{i} as a result of the unconventional splicing of *HAC1* mRNA, which result in replacing 10 aa with the 18 aa known to promote the proteins transactivation activity (Mori et al., 2000).

Mutation of the N49 to L49 within the Hac1^{i} DNA-binding region in the bZIP domain resulted a Hac1^{i} mutant construct (Hac1^{i}-N49L) incapable of completely repressing URS1. High levels of β-galactosidase activity were observed when meiosis was induced by nitrogen starvation in the presence of Hac1^{i}-N49L (Figure 5.2 d), suggesting a role for the conserved invariant asparagine in transcriptional repression of EMGs during vegetative growth.

Mutations in the leucine zipper heptad repeats by altering the three amino acids (L_1, X_6, L_2, X_6, V_3) to proline, is known to disrupt the dimerization of the protein by preventing the protein backbone to conform to an alpha-helix conformation (Morgan and Rubenstein, 2013). The Hac1^{i} triple mutant Hac1^{i}-L67P/L74P/V81P partially repressed induction of β-galactosidase from URS1-controlled reporter plasmids when meiosis was induced by nitrogen starvation (Figure 5.3 d). The apparent low level β-galactosidase induction indicates a role for the leucine zipper in transcriptional repression of EMGs in nitrogen-rich conditions. Given the β-galactosidase results from expressing Hac1^{i} bZIP domain mutants, by either possibly disrupting the DNA-binding or dimerization functions of Hac1^{i}, I propose that to completely abolish Hac1^{i} negative regulation, mutations in both bZIP regions should be tested. The distinct structural motif of Hac1^{i} bZIP domain, which consists of the DNA-binding region adjacent to the leucine zipper, might contribute to the Hac1^{i} mutants (Hac1^{i}-N49L and Hac1^{i}-L67P/L74P/V81P) retaining the ability to partially repress URS1 regulation.

Mutation of the residue responsible for the Hac1^{i} transactivation potential affected Hac1^{i} efficiency to repress β-galactosidase activity (5.4 d), which was mediated by

expressing Hac1^{i}-S238A and measuring activation of the URS1-controlled reporter gene. A single Ser-238 is the key residue in the 18 aa C-terminal domain of Hac1^{i} is suggested to be crucial for transactivation (Mori et al., 2000). This less active mutant derivative of Hac1^{i} Hac1^{i}-S238A showed to be less potent than Hac1^{i} in repressing URS1-*CYC1-lacZ* reporter expression, which agrees with the role of Hac1^{i}-S238A in regulating the UPR (Mori et al., 2000). Looking at results from the mutants Hac1^{u}, lacks the 18 aa containing Ser-238, and Hac1^{i}-S238A, confirming that the splicing of *HAC1* mRNA to produce the highly activated Hac1^{i} is required for efficient negative regulation of EMGs during meiosis through Ser-238.

Northern blot analysis of EMGs (*IME2*, *HOP1*, *SPO13*) showed results consistent with that of the β-galactosidase assays (Figure 5.5).

Overall, disruption of the Hac1 dimerization function and transactivation activity produce a Hac1 transcription factor with a partial effect on the negative regulation of EMGs. While disrupting the invariant asparagine within the Hac1 bZIP domain produced a non-functional negative regulator of EMGs. Given the general views and known structural constraints of bZIP proteins such as Gcn4 (Tzamarias et al., 1992), I propose that the Asn-49 directly contacts specific positions in the target DNA with high affinity and thus aligning the protein along the DNA. Given the results, the presence of the Asn-49 is suggested to be enough to interact, align, and transcribe DNA involved in transcriptional repression of EMGs when expressing Hac1 disrupted for dimerization function or transcriptional activity. The leucine zipper may in part be involved with positioning Hac1 on the DNA and stabilising it, but the basic DNA-binding region is central and more crucial for the Hac1 function. Nonetheless, the lack of Hac1 dimerization and potency render the Hac1 transcription factor unable to completely repress transcription of EMGs. However, from the early finding in this study, the leucine zipper seems to be important along with the invariant asparagine for transcriptional activation of genes involved in the UPR via UPRE. Highlighting an interesting possible difference for the structural role of Hac1 bZIP transcription factor in the UPR and meiosis pathways.

Results suggested that regulation of EMGs repression via Hac1^{i} during nitrogen-rich conditions requires key residues within the bZIP domain and the transactivation potential of Hac1^{i}.

6 Experiments to Measure Steady-State Levels of Hac1 and Hac1 Variants

6.1 Rationale

Detecting Hac1 steady expression levels are important to further justify results from the previous experiments and confirm expression of the Hac1 mutants. Western blotting using SDS-PAGE is the clear method to detect Hac1. In (Schröder et al., 2004) HA-Hac1^{i} expression was detected by Western blotting. HA-Hac1^{i} was detected from inducible p2UG-HA-Hac1^{i}, because the level of *HAC1* mRNA splicing in vegetatively growing cells was too low to detect Hac1^{i} by Western blotting or immunoprecipitation (Schröder et al., 2004). Expression of Hac1^{i} from p2UG-HA-Hac1^{i} is controlled by three glucocorticoid response elements, and strictly dependent on the presence of a glucocorticoid receptor (constitutively expressed from pG-N795; Schena et al, 1991) and steroids. HA-Hac1^{i} expression was induced by adding 50 µM 21-hydroxyprogesterone (deoxycorticosterone) (DOC) for 1 h into a culture grown to mid-log phase on synthetic acetate medium and was further detected using HA-tag antibody in a Western blot. This is made possible by the presence of an HA-tag (YPYDVPDYA) antibody epitope tag fused to the N-terminus of *HAC1*. This tag facilitated the detection of Hac1, its isolation, and purification.
The clear abundance of Hac1^{i} expressed by p2UG-HA-Hac1^{i} plasmid made it readily detectable using SDS-PAGE Western blotting. However, HA-Hac1^{i} was not examined for detectable expression levels when subcloned into pRS314 (Schröder et al., 2004).
In this thesis I used the HA-Hac1^{u}, HA-Hac1^{i} and its mutants subcloned into the low copy plasmid pRS314, a yeast centromeric vector with a *TRP1* marker and a multiple cloning site derived from pBluescript (Sikorski and Hieter, 1989) in the experiments. Therefore, detection of Hac1 and its mutants used in this study expressed from pRS314 was the aim from the following experiments. I used and optimised several methods to precipitate and detect steady levels of Hac1 and its mutants, such as protein precipitation using ammonium sulphate and protein precipitation using immunoprecipitation via beads.

6.2 Experiments to Extract and Detect Hac1^{i}

As mentioned in (Schröder et al., 2004) p2UG-HA- *HAC1^{i}* levels were detected by inducing cultures grown to mid-log in acetate containing media with 50 µM DOC for 1 h. Cells were then lysed with lysis buffer 25 mM sodium phosphate (pH 7.3), 150 mM NaCl, 1 % (v/v) Triton X-100, 10% (v/v) glycerol, 1 mM EDTA, 100 mM NaF, 1 mM Na_3VO_4, 0.05 % (v/v) β-mercaptoethanol, 120 mg/ml PMSF, 1 mg/ml pepstatin, 0.5 mg/ml leupeptin, and 10 mg/ml aprotinin or complete protease inhibitors, EDTA-free (Roche). Here I sought to assess an optimal lysis buffer conditions to extract HA-Hac1 and detect it by Western blotting from cells expressing HA-Hac1 from the low copy plasmid pRS314. This was done by testing detection of HA-Hac1^{i} when using different lysis buffers to extract the protein lysate. I used a similar lysis buffer described previously (Schröder et al., 2004), and two other different compositions of extraction lysis buffers.
Cells transformed with pRS314 or pRS314-HA-Hac1^{i} were grown to mid-log phase in acetate media (PSP2 – Trp) then moved into sporulation media (C-SPO – Trp), and collected at 0, 4, and 8 h time points of nitrogen starvation. Extracts were prepared as described in materials and methods, they were lysed with each of the following buffers: Lysis buffer 1 composed of 25 mM sodium phosphate ($Na_xH_{3-x}PO_4$, pH7.3), 150 mM NaCl, 1% (v/v) Triton X-100, 10% (v/v) glycerol, 10 mM EDTA, the reducing agent and protease inhibitors were then added to the buffer directly before treating the cells with the lysis buffer (5 mM β-mercaptoethanol, 2 mM PMSF, 1 µg/ml pepstatin, 0.5 µg/ml leupeptin, 6 mM AEBSF, and 10 µg/ml aprotinin). Lysis buffer 2 composition was exactly like buffer 1 but β-mercaptoethanol free. Lysis buffer 3 was a urea buffer composed of 8 M urea, 2.5 % (w/v) SDS, 50 mM Tris-HCl, pH7.5 (at 4 °C), 10 mM EDTA, again 5 mM β-mercaptoethanol, 2 mM PMSF, 6 mM AEBSF were added to the lysis buffer before lysing the cells. The whole cell extracts were quantified using either Bradford protein assay, for both extract from lysis buffer 1 and 2, or BCA protein assay for the urea-based buffer lysates. 50 µg of whole protein extracts for each time point (0, 4, 8 h) sample (pRS314 and pRS314-HA-Hac1^{i}) were loaded on to 12 % SDS-PAGE gels for Western blot experiments. Membranes transferred with the sample proteins were incubated with HA-tagged antibody o/n at 4 °C. However, results from probing the membrane with α-rabbit antibody showed no bands at the desired size (Data not shown). Furthermore, Coomassie staining, and destaining of the SDS-PAGE gel whole cell extracts showed that a wide range of proteins (~12 to > 180 kDa) can be reproducibly extracted from yeast cell in rich-nitrogen conditions. Discrete bands over a range of molecular weights are indicative of quality protein extracts from cells lysed with the different lysis buffers

(Figure 6.1). However, the absence of a more intense band in the sample lysates with overexpressed pRS314-HA-Hac1^{i} is suggestive of low amounts of HA-Hac1^{i} levels in the total protein lysates. Also, some protein extracts from the urea-based lysates were not expressed as in the other lysates extracted with the other two buffers.

These results then raised the question, if the absence of the HA-Hac1^{i} band in the Western blot is due to low expression levels of Hac1^{i} or if Hac1^{i} protein is unstable in the extraction lysis buffers. To address this question, I examined the detection of HA-Hac1^{i} when expressed from inducible p2UG-HA-Hac1^{i} and extracted using the different lysis buffers described above. Results showed that HA-Hac1^{i} was detectable when probing membranes with HA-tagged antibodies. 10 µg of whole cell extracts from each lysate sample buffer was loaded on to 12 % SDS-PAGE gels to detect Hac1^{i} (data not shown). This suggests that HA-Hac1^{i} is stable in the experimental lysis buffers, but when expressing the protein from pRS314-HA-Hac1^{i} its levels are not enough to detect using direct extraction methods. This led us to utilise other experiments to precipitate and detect HA-Hac1^{i} from the low copy plasmid pRS314-HA-Hac1^{i}.

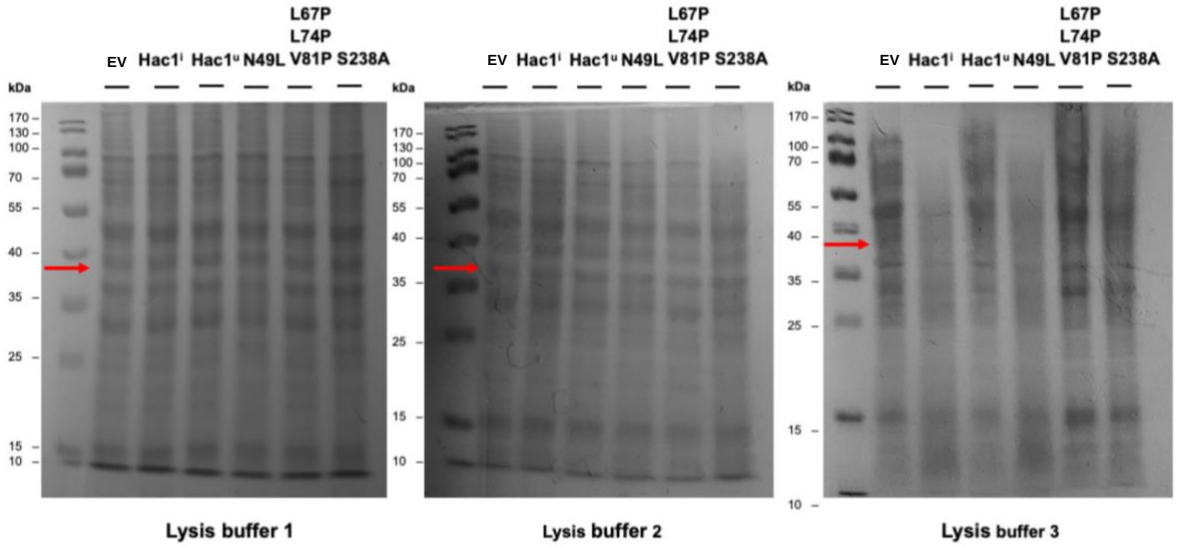

Figure 6-1 Coomassie Blue staining and destaining of whole cell extracts expressing EV and mutant Hac1 proteins.

12 % SDS-PAGE gels were stained with Coomassie brilliant blue. The different cell lysates were extracted using the three different lysis buffers shown under each gel image. The staining shows the presence of visible protein bands at different sizes, however when using buffer 3 (urea based) the protein bands are less present in some of the extract lanes. The red arrow indicates where the Hac1 protein is present.

6.3 **Experiments to Optimise Measurement of Steady-State Levels of Hac1^{i}**

After cell lysis, the most often used second step in protein purification procedures is a kind of rapid, bulk precipitation step. This can be accomplished in many ways, here I use two different precipitation methods to enrich HA-Hac1^{i} in the sample lysates to be detected by Western blotting: 1) ammonium sulfate precipitation $(NH_4)_2SO_4$, which is accomplished by altering the solvent conditions and taking advantage of the changes in solubility of HA-Hac1^{i} relative to other proteins and macromolecules in the whole cell extract. $(NH_4)_2SO_4$ is the reagent of choice for salt precipitation, due to it having a higher solubility when compared to phosphate salts (Wingfield, 1998). The basic theory aims to increase the solubility of globular proteins upon the addition of salt (<0.15 M), an effect known as salting-in. Hence, at higher salt concentrations, protein solubility will decrease, resulting in protein precipitation; this effect is known as salting-out (Green and Hughes, 1955). It should be mentioned that salting-out proteins consequently tends to enhance the stability of proteins native conformation. In contrast, salting-in ions usually tends to cause denaturation (Green and Hughes, 1955).

2) Immunoprecipitation, which is accomplished by purifying and enriching HA-Hac1^{i} levels from a whole cell extract, accomplished by binding the HA-tag to antibodies bound to beads. Furthermore, to optimise these purification methods, I used the inducible p2UG-HA-Hac1^{i} to examine the optimal conditions to enrich and detect ample amounts of Hac1^{i}. I suggest that this will then allow for detection of Hac1 and its mutants when expressed from the low copy plasmid pRS314.

6.3.1 **Hac1^{i} Fractionation by Ammonium Sulfate $(NH_4)_2SO_4$**

Based on previous work, Hac1^{i} in extracts was fractionated by differential precipitation using ammonium sulfate $(NH_4)_2SO_4$ (Kawahara et al., 1997, Mori et al., 1992). I used the lysis buffer described in (Mori et al., 1992) to lyse cultured cells. I aim to enrich and detect HA-Hac1^{i} expressed from the inducible p2UG-HA-Hac1^{i} as described in (Kawahara et al., 1997, Mori et al., 1992). Initially I tested detection of Hac1^{i} expressed from the inducible p2UG-HA-Hac1^{i} when loading 50 µg total protein lysate and compared it to the same total protein loading volume or 300 µg of low copy plasmid pRS314-HA-Hac1^{i}, in which I used the buffer described in (Mori et al., 1992). The results yielded a thin band at the HA-Hac1^{i} position, however a smear also appeared in the lane that can be a result of not enough reducing agent. As expected, no bands were detected in the lanes containing the extracts from pRS314-HA-Hac1^{i} (Figure 6.2 a). The previous results confirmed stable extraction of Hac1^{i} using the lysis buffer described in (Mori et al., 1992).

Whole lysate concentration titration to detect Hac1^{i}

For the following experiment whole cell extracts were collected from 100 ml cell cultures as described in materials and methods. First, to determine the optimal whole cell extract concentration required to detect a clear and sharp HA-Hac1^{i} band without precipitation, I tested detection of Hac1^{i} when loading various concentration of whole cell lysates. For this experiment, after the cells were lysed, the protein samples were then quantified. 8 Sample aliquots from a single extract were prepared with different protein concentrations ranging from 1 µg to 100 µg. The EV negative control sample (p2UG) was adjusted to match the highest concentration of the HA-Hac1^{i} containing sample, 100 µg of total cell lysate. Western blot observation revealed that lysates carrying EV at high concentration does not result in non-specific antibody binding. Furthermore, loading whole cell extract carrying the induced p2UG-HA-Hac1^{i} $\geq$ 10 µg was sufficient to detect a single HA-Hac1^{i} band migrating at ~ 40 kDa in 12 % SDS-PAGE gel (Figure 6.2 b). The HA-Hac1^{i} band detected is appreciably larger than its calculated molecular weight of Hac1^{i} 26,045. This behaviour can be due to the present of the HA-tag or abundance in charged residues as seen before (Kawahara et al., 1997), also failure to fully denature prior to electrophoresis can be a factor. This experiment also showed successful extraction of HA-Hac1^{i} using the lysis buffer described in (Wingfield et al., 1991).

Optimization of DTT concentration required for Hac1^{i} precipitation

I then asked the question, if I can reduce the concentration of DTT used in the extraction buffer from 0.5 mM, while still maintaining prevention of protein oxidation damage. I prepared a titration experiment using a range of DTT concentration from 0 mM to 0.5 mM to test the minimal amount of DTT required to reduce the disulfide bonds of proteins. The extraction buffer was prepared, once the cells were ready, the protease inhibitors were added to the buffer which was aliquoted into different 10 ml tubes. The DTT was then directly added at the appropriate concentration to the different buffers. The results showed that completely removing DTT from the lysis buffer caused Hac1^{i} oxidation, and as the concentration of DTT increased the oxidation damage decreases and a clean single band presented at the 0.5 mM treated extracts lane (Figure 6.2 c). Therefore, the optimal concentration of DTT to add to the lysis buffer is 0.5 mM as described in (Mori et al., 1992). Hence, I used the following lysis buffer as the basis for the protein extraction in this experiment: 200 mM Tris-HCl, pH8.0, 10 mM $MgCl_2$, 10% (v/v) glycerol, and 0.5 mM DTT, and various protease inhibitors (2 mM pepstatin A, 2 mM leupeptin, 2 mg/l chymostatin, 2 mM benzamidine, and 1 mM PMSF).

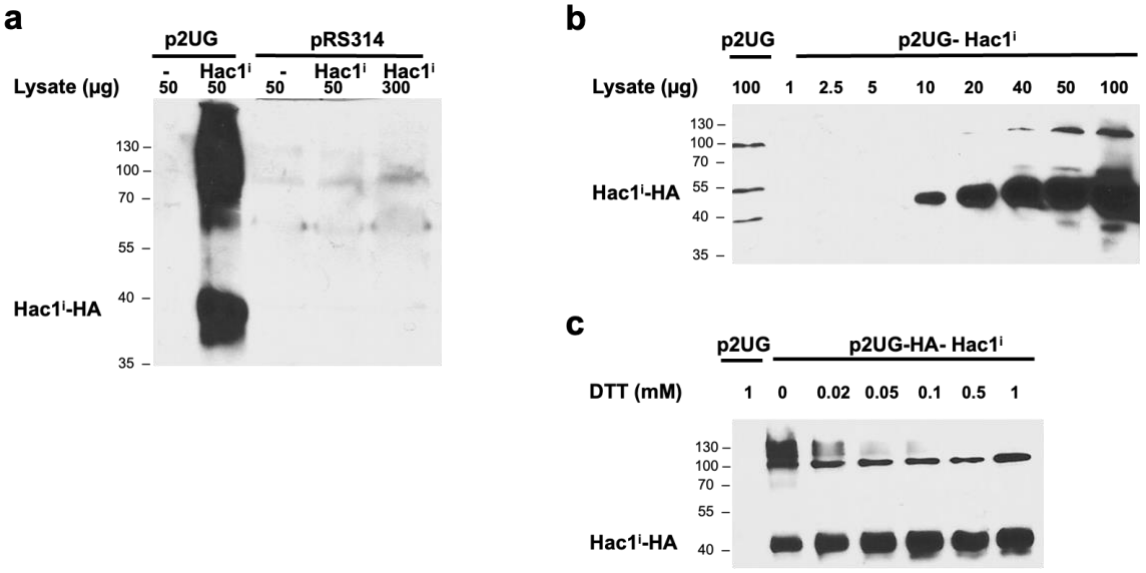

Figure 6-2 Hac1^{i} $(NH_4)_2SO_4$ fractionation.

Strains transformed with p2UG and p2UG-HA-Hac1^{i} are grown to mid-log phase then treated for 1 h with 50 µM deoxycorticosterone (DOC) to induce expression of HA-Hac1^{i}. **(a)** The Western blot showed that extraction and detection of Hac1^{i} using the recommended buffer in (Mori et al., 1992) was successful only when using extracts from strains inducing p2UG-HA-Hac1^{i} but not pRS314-HA-Hac1^{i}. Smearing in lane 2 is a result of inadequate concentrations of DTT added to the lysis buffer. ECL2 was used to detect peroxidase activity from HRP-conjugated antibodies. **(b)** Western blot for HA-tagged Hac1^{i} resulting from whole yeast extract concentration titration, which revealed that loading ~ 10 µg of lysate extract (derived from the induced p2UG-HA-Hac1^{i}) is sufficient to detect HA-Hac1^{i}. Chemiluminescence detection reagents were used to detect the HA-tagged Hac1^{i}. **(c)** Western blot for HA-tagged Hac1^{i} resulting from loading 10 µg whole yeast extracts, which were lysed with buffers containing different concentrations of DTT (DTT titration). 0.5 mM is the optimal concentration of reducing agent DTT to avoid protein oxidation and smearing in the lanes. Chemiluminescence detection reagents were used to detect the HA-tagged Hac1^{i}. Chemiluminescence detection reagents were used to detect the HA-tagged Hac1^{i}.

Observation of Hac1^{i} in the different stages of the whole cell lysate fractionation

Next, I observed the different fractions resulting from the steps involved in salting-out the whole cell protein extracts using $(NH_4)_2SO_4$. This will help us monitor the position of HA-Hac1^{i} throughout the fractionation process and confirm its presence in the fractioned whole cell protein lysate. Two lysis buffers were prepared 200 mM Tris-HCl, pH8.0, 10 mM $MgCl_2$, 10% (v/v) glycerol, and 0.5 mM DTT, and various protease inhibitors (2 mM pepstatinA, 2 mM leupeptin, 2 mg/l chymostatin, 2 mM benzamidine, and 1 mM PMSF). One of the lysis buffers additionally contained 10 % (v/v) $(NH_4)_2SO_4$, which is to be used as the lysis buffer for the salting-out experiment (L1), and the other $(NH_4)_2SO_4$ salt-free buffer was to be used for the control sample extraction (p2UG and p2UG-HA-Hac1^{i}) and resuspension solution for the precipitated fractions (L2). 200 ml of cultured cell containing either p2UG or p2UG-HA-Hac1^{i} were grown and induced as described in material and methods. The final harvested pellet for each sample strain was divided into two 1.5 ml microcentrifuge tubes. The pelleted cells were then resuspended with 450 µl of either L1 or L2 and lysed then quantified, the different whole protein lysate concertation ranged from ~ 20 µg / µl to 25 µg / µl. Control sample extracts (L2) were frozen to be used the next day in the Western blot. However, (L1) extracts were further centrifuged at 10,000 x g, to pellet and remove unwanted cell debris, the supernatant (~ 400 µl) was transferred into a 1 ml polycarbonate round bottom tube. It is important to mention that every centrifugation stage resulted in a fractionated pellet (P) and supernatant (S), the first fraction is (P_1 & S_1) after the first 10,000 x g centrifugation. S_1 was then transferred into a clean polycarbonate tube and centrifuged at 100,000 g for 1 h, at 4°C precipitating a sample pellet (P_2 & S_2), P_1 and P_2 were resuspended in 200 µl of L2. Then, ~ 245 µl of S_2 sample was transferred into a clean polycarbonate tube and 455 µl of $(NH_4)_2SO_4$ for a final concentration of 2.6 M was added to salt-out the whole cell extract including HA-Hac1^{i}, the remaining 155 µl volume of S_2 was collected. The 2.6 M concentrated sample was also centrifuged at 100,000 g for 1 h, at 4°C, producing a visible pellet and supernatant (P_3 & S_3), here P_3 was resuspended in 200 µl of L2 to later be dialysed and 200 µl of S_3 was also collected for dialysis. Finally, from the remaining S_3 I took ~ 350 µl and treat it with 2.9 M of $(NH_4)_2SO_4$ and centrifuged to salt-out any remaining proteins including residual HA-Hac1^{i} (P_4), the pellet here was also resuspended with 200 µl L2 (Figure 6.3).

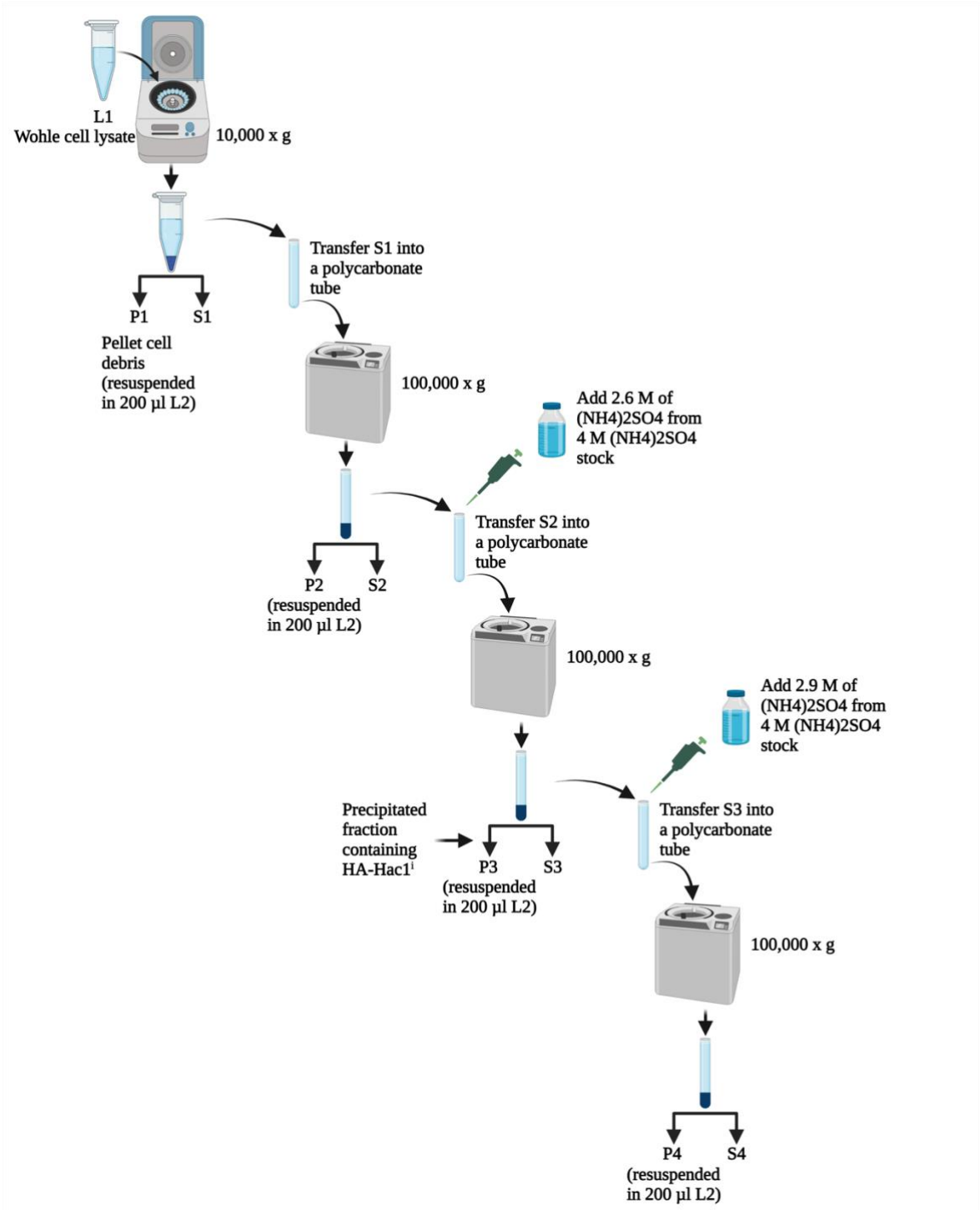

Figure 6-3 **Fractionation scheme to observe Hac1^{i} precipitation.**

Created with BioRender.com.

Dialysing the collected fractions to quantify protein concentration

After fractions were collected, the $(NH_4)_2SO_4$ samples were subjected to dialysis. This allows for the removal of $(NH_4)_2SO_4$. This procedure is necessary to proceed to subsequent steps in the purification process and detect HA-Hac1^i in the collected fractions by immunoblotting. I dialysed the samples (S_1, S_2, P_3, P_4, S_3) extensively o/n against dialysis buffer (20 mM HEPES (pH 7.9), 50 mM KCl, 0.25 mM EDTA (pH 8.0), 0.5 mM DTT) described in materials and methods. The starting sample (S_1), extracted from strains carrying p2UG-HA-Hac1^i, contained ~ 9 mg / ml of total protein in the cell lysate. As expected, results from the Western blot showed HA-Hac1^i detection in the appropriate suggested sample differentiation fractions (Figure 6.4 a). HA-Hac1^i detected from extracts lysed with either L1 or L2 displayed identical migration behaviour and intensity when I loaded 50 µg of each sample and run on 12 % SDS-PAGE gel. Both nontreated S_1 and S_2 kept the ability to solubilise HA-Hac1^i evident from the intense single band detected at the appropriate position (Figure 6.4 a). Figure 6.4 a also showed precipitated whole protein extracts (P_3) to contain HA-Hac1^i when using α-HA, which was clear from the detected intense band at position ~ 37 kDa identical to the position of unfractionated HA-Hac1^i (control). However, P_3 fraction also displays precipitation of other proteins highlighted by the nonspecific α-HA binding or the smearing may indicate non-specific binding of the α-HA antibody. Also, it may be during the lengthy process that the sample precipitates and loses a peptide-based protease inhibitor. Leupeptin is an aldehyde and forms a hemiacetal with active site serines of serine proteases hence the modification is covalent and should be stable. It may be more likely that a non-covalent peptide-based protease inhibitor is precipitated, or at high [NH4+] the aldehyde of leupeptin is converted to an imine. P_4 showed a faint single HA-Hac1^i band. Overall, Hac1^i is present as expected in the different fractions, and specifically in the whole protein fraction. Hac1^i was followed throughout the experiment, it was found to precipitate when adding 2.6 M $(NH_4)_2SO_4$ along with other proteins leaving residual amounts of Hac1^i in the following treated fraction.

Optimization and detection of Hac1^i using various concentrations of $(NH_4)_2SO_4$ from the whole cell lysate precipitant

Given these previous results, it is clear HA-Hac1^i was capable of being fractionated and present in the fractionated whole cell lysate, it further needs to be salted-out using an optimal $(NH_4)_2SO_4$ concentration to obtain a single Hac1^i band (Kawahara et al., 1997). To test the best concentration of $(NH_4)_2SO_4$ required to detect the single band HA-Hac1^i from the whole protein lysate fraction in this study, I further fractionated the total protein fraction (P_3) with different concentration of $(NH_4)_2SO_4$. The 100 ml cultures for this test

were grown and induced as mentioned before. I used both L1 and L2 lysis buffers to extract cell lysates. The protein concentration was between 20 µg and 25 µg / µl. This creates two groups to be tested with various $(NH_4)_2SO_4$ final concentration. I resuspended 3 whole cell extracts pelleted fractions for each group in ~ 400 µl of L2 (group 1 extracted with L1 and group two extracted with L2), which were obtained by precipitating whole cell lysates by a final concentration of 2.6 M $(NH_4)_2SO_4$. Samples of both groups were then treated with $(NH_4)_2SO_4$ to final concentrations of either 1 M, 1.5 M, or 2 M (Kawahara et al., 1997) and adjusted to a final volume of 700 µl in the polycarbonate tube (I used 2 tubes for each sample). Samples were centrifuged at 100,000 g for 1 h, at 4°C to precipitate HA-Hac1^i. Afterwards ~ 200 µl of the supernatants were collected, and the precipitated proteins were resuspended in 200 µl of L2 (collected into one tube). The resulting 12 samples were dialyzed extensively against dialysis buffer o/n at 4°C. The samples were then quantified, the protein concentrations ranged between 2 and 3 mg / ml. I must explain that the result of examining the Western blots loaded with the lysates extracted with either L1 or L2 (group 1 and 2) are comparable (Figure 6.4 b and c), therefore they are explained together here. Immunoblotting experiments with α-HA revealed that, no nonspecific binding of α-HA was detected from extract carrying p2UG plasmids alone; in contrast, as expected HA-Hac1^i was detected from the control extracts carrying p2UG-HA-Hac1^i, first two lanes in (Figure 6.4 b and c). Both positive and negative controls were not fractionated. The third lane shows HA-Hac1^i detection when loading 10 µg from supernatant centrifuged at 10.000 x g for 10 min, at 4°C. Interesting to see, that the samples treated with different final $(NH_4)_2SO_4$ concentrations showed a clear increase in HA-Hac1^i band intensity (P) as it decreased in the supernatant (Figure 6.4 b and c). In other words, in the lanes 5-7 the higher the concentration the less the band strength; subsequently, in the lanes 8-10 the higher the concentration the more the band strength. Thus, from the previous data I observed that precipitating the whole cell extract by a final concentration of 2.6 M $(NH_4)_2SO_4$ results in a whole protein fraction containing HA-Hac1^i. Then resuspending the whole protein fraction precipitated protein pellet in L2 and obtaining a second fraction by a final optimal concentration of 2 M $(NH_4)_2SO_4$ revealed a single Hac1^i band. This fraction has the HA-Hac1^i that ran on an SDS-PAGE 12 % gel as a single band. These results correlate with the previous results seen in (Kawahara et al., 1997). Furthermore, preliminary observations comparing lane 2 (with 10 µg lysate) to lane 10 (with 50 µg of the dialysed solubilised final 2 M pelleted fraction) (Figure 6.4 b and c) indicates less than expected enrichment for the HA-Hac1^i protein. This led me to investigate a different method to precipitate Hac1^i.

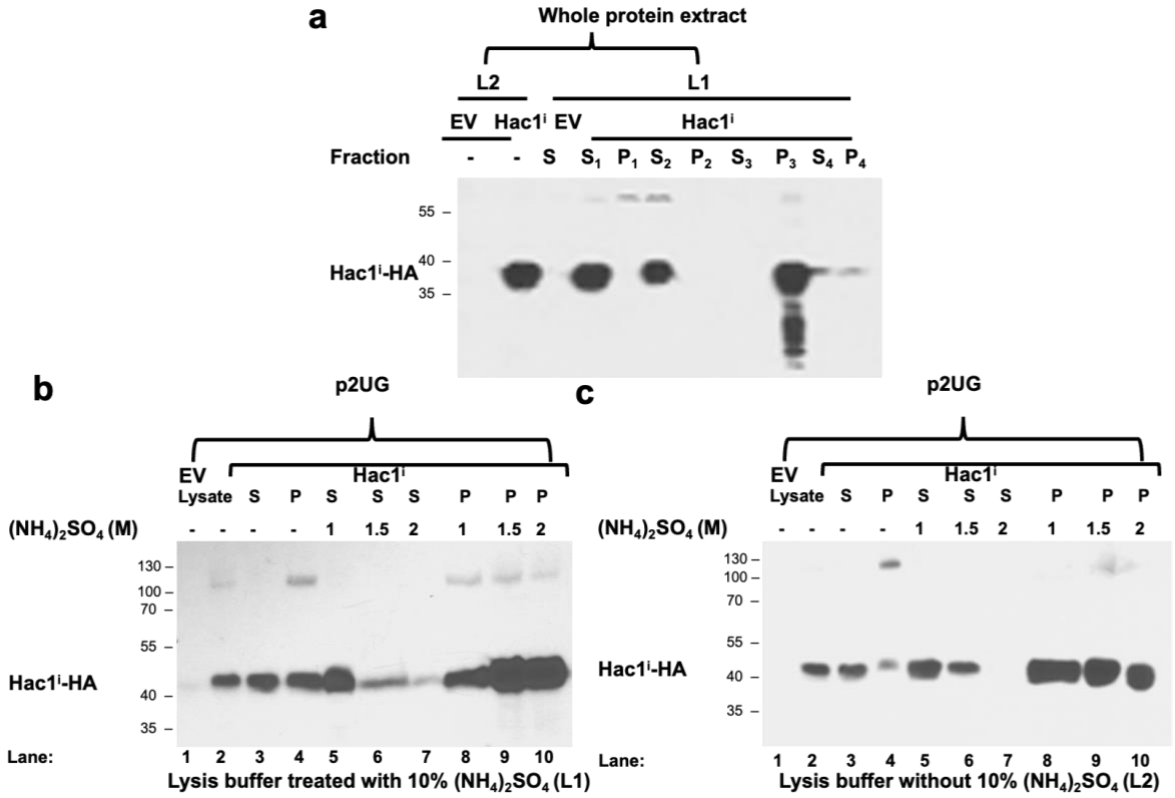

Figure 6-4 Ammonium sulfate ($(NH_4)_2SO_4$) fractionation of HA-tagged p2UG-Hac1^i using different $(NH_4)_2SO_4$ concentrations.

(a) 50 µg of total protein sample was loaded into each lane to detect the presence of HA-tagged Hac1^i within the different samples (S for supernatant and P for pelleted fraction). Western blot revealed 50 µg of proteins in the 2.6 M $(NH_4)_2SO_4$ whole cell protein extract fraction to contain HA-tagged Hac1^i at the appropriate molecular weight when compared to the positive control sample Hac1^i, which was not $(NH_4)_2SO_4$ fractionated. **(b)** A Western blot to detect HA-tagged Hac1^i in the precipitated pellets and supernatant at different $(NH_4)_2SO_4$ concentrations. All protein lysate samples were extracted using lysis buffer treated with 10 % (v/v) $(NH_4)_2SO_4$ (L1) then centrifuged at 10,000 x g for 10 min, sample seen in lane 2 (positive control). All samples were then treated with 2.6 M $(NH_4)_2SO_4$ and centrifuged at 100,000 x g for 1 h, at 4 °C, seen in lane 3 and 4. Then all the pellets were solubilized in either 1 M, 1.5 M, and 2 M $(NH_4)_2SO_4$ and centrifuged at 100,000 x g for 1 h, at 4 °C, shown as S (supernatant) and P (pelleted fraction) on the rest of the lanes. HA-tagged Hac1^i was detected in all the precipitated P samples but with different intensities depending on the $(NH_4)_2SO_4$ concentrations used, S samples of each corresponding P sample also revealed the non-precipitated HA-Hac1^i. ECL2 was used to detect peroxidase activity from HRP-conjugated antibodies. **(c)** Western blot showed identical results to Western blot (a) and is labeled the same, the difference is in the whole cell extract lysis buffer, here the lysis buffer was not treated with 10% (v/v) $(NH_4)_2SO_4$ (L2). Chemiluminescence detection reagents were used to detect the HA-tagged Hac1^i.

6.3.2 Hac1^{i} Immunoprecipitation Using Capture of the anti-HA antibody With Protein A Coupled to Agarose Beads

The lysis buffer used in the previous experiment (L2) was also used to extract whole cell lysates for the Immunoprecipitation (IP), with some modifications. When preparing the lysis buffer I removed $MgCl_2$, used previously to optimise electrophoretic mobility shift assays for DNA specific binding (Mori et al., 1996), a step not required for my study. Also, no glycerol was added to the buffer. I also removed DTT to avoid possible reduction damage of the α-HA antibodies during the incubation step in an IP. In addition, 0.5 % (v/v) Triton X-100 was added to the buffer to insure good solubilisation of protein during IP incubation.

Observation of the of Hac1^{i} stability during o/n incubation with overhead rotation at 4°C

100 ml of cell cultures for strains carrying p2UG-HA-Hac1^{i} were grown and prepared as before, then lysed using the optimised lysis buffer. Whole protein lysates were extracted and prepared as described in material and methods and quantified for all samples. First, I wanted to analyse the stability of the HA-Hac1^{i} protein extracted with optimised lysis buffer and observe its stability throughout different time points of incubation with overhead rotation at 4°C. 10 µg of cell extracts from culture inducing p2UG-HA-Hac1^{i} was added to different microcentrifuge tubes and adjusted with the buffer to a final volume of 200 µl, to test HA-Hac1^{i} detection on Western blot from different time point incubations (0, 1, 2, 3, 4, o/n). Results showed comparable sharp HA-Hac1^{i} bands throughout the various time points of protein lysate incubation, even when compared to lane 2 the 0 h positive input p2UG-HA-Hac1^{i} (Figure 6.5 a). Now that I observed o/n stability of HA-Hac1^{i} protein during incubation with overhead rotation at 4°C.

Hac1^{i} immunoprecipitation using various concentrations of protein lysate

I next asked at what whole protein lysate input in an IP sample do I observed detection of HA-Hac1^{i} expressed from inducible p2UG-HA-Hac1^{i}. For this experiment during IP, free-unbound α-HA antibody form immune complexes with HA-Hac1^{i} in the lysate. The immune complexes are then captured on the Sepharose carrying immobilized protein A. First, I prepared an IP titration experiment to analyse the total protein lysate concentration required to detect HA-Hac1^{i} (expressed from p2UG-HA-Hac1^{i}) on a Western blot. I loaded 10 µg of total protein lysate expressing p2UG-HA-Hac1^{i} as the control input, and prepared a range of 1 x, 2 x, 3 x, 4 x, 5 x of total protein lysate concentration in final volumes of 200

µl, then left the samples to incubate for ~ 1 h, at 4°C with overhead rotation. Samples were then washed and prepared as described in materials and methods. Western blot observation showed that the IP from the negative control sample (p2UG) and the positive samples displayed high background (data not shown). Because of this result it is difficult to conclude efficient concentrations of total protein lysate required to detect HA-Hac1^{i}. The high background can be due to incomplete sample washing, non-specific proteins binding to the beads or antibodies, or high amount of antibody eluting.

Hac1^{i} immunoprecipitation using various concentrations of α-HA antibody

Hence, I decided to use 50 µg of total cell lysate to examine detecting HA-Hac1^{i} when using various concentrations of α-HA antibody to bind our target protein. I hypothesise that adding compatible amounts of α-HA antibody to the sample would overcome the possible non-specific binding of the protein. I prepared the samples and added a volume range of α-HA antibody (0.5, 1, 1.5, 2 µl / 200 µl) to the prepared samples of lysate. Samples were then run on a 12 % SDS-PAGE gel for 2 h, to allow for better resolution. Simultaneously, I ran the positive (p2UG-HA-Hac1^{i}) and negative (p2UG) samples collected from beads that have been eluted before. In which after I eluted the protein using 6 x SDS-PAGE sample buffer with β- mercaptoethanol I then took the beads and treated them again with 6 x SDS-PAGE sample buffer with β- mercaptoethanol and boiled them for another 5 min. This second elution lane 2 (Figure 6.5 b) is to collect a sample to observe if any Hac1^{i} remains bound to the beads after the first elusion. The results shown in (Figure 6.5 b) display the heavy chains of the α-HA antibody signals as before, specifically at position ~ 55 kDa and interfering with HA-Hac1^{i} target protein position. However, the lanes with the second collected elution samples from the beads, that have been eluted before to collect the target protein, have no visible bands as expected. This high background problem could be a result of α-HA antibody being used in both the IP and Western blot, also since the heavy-chain (HC, 55 kDa) of the IP antibody is also eluted from the beads and size-fractionated by SDS-PAGE with HA-Hac1^{i}, the secondary antibody, a HRP conjugated secondary antibody detects the primary antibody and on western blot will also recognise the HC band on Western blot filters.

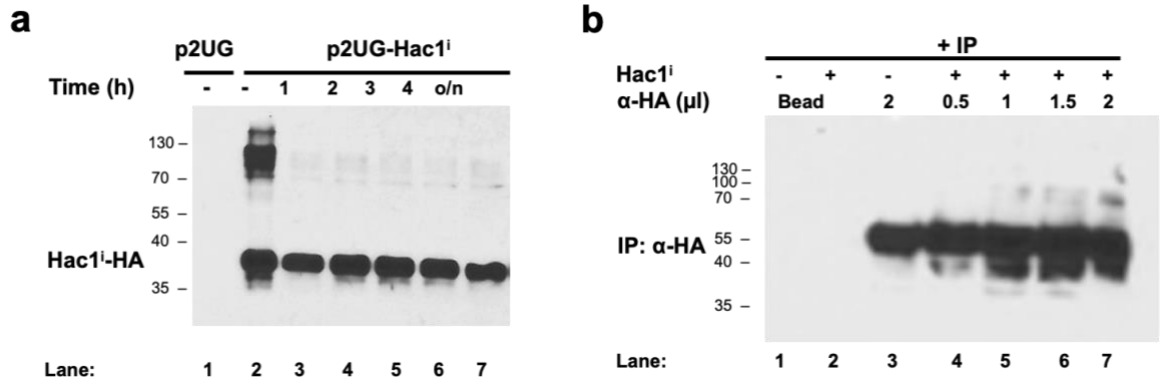

Figure 6-5 Hac1^{i} Immunoprecipitation with α-HA antibodies.

(a) Western blot detecting HA-tagged Hac1^{i} expressed from p2UG-HA-Hac1^{i} after mid-log phase culture induction with 50 µM deoxycortcosterone (DOC) for 1 h. Observe stability of HA-Hac1^{i} protein behaviour during different time point incubation with overhead rotation at 4°C. **(b)** Western blot to detect immunoprecipitated Hac1^{i} revealed heavy chains of α-HA antibody when loading 50 µg of cell lysate and various concentrations of α-HA antibodies. Lanes 1 and 2 show samples collected from the second round of bead elusion remaining from the collected samples shown in lane 3 and 7.

6.3.3 Hac1^{i} Immunoprecipitation Using Magnetic Beads

To overcome the heavy chain binding problem resulting from the use of the Free Antibodies approach and the detachment of the HC, I used magnetic beads. I used highly specific α-HA monoclonal antibody pre-immobilized to magnetic beads to precipitate Hac1^{i} at high levels. For this experiment I optimized the previous mentioned lysis buffer with respect to the protocol recommended by the product provider (Thermo Fisher Scientific). I added 10 mM EDTA and replaced 0.1 % (v/v) Triton-X-100 with the non-ionic detergent 0.05 % (v/v) Tween-20. To test the optimised buffer's ability to extract HA-Hac1^{i} from the strain carrying the inducible p2UG-HA-Hac1^{i}, I grew the cell cultures as described in materials and methods and induced the cultures with DOC for 1 h. I extracted the whole cell lysates using buffer (200 mM Tris-HCl, pH 8.0, 10 mM EDTA, 0.05 % (v/v) Tween-20 and 0.5 mM DTT), and various protease inhibitors added before lysing the cells (2 mM pepstatin A, 2 mM leupeptin, 2 mg / l chymostatin, 2 mM benzamidine, and 1 mM PMSF). Results from loading 10 µg of protein lysate on a 12 % SDS-PAGE gel showed a clear single band migrating at the appropriate HA-Hac1^{i} size of ~ 37 kDa (Figure 6.6 c).

Hac1^{i} immunoprecipitation using various concentrations of protein lysate

Now that I know Hac1^{i} can be extracted successfully using this buffer I asked the question, at what concentration of total cell lysate can I detect HA-Hac1^{i} in an IP using the α-HA magnetic beads. To answer this question, I tested a titration of different input lysate concentration to evaluate at what point do I detect HA-Hac1^{i} using the α-HA magnetic beads. It is important to note that the α-HA magnetic beads have a binding capacity of ≥ 10 µg GST-RRK-HA (70 kDa fusion protein) / mg of beads. For the experiments, as recommended I use 10 µg of beads / sample. The magnetic beads were prepared as described in materials and methods. I set up an IP for samples with concentrations of (10, 25, 50, 100, 500 µg) for whole cell lysate concentration input and adjusted all samples to a final volume of 200 µl using the buffer alone without protease inhibitors. Samples were incubated ~ 2 h, at 4°C with overhead rotation Samples were then washed and prepared as described in materials and methods and loaded onto a 12 % SDS-PAGE gel. Excitingly, immunoblotting revealed that HA-Hac1^{i} can be detected from IP samples as a single band extracted from whole cell lysates ≥ 50 µg (Figure 6.6 a); Hac1^{i} might run higher in the input sample (lane2) compared to the IP Hac1^{i} due to the absence of a reducing agent in the elution buffer, which leads to the formation of disulfide bonds between cysteine amino acids. Lane 2 which contains the positive control input shows HA-tagged Hac1^{i} loaded at 10 µg cell lysate (Figure 6.6 a). These results also support the suggestion that 10 µg of magnetic beads were able to bind the distinguishable increasing concentration of HA-tagged Hac1^{i} from each sample (Figure 6.6 a). Given these results I decided to use 75 µg of whole cell lysate to IP HA-Hac1^{i} expressed from the inducible plasmid p2UG-HA-Hac1^{i} to optimise the IP method. Moreover, even though HA-Hac1^{i} shows a single band migrating at the desired size, there is still some specific signals that increases as the input sample increased. Also, the HA-Hac1^{i} positive control shows nonspecific binding of α-HA indicative of incomplete breakdown of disulfide bonds and sample oxidation. This can be attributed to the elution method used here, in that the 1 x SDS-PAGE sample loading buffer used to elute HA-Hac1^{i} does not contain any reducing agent. Therefore, I proposed that adding a reducing agent, such as β-mercaptoethanol, to the SDS loading dye would prevent the apparent background.

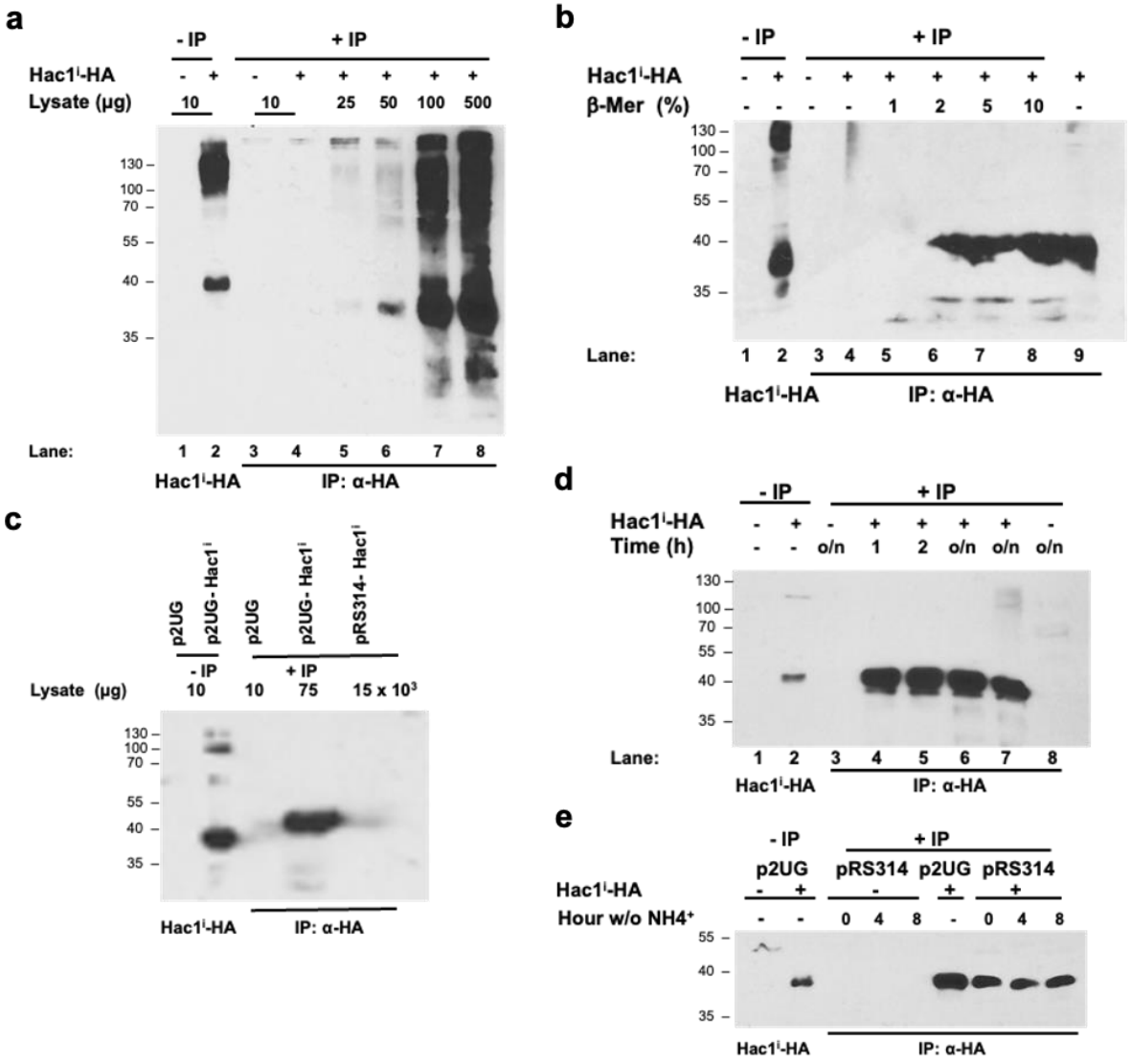

Figure 6-6 Hac1^{i} Immunoprecipitation using magnetic beads (Method optimisation)

-IP indicates samples were lysed but not immunoprecipitated (controls), and + IP indicates samples were lysed and immunoprecipitated **(a)** Western blot of an input lysate concentration titration (10, 25, 50, 100, 500 µg) which is inducing p2UG-HA-Hac1^{i}. Whole cell lysate concentration ≥ 50 µg was enough to detect HA-Hac1^{i} using 10 µg α-HA magnetic beads. Smearing in the lanes is due to eluting the protein sample with 1 x SDS-PAGE dye without β-mercaptoethanol. **(b)** Western blot detecting HA-Hac1^{i} from 75 µg lysate input treated with a concentration titration of β-mercaptoethanol after eluting the IP sample with 1 x SDS-PAGE dye. Treating the eluted sample with ≥ 2 % (v/v) β-mercaptoethanol overcomes the smearing shown in Western blot (a). **(c)** Detection of HA-Hac1^{i} expressed from both p2UG-HA-Hac1^{i} and pRS314-HA-Hac1^{i}. **(d)** Overnight incubation (o/n) at 4°C with overhead rotation of IP samples for lysates expressing p2UG-HA-Hac1^{i} results in comparable HA-Hac1^{i} bands when compared to the other time points. Lane 7 shows HA-Hac1^{i} band IP from 75 µg p2UG-HA-Hac1^{i} containing lysate mixed with ~ 1 ml (19 mg) lysate containing pRS314, lane 8 as expected shows no band from IP lysate containing pRS314. **(e)** Western blot showing comparable and stable levels of HA-Hac1^{i} bands expressed at different sporulation time points.

Detection of Hac1^{i} single band using a titration of different β-mercaptoethanol concentrations

To accomplish this, I created a titration experiment using different concentrations of β-mercaptoethanol to analyse the concentration required to ensure break down of protein HA-Hac1^{i} disulfide bonds in the sample. Usually, 5 % (v/v) β-mercaptoethanol in the SDS-PAGE loading dye (used in my lab) is optimal to ensure complete reduction of disulfide bridges leading to complete Hac1^{i} protein denaturation, as seen from results before. After I run an IP (using 75 µg in a final volume of 200 µl) as described above and eluted the samples after boiling for 5 min with 1 x SDS dye at 100°C I allowed the samples to cool down for 5 min. The samples were then placed in the magnetic racks and the supernatants were collected in clean microcentrifuge tubes. At this stage I added different concentration (0 %, 2 %, 5 %, 7 %, 10 %) (v/v) of β-mercaptoethanol to each sample and boiled again for 5 min. These samples were then loaded onto a 12 % SDS-PAGE gel. Western blot observation revealed that when no β-mercaptoethanol was added in the non-IP positive control sample, a clear lack of complete reduction of HA-Hac1^{i} is apparent from the background present in lane 2 (Figure 6.6 b). Compared to the last lane 9 (Figure 6.6 b) where non-IP positive control shows a single HA-Hac1^{i} band. For this sample, I prepared 10 µg of whole protein lysate that has been incubated alongside the IP samples with 5 % (v/v) β-mercaptoethanol lane 9 (Figure 6.6 b). Furthermore, the IP positive control with 0 % (v/v) β-Mercaptoethanol also showed some smearing and background, however there was no detection of a single band. Nevertheless, when looking at the IP sample lanes treated with ≥ 2 % β-Mercaptoethanol they all displayed a single band at the position expected for HA-Hac1^{i} and comparable to the non-IP positive control HA-Hac1^{i} position (Figure 6.6 b). This further suggest that adding at least 2 % (v/v) β-Mercaptoethanol was optimal to reduce HA-Hac1^{i} disulfide bonds allowing for complete protein denaturation and allow for the appearance of a HA-Hac1^{i} single band.

Hac1^{i} immunoprecipitation and detection expressed from the single copy plasmid pRS314-HA-Hac1^{i}

Given these results I now have an optimised IP method to detect HA-Hac1^{i} from p2UG-HA-Hac1^{i} and asked if I can now detect HA-Hac1^{i} from single copy plasmid pRS314-HA-Hac1^{i} using the same method. 250 ml culture of cells expressing pRS314-HA-Hac1^{i} were grown to mid-log phase (A_{600} = 0.4- 0.8) in acetate selective growth media (PSP2-Trp). The cells were collected and prepared as described in materials and methods. The samples were lysed, and the IP was set up as previously mentioned. Again, for the IP positive

control I used 75 µg of whole protein cell lysate extracted from p2UG-HA-Hac1^{i} and 15 mg of whole protein cell lysate sample carrying the single-copy plasmid pRS314-HA-Hac1^{i}. Because the volume of the single copy plasmid lysate extract is ~ 1 ml, I added lysis buffer (free from DTT and protease inhibitors) to the positive control IP sample to reach a final volume of 1 ml. After ~ 2 h, at 4°C of incubation with overhead rotation, the samples were collected, washed, and run on a 12 % SDS-PAGE gel. When examining the immunoblot I observed that 10 µg of α-HA magnetic beads retain the ability to bind and present HA-Hac1^{i} in a volume of 1 ml with ~ 2 h, at 4°C incubation with overhead rotation (Figure 6.6 c). Furthermore, the IP sample from the lysate carrying pRS314-HA-Hac1^{i} showed a faint band at the position of Hac1^{i}. This result was exciting, I finally observed a possible HA-Hac1^{i} band from the single-copy plasmid. Given this observation suggest that the IP method requires some optimisation to clearly detect pRS314-HA-Hac1^{i}. Thus, I asked if the components (protease inhibitors, DTT and other proteins) present in the single-copy plasmid lysate extract interferes with the magnetic bead's immune complex formation. To address this question, I incubated 75 µg of whole cell lysate carrying p2UG-HA-Hac1^{i} in 1 ml final volume of lysate extract from cultures carrying pRS314 alone. I also tested the positive IP samples at different incubation time points 1 h, 2 h, and o/n at 4°C with overhead rotation. Previous results from this study showed there is no visible difference in detection of HA-Hac1^{i} when incubating the lysate sample alone for 1 h or o/n (Figure 6.6 a). However, testing detection of HA-Hac1^{i} from the whole cell lysate when incubating with α-HA magnetic beads at different time points was done because later in the experiment, when testing sample extracts containing Hac1 mutants expressed from pRS314 extracted from different time points, the IP samples will be incubated o/n at 4°C with overhead rotation. First, I set up the o/n IP samples 75 µg lysate extract containing p2UG-HA-Hac1^{i} and adjusting to a final volume of 1 ml, and placed them in the overhead rotator, then the next day I incubated the 1h and 2 h samples. Afterwards samples were washed and run on a 12 % SDS-PAGE gel. Figure 6.6 d shows that 4°C o/n IP incubation does not effect the efficiency of the IP when comparing (lane 4, 5, and 6) 1, 2 h detected protein to the o/n HA-Hac1^{i} single bands detected on a Western blot when loading 75 µg of lysate extract containing p2UG-HA-Hac1^{i}. Also, o/n IP incubation of empty vector with α-HA magnetic beads did not yield any non-specific binding (lane 1, Figure 6.6 d). Moreover, I detected HA-Hac1^{i} (lane 7) (Figure 6.6 d) from the o/n IP incubation of 75 µg p2UG-HA-Hac1^{i} expressing lysate mixed with the single-copy plasmid lysate, which indicates that the components in the lysate extracts from the cultures expressing the single-copy plasmid does not affect the IP efficiency when compared to the o/n IP in lane 6. Lane

8 indicates that when incubating the lysates carrying the pRS314 o/n, the beads do not bind to other nonspecific proteins within the lysates and thus no bands appeared (Figure 6.6 d). Hence given these results, I hypothesised that longer incubation of the IP sample with the single-copy plasmids o/n will increase the binding probability for the HA-Hac1^{i}.

Observation of Hac1^{i} expressed from low-copy plasmid after o/n incubation with overhead rotation at 4°C

To test this hypothesis, ~ 650 ml of cultures expressing pRS314-HA-Hac1^{i} were grown to mid-log phase (A_{600} = 0.4-0.8) in acetate selective growth media (PSP2-Trp) then transferred into sporulation media (C-SPO-Trp). ~ 200 ml of culture was collected for each time point of sporulation 0 h, 4 h, and 8 h. Cells were then harvested, and lysates were extracted as described before for the IP samples. I set up the IP using 20 mg of whole cell lysates in a final volume of 1 ml, and samples were incubated o/n in an overhead rotator at 4°C. Excitingly, immunoblotting results showed comparable levels of HA-Hac1^{i} expressed at different sporulation time points (Figure 6.6 e). I also ran a positive control IP (p2UG-HA-Hac1^{i}) to analyse the success of the IP procedure. All the detected HA-Hac1^{i} run as single bands at the appropriate size ~ 37 kDa (Figure 6.6 e).

Detection of the mutant Hac1^{i} expressed from the low-copy plasmid at different nitrogen starvation time points

Furthermore, since HA-Hac1^{i} expressed at the different nitrogen starvation time points are comparable, I decided to test the expression levels from the Hac1^{u} and Hac1^{i} mutants at 0 h and 8 h. These results were indicative of a working method to extract, precipitate and detect steady levels of HA-Hac1^{i} induced from the low-copy plasmid pRS314-HA-Hac1^{i}. In which the cells were lysed with ice-cold lysis buffer (200 mM Tris-HCl, pH8.0, 10 mM EDTA, 0.05 % (v/v) Tween-20 and 0.5 mM DTT), and various protease inhibitors added before lysing the cells (2 mM pepstatin A, 2 mM leupeptin, 2 mg / l chymostatin, 2 mM benzamidine, and 1 mM PMSF). Once cells were lysed, protein lysates were quantified, and the IP samples were set up in a 1.5 ml microcentrifuge tube (x µl of lysate + 10 µg α-HA magnetic beads and adjusted with lysis buffer to desired final volume) on ice. Samples were then left to incubate for the allocated time in with overhead rotation at 4°C. Then the HA-Hac1^{i} bound to the α-HA magnetic beads were collected by placing the tubes in a magnetic rack and washed. Samples were then eluted with 1 x SDS-PAGE sample buffer boiled for 5 min at 100°C, the eluted samples were then transferred into a clean 1.5 ml microcentrifuge tube and ~ 2 – 3 % (v/v) β-Mercaptoethanol were added to each sample

and boiled again for 5 min at 100°C. Sample tubes were spun and ready to load and run for ~ 2 h in 12 % SDS-PAGE gel for Western blotting.

Now, using the working method as described before I prepared the samples for cultures expressing HA-Hac1^{i}, HA-Hac1^{u}, HA-Hac1^{i}-N49L, HA-Hac1^{i}- L67P/L74P/V81P and HA-Hac1^{i}-S238A and set up the IP with 18 mg input of whole cell lysate in a final volume of 1 ml and incubated them o/n with overhead rotation at 4°C. The next day I treated the beads as described before and run the eluted samples. The results in (Figure 6.7 a) shows detection of HA-Hac1 and its mutants in some of the IP samples. As expected, EV shows no bands while Hac1^{i} is observed at the appropriate position ~ 37 kDa during 0 and 8 h nitrogen starvation (Figure 6.7 a). HA-Hac1^{u}, HA-Hac1^{i}-N49L, and HA-Hac1^{i}-L67P/L74P/V81P is also detected at 0 h nitrogen starvation, but at different expression levels (Figure 6.7 a). HA-Hac1^{u} migrates at a lower size ~ 36 kDa, given that Hac1^{u} protein is smaller than Hac1^{i}. At 8 h nitrogen starvation bands for HA-Hac1^{i}-N49L and HA-Hac1^{i}-L67P/L74P/V81P are observed, but not for HA-Hac1^{u}. Also, at both 0 and 8 h starvation no clear detection of HA-Hac1^{i}-S238A was observed (Figure 6.7 a). Expression and observation of Hac1^{i} and some of the mutants at the desired molecular weight supports the β-galactosidase assays and Northern blots results, previously discussed. I also noticed some nonspecific signals in the Western blot which may be a result of protein degradation (Figure 6.7 a). I then asked if adjusting the lysis buffer pH from 8.0 to 8.5 would produce desirable results. At the same time, I tested using a different detergent (0.1 % (v/v) Triton-X-100) in the extraction buffer.

Observation of Hac1^{i} using the lysis buffer adjusted for pH 8.5 and detergent (0.1 % (v/v) **Triton-X-100)**

For these experiments I first tested extraction and detection of HA-Hac1^{i} induced from p2UG-HA-Hac1^{i}. The IPs were set up and Western blot results showed detection of the HA-Hac1^{i} band when samples where IP from lysates extracted with either lysis buffer at pH 8.5 or containing 0.1 % (v/v) Triton-X-100 (Figure 6.7 b). Each IP sample was run with a positive control. Next, I first tested the lysates extracted with the lysis buffer at pH 8.5. Unfortunately, the repeated experiment also resulted in detecting different levels of HA-Hac1 and its mutants in some samples (Figure 6.7 c). I then suggested testing supplementing detergent 0.05 % (v/v) Tween-20 for 0.1 % (v/v) Triton-X-100, as this detergent might work better in the o/n IP. However, the immunoblot results still showed non-comparable HA-Hac1 bands. Also, nonspecific signals are seen in some of the lanes that may suggest protein degradation (Figure 6.7 d).

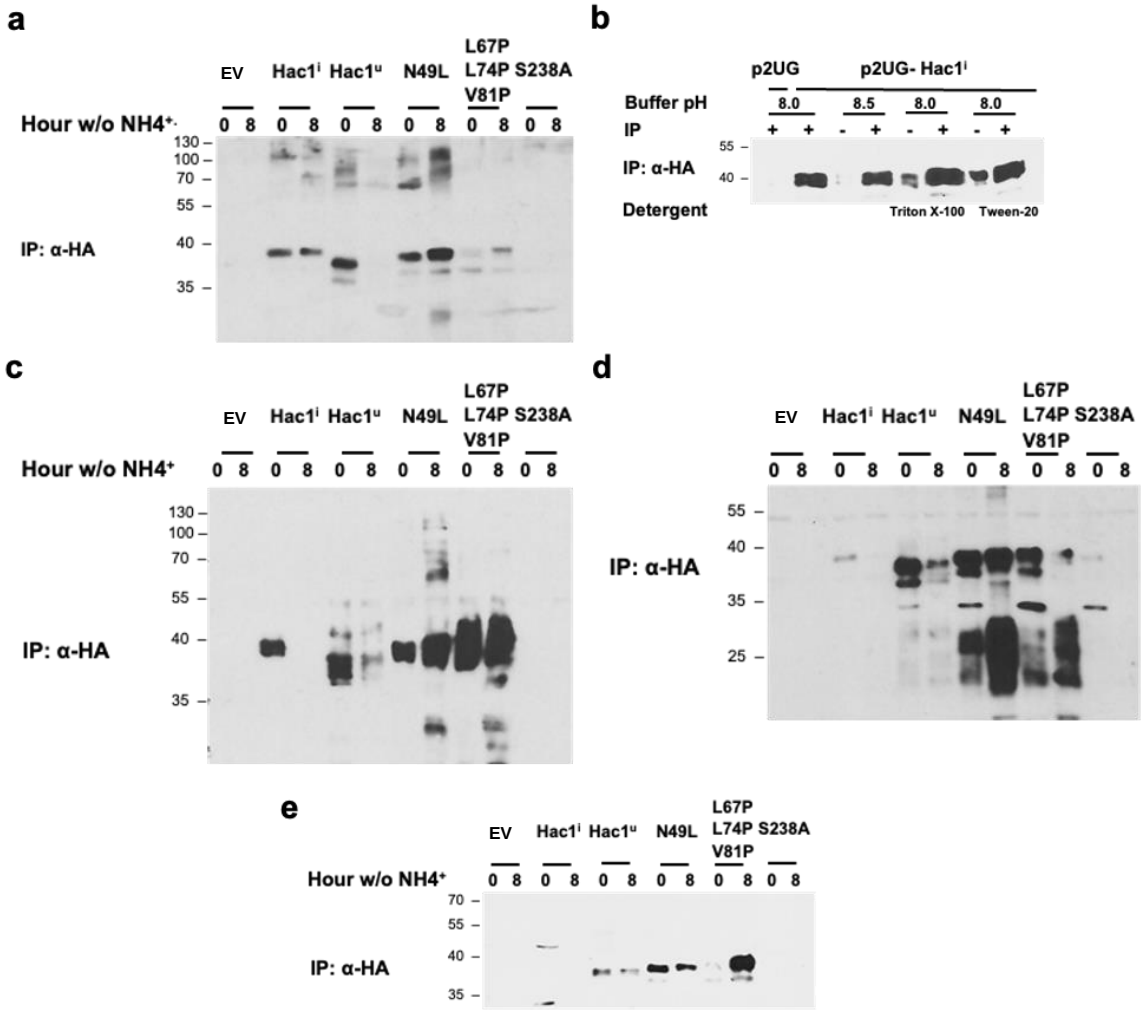

Figure 6-7 Hac1^{i} Immunoprecipitation using magnetic beads.

Input whole cell lysate from cultures expressing low-copy plasmid was at a concentration of 18 mg. Cultures were grown to mid-log phase in acetate media then transferred into sporulation media, samples were collected at 0 h and 8 h of nitrogen starvation. Exposure times in for Western blots a, c, d, and e are the same, 5 min **(a)** Western blot detection of HA-Hac1^{i} and its mutants expressed from low-copy plasmids. The immunoblotting shows variable detection levels of HA-Hac1^{i} in the different lanes when using the previously optimized IP Method. **(b)** Alterations in the lysis buffer pH from 8.0 to 8.5 or detergent from 0.05 % (v/v) Tween-20 for 0.1 % (v/v) Triton-X-100 revealed detectable levels of HA-Hac1^{i} expressed from p2UG-HA-Hac1^{i} on the Western blot. **(c)** Western blot detection of HA-Hac1^{i} and its mutants extracted with lysis buffer with a pH 8.5 revealed various levels of HA-Hac1^{i} and its mutant. **(d)** Western blot detection of HA-Hac1^{i} and its mutants extracted with lysis buffer with detergent 0.1 % (v/v) Triton-X-100 revealed various levels of HA-Hac1^{i} and its mutant along with high background and smearing. **(e)** Altering the reducing agent used in the lysis buffer from DTT to TCEP allowed for cleaner Western blots, but HA-Hac1^{i} and its mutants were still not detected at comparable amounts in all lanes.

Observation of Hac1^{i} using lysis buffer adjusted for reducing agent TCEP

Finally, I decided to use a more stable reducing agent in the extraction lysis buffer to try and overcome the oxidation of the samples. I replaced 0.5 mM DTT with 0.5 mM (tris(2-carboxyethyl) phosphine) (TCEP) in the extraction lysis buffer. TCEP is more resistant to oxidation in air and is significantly more stable than DTT at pH values above 7.5. The change from DTT to TCEP was motivated by that β-mercaptoethanol and DTT will counteract some of the protease inhibition. The PMSF (while it is a serine protease inhibitor that covalently modifies the active site serine of serine proteases) will also covalently modify the active site cysteine of cysteine proteases and inactivate these. However, PMSF can be competed off this active site cysteine by other thiols (β-mercaptoethanol, DTT, not TCEP), leading to reactivation of cysteine proteases.

Replacing the reducing agent DTT in the lysis buffer with TCEP may create a preferable IP incubation environment. The goal is to remove the problem that maybe rising from the IP samples incubating o/n in a large ~ 1 ml volume of lysis buffer. The IP experiment was repeated the same way as before. Results showed cleaner blots, and I got single bands that have been fully reduced and the lanes show no smearing. However, like before I still got variable detection levels of HA-Hac1^{i} (Figure 6.7 e). The bands at migration positions below monomeric HA-Hac1^{i} suggest degradation. The degradation may be partial in some samples and complete in other samples. If degradation is partial, then bands below the running position of monomeric HA-Hac1^{i} and some (or none) monomeric HA-Hac1^{i} can be observed. If degradation is complete, then no signal in the lane can be observed (Figure 6.7 e).

Observation of Hac1^{i} and Hac1 mutants expression in the different experiments

In figure 6.7 a Hac1^{i} is detected as a single band at the desired position at both 0 and 8 h nitrogen starvation, in figure 6.7 c, Hac1^{i} was only detected at 0 h nitrogen starvation. However, in figure 6.7 d and e no bands were seen at 0 and 8 h nitrogen starvation. The Hac1^{u} was observed as a single band expressed from 0 h nitrogen starvation in figures 6.7 a, c, d, and e; however, Hac1^{u} was observed at 8 h nitrogen starvation as a faint band in figures 6.7 c, d, and e but none in 6.7 a. As for the Hac1^{i}-N49L mutant, expression at 0 and 8 h nitrogen starvation was detected. Hac1^{i}-N49L mutant signals were observed in figures 6.7 a, c, d, and e, as mentioned before the signals running under the Hac1^{i}-N49L mutant may be a result of partial protein degradation. HA-Hac1^{i}- L67P/L74P/V81P mutant expressed at 0 and 8 h nitrogen starvation was observed as faint signals compared to

detected Hac1^{i} and Hac1 mutants (Figure 6.7 a). In figure 6.7 c, HA-Hac1^{i}-L67P/L74P/V81P was observed at 0 and 8 h nitrogen starvation with high signal compared to detected Hac1^{i} and Hac1 mutants, maybe a result of partial protein degradation. Looking at figure 6.7 d, HA-Hac1^{i}- L67P/L74P/V81P mutant was observed as a clear band at 0 h nitrogen starvation, but as a partial signal at 8 h nitrogen starvation, both running samples display a degree of possible partial protein degradation. A faint single HA-Hac1^{i}-L67P/L74P/V81P band was seen at 0 h nitrogen starvation compared to the clear band detected at 8 h nitrogen starvation (Figure 6.7 e). Finally, Hac1^{i}-S238A mutants was observed as a faint signal at 0 h nitrogen starvation in figure 6.7 d, but was not observed in figures 6.7 a, c, and e. Further optimisation of the IP method is required, possibly by minimising the time for the IP. Instead of o/n, for the minimum amount of time to capture all HA-Hac1^{i} protein, thus overcoming possible unwanted reactions taking place given the long incubation time.

6.4 Discussion

Several studies, using the yeast strain S288C, estimate that the Hac1 protein abundance is between 1800 and 8500 molecules per cell. This has been documented by confocal microscopy, immunoblotting, and flow cytometry (Ghaemmaghami et al., 2003, Lee et al., 2007, Tkach et al., 2012, Chong et al., 2015). Detection of Hac1^{i} expressed protein through immunoblotting is observed in multiple studies, in which the cells were treated with DTT or Tm to induce ER stress activating UPR (Uppala et al., 2022, Sathe et al., 2015, Rüegsegger et al., 2001, Kawahara et al., 1997). In a study to observe Hac1^{u}, specific modifications were made to enhance detection of HA-tagged Hac1^{u}: 1) the use of a more sensitive α-HA antibody, 2) the use of an *IRE1* knockout strain, which eliminates the Ire1-dependent splicing of HAC1 mRNA, 3) deletion of *DUH1* to stabilize protein produced by *HAC1^{u}* mRNA, given that Duh1 acts on targeting Hac1^{u} for degradation (Di Santo et al., 2016).

This chapter presents the different attempts of HA-Hac1^{i} and its mutant's expression, precipitation and detection, to confirm and measure steady state expression of the protein in the β-galactosidase assays and Northern blots. Using Western blots to observe the purification and detection of the Hac1 target protein, I analysed the protein precipitation using different methods. Throughout the optimization process, Hac1^{i} expressed from the inducible p2UG-HA-Hac1^{i} plasmid seemed to be stable and was used as the positive control to which the different methods were analysed.

Successful whole cell extract, $(NH_4)_2SO_4$ fractionation and precipitation of $Hac1^i$ was reported in a previous study, however, detection of $Hac1^i$ was reported only from extracts of cells treated with Tm (Kawahara et al., 1997). This data suggests the $Hac1^i$ protein is amenable to precipitation and resuspension. In this study precipitation and detection of $Hac1^i$ when utilizing ammonium sulfate $(NH_4)_2SO_4$ precipitation protocol did not yield measurable levels of $Hac1^i$ when expressed from pRS314-HA-$Hac1^i$. While when salting out the $Hac1^i$ expressed from p2UG-HA-$Hac1^i$, results displayed purified detectable levels of the target protein. The observed data suggested that I will require very large amounts of cell culture at mid-log phase, and for the different nitrogen starvation time points, to concentrate $Hac1^i$ and its mutants using the ammonium sulfate $(NH_4)_2SO_4$ precipitation protocol. Thus, the protein concentration was insufficient for further analysis steps. Hence, I decided to use immunoprecipitation protocols.

Expression and detection of stable $Hac1^i$ expressed from p2UG-HA-$Hac1^i$ was observed at various incubation time points via immunoblotting (Figure 6.5 a). However, immunoprecipitation using free HA antibodies was unsuccessful to purify and analyse $Hac1^i$ expressed from p2UG-HA-$Hac1^i$. The high nonspecific signals in the Western blot results suggested the presence of the denatured primary antibody heavy chains (~ 50 kDa). This is a common problem associated with secondary antibodies for Western blotting after immunoprecipitation step, making it difficult to distinguish my target protein in these blots. Furthermore, creating an α-HA antibody titration, by increasing the α-HA concentration added to each lysate sample did not resolve the nonspecific binding of the primary antibody heavy chains (Figure 6.5 b). To overcome this masking effect, I decided to use α-HA magnetic beads to purify $Hac1^i$ and its mutants in the immunoprecipitation protocol. The blocked magnetic bead surface is coated with α-HA antibody, a highly specific mouse IgG1 monoclonal antibody that recognizes the HA-epitope tag (YPYDVPDYA). Results from the titration experiment using different lysate concentration with 10 µg α-HA magnetic beads, suggest that during the IP the beads are not being saturated at lysate concentrations ≤ 500 µg, which contain the highly inducible 2 µm p2UG-HA-$Hac1^i$ plasmid (Figure 6.6 a). Since the target Hac1 is expressed by a low-copy plasmid, it is safe to speculate that incubating large concentrations of lysate ~ 20 (with low-copy plasmid pRS314- HA-$Hac1^i$) with 10 µg of α-HA magnetic beads will not saturate the beads. Using the α-HA magnetic beads I was able to purify and detect $Hac1^i$ expressed from p2UG-HA-$Hac1^i$, while using 75 µg of whole lysate input in the IP (Figure 6.6 c). Successfully, I was also able to detect $Hac1^i$, expressed from pRS314-HA-$Hac1^i$ at the different sporulation time points (0, 4, 8 h) using the α-HA magnetic beads, when loading

a high concentration of protein lysate ~ 19 mg. Further optimization of the cell culture extraction buffer was investigated to try and extract steady levels of Hac1^{i}, Hac1^{u}, Hac1^{i}-N49L, Hac1^{i}- L67P/L74P/V81P, and Hac1^{i}- S238A. Results from IP experiments at the different sporulation time points did not show comparable levels of target protein in Western blots, this suggests the need for further optimization of the IP.

Nevertheless, from the observed data in figures 6.6 e and 6.7 a, c, d, and e, it may be concluded that HA-Hac1^{i} does not change in sporulation over 8 h. Also, from figure 6.7 a, c, d, and e, when taking together the four partially successful repeats it maybe concluded that Hac1^{u}, Hac1^{i}-N49L, Hac1^{i}- L67P/L74P/V81P are likely expressed, maybe not at the same level. Previous growth assays, β-galactosidase, and immunoprecipitation analysis revealed that the mutant Hac1^{i}-S238A has been constructed, expressed, and detected successfully (Mori et al., 2000). This suggests that Hac1^{i}-S238A in this study is expressed and functional, further evident from the mutant's ability to partially repress transcription of EMG (Figure 5.4 and 5.5) and partial induction of β-galactosidase activity through UPRE (Figure 4.1 a). Lack of expression of some Hac1^{i} and Hac1 mutants maybe due to their degradation. When the UPR is inactive accelerated Hac1 protein degradation prevents the accumulation of Hac1, thus protein degradation serves as a fail-safe mechanism (Di Santo et al., 2016). Such tight control is required since inappropriate induction of the UPR in the absence of unfolded proteins in the ER is toxic to cells (Kawahara et al., 1997). Hac1^{u} accumulation, even though it possesses low UPR activation potential, is undesirable. Hence, the unique C-terminal tail of Hac1^{u} is recognised as a "degron" by Duh1 and is rapidly degraded by the proteasome (Di Santo et al., 2016). Overall, detection of Hac1^{i} through immunoblotting, after using lysate extractions or precipitations, has been observed when cells have been stressed and the UPR was activated (Uppala et al., 2022, Sathe et al., 2015, Rüegsegger et al., 2001, Kawahara et al., 1997).

7 Transcription of Known Components of *RPD3L* (HDA) are not regulated by Hac1^{i}

7.1 Rationale

In a previous study (Schröder et al., 2004) co-immunoprecipitation experiments showed that Hac1^{i} can interact with the *RPD3-SIN3* histone deacetylase complex (HDAC) *in vivo*. They also demonstrated that *HAC1* is a peripheral component of the HDAC. *RPD3* encodes a histone deacetylase (Rundlett et al., 1996). *SIN3*/HDAC is a component of Rpd3 producing a co-repressor complex involved in transcriptional repression (Silverstein and Ekwall, 2005). In yeast, Rpd3L contains the three core subunits: Rpd3, Sin3 and Ume1(Carrozza et al., 2005b, Keogh et al., 2005) involved in transcriptional repression (Kadosh and Struhl, 1998a). Ime1 is a key regulator of meiosis and activation of EMGs through interactions with Ume6 (Kassir et al., 2003). Ume6 is an Rpd3 HDAC subunit that recognises and binds to the URS1 regulatory sequence (Strich et al., 1994, Kadosh and Struhl, 1997). The *RPD3-SIN3* HDAC is required for negative regulation of EMGs transcription by Hac1^{i}. Furthermore, the *RPD3-SIN3* HDAC is recruited to the URS1 promoter sites of EMGs by bound Ume6 to negatively regulate EMGs and meiosis by Hac1^{i}. The study also showed that the HDAC catalytic activity is required for the complex to mediate repression of EMG by Hac1^{i} during nitrogen starvation (Schröder et al., 2004). It is not clear how the association of Hac1^{i} with the HDAC alters some aspects of HDAC function, for example increases its specific deacetylation, or alters its substrate spectrum through altering the conformation of composition of the HDAC. Rpd3 is the enzymatic HDAC component of a large complex that primarily targets H3 and H4 (Sabet et al., 2004, Rundlett et al., 1998). Many subunits of this large complex have been identified by mass spectrometry and MudPIT. These include Sin3, Pho23, Sds3, Sap30, Dep1, Cti6, Rxt2, Rxt3, and Ash1 (Carrozza et al., 2005a). It is not clear what other subunits associated with the HDAC are involved in negatively regulating transcription of EMG by Hac1^{i} under nitrogen starvation, if any.

Here I investigate the requirement for the transcriptional regulation of the bZIP transcription factor Hac1^{i} for regulating specific component of the Rpd3 HDAC, during repressing transcription of EMGs when subjected to nitrogen starvation. Simultaneously, identifying potential transcriptional targets of Hac1^{i} involved in transcriptional repression of EMGs in response to nitrogen sensing. For this study, I investigated the following subunits of Pho23, Sds3, Sap30, Dep1, Cti6, Rxt2, Rxt3.

7.2 Hac1^{i} is not required to transcribe known constituents of HDAC (*DEP1, CTI6, RXT2, RXT3, PHO23, SDS3, SAP30*)

Given that Rpd3L is part of large complex, I asked if any of its known subunits are repressed by overexpressing Hac1^{i} during nitrogen sensing response. Furthermore, examining Hac1 function as a transcriptional regulator during meiosis in response to nitrogen starvation on Rpd3L. In order to answer this question, I examined mRNA expression levels of the Rpd3L subunits, during nitrogen starvation through expressing Hac1^{i}. The expression levels of *DEP1*, *CTI6*, *RXT2*, *RXT3*, *PHO23*, *SDS3*, *SAP30* transcription were analysed by Northern hybridization.

First ~ 500 bp long DNA fragments, of the target mRNA genes, were amplified by PCR to produce specific DNA templates. This was accomplished by amplifying the target gene using the yeast whole genome extract (PWY-260) as template for the PCR. The resulting ~ 500 bp fragments were run on an agarose gel and purified and quantified for Northern blot hybridization (Figure 7.1 a). Preliminary result shown in (Figure 7.1 b) indicate that the expressed endogenous mRNA levels of the genes coding for Rpd3L components are not affected by overexpression of Hac1^{i} under nitrogen starvation. The results showed undisguisable levels of mRNA expression when comparing mRNA levels expressed from strains expressing empty vector (-) and Hac1^{i} (Figure 7.1 b).

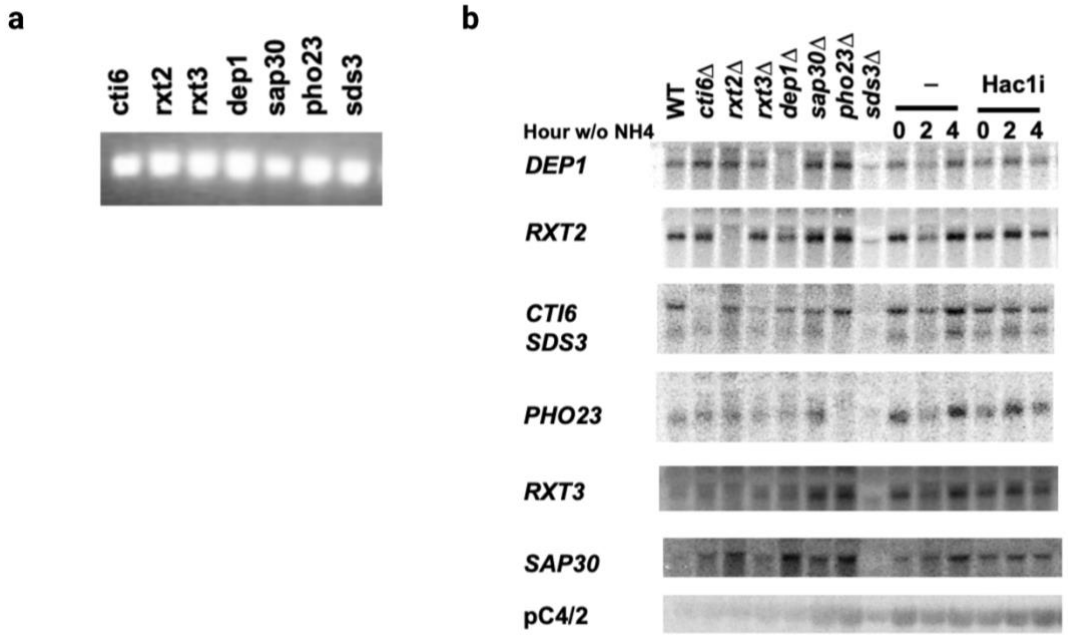

Figure 7-1 Hac1^{i} is not required to regulate early meiotic genes repression through known components of the Rpd3L complex.

(a) Agarose gel analysis of the DNA templates for the target mRNAs (*DEP1, CTI6, RXT2, RXT3, PHO23, SDS3, SAP30*). **(b)** Northern blot for the mRNA targets mentioned in (a), and the loading control pC4/2 on RNA extracted from MSY-134-36 carrying empty vector (-) or Hac1^{i}. RNA samples were extracted at different time points of nitrogen starvation. Three independent clones were examined.

7.3 Discussion

Expressing Hac1^{i} did not affect mRNA expression levels of know subunit proteins of the Rpd3 complex (Figure 7.1 b). Results from this finding is consistent with the data from the previous experiments, in that Hac1^{i} functions at a transcriptional level. Hac1^{i} most likely is involved in regulating transcription of a component of the Rpd3L, in a direct or indirect manner. Also, the results suggested that Hac1^{i} transcriptions factor regulates suppression of EMGs through other target genes than (*DEP1*, *CTI6*, *RXT2*, *RXT3*, *PHO23*, *SDS3*, *SAP30*). Developing a method and phenotype to screen and identify Hac1^{i} potential targets during sporulation may help identify possible targets for Hac1^{i} transcriptional regulation in meiosis.

8 Conclusion and Future Work

In yeast *S. cerevisiae* the differentiation responses are dictated by the nutritional environment. Yeast can differentiate under shifting environmental conditions to multiple cell forms that vary in their physiology, metabolism, and regulation. These forms are then better adapted to conditions for survival, stress defence and reproduction. One such form is spore formation as a result of meiosis under less favourable nutritional conditions. Repression of meiotic differentiation via extracellular nutrients, mostly glucose and nitrogen sources, is a well understood phenomenon (Kassir and Simchen, 1989, Pan and Heitman, 1999, Honigberg and Purnapatre, 2003). Even though little is known about the mechanisms that directly control meiosis by nitrogen, a mechanism that contributes to nitrogen repression of the early meiotic genes (EMGs) has been reported (Kassir and Simchen, 1989, Kupiec, 1997, Honigberg and Purnapatre, 2003, Schröder et al., 2000, Schröder et al., 2004). In a previous study done by my lab, the activity of the unfolded protein response (UPR) signalling pathway, from the ER to the nucleus, correlated with the abundance of extracellular nitrogen sources. And the nitrogen-rich conditions correlated with the repression of EMGs (Schröder et al., 2000, Schröder et al., 2004). Moreover, the study recognised $Hac1^{i}$, a positive regulator of the UPR, as a negative regulator of EMGs (Schröder et al., 2000). Therefore, the information of nutritional state of the cell is sensed by the UPR, which represses nitrogen starvation responses, promotes growth, and decides the fate of developmental pathways. The (Schröder et al., 2004) study proposed the following model for nitrogen-mediated regulation of EMGs by $Hac1^{i}$ (Figure 1.11 a). In nitrogen-rich conditions, *HAC1* mRNA is spliced and translated to the trans-actively potent $Hac1^{i}$ protein (Schröder et al., 2000, Chapman and Walter, 1997, Rüegsegger et al., 2001, Mori et al., 2000). The level of $Hac1^{i}$ product compares greatly with the quantity of *HAC1* mRNA splicing, due to the half-life of $Hac1^{i}$ being approximately 2 min (Kawahara et al., 1997). $Hac1^{i}$ then associates with the *RPD3-SIN3* histone deacetylase complex ($Hac1^{i}$-HDAC complex), which is recruited by Ume6 to URS1 promoters of EMGs, suppressing transcription of EMGs and entry into meiosis (Schröder et al., 2004, Kadosh and Struhl, 1997). The *RPD3-SIN3* HDAC catalytic domain plays a role in transcriptional repression of EMGs (Schröder et al., 2004). The importance of the highly conserved residues of bZIP transcription factors is further supported by findings discussed in this thesis.

In the current study, the $Hac1^{i}$ bZIP transcription factor has an enhanced ability to repress transcriptional activation, as shown by a decrease in T_4C -URS1-controlled activation reporter plasmid (Figure 5.1) and EMGs (Figure 5.5) by nitrogen starvation in cells

overexpressing Hac1^{i}, which correlates with previous findings (Schröder et al., 2004). The negative regulation of EMGs by key conserved residues within the Hac1^{i} domains was investigated by using the T$_4$C-URS1-*CYC1-lacZ* reporter plasmid when inducing meiosis by nitrogen starvation. Mutations in the invariant asparagine within the DNA-binding domain and the triple mutation in the leucine zipper of Hac1^{i} resulted in Hac1^{i} mutants which partially repressed transcriptional activation, evident by a decrease in T$_4$C-URS1-*CYC1-lacZ* reporter (Figure 5.2 and 5.3) and EMGs (Figure 5.5) expression. The ability of the Hac1^{i} mutant (Hac1^{i}- L67P/L74P/V81P) to retain repression function suggests other residues within the bZIP domain may function to overcome the apparent mutations limitations. For example, this mutant still retains a functional DNA-binding domain, which may be maintaining the monomers transcription function, albeit at lower potential. The conserved Asn-49 is also present in the well-studied Gcn4-235, which when mutated to various amino acids abolished DNA-binding activity in *vitro*. Additionally, of three residues shown to functionally substitute for Asn-235 in GCN4 and Jun-GCN4, all clearly reduce DNA-binding affinity and alter specificities at the ± 4 position of the Gcn4 target site. This suggests that Asn-235 makes direct (base specific) contacts with the fourth position of the Gcn4 target sites (Pu and Struhl, 1991a, Pu and Struhl, 1991b). Moving forward, additional mutations within the conserved Hac1^{i} DNA-binding region, such as Arg-48, Ala-52, Ala-53, might produce functionally inactive Hac1^{i} with no negative regulation of EMGs. Producing a complete Hac1^{i} functional mutant that can be investigated in both the UPR and meiosis pathway, highlighting yeast Hac1^{i} as a transcriptional activator or repressor that bind DNA via a bZIP domain consisting of a leucine zipper dimerization element and an adjacent basic region that directly contacts DNA. Also, a combined mutation of the invariant asparagine and leucine zipper is worth investigating. Results will help identify the structural regions involved in regulating transcription of Hac1^{i} target genes in the UPR and meiosis pathway.

As it was previously illustrated the spliced *HAC1* mRNA Hac1^{i} represses transcription of EMGs through URS1, here I investigated negative the regulation of the translatable unspliced form of *HAC1* mRNA Hac1^{u} during induction of meiosis. Results show that the Hac1^{u} mutant slightly repressed activation of T$_4$C-URS1-*CYC1-lacZ* reporter and EMGs (Figure 5.1 and 5.5). Moreover, given that the major difference between Hac1^{i} and Hac1^{u} is the C-terminus; specifically, the presence of the Ser-238 in Hac1^{i}, the Hac1^{i}-S238A mutant was also characterized for repression function. It is important to note that Hac1^{i} is a significantly more potent transcription factor in regulating EMGs repression compared to Hac1^{u} and Hac1^{i}-S238A as observed from (Figure 4.1 a), further correlating with a previous study (Mori et al., 2000). Also, the inability of Hac1^{i}-S238A to fully repress

transcriptional activation of T_4C-URS1-*CYC1-lacZ* reporter plasmids and EMGs (Figure 5.4 and 5.5) suggests that the transactivation potential of Hac1^i is required to efficiently repress transcription of EMGs through URS1. Overall, characterization of key residues in the Hac1^i bZIP domain suggested a transcriptional role for Hac1^i bZIP transcription factor in transcribing target genes involved in negatively regulating transcription of EMGs through the *RPD3-SIN3* HDAC.

Hac1^i is a bZIP transcription factor, activates transcription of genes containing UPR element (UPRE) and *INO1* gene (Chapman et al., 1998). According to the genome-wide screen, no apparent targets of Hac1^i have been identified so far (Uetz et al., 2000). A poorly understood aspect of meiotic gene regulation is how transcriptional repression is mediated under nutrient rich conditions through Hac1^i. In this study I aimed to identify potential targets for Hac1^i involved in EMGs transcriptional repression under nutrient rich condition via *RPD3-SIN3* HDAC. Hac1^i displayed a physiological-peripheral communication with the HDAC (Schröder et al., 2004). Observation of mRNA levels for well-known components of the Rpd3L histone deacetylase complex (*DEP1*, *CTI6*, *RXT2*, *RXT3, PHO23, SDS3*, *SAP30*), suggested that Hac1^i transduces transcriptional repression via other regulators of the *RPD3-SIN3* HDAC (Figure 7.1). Still *UME1* and *ASH1*, which are also components of the Rpd3-Sin3 HDAC, might be targets of Hac1^i. Additional examination of these subunits may shed the light into potential targets for Hac1^i involved in negatively regulating meiosis. Partial loss of repression by presumably transcriptional mutants (zipper mutant) is consistent with Hac1^i acting as a transcriptional factor, by inducing another protein that inhibits Rpd3L. Result from this study support the suggestion that Hac1^i transcribes a gene involved in regulating repression of EMG through Rpd3-Sin3 HDAC. Furthermore, chromatin immunoprecipitation (ChIP) will contribute to further understanding the interactions between the protein and DNA.

The conclusion that Hac1^i negatively mediates transcription of EMGs through URS1 composes an innovative function for this bZIP protein (Schröder et al., 2004).
The novel role for the negative transcriptional regulation by a bZIP transcription factor is exciting for my study. Data collected from my study suggest that Hac1^i functions as a repressor in regulating meiosis at a transcriptional level, given that specific manipulations in the transcription factor bZIP domain rendered Hac1 unable to function with high potential as a negative regulator. bZIP transcription factors repress transcription across several mechanisms. Many can form repressive homo- and heterodimers, for example, ATF3 (Hai et al., 1999, Hai and Hartman, 2001), the small Maf proteins (Motohashi et al.,

2002), bach1 and bach2 (Oyake et al., 1996), and substitute translation products of C/EBPα and C/EBPβ (Chol et al., 1994). Small Maf proteins recruit gene loci into heterochromatin (Motohashi et al., 2002), and many recruit co-repressors to the promoter, for example, Dr_1 by E4BP4 (Cowell and Hurst, 1996), *SSN6-TUP1* by Sko1 (Proft and Struhl, 2002), and Sin3 by Opi1 (Wagner et al., 2001, Kaadige and Lopes, 2003). In addition, direct inhibition of the transactivation domain of the basic helix–loop–helix transcription factor complex Ino2–Ino4 by association with Opi1 was proposed (Wagner et al., 2001). These observations defined the novel framework for negative transcriptional regulation by a bZIP transcription factor. Repression of EMGs by $Hac1^i$ does not involve direct binding of $Hac1^i$ to DNA, since it is dependent on Ume6, which is constitutively bound to URS1. Also, $Hac1^i$ does not recruit the HDAC to URS1 or Ume6, since repression by the HDAC on URS1 was mostly intact in *hac1Δ* strains (Schröder et al., 2004).

Gcn4 was identified to act with $Hac1^i$ to induce transcription of UPR target genes regulated by UPRE. A gel-mobility shift study revealed that when Gcn4 and $Hac1^i$ were bound to separate complexes no ultrashift occurred. Therefore, both Gcn4 and $Hac1^i$ are required to positively regulate transcription of UPR target genes controlled by UPRE. It is suggested that because of the demonstrated direct physical association between $Hac1^i$ and Gcn4 and the sequence motif UPRE, that it is likely that Gcn4 and $Hac1^i$ activate transcription by binding promoter DNA as a heterodimer. The binding of target DNA by a Gcn4-$Hac1^i$ heterodimer results in a transcriptionally active and stable complex. Gcn4 knockout phenotypes closely resembles *Δire1* and *Δhac1*, the deletion of any of these genes inhibits transcriptional activation by ER stress (Patil et al., 2004). Disruption of the $Hac1^i$ leucine zipper in this context prevents the Gcn4-$Hac1^i$ heterodimer formation, which results in the inability of the $Hac1^i$ leucine zipper mutant to induce UPRE-*lacZ* (Figure 4.1 b). The study (Patil et al., 2004) also proposed that given the important role of Gcn4 in the UPR, Gcn4 and its upstream activator Gcn2 hence join Ire1, $Hac1^i$, and Rlg1 in the list of crucial players in the yeast UPR.

The $Hac1^i$ leucine zipper mutant also partially represses EMGs transcription. I propose that $Hac1^i$ can bind DNA and stimulate transcriptional activation of genes involved in regulating repression of EMGs as a monomer. The partial loss of $Hac1^i$ leucine zipper mutant transcriptional repression function might be due to the $Hac1^i$ monomer regulating transcriptional repression with less efficiency than $Hac1^i$ dimer. Thus, $Hac1^i$ dimerization may be required for competently regulating transcriptional repression of EMGs by Rpd3-

Sin3 HDAC. Another proposal is that Hac1^{i} monomer may be interacting with Rpd3L to repress EMGs with less potency than a homo- or heterodimer.
Replacement of unspliced Hac1 10 aa with the 18 aa in the mature Hac1 produces a Hac1^{i} transcription factor with higher transactivation potential to regulate UPR (Mori et al., 2000). Hac1^{u} and the transactivation domain mutant display similar partial repression regulation of T$_4$C-URS1-*CYC1-lacZ* and EMGs. Given these results, I propose that along with Hac1 dimerization transactivation of the Hac1^{i} protein is required to sufficiently repress EMGs mediated by URS1 promoter. In which Ser-238 promotes transactivation potential of Hac1^{i} to repress transcriptional activation of EMGs through Rpd3-Sin3 HDAC during nitrogen-rich condition.
The disruption of the invariant asparagine in the Hac1^{i} DNA-binding domain abolishes repression regulation of EMG by Hac1^{i}. Overall, during nitrogen-rich condition *HAC1* mRNA is spliced to produce Hac1^{i} (Schröder et al., 2004), I propose a model in which Hac1^{i} bZIP transcription factor bounds a target DNA or *RPD3L* as a transactivated homo- or heterodimer, where the invariant asparagine recognises and binds the target sequence position in the DNA. The leucine zipper dimerization promotes stability of the Hac1^{i} protein-DNA binding, thus regulating transcriptional repression of EMGs via Rpd3-Sin3 HDAC.

In previous studies the functional homolog for *HAC1* in metazoans, *XBP-1* was found to be required for differentiation into cells specialized in secretion, for example, plasma cell differentiation (Reimold et al., 2001). Both *XBP-1* and *HAC1* belong to the family of ATF/CREB bZIP transcription factors. *XBP-1* controls genes containing a CRE (cAMP response element)-like element (Clauss et al., 1996). As in *HAC1*, *XBP-1* splicing introduces a frameshift and an alternative C-terminus with increased transcriptional activation potential. However, there is no differential translational control of unspliced and spliced *XBP-1* mRNAs (Lee et al., 2003). Splicing of *XBP-1* mRNA was observed in B cells undergoing terminal differentiation (Calfon et al., 2002, Iwakoshi et al., 2003). Terminal differentiation of B cells involves transcriptional repression of c-*myc* (Lin et al., 2000). c-*myc* repression is mediated by recruitment of mammalian orthologs of yeast Rpd3 to the c-*myc* promoter by Blimp-1 (Yu et al., 2000, Lin et al., 1997). Also, the kinetics of activation of the UPR, splicing of *XBP-1* mRNA, downregulation of c-*myc* expression, and activation of Blimp-1 expression are similar. Thus, the UPR decreases the biosynthetic burden of the secretory pathway by downregulating expression of genes encoding secreted proteins. A model was proposed in which the activity of UPR signalling pathways reflects the biosynthetic activity of the ER. Further demonstrating that the ER signalling pathway

controls cellular events, such as execution of differentiation and starvation programs (Schröder and Kaufman, 2005). Put together these data support the idea of a crosstalk mechanism existing between the UPR and differentiation programs, as shown from my study in the case for yeast.

I utilised and optimised several methods to express and detect steady levels of Hac1 protein expressed from $Hac1^{i}$ and the genetically constructed Hac1 mutants. Results from an immunoprecipitation-Western blotting technique using α-HA magnetic beads was successful to detect Hac1 protein expressed from its own promoter from a single copy plasmid. Development of this technique was helpful to enrich and detect the expression of the protein, because $Hac1^{i}$ might be at low abundance during nitrogen starvation. Failure to observe $Hac1^{i}$ expressed from the low-copy plasmid, from whole extracts without precipitation during nitrogen starvation, may be due to its low induction levels. Which is not the case with $Hac1^{i}$ induced during UPR activation by DTT or Tm, where $Hac1^{i}$ is observed by immunoblotting given its high induction levels to alleviate UPR (Uppala et al., 2022, Sathe et al., 2015, Rüegsegger et al., 2001, Kawahara et al., 1997). Furthermore, detection of Hac1 and its mutants expressed from the low-copy plasmid is important to observe the proteins behaviour throughout 8 h sporulation, and to support β-galactosidase reporter assays and Northern blotting in this study. For further detection reproducing of comparable steady levels of the protein expressed from the various derivatives of Hac1, I propose cloning the Hac1 and its mutants into p2UG. This allows for induction of abundant levels of Hac1, under the control of its own promoter, to observe the expression levels of protein and detection with ease.

This study further opens the door for characterisation of whether Hac1 bZIP transcription factor inhibits nucleosomal acetylation in the promoters of EMGs. Also, compare the effects of expression and/or deletion of Hac1 on nucleosomal acetylation using chromatin immunoprecipitation to WT cells. In addition, produce yeast strains carrying deletions of N-terminal histone tails or that carry point mutations in acetylation sites in these tails and then characterise whether these genetic manipulations abolish the effects of overexpression and/or deletion of Hac1 on expression of EMGs using β-galactosidase reporter assays and Northern blotting. The findings would highlight the role of Hac1 in chromatin remodelling via Rpd3-Sin3 HDAC.

The UPR pathway's roles in the biological responses towards different environmental stressors in fungi have been well characterised. Nonetheless, not much is known about the

biological functions of the UPR pathway in morphological development and differentiation. In the *Ustilago maydis* corn smut fungus, *ire1Δ* strains display reduced filamentous growth, while agitation of the *HAC1* homolog, *CIB1* does not affect filamentous growth (Heimel et al., 2013). In the *Magnaporthe oryzae* rice blast fungus, Hac1 is required for conidia production in asexual development, while the regulatory mechanism involving the UPR pathway during asexual development has yet to be fully characterised (Tang et al., 2015). In the *Alternaria alternata* phytopathogenic fungus in plants, showed that both Hac1 and Gcn4 bZIP transcription factors are essential for colony morphogenesis. Deletion of *HAC1* produced decreased aerial hypha and are hypersensitive to ER stressors, such as Tm and DTT (Gai et al., 2022). In the *Candida albicans* human fungal pathogen, hyphal development is reduced in a *hac1Δ* mutant during serum stimulation. However, the regulation of Ire1 in hyphal development has not been characterised (Wimalasena et al., 2008). In *Cryptococcus neoformans* global fungal meningitis pathogen, the UPR pathway directs sexual and unisexual differentiation in an Ire1-dependent but Hxl1-independent manner, where Hxl1 is a homolog of Hac1 (Jung et al., 2016). Taken together, bZIP transcription factors involved in the UPR pathway are key regulators of fungal morphogenesis and differentiation. A clear crosstalk is clearly identified between the UPR pathway and pathways that regulate pathogenic development and cellular responses to environmental changes.

Overall, my research has provided very interesting insights into how Hac1 represses early meiotic genes in *Saccharomyces cerevisiae*. Characterising crosstalk between stress and nutrient signalling pathways that controls development and differentiation in fungi. Investigating how the transcription factor Hac1, whose synthesis is controlled by endoplasmic reticulum stress signalling pathways, represses transcription of a set of genes induced by severe starvation, the early meiotic genes in the yeast *S. cerevisiae*. Transcriptional induction of the early meiotic genes controls meiotic development and sporulation in *S. cerevisiae*. This research will advance our knowledge of crosstalk between stress and nutrient signalling pathways in yeasts and fungi and will open new avenues for the development of anti-fungal drugs and fungicides. Furthermore, understanding the intricacy of HDAC regulation and function in cells is hence of utmost importance to design pharmacological approaches to inhibit or moderate their action in the insurgence and sustenance of pathogenesis.

9 BIBLIOGRAPHY

Bibliography

ADAMS, C. J., KOPP, M. C., LARBURU, N., NOWAK, P. R. & ALI, M. M. 2019. Structure and molecular mechanism of ER stress signaling by the unfolded protein response signal activator IRE1. *Frontiers in Molecular Biosciences,* 6**,** 11.

AEBI, M., BERNASCONI, R., CLERC, S. & MOLINARI, M. 2010. N-glycan structures: recognition and processing in the ER. *Trends in biochemical sciences,* 35**,** 74-82.

AGARWALA, S. D., BLITZBLAU, H. G., HOCHWAGEN, A. & FINK, G. R. 2012. RNA methylation by the MIS complex regulates a cell fate decision in yeast. *PLoS genetics,* 8**,** e1002732.

AGRE, P., JOHNSON, P. F. & MCKNIGHT, S. L. 1989. Cognate DNA binding specificity retained after leucine zipper exchange between GCN4 and C/EBP. *Science,* 246**,** 922-926.

AHMED, N. T. 2010. *Regulation of middle meiotic gene expression by the Sum1 repressor in Saccharomyces cerevisiae.* Thomas Jefferson University.

ALBER, T. 1992. Structure of the leucine zipper. *Current opinion in genetics & development,* 2**,** 205-210.

ALLERS, T. & LICHTEN, M. 2001. Differential timing and control of noncrossover and crossover recombination during meiosis. *Cell,* 106**,** 47-57.

AMEYAR, M., WISNIEWSKA, M. & WEITZMAN, J. 2003. A role for AP-1 in apoptosis: the case for and against. *Biochimie,* 85**,** 747-752.

ANDERSON, S. F., STEBER, C. M., ESPOSITO, R. E. & COLEMAN, J. E. 1995. UME6, a negative regulator of meiosis in Saccharomyces cerevisiae, contains a C-terminal Zn2Cys6 binuclear cluster that binds the URS1 DNA sequence in a zinc-dependent manner. *Protein Science,* 4**,** 1832-1843.

ANSHU, A., MANNAN, M. A.-U., CHAKRABORTY, A., CHAKRABARTI, S. & DEY, M. 2015. A novel role for protein kinase Kin2 in regulating HAC1 mRNA translocation, splicing, and translation. *Molecular and Cellular Biology,* 35**,** 199-210.

ARAGÓN, T., VAN ANKEN, E., PINCUS, D., SERAFIMOVA, I. M., KORENNYKH, A. V., RUBIO, C. A. & WALTER, P. 2009. Messenger RNA targeting to endoplasmic reticulum stress signalling sites. *Nature,* 457**,** 736-740.

ARNDT, K. & FINK, G. R. 1986. GCN4 protein, a positive transcription factor in yeast, binds general control promoters at all 5'TGACTC 3'sequences. *Proceedings of the National Academy of Sciences,* 83**,** 8516-8520.

ARONOVA, S., WEDAMAN, K., ANDERSON, S., YATES III, J. & POWERS, T. 2007. Probing the membrane environment of the TOR kinases reveals functional interactions between TORC1, actin, and membrane trafficking in Saccharomyces cerevisiae. *Molecular biology of the cell,* 18**,** 2779-2794.

ASADA, R., KANEMOTO, S., KONDO, S., SAITO, A. & IMAIZUMI, K. 2011. The signalling from endoplasmic reticulum-resident bZIP transcription factors involved in diverse cellular physiology. *The Journal of Biochemistry,* 149**,** 507-518.

ASHRAFI, K., LIN, S. S., MANCHESTER, J. K. & GORDON, J. I. 2000. Sip2p and its partner snf1p kinase affect aging in S. cerevisiae. *Genes & development,* 14**,** 1872-1885.

AT, G. 1958. Some observations on sporulation in Saccharomyces. *Comptes rendus des travaux du Laboratoire Carlsberg. Serie chimique,* 31**,** 1-6.

AUKERMAN, M. J., SCHMIDT, R. J., BURR, B. & BURR, F. A. 1991. An arginine to lysine substitution in the bZIP domain of an opaque-2 mutant in maize abolishes specific DNA binding. *Genes & development,* 5**,** 310-320.

BACK, S. H., SCHRÖDER, M., LEE, K., ZHANG, K. & KAUFMAN, R. J. 2005. ER stress signaling by regulated splicing: IRE1/HAC1/XBP1. *Methods,* 35**,** 395-416.

BARBET, N. C., SCHNEIDER, U., HELLIWELL, S. B., STANSFIELD, I., TUITE, M. F. & HALL, M. N. 1996. TOR controls translation initiation and early G1 progression in yeast. *Molecular biology of the cell,* 7**,** 25-42.

BARDWELL, L., COOK, J. G., ZHU-SHIMONI, J. X., VOORA, D. & THORNER, J. 1998. Differential regulation of transcription: repression by unactivated mitogen-activated protein kinase Kss1 requires the Dig1 and Dig2 proteins. *Proceedings of the National Academy of Sciences,* 95**,** 15400-15405.

BASH, R., WANG, H., ANDERSON, C., YODH, J., HAGER, G., LINDSAY, S. & LOHR, D. 2006. AFM imaging of protein movements: histone H2A–H2B release during nucleosome remodeling. *FEBS letters,* 580**,** 4757-4761.

BATLLE, M., LU, A., GREEN, D. A., XUE, Y. & HIRSCH, J. P. 2003. Krh1p and Krh2p act downstream of the Gpa2p Gα subunit to negatively regulate haploid invasive growth. *Journal of cell science,* 116**,** 701-710.

BECK, T. & HALL, M. N. 1999. The TOR signalling pathway controls nuclear localization of nutrient-regulated transcription factors. *Nature,* 402**,** 689-692.

BEN-ARI, G., ZENVIRTH, D., SHERMAN, A., DAVID, L., KLUTSTEIN, M., LAVI, U., HILLEL, J. & SIMCHEN, G. 2006. Four linked genes participate in controlling sporulation efficiency in budding yeast. *PLoS genetics,* 2**,** e195.

BENJAMIN, K. R., ZHANG, C., SHOKAT, K. M. & HERSKOWITZ, I. 2003. Control of landmark events in meiosis by the CDK Cdc28 and the meiosis-specific kinase Ime2. *Genes & development,* 17**,** 1524-1539.

BERTRAM, P. G., CHOI, J. H., CARVALHO, J., AI, W., ZENG, C., CHAN, T.-F. & ZHENG, X. S. 2000. Tripartite regulation of Gln3p by TOR, Ure2p, and phosphatases. *Journal of Biological Chemistry,* 275**,** 35727-35733.

BERTRAM, P. G., CHOI, J. H., CARVALHO, J., CHAN, T.-F., AI, W. & ZHENG, X. S. 2002. Convergence of TOR-nitrogen and Snf1-glucose signaling pathways onto Gln3. *Molecular and cellular biology,* 22**,** 1246-1252.

BIANCONI, M. L. 2003. Calorimetric determination of thermodynamic parameters of reaction reveals different enthalpic compensations of the yeast hexokinase isozymes. *Journal of Biological Chemistry,* 278**,** 18709-18713.

BICKNELL, A. A., BABOUR, A., FEDEROVITCH, C. M. & NIWA, M. 2007. A novel role in cytokinesis reveals a housekeeping function for the unfolded protein response. *The Journal of cell biology,* 177**,** 1017-1027.

BISSON, L. F. & FRAENKEL, D. G. 1983. Involvement of kinases in glucose and fructose uptake by Saccharomyces cerevisiae. *Proceedings of the National Academy of Sciences,* 80**,** 1730-1734.

BLINDER, D. & MAGASANIK, B. 1995. Recognition of nitrogen-responsive upstream activation sequences of Saccharomyces cerevisiae by the product of the GLN3 gene. *Journal of Bacteriology,* 177**,** 4190-4193.

BOEGER, H., GRIESENBECK, J., STRATTAN, J. S. & KORNBERG, R. D. 2004. Removal of promoter nucleosomes by disassembly rather than sliding in vivo. *Molecular cell,* 14**,** 667-673.

BORNEMAN, A. R., LEIGH-BELL, J. A., YU, H., BERTONE, P., GERSTEIN, M. & SNYDER, M. 2006. Target hub proteins serve as master regulators of development in yeast. *Genes & development,* 20**,** 435-448.

BOWDISH, K. & MITCHELL, A. 1993. Bipartite structure of an early meiotic upstream activation sequence from Saccharomyces cerevisiae. *Molecular and Cellular Biology,* 13**,** 2172-2181.

BOWDISH, K. S., YUAN, H. E. & MITCHELL, A. P. 1995. Positive control of yeast meiotic genes by the negative regulator UME6. *Molecular and cellular biology,* 15**,** 2955-2961.

BRIZA, P., BREITENBACH, M., ELLINGER, A. & SEGALL, J. 1990. Isolation of two developmentally regulated genes involved in spore wall maturation in Saccharomyces cerevisiae. *Genes & Development,* 4**,** 1775-1789.

BROACH, J. R. 2012. Nutritional control of growth and development in yeast. *Genetics,* 192**,** 73-105.

BROACH, J. R. & DESCHENES, R. J. 1990. The function of ras genes in Saccharomyces cerevisiae. *Advances in cancer research,* 54**,** 79-139.

BRODSKY, J. L. & SKACH, W. R. 2011. Protein folding and quality control in the endoplasmic reticulum: Recent lessons from yeast and mammalian cell systems. *Current opinion in cell biology,* 23**,** 464-475.

BROEK, D., TODA, T., MICHAELI, T., LEVIN, L., BIRCHMEIER, C., ZOLLER, M., POWERS, S. & WIGLER, M. 1987. The S. cerevisiae CDC25 gene product regulates the RAS/adenylate cyclase pathway. *Cell,* 48**,** 789-799.

BUKAU, B. & HORWICH, A. L. 1998. The Hsp70 and Hsp60 chaperone machines. *Cell,* 92**,** 351-366.

BURGESS, S. M., AJIMURA, M. & KLECKNER, N. 1999. GCN5-dependent histone H3 acetylation and RPD3-dependent histone H4 deacetylation have distinct, opposing effects on IME2 transcription, during meiosis and during vegetative growth, in budding yeast. *Proceedings of the National Academy of Sciences,* 96**,** 6835-6840.

BUSHKIN, G. G., PINCUS, D., MORGAN, J. T., RICHARDSON, K., LEWIS, C., CHAN, S. H., BARTEL, D. P. & FINK, G. R. 2019. m6A modification of a 3′ UTR site reduces RME1 mRNA levels to promote meiosis. *Nature Communications,* 10**,** 1-13.

BYERS, B. 1981. Cytology of the yeast life cycle. *The molecular biology of the yeast Saccharomyces: life cycle and inheritance.***,** 59-96.

CALFON, M., ZENG, H., URANO, F., TILL, J. H., HUBBARD, S. R., HARDING, H. P., CLARK, S. G. & RON, D. 2002. IRE1 couples endoplasmic reticulum load to secretory capacity by processing the XBP-1 mRNA. *Nature,* 415**,** 92-96.

CARDENAS, M. E., CUTLER, N. S., LORENZ, M. C., DI COMO, C. J. & HEITMAN, J. 1999. The TOR signaling cascade regulates gene expression in response to nutrients. *Genes & development,* 13**,** 3271-3279.

CARLSON, M. 1999. Glucose repression in yeast. *Current opinion in microbiology,* 2**,** 202-207.

CARLSON, M., OSMOND, B. C. & BOTSTEIN, D. 1981. Mutants of yeast defective in sucrose utilization. *Genetics,* 98**,** 25-40.

CARROZZA, M. J., FLORENS, L., SWANSON, S. K., SHIA, W.-J., ANDERSON, S., YATES, J., WASHBURN, M. P. & WORKMAN, J. L. 2005a. Stable incorporation of sequence specific repressors Ash1 and Ume6 into the Rpd3L complex. *Biochimica et Biophysica Acta (BBA)-Gene Structure and Expression,* 1731**,** 77-87.

CARROZZA, M. J., LI, B., FLORENS, L., SUGANUMA, T., SWANSON, S. K., LEE, K. K., SHIA, W.-J., ANDERSON, S., YATES, J. & WASHBURN, M. P. 2005b. Histone H3 methylation by Set2 directs deacetylation of coding regions by Rpd3S to suppress spurious intragenic transcription. *Cell,* 123**,** 581-592.

CHAPMAN, R., SIDRAUSKI, C. & WALTER, P. 1998. Intracellular signaling from the endoplasmic reticulum to the nucleus. *Annual review of cell and developmental biology,* 14**,** 459-485.

CHAPMAN, R. E. & WALTER, P. 1997. Translational attenuation mediated by an mRNA intron. *Curr Biol,* 7**,** 850-9.

CHAUDHURI, T. K. & PAUL, S. 2006. Protein-misfolding diseases and chaperone-based therapeutic approaches. *The FEBS journal,* 273**,** 1331-1349.

CHEN, E. J. & KAISER, C. A. 2003. LST8 negatively regulates amino acid biosynthesis as a component of the TOR pathway. *The Journal of cell biology,* 161**,** 333-347.
CHEN, H., FAN, M., PFEFFER, L. M. & LARIBEE, R. N. 2012. The histone H3 lysine 56 acetylation pathway is regulated by target of rapamycin (TOR) signaling and functions directly in ribosomal RNA biogenesis. *Nucleic acids research,* 40**,** 6534-6546.
CHEN, H. & FINK, G. R. 2006. Feedback control of morphogenesis in fungi by aromatic alcohols. *Genes & development,* 20**,** 1150-1161.
CHEN, S., LEE, C. N., LEE, W. R., MCINTOSH, K. & LEE, T. H. 1993. Mutational analysis of the leucine zipper-like motif of the human immunodeficiency virus type 1 envelope transmembrane glycoprotein. *Journal of Virology,* 67**,** 3615-3619.
CHEN, S. S.-L., LEE, S.-F., HAO, H.-J. & CHUANG, C.-K. 1998. Mutations in the leucine zipper-like heptad repeat sequence of human immunodeficiency virus type 1 gp41 dominantly interfere with wild-type virus infectivity. *Journal of virology,* 72**,** 4765-4774.
CHOL, K.-Y., SATTERBERG, B., LYONS, D. M. & ELION, E. A. 1994. Ste5 tethers multiple protein kinases in the MAP kinase cascade required for mating in S. cerevisiae. *Cell,* 78**,** 499-512.
CHONG, Y. T., KOH, J. L., FRIESEN, H., DUFFY, S. K., COX, M. J., MOSES, A., MOFFAT, J., BOONE, C. & ANDREWS, B. J. 2015. Yeast proteome dynamics from single cell imaging and automated analysis. *Cell,* 161**,** 1413-1424.
CHRISTIANSON, T. W., SIKORSKI, R. S., DANTE, M., SHERO, J. H. & HIETER, P. 1992. Multifunctional yeast high-copy-number shuttle vectors. *Gene,* 110**,** 119-122.
CHU, S., DERISI, J., EISEN, M., MULHOLLAND, J., BOTSTEIN, D., BROWN, P. O. & HERSKOWITZ, I. 1998. The transcriptional program of sporulation in budding yeast. *Science,* 282**,** 699-705.
CHU, S. & HERSKOWITZ, I. 1998. Gametogenesis in yeast is regulated by a transcriptional cascade dependent on Ndt80. *Molecular cell,* 1**,** 685-696.
CLAPIER, C. R. & CAIRNS, B. R. 2009. The biology of chromatin remodeling complexes. *Annual review of biochemistry,* 78**,** 273-304.
CLAUSS, I. M., CHU, M., ZHAO, J.-L. & GLIMCHER, L. H. 1996. The basic domain/leucine zipper protein hXBP-1 preferentially binds to and transactivates CRE-like sequences containing an ACGT core. *Nucleic acids research,* 24**,** 1855-1864.
CLIFFORD, D. M., MARINCO, S. M. & BRUSH, G. S. 2004. The meiosis-specific protein kinase Ime2 directs phosphorylation of replication protein A. *Journal of Biological Chemistry,* 279**,** 6163-6170.
COLOMBO, S., MA, P., CAUWENBERG, L., WINDERICKX, J., CRAUWELS, M., TEUNISSEN, A., NAUWELAERS, D., DE WINDE, J. H., GORWA, M. F. & COLAVIZZA, D. 1998. Involvement of distinct G-proteins, Gpa2 and Ras, in glucose-and intracellular acidification-induced cAMP signalling in the yeast Saccharomyces cerevisiae. *The EMBO journal,* 17**,** 3326-3341.
COLOMINA, N., GARÍ, E., GALLEGO, C., HERRERO, E. & ALDEA, M. 1999. G1 cyclins block the Ime1 pathway to make mitosis and meiosis incompatible in budding yeast. *The EMBO journal,* 18**,** 320-329.
CONRAD, M., SCHOTHORST, J., KANKIPATI, H. N., VAN ZEEBROECK, G., RUBIO-TEXEIRA, M. & THEVELEIN, J. M. 2014. Nutrient sensing and signaling in the yeast Saccharomyces cerevisiae. *FEMS microbiology reviews,* 38**,** 254-299.
COOK, J. G., BARDWELL, L., KRON, S. J. & THORNER, J. 1996. Two novel targets of the MAP kinase Kss1 are negative regulators of invasive growth in the yeast Saccharomyces cerevisiae. *Genes & development,* 10**,** 2831-2848.

COOK, J. G., BARDWELL, L. & THORNER, J. 1997. Inhibitory and activating functions for MAPK Kss1 in the S. cerevisiae filamentous-growth signalling pathway. *Nature,* 390**,** 85-88.
COOPER, K. F. & STRICH, R. 2002. Saccharomyces cerevisiae C-type cyclin Ume3p/Srb11p is required for efficient induction and execution of meiotic development. *Eukaryotic cell,* 1**,** 66-74.
COOPER, T. G. 2002. Transmitting the signal of excess nitrogen in Saccharomyces cerevisiae from the Tor proteins to the GATA factors: connecting the dots. *FEMS microbiology reviews,* 26**,** 223-238.
COURCHESNE, W. E. & MAGASANIK, B. 1983. Ammonia regulation of amino acid permeases in Saccharomyces cerevisiae. *Molecular and cellular biology,* 3**,** 672-683.
COVITZ, P., HERSKOWITZ, I. & MITCHELL, A. 1991. The yeast RME1 gene encodes a putative zinc finger protein that is directly repressed by a1-alpha 2. *Genes & development,* 5**,** 1982-1989.
COVITZ, P. A. & MITCHELL, A. P. 1993. Repression by the yeast meiotic inhibitor RME1. *Genes & development,* 7**,** 1598-1608.
COWELL, I. G. & HURST, H. C. 1996. Protein-protein interaction between the transcriptional repressor E4BP4 and the TBP-binding protein Dr1. *Nucleic acids research,* 24**,** 3607-3613.
COX, J. S., CHAPMAN, R. E. & WALTER, P. 1997. The unfolded protein response coordinates the production of endoplasmic reticulum protein and endoplasmic reticulum membrane. *Molecular biology of the cell,* 8**,** 1805-1814.
COX, J. S., SHAMU, C. E. & WALTER, P. 1993. Transcriptional induction of genes encoding endoplasmic reticulum resident proteins requires a transmembrane protein kinase. *Cell,* 73**,** 1197-1206.
COX, J. S. & WALTER, P. 1996. A novel mechanism for regulating activity of a transcription factor that controls the unfolded protein response. *Cell,* 87**,** 391-404.
CULLEN, P. J., SABBAGH, W., GRAHAM, E., IRICK, M. M., VAN OLDEN, E. K., NEAL, C., DELROW, J., BARDWELL, L. & SPRAGUE, G. F. 2004. A signaling mucin at the head of the Cdc42-and MAPK-dependent filamentous growth pathway in yeast. *Genes & development,* 18**,** 1695-1708.
CULLEN, P. J. & SPRAGUE JR, G. F. 2012. The regulation of filamentous growth in yeast. *Genetics,* 190**,** 23-49.
DANG, W., KAGALWALA, M. N. & BARTHOLOMEW, B. 2007. The Dpb4 subunit of ISW2 is anchored to extranucleosomal DNA. *Journal of Biological Chemistry,* 282**,** 19418-19425.
DAVENPORT, K., WILLIAMS, K., ULLMANN, B. & GUSTIN, M. 1999. Activation of the Saccharomyces cerevisiae filamentation/invasion pathway by osmotic stress in high-osmolarity glycogen pathway mutants. *Genetics,* 153**,** 1091-1103.
DE NADAL, E., ZAPATER, M., ALEPUZ, P. M., SUMOY, L., MAS, G. & POSAS, F. 2004. The MAPK Hog1 recruits Rpd3 histone deacetylase to activate osmoresponsive genes. *Nature,* 427**,** 370-374.
DE SILVA-UDAWATTA, M. N. & CANNON, J. F. 2001. Roles of trehalose phosphate synthase in yeast glycogen metabolism and sporulation. *Molecular microbiology,* 40**,** 1345-1356.
DENG, C. & SAUNDERS, W. 2001. RIM4 encodes a meiotic activator required for early events of meiosis in Saccharomyces cerevisiae. *Molecular Genetics and Genomics,* 266**,** 497-504.
DEUTSCHBAUER, A. M. & DAVIS, R. W. 2005. Quantitative trait loci mapped to single-nucleotide resolution in yeast. *Nature genetics,* 37**,** 1333-1340.

DI COMO, C. J. & ARNDT, K. T. 1996. Nutrients, via the Tor proteins, stimulate the association of Tap42 with type 2A phosphatases. *Genes & development,* 10**,** 1904-1916.
DI SANTO, R., ABOULHOUDA, S. & WEINBERG, D. E. 2016. The fail-safe mechanism of post-transcriptional silencing of unspliced HAC1 mRNA. *Elife,* 5**,** e20069.
DICKINSON, J. R. 1996. Fuse1 alcohols induce hyphal-like extensions and pseudohyphal formationin yeasts. *Microbiology,* 142**,** 1391-1397.
DIDERICH, J. A., SCHEPPER, M., VAN HOEK, P., LUTTIK, M. A., VAN DIJKEN, J. P., PRONK, J. T., KLAASSEN, P., BOELENS, H. F., DE MATTOS, M. J. T. & VAN DAM, K. 1999. Glucose uptake kinetics and transcription of HXTGenes in chemostat cultures of Saccharomyces cerevisiae. *Journal of Biological Chemistry,* 274**,** 15350-15359.
DIETZEL, C. & KURJAN, J. 1987. The yeast SCG1 gene: a Gα-like protein implicated in the a-and α-factor response pathway. *Cell,* 50**,** 1001-1010.
DIRICK, L., BÖHM, T. & NASMYTH, K. 1995. Roles and regulation of Cln-Cdc28 kinases at the start of the cell cycle of Saccharomyces cerevisiae. *The EMBO journal,* 14**,** 4803-4813.
DIRICK, L., GOETSCH, L., AMMERER, G. & BYERS, B. 1998. Regulation of meiotic S phase by Ime2 and a Clb5, 6-associated kinase in Saccharomyces cerevisiae. *Science,* 281**,** 1854-1857.
DOHLMAN, H. G. & THORNER, J. 2001. Regulation of G protein–initiated signal transduction in yeast: paradigms and principles. *Annual review of biochemistry,* 70**,** 703-754.
DONATON, M. C., HOLSBEEKS, I., LAGATIE, O., VAN ZEEBROECK, G., CRAUWELS, M., WINDERICKX, J. & THEVELEIN, J. M. 2003. The Gap1 general amino acid permease acts as an amino acid sensor for activation of protein kinase A targets in the yeast Saccharomyces cerevisiae. *Molecular microbiology,* 50**,** 911-929.
DONZEAU, M. & BANDLOW, W. 1999. The yeast trimeric guanine nucleotide-binding protein α subunit, Gpa2p, controls the meiosis-specific kinase Ime2p activity in response to nutrients. *Molecular and cellular biology,* 19**,** 6110-6119.
DORA, E. G., RUDIN, N., MARTELL, J. R., ESPOSITO, M. S. & RAMÍREZ, R. M. 1999. RPD3 (REC3) mutations affect mitotic recombination in Saccharomyces cerevisiae. *Current genetics,* 35**,** 68-76.
DÜVEL, K., SANTHANAM, A., GARRETT, S., SCHNEPER, L. & BROACH, J. R. 2003. Multiple roles of Tap42 in mediating rapamycin-induced transcriptional changes in yeast. *Molecular cell,* 11**,** 1467-1478.
DWARKI, V., MONTMINY, M. & VERMA, I. 1990. Both the basic region and the 'leucine zipper'domain of the cyclic AMP response element binding (CREB) protein are essential for transcriptional activation. *The EMBO journal,* 9**,** 225-232.
EHRENTRAUT, S., WEBER, J. M., DYBOWSKI, J. N., HOFFMANN, D. & EHRENHOFER-MURRAY, A. E. 2010. Rpd3-dependent boundary formation at telomeres by removal of Sir2 substrate. *Proceedings of the National Academy of Sciences,* 107**,** 5522-5527.
ELLENBERGER, T. 1994. Getting a grip on DNA recognition: structures of the basic region leucine zipper, and the basic region helix-loop-helix DNA-binding domains. *Current Opinion in Structural Biology,* 4**,** 12-21.
ELLENBERGER, T. E., BRANDL, C. J., STRUHL, K. & HARRISON, S. C. 1992. The GCN4 basic region leucine zipper binds DNA as a dimer of uninterrupted α helices: crystal structure of the protein-DNA complex. *Cell,* 71**,** 1223-1237.
ENYENIHI, A. H. & SAUNDERS, W. S. 2003. Large-scale functional genomic analysis of sporulation and meiosis in Saccharomyces cerevisiae. *Genetics,* 163**,** 47-54.

ESPOSITO, M. S. & ESPOSITO, R. E. 1974. Genes controlling meiosis and spore formation in yeast. *Genetics,* 78**,** 215.
FABRIZIO, P., BATTISTELLA, L., VARDAVAS, R., GATTAZZO, C., LIOU, L.-L., DIASPRO, A., DOSSEN, J. W., GRALLA, E. B. & LONGO, V. D. 2004. Superoxide is a mediator of an altruistic aging program in Saccharomyces cerevisiae. *The Journal of cell biology,* 166**,** 1055-1067.
FAZZIO, T. G., KOOPERBERG, C., GOLDMARK, J. P., NEAL, C., BASOM, R., DELROW, J. & TSUKIYAMA, T. 2001. Widespread collaboration of Isw2 and Sin3-Rpd3 chromatin remodeling complexes in transcriptional repression. *Molecular and cellular biology,* 21**,** 6450-6460.
FITZGERALD, D. J., DELUCA, C., BERGER, I., GAILLARD, H., SIGRIST, R., SCHIMMELE, K. & RICHMOND, T. J. 2004. Reaction cycle of the yeast Isw2 chromatin remodeling complex. *The EMBO journal,* 23**,** 3836-3843.
FOIANI, M., NADJAR-BOGER, E., CAPONE, R., SAGEE, S., HASHIMSHONI, T. & KASSIR, Y. 1996. A meiosis-specific protein kinase, Ime2, is required for the correct timing of DNA replication and for spore formation in yeast meiosis. *Molecular and General Genetics MGG,* 253**,** 278-288.
FOLCO, H. D., CHALAMCHARLA, V. R., SUGIYAMA, T., THILLAINADESAN, G., ZOFALL, M., BALACHANDRAN, V., DHAKSHNAMOORTHY, J., MIZUGUCHI, T. & GREWAL, S. I. 2017. Untimely expression of gametogenic genes in vegetative cells causes uniparental disomy. *Nature,* 543**,** 126-130.
FORDYCE, P. M., PINCUS, D., KIMMIG, P., NELSON, C. S., EL-SAMAD, H., WALTER, P. & DERISI, J. L. 2012. Basic leucine zipper transcription factor Hac1 binds DNA in two distinct modes as revealed by microfluidic analyses. *Proceedings of the National Academy of Sciences,* 109**,** E3084-E3093.
FRAND, A. R. & KAISER, C. A. 1998. The ERO1 gene of yeast is required for oxidation of protein dithiols in the endoplasmic reticulum. *Molecular cell,* 1**,** 161-170.
FREESE, E. B., CHU, M. I. & FREESE, E. 1982. Initiation of yeast sporulation by partial carbon, nitrogen, or phosphate deprivation. *Journal of Bacteriology,* 149**,** 840-851.
FREESE, E. B., OLEMPSKA-BEER, Z., HARTIG, A. & FREESE, E. 1984. Initiation of meiosis and sporulation of Saccharomyces cerevisiae by sulfur or guanine deprivation. *Developmental biology,* 102**,** 438-451.
FRENZ, L., JOHNSON, A. & JOHNSTON, L. 2001. Rme1, which controls CLN2 expression in Saccharomyces cerevisiae, is a nuclear protein that is cell cycle regulated. *Molecular Genetics and Genomics,* 266**,** 374-384.
FRIEDLANDER, R., JAROSCH, E., URBAN, J., VOLKWEIN, C. & SOMMER, T. 2000. A regulatory link between ER-associated protein degradation and the unfolded-protein response. *Nature cell biology,* 2**,** 379-384.
FUJII, Y., SHIMIZU, T., TODA, T., YANAGIDA, M. & HAKOSHIMA, T. 2000. Structural basis for the diversity of DNA recognition by bZIP transcription factors. *Nature structural biology,* 7**,** 889-893.
FUJITA, A., TONOUCHI, A., HIROKO, T., INOSE, F., NAGASHIMA, T., SATOH, R. & TANAKA, S. 1999. Hsl7p, a negative regulator of Ste20p protein kinase in the Saccharomyces cerevisiae filamentous growth-signaling pathway. *Proceedings of the National Academy of Sciences,* 96**,** 8522-8527.
GAGIANO, M., BAUER, F. F. & PRETORIUS, I. S. 2002. The sensing of nutritional status and the relationship to filamentous growth in Saccharomyces cerevisiae. *FEMS yeast research,* 2**,** 433-470.
GAI, Y., LI, L., LIU, B., MA, H., CHEN, Y., ZHENG, F., SUN, X., WANG, M., JIAO, C. & LI, H. 2022. Distinct and essential roles of bZIP transcription factors in the stress response and pathogenesis in Alternaria alternata. *Microbiological Research,* 256**,** 126915.

GAILUS-DURNER, V., XIE, J., CHINTAMANENI, C. & VERSHON, A. K. 1996. Participation of the yeast activator Abf1 in meiosis-specific expression of the HOP1 gene. *Molecular and Cellular Biology,* 16**,** 2777-2786.
GALLEGO, C., GARÍ, E., COLOMINA, N., HERRERO, E. & ALDEA, M. 1997. The Cln3 cyclin is down-regulated by translational repression and degradation during the G1 arrest caused by nitrogen deprivation in budding yeast. *The EMBO journal,* 16**,** 7196-7206.
GANCEDO, J. M. 1993. Carbon catabolite repression in yeast. *EJB Reviews***,** 105-121.
GANCEDO, J. M. 1998. Yeast carbon catabolite repression. *Microbiology and molecular biology reviews,* 62**,** 334-361.
GANCEDO, J. M. 2001. Control of pseudohyphae formation in Saccharomyces cerevisiae. *FEMS microbiology reviews,* 25**,** 107-123.
GARDNER, B. M., PINCUS, D., GOTTHARDT, K., GALLAGHER, C. M. & WALTER, P. 2013. Endoplasmic reticulum stress sensing in the unfolded protein response. *Cold Spring Harbor perspectives in biology,* 5**,** a013169.
GARREAU, H., HASAN, R. N., RENAULT, G., ESTRUCH, F., BOY-MARCOTTE, E. & JACQUET, M. 2000. Hyperphosphorylation of Msn2p and Msn4p in response to heat shock and the diauxic shift is inhibited by cAMP in Saccharomyces cerevisiae. *Microbiology,* 146**,** 2113-2120.
GAVADE, J. N., PUCCIA, C. M., HEROD, S. G., TRINIDAD, J. C., BERCHOWITZ, L. E. & LACEFIELD, S. 2022. Identification of 14-3-3 proteins, Polo kinase, and RNA-binding protein Pes4 as key regulators of meiotic commitment in budding yeast. *Current Biology,* 32**,** 1534-1547. e9.
GAVRIAS, V., ANDRIANOPOULOS, A., GIMENO, C. J. & TIMBERLAKE, W. E. 1996. Saccharomyces cerevisiae TEC1 is required for pseudohyphal growth. *Molecular microbiology,* 19**,** 1255-1263.
GELBART, M. E., RECHSTEINER, T., RICHMOND, T. J. & TSUKIYAMA, T. 2001. Interactions of Isw2 chromatin remodeling complex with nucleosomal arrays: analyses using recombinant yeast histones and immobilized templates. *Molecular and cellular biology,* 21**,** 2098-2106.
GENTZ, R., RAUSCHER, F. J., ABATE, C. & CURRAN, T. 1989. Parallel association of Fos and Jun leucine zippers juxtaposes DNA binding domains. *Science,* 243**,** 1695-1699.
GETHING, M.-J. & SAMBROOK, J. 1992. Protein folding in the cell. *Nature,* 355**,** 33-45.
GHAEMMAGHAMI, S., HUH, W.-K., BOWER, K., HOWSON, R. W., BELLE, A., DEPHOURE, N., O'SHEA, E. K. & WEISSMAN, J. S. 2003. Global analysis of protein expression in yeast. *Nature,* 425**,** 737-741.
GIETZ, R. D. & SCHIESTL, R. H. 2007. High-efficiency yeast transformation using the LiAc/SS carrier DNA/PEG method. *Nature protocols,* 2**,** 31-34.
GIMENO, C. J., LJUNGDAHL, P. O., STYLES, C. A. & FINK, G. R. 1992. Unipolar cell divisions in the yeast S. cerevisiae lead to filamentous growth: regulation by starvation and RAS. *Cell,* 68**,** 1077-1090.
GLOVER, J. M. & HARRISON, S. C. 1995. Crystal structure of the heterodimeric bZIP transcription factor c-Fos–c-Jun bound to DNA. *Nature,* 373**,** 257-261.
GOLDMARK, J. P., FAZZIO, T. G., ESTEP, P. W., CHURCH, G. M. & TSUKIYAMA, T. 2000. The Isw2 chromatin remodeling complex represses early meiotic genes upon recruitment by Ume6p. *Cell,* 103**,** 423-433.
GOVIND, C. K., QIU, H., GINSBURG, D. S., RUAN, C., HOFMEYER, K., HU, C., SWAMINATHAN, V., WORKMAN, J. L., LI, B. & HINNEBUSCH, A. G. 2010. Phosphorylated Pol II CTD recruits multiple HDACs, including Rpd3C (S), for methylation-dependent deacetylation of ORF nucleosomes. *Molecular cell,* 39**,** 234-246.

GRANOT, D., MARGOLSKEE, J. P. & SIMCHEN, G. 1989. A long region upstream of the IME1 gene regulates meiosis in yeast. *Molecular and General Genetics MGG,* 218**,** 308-314.
GRANT, P. A., DUGGAN, L., CÔTÉ, J., ROBERTS, S. M., BROWNELL, J. E., CANDAU, R., OHBA, R., OWEN-HUGHES, T., ALLIS, C. D. & WINSTON, F. 1997. Yeast Gcn5 functions in two multisubunit complexes to acetylate nucleosomal histones: characterization of an Ada complex and the SAGA (Spt/Ada) complex. *Genes & development,* 11**,** 1640-1650.
GRAY, S. G. & EKSTRÖM, T. J. 2001. The human histone deacetylase family. *Experimental cell research,* 262**,** 75-83.
GREEN, A. A. & HUGHES, W. L. 1955. [10] Protein fractionation on the basis of solubility in aqueous solutions of salts and organic solvents.
GUO, J. & POLYMENIS, M. 2006. Dcr2 targets Ire1 and downregulates the unfolded protein response in Saccharomyces cerevisiae. *EMBO reports,* 7**,** 1124-1127.
GUSTIN, M. C., ALBERTYN, J., ALEXANDER, M. & DAVENPORT, K. 1998. MAP kinase pathways in the yeast Saccharomyces cerevisiae. *Microbiology and Molecular biology reviews,* 62**,** 1264-1300.
GUTTMANN-RAVIV, N., MARTIN, S. & KASSIR, Y. 2002. Ime2, a meiosis-specific kinase in yeast, is required for destabilization of its transcriptional activator, Ime1. *Molecular and cellular biology,* 22**,** 2047-2056.
HAI, T. & HARTMAN, M. G. 2001. The molecular biology and nomenclature of the activating transcription factor/cAMP responsive element binding family of transcription factors: activating transcription factor proteins and homeostasis. *Gene,* 273**,** 1-11.
HAI, T., WOLFGANG, C. D., MARSEE, D. K., ALLEN, A. E. & SIVAPRASAD, U. 1999. ATF3 and stress responses. *Gene Expression The Journal of Liver Research,* 7**,** 321-335.
HALAZONETIS, T. D., GEORGOPOULOS, K., GREENBERG, M. E. & LEDER, P. 1988. c-Jun dimerizes with itself and with c-Fos, forming complexes of different DNA binding affinities. *Cell,* 55**,** 917-924.
HAMPTON, R. Y. 2000. ER stress response: getting the UPR hand on misfolded proteins. *Current Biology,* 10**,** R518-R521.
HARASHIMA, T., ANDERSON, S., YATES III, J. R. & HEITMAN, J. 2006. The kelch proteins Gpb1 and Gpb2 inhibit Ras activity via association with the yeast RasGAP neurofibromin homologs Ira1 and Ira2. *Molecular cell,* 22**,** 819-830.
HARDWICK, J. S., KURUVILLA, F. G., TONG, J. K., SHAMJI, A. F. & SCHREIBER, S. L. 1999. Rapamycin-modulated transcription defines the subset of nutrient-sensitive signaling pathways directly controlled by the Tor proteins. *Proceedings of the National Academy of Sciences,* 96**,** 14866-14870.
HARRISON, S. C. 1991. A structural taxonomy of DNA-binding domains. *Nature,* 353**,** 715-719.
HARTL, F. U. 1996. Molecular chaperones in cellular protein folding. *Nature,* 381**,** 571-580.
HARTWELL, L. H. 1974. Saccharomyces cerevisiae cell cycle. *Bacteriological reviews,* 38**,** 164-198.
HEIMEL, K., FREITAG, J., HAMPEL, M., AST, J., BÖLKER, M. & KÄMPER, J. 2013. Crosstalk between the unfolded protein response and pathways that regulate pathogenic development in Ustilago maydis. *The Plant Cell,* 25**,** 4262-4277.
HEPWORTH, S. R., FRIESEN, H. & SEGALL, J. 1998. NDT80 and the meiotic recombination checkpoint regulate expression of middle sporulation-specific genes in Saccharomyces cerevisiae. *Molecular and cellular biology,* 18**,** 5750-5761.
HERMAN, P. K. & RINE, J. 1997. Yeast spore germination: a requirement for Ras protein activity during re-entry into the cell cycle. *The EMBO journal,* 16**,** 6171-6181.

HERSKOWITZ, I. 1988. Life cycle of the budding yeast Saccharomyces cerevisiae. *Microbiological reviews,* 52**,** 536-553.
HERSKOWITZ, I. 1992. Mating-type determination and mating-type interconversion in Saccharomyces cerevisiae. *The molecular and cellular biology of the yeast Saccharomyces; Vol. 2, Gene expression***,** 586-656.
HERSKOWITZ, I. 1995. MAP kinase pathways in yeast: for mating and more. *Cell,* 80**,** 187-197.
HESS, J., ANGEL, P. & SCHORPP-KISTNER, M. 2004. AP-1 subunits: quarrel and harmony among siblings. *Journal of cell science,* 117**,** 5965-5973.
HINNEBUSCH, A. G. & NATARAJAN, K. 2002. Gcn4p, a master regulator of gene expression, is controlled at multiple levels by diverse signals of starvation and stress. *Eukaryotic cell,* 1**,** 22-32.
HIRSCHBERG, J. & SIMCHEN, G. 1977. Commitment to the mitotic cell cycle in yeast in relation to meiosis. *Experimental cell research,* 105**,** 245-252.
HODGES, R. S., SODEK, J., SMILLIE, L. & JURASEK, L. Tropomyosin: amino acid sequence and coiled-coil structure. Cold Spring Harbor Symposia on Quantitative Biology, 1973. Cold Spring Harbor Laboratory Press, 299-310.
HOFMAN-BANG, J. 1999. Nitrogen catabolite repression in Saccharomyces cerevisiae. *Molecular biotechnology,* 12**,** 35-71.
HOHMANN, S., KRANTZ, M. & NORDLANDER, B. 2007. Yeast osmoregulation. *Methods in enzymology,* 428**,** 29-45.
HONGAY, C. F., GRISAFI, P. L., GALITSKI, T. & FINK, G. R. 2006. Antisense transcription controls cell fate in Saccharomyces cerevisiae. *Cell,* 127**,** 735-745.
HONIGBERG, S. M. 2004. Ime2p and Cdc28p: co-pilots driving meiotic development. *Journal of cellular biochemistry,* 92**,** 1025-1033.
HONIGBERG, S. M., CONICELLA, C. & ESPOSITIO, R. E. 1992. Commitment to meiosis in Saccharomyces cerevisiae: involvement of the SPO14 gene. *Genetics,* 130**,** 703-716.
HONIGBERG, S. M. & LEE, R. H. 1998. Snf1 kinase connects nutritional pathways controlling meiosis in Saccharomyces cerevisiae. *Molecular and cellular biology,* 18**,** 4548-4555.
HONIGBERG, S. M. & PURNAPATRE, K. 2003. Signal pathway integration in the switch from the mitotic cell cycle to meiosis in yeast. *Journal of cell science,* 116**,** 2137-2147.
HOTA, S. K. & BARTHOLOMEW, B. 2011. Diversity of operation in ATP-dependent chromatin remodelers. *Biochimica et Biophysica Acta (BBA)-Gene Regulatory Mechanisms,* 1809**,** 476-487.
HU, J. C., O'SHEA, E. K., KIM, P. S. & SAUER, R. T. 1990. Sequence requirements for coiled-coils: analysis with lambda repressor-GCN4 leucine zipper fusions. *Science,* 250**,** 1400-1403.
HUBBARD, S. C. & IVATT, R. J. 1981. Synthesis and processing of asparagine-linked oligosaccharides. *Annual review of biochemistry,* 50**,** 555-583.
IFTODE, C., DANIELY, Y. & BOROWIEC, J. A. 1999. Replication protein A (RPA): the eukaryotic SSB. *Critical reviews in biochemistry and molecular biology,* 34**,** 141-180.
ISHIWATA-KIMATA, Y., YAMAMOTO, Y.-H., TAKIZAWA, K., KOHNO, K. & KIMATA, Y. 2013. F-actin and a type-II myosin are required for efficient clustering of the ER stress sensor Ire1. *Cell structure and function***,** 12033.
IWAKOSHI, N. N., LEE, A.-H., VALLABHAJOSYULA, P., OTIPOBY, K. L., RAJEWSKY, K. & GLIMCHER, L. H. 2003. Plasma cell differentiation and the unfolded protein response intersect at the transcription factor XBP-1. *Nature immunology,* 4**,** 321-329.

JAMBHEKAR, A. & AMON, A. 2008. Control of meiosis by respiration. *Current Biology,* 18**,** 969-975.
JIANG, Y. & BROACH, J. R. 1999. Tor proteins and protein phosphatase 2A reciprocally regulate Tap42 in controlling cell growth in yeast. *The EMBO journal,* 18**,** 2782-2792.
JOHNSON, P. F. & MCKNIGHT, S. L. 1989. Eukaryotic transcriptional regulatory proteins. *Annual review of biochemistry,* 58**,** 799-839.
JOHNSTON, G. 1977. Cell size and budding during starvation of the yeast Saccharomyces cerevisiae. *Journal of Bacteriology,* 132**,** 738-739.
JOHNSTON, M. 1992. Regulation of carbon and phosphate utilization. *The molecular and cellular biology of the yeast Saccharomyces***,** 193-281.
JOHNSTON, M. & KIM, J.-H. 2005. Glucose as a hormone: receptor-mediated glucose sensing in the yeast Saccharomyces cerevisiae. Portland Press Ltd.
JOSHI, A., NEWBATT, Y., MCANDREW, P. C., STUBBS, M., BURKE, R., RICHARDS, M. W., BHATIA, C., CALDWELL, J. J., MCHARDY, T. & COLLINS, I. 2015. Molecular mechanisms of human IRE1 activation through dimerization and ligand binding. *Oncotarget,* 6**,** 13019.
JOSHI, A. A. & STRUHL, K. 2005. Eaf3 chromodomain interaction with methylated H3-K36 links histone deacetylation to Pol II elongation. *Molecular cell,* 20**,** 971-978.
JUNG, K.-W., SO, Y.-S. & BAHN, Y.-S. 2016. Unique roles of the unfolded protein response pathway in fungal development and differentiation. *Scientific reports,* 6**,** 1-14.
JUNGBLUT, A., HOPFNER, K.-P. & EUSTERMANN, S. 2020. Megadalton chromatin remodelers: common principles for versatile functions. *Current Opinion in Structural Biology,* 64**,** 134-144.
KAADIGE, M. R. & LOPES, J. M. 2003. Opi1p, Ume6p and Sin3p control expression from the promoter of the INO2 regulatory gene via a novel regulatory cascade. *Molecular microbiology,* 48**,** 823-832.
KADOSH, D. & STRUHL, K. 1997. Repression by Ume6 involves recruitment of a complex containing Sin3 corepressor and Rpd3 histone deacetylase to target promoters. *Cell,* 89**,** 365-371.
KADOSH, D. & STRUHL, K. 1998a. Histone deacetylase activity of Rpd3 is important for transcriptional repression in vivo. *Genes & development,* 12**,** 797-805.
KADOSH, D. & STRUHL, K. 1998b. Targeted recruitment of the Sin3-Rpd3 histone deacetylase complex generates a highly localized domain of repressed chromatin in vivo. *Molecular and cellular biology,* 18**,** 5121-5127.
KAGALWALA, M. N., GLAUS, B. J., DANG, W., ZOFALL, M. & BARTHOLOMEW, B. 2004. Topography of the ISW2–nucleosome complex: insights into nucleosome spacing and chromatin remodeling. *The EMBO journal,* 23**,** 2092-2104.
KAHANA, S., PNUELI, L., KAINTH, P., SASSI, H. E., ANDREWS, B. & KASSIR, Y. 2010. Functional dissection of IME1 transcription using quantitative promoter–reporter screening. *Genetics,* 186**,** 829-841.
KANE, S. M. & ROTH, R. 1974. Carbohydrate metabolism during ascospore development in yeast. *Journal of bacteriology,* 118**,** 8-14.
KANIAK, A., XUE, Z., MACOOL, D., KIM, J.-H. & JOHNSTON, M. 2004. Regulatory network connecting two glucose signal transduction pathways in Saccharomyces cerevisiae. *Eukaryotic cell,* 3**,** 221-231.
KASSIR, Y., ADIR, N., BOGER-NADJAR, E., RAVIV, N. G., RUBIN-BEJERANO, I., SAGEE, S. & SHENHAR, G. 2003. Transcriptional regulation of meiosis in budding yeast. *International review of cytology,* 224**,** 111-171.
KASSIR, Y., GRANOT, D. & SIMCHEN, G. 1988. IME1, a positive regulator gene of meiosis in S. cerevisiae. *Cell,* 52**,** 853-62.

KASSIR, Y. & SIMCHEN, G. 1976. Regulation of mating and meiosis in yeast by the mating-type region. *Genetics,* 82**,** 187-206.
KASSIR, Y. & SIMCHEN, G. 1989. Pathways leading to meiotic differentiation in the yeast Saccharomyces cerevisiae. *Current genetics*.
KATAOKA, T., BROEK, D. & WIGLER, M. 1985. DNA sequence and characterization of the S. cerevisiae gene encoding adenylate cyclase. *Cell,* 43**,** 493-505.
KAUFMAN, R. J., SCHEUNER, D., SCHRÖDER, M., SHEN, X., LEE, K., LIU, C. Y. & ARNOLD, S. M. 2002. The unfolded protein response in nutrient sensing and differentiation. *Nature reviews Molecular cell biology,* 3**,** 411-421.
KAWAHARA, T., YANAGI, H., YURA, T. & MORI, K. 1997. Endoplasmic reticulum stress-induced mRNA splicing permits synthesis of transcription factor Hac1p/Ern4p that activates the unfolded protein response. *Molecular biology of the cell,* 8**,** 1845-1862.
KELLER, W., KÖNIG, P. & RICHMOND, T. J. 1995. Crystal structure of a bZIP/DNA complex at 2.2 Å: determinants of DNA specific recognition. *Journal of molecular biology,* 254**,** 657-667.
KENT, N. A., KARABETSOU, N., POLITIS, P. K. & MELLOR, J. 2001. In vivo chromatin remodeling by yeast ISWI homologs Isw1p and Isw2p. *Genes & development,* 15**,** 619-626.
KEOGH, M.-C., KURDISTANI, S. K., MORRIS, S. A., AHN, S. H., PODOLNY, V., COLLINS, S. R., SCHULDINER, M., CHIN, K., PUNNA, T. & THOMPSON, N. J. 2005. Cotranscriptional set2 methylation of histone H3 lysine 36 recruits a repressive Rpd3 complex. *Cell,* 123**,** 593-605.
KIM, S., BENGURIA, A., LAI, C.-Y. & JAZWINSKI, S. M. 1999. Modulation of life-span by histone deacetylase genes in Saccharomyces cerevisiae. *Molecular biology of the cell,* 10**,** 3125-3136.
KIM, S., SIDERIS, D. P., SEVIER, C. S. & KAISER, C. A. 2012. Balanced Ero1 activation and inactivation establishes ER redox homeostasis. *Journal of Cell Biology,* 196**,** 713-725.
KIMATA, Y., KIMATA, Y. I., SHIMIZU, Y., ABE, H., FARCASANU, I. C., TAKEUCHI, M., ROSE, M. D. & KOHNO, K. 2003. Genetic evidence for a role of BiP/Kar2 that regulates Ire1 in response to accumulation of unfolded proteins. *Molecular biology of the cell,* 14**,** 2559-2569.
KIMATA, Y., OIKAWA, D., SHIMIZU, Y., ISHIWATA-KIMATA, Y. & KOHNO, K. 2004. A role for BiP as an adjustor for the endoplasmic reticulum stress-sensing protein Ire1. *The Journal of cell biology,* 167**,** 445-456.
KNOEPFLER, P. S. & EISENMAN, R. N. 1999. Sin meets NuRD and other tails of repression. *Cell,* 99**,** 447-450.
KOHNO, K., NORMINGTON, K., SAMBROOK, J., GETHING, M. & MORI, K. 1993. The promoter region of the yeast KAR2 (BiP) gene contains a regulatory domain that responds to the presence of unfolded proteins in the endoplasmic reticulum. *Molecular and cellular biology,* 13**,** 877-890.
KÖNIG, P. & RICHMOND, T. J. 1993. The X-ray structure of the GCN4-bZIP bound to ATF/CREB site DNA shows the complex depends on DNA flexibility. *Journal of molecular biology,* 233**,** 139-154.
KOUZARIDES, T. & ZIFF, E. 1988. The role of the leucine zipper in the fos–jun interaction. *Nature,* 336**,** 646-651.
KRAAKMAN, L., LEMAIRE, K., MA, P., TEUNISSEN, A. W., DONATON, M. C., VAN DIJCK, P., WINDERICKX, J., DE WINDE, J. H. & THEVELEIN, J. M. 1999. A Saccharomyces cerevisiae G-protein coupled receptor, Gpr1, is specifically required for glucose activation of the cAMP pathway during the transition to growth on glucose. *Molecular microbiology,* 32**,** 1002-1012.

KRON, S. J. & GOW, N. A. 1995. Budding yeast morphogenesis: signalling, cytoskeleton and cell cycle. *Current opinion in cell biology,* 7**,** 845-855.
KRON, S. J., STYLES, C. A. & FINK, G. R. 1994. Symmetric cell division in pseudohyphae of the yeast Saccharomyces cerevisiae. *Molecular biology of the cell,* 5**,** 1003-1022.
KU, H. H. 1966. Notes on the use of propagation of error formulas. *Journal of Research of the National Bureau of Standards,* 70**,** 263-273.
KÜBLER, E., MÖSCH, H.-U., RUPP, S. & LISANTI, M. P. 1997. Gpa2p, a G-protein α-subunit, regulates growth and pseudohyphal development in Saccharomyces cerevisiae via a cAMP-dependent mechanism. *Journal of Biological Chemistry,* 272**,** 20321-20323.
KUCHIN, S., VYAS, V. K. & CARLSON, M. 2002. Snf1 protein kinase and the repressors Nrg1 and Nrg2 regulate FLO11, haploid invasive growth, and diploid pseudohyphal differentiation. *Molecular and cellular biology,* 22**,** 3994-4000.
KUKURUZINSKA, M. A. & LENNON, K. 1998. Protein N-Glycosylation: Molecular Genetics and Functional Significance. *Critical Reviews in Oral Biology & Medicine,* 9**,** 415-448.
KUPIEC, M. 1997. Meiosis and sporulation in Saccharomyces cerevisiae. *The Molecular and Cellular Biology of the Yeast Saccharomyces,* 3**,** 889-1036.
KURDISTANI, S. K. & GRUNSTEIN, M. 2003. Histone acetylation and deacetylation in yeast. *Nature reviews Molecular cell biology,* 4**,** 276-284.
KURDISTANI, S. K., ROBYR, D., TAVAZOIE, S. & GRUNSTEIN, M. 2002. Genome-wide binding map of the histone deacetylase Rpd3 in yeast. *Nature genetics,* 31**,** 248-254.
LAMB, T. M., XU, W., DIAMOND, A. & MITCHELL, A. P. 2001. Alkaline response genes of Saccharomyces cerevisiaeand their relationship to the RIM101 pathway. *Journal of Biological Chemistry,* 276**,** 1850-1856.
LANDSCHULZ, W. H., JOHNSON, P. F. & MCKNIGHT, S. L. 1988. The leucine zipper: a hypothetical structure common to a new class of DNA binding proteins. *Science,* 240**,** 1759-1764.
LÄNGST, G. & BECKER, P. B. 2001. Nucleosome mobilization and positioning by ISWI-containing chromatin-remodeling factors. *Journal of cell science,* 114**,** 2561-2568.
LAPORTE, D., COURTOUT, F., SALIN, B., CESCHIN, J. & SAGOT, I. 2013. An array of nuclear microtubules reorganizes the budding yeast nucleus during quiescence. *Journal of Cell Biology,* 203**,** 585-594.
LARDENOIS, A., STUPAREVIC, I., LIU, Y., LAW, M. J., BECKER, E., SMAGULOVA, F., WAERN, K., GUILLEUX, M.-H., HORECKA, J. & CHU, A. 2015. The conserved histone deacetylase Rpd3 and its DNA binding subunit Ume6 control dynamic transcript architecture during mitotic growth and meiotic development. *Nucleic acids research,* 43**,** 115-128.
LEBER, J. H., BERNALES, S., WALTER, P. & MCKNIGHT, S. 2004. IRE1-independent gain control of the unfolded protein response. *PLoS biology,* 2**,** e235.
LECHNER, T., CARROZZA, M. J., YU, Y., GRANT, P. A., EBERHARTER, A., VANNIER, D., BROSCH, G., STILLMAN, D. J., SHORE, D. & WORKMAN, J. L. 2000. Sds3 (suppressor of defective silencing 3) is an integral component of the yeast Sin3· Rpd3 histone deacetylase complex and is required for histone deacetylase activity. *Journal of biological chemistry,* 275**,** 40961-40966.
LEE, A.-H., IWAKOSHI, N. N. & GLIMCHER, L. H. 2003. XBP-1 regulates a subset of endoplasmic reticulum resident chaperone genes in the unfolded protein response. *Molecular and cellular biology,* 23**,** 7448-7459.
LEE, J., SHIN, M.-K., RYU, D.-K., KIM, S. & RYU, W.-S. 2010. Insertion and deletion mutagenesis by overlap extension PCR. *In vitro mutagenesis protocols.* Springer.

LEE, M. W., KIM, B. J., CHOI, H. K., RYU, M. J., KIM, S. B., KANG, K. M., CHO, E. J., YOUN, H. D., HUH, W. K. & KIM, S. T. 2007. Global protein expression profiling of budding yeast in response to DNA damage. *Yeast,* 24**,** 145-154.

LEE, R. H. & HONIGBERG, S. M. 1996. Nutritional regulation of late meiotic events in Saccharomyces cerevisiae through a pathway distinct from initiation. *Molecular and cellular biology,* 16**,** 3222-3232.

LEMAIRE, K., VAN DE VELDE, S., VAN DIJCK, P. & THEVELEIN, J. M. 2004. Glucose and sucrose act as agonist and mannose as antagonist ligands of the G protein-coupled receptor Gpr1 in the yeast Saccharomyces cerevisiae. *Molecular cell,* 16**,** 293-299.

LEVINE, K., HUANG, K. & CROSS, F. R. 1996. Saccharomyces cerevisiae G1 cyclins differ in their intrinsic functional specificities. *Molecular and cellular biology,* 16**,** 6794-6803.

LIN, K.-I., LIN, Y. & CALAME, K. 2000. Repression of c-myc is necessary but not sufficient for terminal differentiation of B lymphocytes in vitro. *Molecular and cellular biology,* 20**,** 8684-8695.

LIN, Y., WONG, K.-K. & CALAME, K. 1997. Repression of c-myc transcription by Blimp-1, an inducer of terminal B cell differentiation. *Science,* 276**,** 596-599.

LIU, H., STYLES, C. A. & FINK, G. R. 1993. Elements of the yeast pheromone response pathway required for filamentous growth of diploids. *Science,* 262**,** 1741-1744.

LO, W.-S. & DRANGINIS, A. 1996. FLO11, a yeast gene related to the STA genes, encodes a novel cell surface flocculin. *Journal of bacteriology,* 178**,** 7144-7151.

LO, W.-S. & DRANGINIS, A. M. 1998. The cell surface flocculin Flo11 is required for pseudohyphae formation and invasion by Saccharomyces cerevisiae. *Molecular biology of the cell,* 9**,** 161-171.

LOEWITH, R. & HALL, M. N. 2011. Target of rapamycin (TOR) in nutrient signaling and growth control. *Genetics,* 189**,** 1177-1201.

LOEWITH, R., JACINTO, E., WULLSCHLEGER, S., LORBERG, A., CRESPO, J. L., BONENFANT, D., OPPLIGER, W., JENOE, P. & HALL, M. N. 2002. Two TOR complexes, only one of which is rapamycin sensitive, have distinct roles in cell growth control. *Molecular cell,* 10**,** 457-468.

LOEWITH, R., SMITH, J. S., MEIJER, M., WILLIAMS, T. J., BACHMAN, N., BOEKE, J. D. & YOUNG, D. 2001. Pho23 is associated with the Rpd3 histone deacetylase and is required for its normal function in regulation of gene expression and silencing in Saccharomyces cerevisiae. *Journal of Biological Chemistry,* 276**,** 24068-24074.

LOPES, J. M., SCHULZE, K., YATES, J., HIRSCH, J. & HENRY, S. 1993. The INO1 promoter of Saccharomyces cerevisiae includes an upstream repressor sequence (URS1) common to a diverse set of yeast genes. *Journal of bacteriology,* 175**,** 4235-4238.

LORENZ, M. C. & HEITMAN, J. 1997. Yeast pseudohyphal growth is regulated by GPA2, a G protein α homolog. *The EMBO journal,* 16**,** 7008-7018.

LORENZ, M. C. & HEITMAN, J. 1998a. The MEP2 ammonium permease regulates pseudohyphal differentiation in Saccharomyces cerevisiae. *The EMBO journal,* 17**,** 1236-1247.

LORENZ, M. C. & HEITMAN, J. 1998b. Regulators of pseudohyphal differentiation in Saccharomyces cerevisiae identified through multicopy suppressor analysis in ammonium permease mutant strains. *Genetics,* 150**,** 1443-1457.

LORENZ, M. C., PAN, X., HARASHIMA, T., CARDENAS, M. E., XUE, Y., HIRSCH, J. P. & HEITMAN, J. 2000. The G protein-coupled receptor Gpr1 is a nutrient sensor that regulates pseudohyphal differentiation in Saccharomyces cerevisiae. *Genetics,* 154**,** 609-622.

LYON, M. F., JAMIESON, R. V., PERVEEN, R., GLENISTER, P. H., GRIFFITHS, R., BOYD, Y., GLIMCHER, L. H., FAVOR, J., MUNIER, F. L. & BLACK, G. C. 2003. A dominant mutation within the DNA-binding domain of the bZIP transcription factor Maf causes murine cataract and results in selective alteration in DNA binding. *Human molecular genetics,* 12**,** 585-594.

MACARTHUR, M. W. & THORNTON, J. M. 1991. Influence of proline residues on protein conformation. *Journal of molecular biology,* 218**,** 397-412.

MADHANI, H. D. & FINK, G. R. 1997. Combinatorial control required for the specificity of yeast MAPK signaling. *Science,* 275**,** 1314-1317.

MADHANI, H. D., STYLES, C. A. & FINK, G. R. 1997. MAP kinases with distinct inhibitory functions impart signaling specificity during yeast differentiation. *Cell,* 91**,** 673-684.

MAGASANIK, B. & KAISER, C. A. 2002. Nitrogen regulation in Saccharomyces cerevisiae. *Gene,* 290**,** 1-18.

MALATHI, K., XIAO, Y. & MITCHELL, A. P. 1997. Interaction of yeast repressor-activator protein Ume6p with glycogen synthase kinase 3 homolog Rim11p. *Molecular and cellular biology,* 17**,** 7230-7236.

MALATHI, K., XIAO, Y. & MITCHELL, A. P. 1999. Catalytic roles of yeast GSK3β/shaggy homolog Rim11p in meiotic activation. *Genetics,* 153**,** 1145-1152.

MALLORY, M. J., COOPER, K. F. & STRICH, R. 2007. Meiosis-specific destruction of the Ume6p repressor by the Cdc20-directed APC/C. *Molecular cell,* 27**,** 951-961.

MALLORY, M. J., LAW, M. J., STERNER, D. E., BERGER, S. L. & STRICH, R. 2012. Gcn5p-dependent acetylation induces degradation of the meiotic transcriptional repressor Ume6p. *Molecular biology of the cell,* 23**,** 1609-1617.

MANDEL, S., ROBZYK, K. & KASSIR, Y. 1994. IME1 gene encodes a transcription factor which is required to induce meiosis in Saccharomyces cerevisiae. *Developmental genetics,* 15**,** 139-147.

MARINI, A.-M., SOUSSI-BOUDEKOU, S., VISSERS, S. & ANDRE, B. 1997. A family of ammonium transporters in Saccharomyces cerevisiae. *Molecular and cellular biology,* 17**,** 4282-4293.

MARINI, A.-M., VISSERS, S., URRESTARAZU, A. & ANDRE, B. 1994. Cloning and expression of the MEP1 gene encoding an ammonium transporter in Saccharomyces cerevisiae. *The EMBO journal,* 13**,** 3456-3463.

MATALLANA, E. & ARANDA, A. 2017. Biotechnological impact of stress response on wine yeast. *Letters in applied microbiology,* 64**,** 103-110.

MATSUMOTO, K., UNO, I. & ISHIKAWA, T. 1983. Initiation of meiosis in yeast mutants defective in adenylate cyclase and cyclic AMP-dependent protein kinase. *Cell,* 32**,** 417-423.

MATSUURA, A., TREININ, M., MITSUZAWA, H., KASSIR, Y., UNO, I. & SIMCHEN, G. 1990. The adenylate cyclase/protein kinase cascade regulates entry into meiosis in Saccharomyces cerevisiae through the gene IME1. *The EMBO journal,* 9**,** 3225-3232.

MCCONNELL, A. D., GELBART, M. E. & TSUKIYAMA, T. 2004. Histone fold protein Dls1p is required for Isw2-dependent chromatin remodeling in vivo. *Molecular and cellular biology,* 24**,** 2605-2613.

MCKNIGHT, J. N., BOERMA, J. W., BREEDEN, L. L. & TSUKIYAMA, T. 2015. Global promoter targeting of a conserved lysine deacetylase for transcriptional shutoff during quiescence entry. *Molecular cell,* 59**,** 732-743.

MEIMOUN, A., HOLTZMAN, T., WEISSMAN, Z., MCBRIDE, H. J., STILLMAN, D. J., FINK, G. R. & KORNITZER, D. 2000. Degradation of the transcription factor Gcn4 requires the kinase Pho85 and the SCFCDC4 ubiquitin–ligase complex. *Molecular Biology of the Cell,* 11**,** 915-927.

MENDENHALL, M. D. & HODGE, A. E. 1998. Regulation of Cdc28 cyclin-dependent protein kinase activity during the cell cycle of the yeast Saccharomyces cerevisiae. *Microbiology and Molecular Biology Reviews,* 62**,** 1191-1243.
MESSENGUY, F., VIERENDEELS, F., SCHERENS, B. & DUBOIS, E. 2000. In Saccharomyces cerevisiae, expression of arginine catabolic genes CAR1 and CAR2 in response to exogenous nitrogen availability is mediated by the Ume6 (CargRI)-Sin3 (CargRII)-Rpd3 (CargRIII) complex. *Journal of Bacteriology,* 182**,** 3158-3164.
MILES, S., LI, L., DAVISON, J. & BREEDEN, L. L. 2013. Xbp1 directs global repression of budding yeast transcription during the transition to quiescence and is important for the longevity and reversibility of the quiescent state. *PLoS genetics,* 9**,** e1003854.
MILLER, J. H. 1972. Assay of β-galactosidase. *Experiments in molecular genetics*.
MILLER, M. 2009. The importance of being flexible: the case of basic region leucine zipper transcriptional regulators. *Current protein and peptide science,* 10**,** 244-269.
MITCHELL, A. P. 1994. Control of meiotic gene expression in Saccharomyces cerevisiae. *Microbiological reviews,* 58**,** 56-70.
MITCHELL, A. P., DRISCOLL, S. E. & SMITH, H. E. 1990. Positive control of sporulation-specific genes by the IME1 and IME2 products in Saccharomyces cerevisiae. *Molecular and cellular biology,* 10**,** 2104-2110.
MOLINARI, M., GALLI, C., VANONI, O., ARNOLD, S. M. & KAUFMAN, R. J. 2005. Persistent glycoprotein misfolding activates the glucosidase II/UGT1-driven calnexin cycle to delay aggregation and loss of folding competence. *Molecular cell,* 20**,** 503-512.
MORGAN, A. A. & RUBENSTEIN, E. 2013. Proline: the distribution, frequency, positioning, and common functional roles of proline and polyproline sequences in the human proteome. *PloS one,* 8**,** e53785.
MORI, K. 2000. Tripartite management of unfolded proteins in the endoplasmic reticulum. *Cell,* 101**,** 451-454.
MORI, K. 2003. Frame switch splicing and regulated intramembrane proteolysis: key words to understand the unfolded protein response. *Traffic,* 4**,** 519-528.
MORI, K., KAWAHARA, T., YOSHIDA, H., YANAGI, H. & YURA, T. 1996. Signalling from endoplasmic reticulum to nucleus: transcription factor with a basic-leucine zipper motif is required for the unfolded protein-response pathway. *Genes to Cells,* 1**,** 803-817.
MORI, K., OGAWA, N., KAWAHARA, T., YANAGI, H. & YURA, T. 1998. Palindrome with Spacer of One Nucleotide Is Characteristic of the cis-Acting Unfolded Protein Response Element inSaccharomyces cerevisiae. *Journal of Biological Chemistry,* 273**,** 9912-9920.
MORI, K., OGAWA, N., KAWAHARA, T., YANAGI, H. & YURA, T. 2000. mRNA splicing-mediated C-terminal replacement of transcription factor Hac1p is required for efficient activation of the unfolded protein response. *Proceedings of the National Academy of Sciences,* 97**,** 4660-4665.
MORI, K., SANT, A., KOHNO, K., NORMINGTON, K., GETHING, M. & SAMBROOK, J. 1992. A 22 bp cis-acting element is necessary and sufficient for the induction of the yeast KAR2 (BiP) gene by unfolded proteins. *The EMBO journal,* 11**,** 2583-2593.
MORL, K., MA, W., GETHING, M.-J. & SAMBROOK, J. 1993. A transmembrane protein with a cdc2+ CDC28-related kinase activity is required for signaling from the ER to the nucleus. *Cell,* 74**,** 743-756.
MOSCH, H.-U., KUBLER, E., KRAPPMANN, S., FINK, G. R. & BRAUS, G. H. 1999. Crosstalk between the Ras2p-controlled mitogen-activated protein kinase and

cAMP pathways during invasive growth of Saccharomyces cerevisiae. *Molecular biology of the cell,* 10**,** 1325-1335.
MÖSCH, H.-U., ROBERTS, R. L. & FINK, G. R. 1996. Ras2 signals via the Cdc42/Ste20/mitogen-activated protein kinase module to induce filamentous growth in Saccharomyces cerevisiae. *Proceedings of the National Academy of Sciences,* 93**,** 5352-5356.
MOTOHASHI, H., O'CONNOR, T., KATSUOKA, F., ENGEL, J. D. & YAMAMOTO, M. 2002. Integration and diversity of the regulatory network composed of Maf and CNC families of transcription factors. *Gene,* 294**,** 1-12.
MUNDER, M. C., MIDTVEDT, D., FRANZMANN, T., NUSKE, E., OTTO, O., HERBIG, M., ULBRICHT, E., MÜLLER, P., TAUBENBERGER, A. & MAHARANA, S. 2016. A pH-driven transition of the cytoplasm from a fluid-to a solid-like state promotes entry into dormancy. *elife,* 5**,** e09347.
MUTHUKUMAR, G., SUHNG, S., MAGEE, P., JEWELL, R. & PRIMERANO, D. 1993. The Saccharomyces cerevisiae SPR1 gene encodes a sporulation-specific exo-1, 3-beta-glucanase which contributes to ascospore thermoresistance. *Journal of bacteriology,* 175**,** 386-394.
NACHMAN, I., REGEV, A. & RAMANATHAN, S. 2007. Dissecting timing variability in yeast meiosis. *Cell,* 131**,** 544-556.
NADJAR-BOGER, E. 2000. *Regulation of DNA replication in mitosis and meiosis in the budding yeast Saccharomyces cerevisiae*, Technion-Israel Institute of Technology, Faculty of Biology.
NAKAZAWA, N., NIIJIMA, S., TANAKA, Y. & ITO, T. 2012. Immunosuppressive drug rapamycin restores sporulation competence in industrial yeasts. *Journal of bioscience and bioengineering,* 113**,** 491-495.
NAKAZAWA, N., SATO, A. & HOSAKA, M. 2016. TORC1 activity is partially reduced under nitrogen starvation conditions in sake yeast Kyokai no. 7, Saccharomyces cerevisiae. *Journal of bioscience and bioengineering,* 121**,** 247-252.
NASH, P., TANG, X., ORLICKY, S., CHEN, Q., GERTLER, F. B., MENDENHALL, M. D., SICHERI, F., PAWSON, T. & TYERS, M. 2001. Multisite phosphorylation of a CDK inhibitor sets a threshold for the onset of DNA replication. *Nature,* 414**,** 514-521.
NEHLIN, J. O., CARLBERG, M. & RONNE, H. 1992. Yeast SKO1 gene encodes a bZIP protein that binds to the CRE motif and acts as a repressor of transcription. *Nucleic acids research,* 20**,** 5271-5278.
NEIMAN, A. M. 2005. Ascospore formation in the yeast Saccharomyces cerevisiae. *Microbiology and Molecular Biology Reviews,* 69**,** 565-584.
NEIMAN, A. M. 2011. Sporulation in the budding yeast Saccharomyces cerevisiae. *Genetics,* 189**,** 737-65.
NG, H. H. & BIRD, A. 2000. Histone deacetylases: silencers for hire. *Trends in biochemical sciences,* 25**,** 121-126.
NIJHAWAN, A., JAIN, M., TYAGI, A. K. & KHURANA, J. P. 2008. Genomic survey and gene expression analysis of the basic leucine zipper transcription factor family in rice. *Plant physiology,* 146**,** 333-350.
NIKAWA, J.-I., AKIYOSHI, M., HIRATA, S. & FUKUDA, T. 1996. Saccharomyces cerevisiae IRE2/HAC1 is involved in IRE1-mediated KAR2 expression. *Nucleic acids research,* 24**,** 4222-4226.
NISHITOH, H., MATSUZAWA, A., TOBIUME, K., SAEGUSA, K., TAKEDA, K., INOUE, K., HORI, S., KAKIZUKA, A. & ICHIJO, H. 2002. ASK1 is essential for endoplasmic reticulum stress-induced neuronal cell death triggered by expanded polyglutamine repeats. *Genes & development,* 16**,** 1345-1355.
NOJIMA, H., LEEM, S.-H., ARAKI, H., SAKAI, A., NAKASHIMA, N., KANAOKA, Y. & ONO, Y. 1994. Hac1: A novel yeast bZIP protein binding to the CRE motif is a

multicopy suppressor for cdcW mutant of Schizosaccharomyces pombe. *Nucleic acids research,* 22**,** 5279-5288.
NORMINGTON, K., KOHNO, K., KOZUTSUMI, Y., GETHING, M.-J. & SAMBROOK, J. 1989. S. cerevisiae encodes an essential protein homologous in sequence and function to mammalian BiP. *Cell,* 57**,** 1223-1236.
O'NEIL, K. T., HOESS, R. H. & DEGRADO, W. F. 1990. Design of DNA-binding peptides based on the leucine zipper motif. *Science,* 249**,** 774-778.
O'SHEA, E. K., RUTKOWSKI, R. & KIM, P. S. 1989. Evidence that the leucine zipper is a coiled coil. *Science,* 243**,** 538-542.
O'ROURKE, S. M. & HERSKOWITZ, I. 1998. The Hog1 MAPK prevents cross talk between the HOG and pheromone response MAPK pathways in Saccharomyces cerevisiae. *Genes & development,* 12**,** 2874-2886.
OAS, T. G., MCINTOSH, L. P., O'SHEA, E. K., DAHLQUIST, F. W. & KIM, P. S. 1990. Secondary structure of a leucine zipper determined by nuclear magnetic resonance spectroscopy. *Biochemistry,* 29**,** 2891-2894.
OGAWA, N. & MORI, K. 2004. Autoregulation of the HAC1 gene is required for sustained activation of the yeast unfolded protein response. *Genes to Cells,* 9**,** 95-104.
OHKUNI, K. & YAMASHITA, I. 2000. A transcriptional autoregulatory loop for KIN28–CCL1 and SRB10–SRB11, each encoding RNA polymerase II CTD kinase–cyclin pair, stimulates the meiotic development of S. cerevisiae. *Yeast,* 16**,** 829-846.
OIKAWA, D., KIMATA, Y. & KOHNO, K. 2007. Self-association and BiP dissociation are not sufficient for activation of the ER stress sensor Ire1. *Journal of cell science,* 120**,** 1681-1688.
OLIPHANT, A. R., BRANDL, C. J. & STRUHL, K. 1989. Defining the sequence specificity of DNA-binding proteins by selecting binding sites from random-sequence oligonucleotides: analysis of yeast GCN4 protein. *Molecular and cellular biology,* 9**,** 2944-2949.
OYAKE, T., ITOH, K., MOTOHASHI, H., HAYASHI, N., HOSHINO, H., NISHIZAWA, M., YAMAMOTO, M. & IGARASHI, K. 1996. Bach proteins belong to a novel family of BTB-basic leucine zipper transcription factors that interact with MafK and regulate transcription through the NF-E2 site. *Molecular and cellular biology,* 16**,** 6083-6095.
ÖZCAN, S. 2002. Two different signals regulate repression and induction of gene expression by glucose. *Journal of Biological Chemistry,* 277**,** 46993-46997.
ÖZCAN, S., DOVER, J. & JOHNSTON, M. 1998. Glucose sensing and signaling by two glucose receptors in the yeast Saccharomyces cerevisiae. *The EMBO journal,* 17**,** 2566-2573.
OZCAN, S., DOVER, J., ROSENWALD, A. G., WÖLFL, S. & JOHNSTON, M. 1996. Two glucose transporters in Saccharomyces cerevisiae are glucose sensors that generate a signal for induction of gene expression. *Proceedings of the National Academy of Sciences,* 93**,** 12428-12432.
ÖZCAN, S. & JOHNSTON, M. 1999. Function and regulation of yeast hexose transporters. *Microbiology and Molecular Biology Reviews,* 63**,** 554-569.
ÖZCAN, U., CAO, Q., YILMAZ, E., LEE, A.-H., IWAKOSHI, N. N., ÖZDELEN, E., TUNCMAN, G., GÖRGÜN, C., GLIMCHER, L. H. & HOTAMISLIGIL, G. S. 2004. Endoplasmic reticulum stress links obesity, insulin action, and type 2 diabetes. *Science,* 306**,** 457-461.
PADMORE, R., CAO, L. & KLECKNER, N. 1991. Temporal comparison of recombination and synaptonemal complex formation during meiosis in S. cerevisiae. *Cell,* 66**,** 1239-1256.
PAGE, S. L. & HAWLEY, R. S. 2004. The genetics and molecular biology of the synaptonemal complex. *Annu. Rev. Cell Dev. Biol.,* 20**,** 525-558.

PAIRA, S. & DAS, B. 2022. Determination of the Stability and Intracellular (Intra-Nuclear) Targeting and Recruitment of Pre-HAC1 mRNA in the Saccharomyces cerevisiae During the Activation of UPR. *The Unfolded Protein Response.* Springer.

PAK, J. & SEGALL, J. 2002. Regulation of the premiddle and middle phases of expression of the NDT80 gene during sporulation of Saccharomyces cerevisiae. *Molecular and cellular biology,* 22**,** 6417-6429.

PAL, B., CHAN, N. C., HELFENBAUM, L., TAN, K., TANSEY, W. P. & GETHING, M.-J. 2007. SCFCdc4-mediated degradation of the Hac1p transcription factor regulates the unfolded protein response in Saccharomyces cerevisiae. *Molecular biology of the cell,* 18**,** 426-440.

PALECEK, S. P., PARIKH, A. S., HUH, J. H. & KRON, S. J. 2002. Depression of Saccharomyces cerevisiae invasive growth on non-glucose carbon sources requires the Snf1 kinase. *Molecular microbiology,* 45**,** 453-469.

PAN, X., HARASHIMA, T. & HEITMAN, J. 2000. Signal transduction cascades regulating pseudohyphal differentiation of Saccharomyces cerevisiae. *Current opinion in microbiology,* 3**,** 567-572.

PAN, X. & HEITMAN, J. 1999. Cyclic AMP-dependent protein kinase regulates pseudohyphal differentiation in Saccharomyces cerevisiae. *Molecular and cellular biology,* 19**,** 4874-4887.

PAPA, F. R., ZHANG, C., SHOKAT, K. & WALTER, P. 2003. Bypassing a kinase activity with an ATP-competitive drug. *Science,* 302**,** 1533-1537.

PARVIZ, F. & HEIDEMAN, W. 1998. Growth-independent regulation of CLN3 mRNA levels by nutrients in Saccharomyces cerevisiae. *Journal of bacteriology,* 180**,** 225-230.

PATIL, C. & WALTER, P. 2001. Intracellular signaling from the endoplasmic reticulum to the nucleus: the unfolded protein response in yeast and mammals. *Current opinion in cell biology,* 13**,** 349-355.

PATIL, C. K., LI, H., WALTER, P. & MCKNIGHT, S. 2004. Gcn4p and novel upstream activating sequences regulate targets of the unfolded protein response. *PLoS biology,* 2**,** e246.

PAZIN, M. J. & KADONAGA, J. T. 1997. What's up and down with histone deacetylation and transcription? *Cell,* 89**,** 325-328.

PEDRUZZI, I., DUBOULOZ, F., CAMERONI, E., WANKE, V., ROOSEN, J., WINDERICKX, J. & DE VIRGILIO, C. 2003. TOR and PKA signaling pathways converge on the protein kinase Rim15 to control entry into G0. *Molecular cell,* 12**,** 1607-1613.

PINCUS, D., CHEVALIER, M. W., ARAGÓN, T., VAN ANKEN, E., VIDAL, S. E., EL-SAMAD, H. & WALTER, P. 2010. BiP binding to the ER-stress sensor Ire1 tunes the homeostatic behavior of the unfolded protein response. *PLoS biology,* 8**,** e1000415.

PITONIAK, A., BIRKAYA, B., DIONNE, H. M., VADAIE, N. & CULLEN, P. J. 2009. The signaling mucins Msb2 and Hkr1 differentially regulate the filamentation mitogen-activated protein kinase pathway and contribute to a multimodal response. *Molecular biology of the cell,* 20**,** 3101-3114.

PLANK, M. 2022. Interaction of TOR and PKA Signaling in S. cerevisiae. *Biomolecules,* 12**,** 210.

PNUELI, L., EDRY, I., COHEN, M. & KASSIR, Y. 2004. Glucose and nitrogen regulate the switch from histone deacetylation to acetylation for expression of early meiosis-specific genes in budding yeast. *Molecular and cellular biology,* 24**,** 5197-5208.

PRAY-GRANT, M. G., DANIEL, J. A., SCHIELTZ, D., YATES, J. R. & GRANT, P. A. 2005. Chd1 chromodomain links histone H3 methylation with SAGA-and SLIK-dependent acetylation. *Nature,* 433**,** 434-438.

PRIMIG, M., WILLIAMS, R. M., WINZELER, E. A., TEVZADZE, G. G., CONWAY, A. R., HWANG, S. Y., DAVIS, R. W. & ESPOSITO, R. E. 2000. The core meiotic transcriptome in budding yeasts. *Nature genetics,* 26**,** 415-423.

PRINGLE, J. R. & HARTWELL, L. 1981. The molecular biology of the yeast Saccharomyces cerevisiae: life cycle and inheritance. *The Saccharomyces Cerevisiae Cell Cycle***,** 97-142.

PROFT, M. & STRUHL, K. 2002. Hog1 kinase converts the Sko1-Cyc8-Tup1 repressor complex into an activator that recruits SAGA and SWI/SNF in response to osmotic stress. *Molecular cell,* 9**,** 1307-1317.

PU, W. T. & STRUHL, K. 1991a. Highly conserved residues in the bZIP domain of yeast GCN4 are not essential for DNA binding. *Molecular and cellular biology,* 11**,** 4918-4926.

PU, W. T. & STRUHL, K. 1991b. The leucine zipper symmetrically positions the adjacent basic regions for specific DNA binding. *Proceedings of the National Academy of Sciences,* 88**,** 6901-6905.

PUIG, S., LAU, M. & THIELE, D. J. 2004. Cti6 is an Rpd3-Sin3 histone deacetylase-associated protein required for growth under iron-limiting conditions in Saccharomyces cerevisiae. *Journal of Biological Chemistry,* 279**,** 30298-30306.

PURNAPATRE, K., PICCIRILLO, S., SCHNEIDER, B. L. & HONIGBERG, S. M. 2002. The CLN3/SWI6/CLN2 pathway and SNF1 act sequentially to regulate meiotic initiation in Saccharomyces cerevisiae. *Genes to Cells,* 7**,** 675-691.

RAITHATHA, S. A., VAZA, S., ISLAM, M. T., GREENWOOD, B. & STUART, D. T. 2021. Ume6 Acts as a Stable Platform To Coordinate Repression and Activation of Early Meiosis-Specific Genes in Saccharomyces cerevisiae. *Molecular and Cellular Biology,* 41**,** e00378-20.

RAUGHT, B., GINGRAS, A.-C. & SONENBERG, N. 2001. The target of rapamycin (TOR) proteins. *Proceedings of the National Academy of Sciences,* 98**,** 7037-7044.

RAYNER, T. F., GRAY, J. V. & THORNER, J. W. 2002. Direct and novel regulation of cAMP-dependent protein kinase by Mck1p, a yeast glycogen synthase kinase-3. *Journal of Biological Chemistry,* 277**,** 16814-16822.

REIMOLD, A. M., IWAKOSHI, N. N., MANIS, J., VALLABHAJOSYULA, P., SZOMOLANYI-TSUDA, E., GRAVALLESE, E. M., FRIEND, D., GRUSBY, M. J., ALT, F. & GLIMCHER, L. H. 2001. Plasma cell differentiation requires the transcription factor XBP-1. *Nature,* 412**,** 300-307.

REINDERS, A., BÜRCKERT, N., BOLLER, T., WIEMKEN, A. & DE VIRGILIO, C. 1998. Saccharomyces cerevisiae cAMP-dependent protein kinase controls entry into stationary phase through the Rim15p protein kinase. *Genes & development,* 12**,** 2943-2955.

REINKE, A., ANDERSON, S., MCCAFFERY, J. M., YATES, J., ARONOVA, S., CHU, S., FAIRCLOUGH, S., IVERSON, C., WEDAMAN, K. P. & POWERS, T. 2004. TOR complex 1 includes a novel component, Tco89p (YPL180w), and cooperates with Ssd1p to maintain cellular integrity in Saccharomyces cerevisiae. *Journal of Biological Chemistry,* 279**,** 14752-14762.

ROBERTS, R. L. & FINK, G. R. 1994. Elements of a single MAP kinase cascade in Saccharomyces cerevisiae mediate two developmental programs in the same cell type: mating and invasive growth. *Genes & development,* 8**,** 2974-2985.

ROBERTS, R. L., MÖSCH, H.-U. & FINK, G. R. 1997. 14-3-3 proteins are essential for RAS/MAPK cascade signaling during pseudohyphal development in S. cerevisiae. *Cell,* 89**,** 1055-1065.

ROBERTSON, L. S. & FINK, G. R. 1998. The three yeast A kinases have specific signaling functions in pseudohyphal growth. *Proceedings of the National Academy of Sciences,* 95**,** 13783-13787.

RØDKÆR, S. V. & FÆRGEMAN, N. J. 2014. Glucose-and nitrogen sensing and regulatory mechanisms in Saccharomyces cerevisiae. *FEMS yeast research,* 14**,** 683-696.
ROHDE, J. & CARDENAS, M. 2004. Nutrient signaling through TOR kinases controls gene expression and cellular differentiation in fungi. *TOR***,** 53-72.
ROHDE, J., HEITMAN, J. & CARDENAS, M. E. 2001. The TOR kinases link nutrient sensing to cell growth. *Journal of Biological Chemistry,* 276**,** 9583-9586.
ROHDE, J. R., CAMPBELL, S., ZURITA-MARTINEZ, S. A., CUTLER, N. S., ASHE, M. & CARDENAS, M. E. 2004. TOR controls transcriptional and translational programs via Sap-Sit4 protein phosphatase signaling effectors. *Molecular and cellular biology,* 24**,** 8332-8341.
ROLLAND, F., WINDERICKX, J. & THEVELEIN, J. M. 2001. Glucose-sensing mechanisms in eukaryotic cells. *Trends in biochemical sciences,* 26**,** 310-317.
ROLLAND, F., WINDERICKX, J. & THEVELEIN, J. M. 2002. Glucose-sensing and-signalling mechanisms in yeast. *FEMS yeast research,* 2**,** 183-201.
RON, D. & WALTER, P. 2007. Signal integration in the endoplasmic reticulum unfolded protein response. *Nature reviews Molecular cell biology,* 8**,** 519-529.
RONNE, H. 1995. Glucose repression in fungi. *Trends in Genetics,* 11**,** 12-17.
ROSE, M., ALBIG, W. & ENTIAN, K. D. 1991. Glucose repression in Saccharomyces cerevisiae is directly associated with hexose phosphorylation by hexokinases PI and PII. *European journal of biochemistry,* 199**,** 511-518.
RUBIN-BEJERANO, I., MANDEL, S., ROBZYK, K. & KASSIR, Y. 1996. Induction of meiosis in Saccharomyces cerevisiae depends on conversion of the transcriptional represssor Ume6 to a positive regulator by its regulated association with the transcriptional activator Ime1. *Molecular and cellular biology,* 16**,** 2518-2526.
RUBINSTEIN, A., GUREVICH, V., KASULIN-BONEH, Z., PNUELI, L., KASSIR, Y. & PINTER, R. Y. 2007. Faithful modeling of transient expression and its application to elucidating negative feedback regulation. *Proceedings of the National Academy of Sciences,* 104**,** 6241-6246.
RÜEGSEGGER, U., LEBER, J. H. & WALTER, P. 2001. Block of HAC1 mRNA translation by long-range base pairing is released by cytoplasmic splicing upon induction of the unfolded protein response. *Cell,* 107**,** 103-114.
RUIZ-ROIG, C., VIÉITEZ, C., POSAS, F. & DE NADAL, E. 2010. The Rpd3L HDAC complex is essential for the heat stress response in yeast. *Molecular microbiology,* 76**,** 1049-1062.
RUNDLETT, S. E., CARMEN, A. A., KOBAYASHI, R., BAVYKIN, S., TURNER, B. M. & GRUNSTEIN, M. 1996. HDA1 and RPD3 are members of distinct yeast histone deacetylase complexes that regulate silencing and transcription. *Proceedings of the National Academy of Sciences,* 93**,** 14503-14508.
RUNDLETT, S. E., CARMEN, A. A., SUKA, N., TURNER, B. M. & GRUNSTEIN, M. 1998. Transcriptional repression by UME6 involves deacetylation of lysine 5 of histone H4 by RPD3. *Nature,* 392**,** 831-835.
RUPP, S., SUMMERS, E., LO, H. J., MADHANI, H. & FINK, G. 1999. MAP kinase and cAMP filamentation signaling pathways converge on the unusually large promoter of the yeast FLO11 gene. *The EMBO journal,* 18**,** 1257-1269.
RUTHERFORD, J. C., CHUA, G., HUGHES, T., CARDENAS, M. E. & HEITMAN, J. 2008. A Mep2-dependent transcriptional profile links permease function to gene expression during pseudohyphal growth in Saccharomyces cerevisiae. *Molecular biology of the cell,* 19**,** 3028-3039.
RUTKOWSKI, D. T. & HEGDE, R. S. 2010. Regulation of basal cellular physiology by the homeostatic unfolded protein response. *Journal of Cell Biology,* 189**,** 783-794.
SABET, N., VOLO, S., YU, C., MADIGAN, J. P. & MORSE, R. H. 2004. Genome-wide analysis of the relationship between transcriptional regulation by Rpd3p and the

histone H3 and H4 amino termini in budding yeast. *Molecular and cellular biology,* 24**,** 8823-8833.
SAGEE, S., SHERMAN, A., SHENHAR, G., ROBZYK, K., BEN-DOY, N., SIMCHEN, G. & KASSIR, Y. 1998. Multiple and distinct activation and repression sequences mediate the regulated transcription of IME1, a transcriptional activator of meiosis-specific genes in Saccharomyces cerevisiae. *Molecular and cellular biology,* 18**,** 1985-1995.
SANTANGELO, G. M. 2006. Glucose signaling in Saccharomyces cerevisiae. *Microbiology and Molecular Biology Reviews,* 70**,** 253-282.
SARKAR, S., DALGAARD, J. Z., MILLAR, J. B. & ARUMUGAM, P. 2014. The Rim15-endosulfine-PP2ACdc55 signalling module regulates entry into gametogenesis and quiescence via distinct mechanisms in budding yeast. *PLoS genetics,* 10**,** e1004456.
SATHE, L., BOLINGER, C., MANNAN, M. A.-U., DEVER, T. E. & DEY, M. 2015. Evidence that base-pairing interaction between intron and mRNA leader sequences inhibits initiation of HAC1 mRNA translation in yeast. *Journal of Biological Chemistry,* 290**,** 21821-21832.
SAUDEK, V., PASTORE, A., MORELLI, M. C., FRANK, R., GAUSEPOHL, H. & GIBSON, T. 1991. The solution structure of a leucine-zipper motif peptide. *Protein Engineering, Design and Selection,* 4**,** 519-529.
SCHENA, M., PICARD, D. & YAMAMOTO, K. R. 1991. [26] Vectors for constitutive and inducible gene expression in yeast. *Methods in enzymology.* Elsevier.
SCHENBORN, E. & GOIFFON, V. 1993. A sensitive assay for firefly luciferase activity. *Promega Notes,* 41**,** 11-14.
SCHERENS, B., FELLER, A., VIERENDEELS, F., MESSENGUY, F. & DUBOIS, E. 2006. Identification of direct and indirect targets of the Gln3 and Gat1 activators by transcriptional profiling in response to nitrogen availability in the short and long term. *FEMS yeast research,* 6**,** 777-791.
SCHNEPER, L., DÜVEL, K. & BROACH, J. R. 2004. Sense and sensibility: nutritional response and signal integration in yeast. *Current opinion in microbiology,* 7**,** 624-630.
SCHNEPPENHEIM, R., BUDDE, U., DAHLMANN, N. & RAUTENBERG, P. 1991. Luminography–a new, highly sensitive visualization method for electrophoresis. *Electrophoresis,* 12**,** 367-372.
SCHRÖDER, M., CHANG, J. S. & KAUFMAN, R. J. 2000. The unfolded protein response represses nitrogen-starvation induced developmental differentiation in yeast. *Genes & development,* 14**,** 2962-2975.
SCHRÖDER, M., CLARK, R. & KAUFMAN, R. J. 2003. IRE1-and HAC1-independent transcriptional regulation in the unfolded protein response of yeast. *Molecular microbiology,* 49**,** 591-606.
SCHRÖDER, M., CLARK, R., LIU, C. Y. & KAUFMAN, R. J. 2004. The unfolded protein response represses differentiation through the RPD3-SIN3 histone deacetylase. *The EMBO journal,* 23**,** 2281-2292.
SCHRÖDER, M. & KAUFMAN, R. J. 2005. ER stress and the unfolded protein response. *Mutation Research/Fundamental and Molecular Mechanisms of Mutagenesis,* 569**,** 29-63.
SCHWARTZ, M. A. & MADHANI, H. D. 2004. Principles of MAP kinase signaling specificity in Saccharomyces cerevisiae. *Annu. Rev. Genet.,* 38**,** 725-748.
SEHGAL, S. Sirolimus: its discovery, biological properties, and mechanism of action. Transplantation proceedings, 2003. Elsevier, S7-S14.
SENGUPTA, N., VINOD, P. & VENKATESH, K. 2007. Crosstalk between cAMP-PKA and MAP kinase pathways is a key regulatory design necessary to regulate FLO11 expression. *Biophysical chemistry,* 125**,** 59-71.

SHAH, J. & CLANCY, M. 1992. IME4, a gene that mediates MAT and nutritional control of meiosis in Saccharomyces cerevisiae. *Molecular and cellular biology,* 12**,** 1078-1086.
SHAMU, C. E. & WALTER, P. 1996. Oligomerization and phosphorylation of the Ire1p kinase during intracellular signaling from the endoplasmic reticulum to the nucleus. *The EMBO journal,* 15**,** 3028-3039.
SHANER, L., WEGELE, H., BUCHNER, J. & MORANO, K. A. 2005. The yeast Hsp110 Sse1 functionally interacts with the Hsp70 chaperones Ssa and Ssb. *Journal of Biological Chemistry,* 280**,** 41262-41269.
SHEFER-VAIDA, M., SHERMAN, A., ASHKENAZI, T., ROBZYK, K. & KASSIR, Y. 1995. Positive and negative feedback loops affect the transcription of IME1, a positive regulator of meiosis in Saccharomyces cerevisiae. *Developmental genetics,* 16**,** 219-228.
SHENHAR, G. & KASSIR, Y. 2001. A positive regulator of mitosis, Sok2, functions as a negative regulator of meiosis in Saccharomyces cerevisiae. *Molecular and cellular biology,* 21**,** 1603-1612.
SHERMAN, A., SHEFER, M., SAGEE, S. & KASSIR, Y. 1993. Post-transcriptional regulation of IME1 determines initiation of meiosis in Saccharomyces cerevislae. *Molecular and General Genetics MGG,* 237**,** 375-384.
SHERMAN, F. 1991. [1] Getting started with yeast. *Methods in enzymology.* Elsevier.
SHERMAN, F. & ROMAN, H. 1963. Evidence for two types of allelic recombination in yeast. *Genetics,* 48**,** 255.
SHILO, V., SIMCHEN, G. & SHILO, B. 1978. Initiation of meiosis in cell cycle initiation mutants of Saccharomyces cerevisiae. *Experimental cell research,* 112**,** 241-248.
SHIMIZU, M., HARA, M., MURASE, A., SHINDO, H. & MITCHELL, A. Dissection of the DNA binding domain of yeast Zn-finger protein Rme1p, a repressor of meiotic activator IME1. Nucleic acids symposium series, 1997. 175-176.
SHIMIZU, M., TAKAHASHI, K., LAMB, T. M., SHINDO, H. & MITCHELL, A. P. 2003. Yeast Ume6p repressor permits activator binding but restricts TBP binding at the HOP1 promoter. *Nucleic acids research,* 31**,** 3033-3037.
SIA, R. & MITCHELL, A. P. 1995. Stimulation of later functions of the yeast meiotic protein kinase Ime2p by the IDS2 gene product. *Molecular and cellular biology,* 15**,** 5279-5287.
SIDRAUSKI, C., COX, J. S. & WALTER, P. 1996. tRNA ligase is required for regulated mRNA splicing in the unfolded protein response. *Cell,* 87**,** 405-413.
SIDRAUSKI, C. & WALTER, P. 1997. The transmembrane kinase Ire1p is a site-specific endonuclease that initiates mRNA splicing in the unfolded protein response. *Cell,* 90**,** 1031-1039.
SIEWE, R. M., WEIL, B., BURKOVSKI, A., EIKMANNS, B. J., EIKMANNS, M. & KRÄMER, R. 1996. Functional and Genetic Characterization of the (Methyl) ammonium Uptake Carrier of Corynebacterium glutamicum (∗). *Journal of Biological Chemistry,* 271**,** 5398-5403.
SIKORSKI, R. S. & HIETER, P. 1989. A system of shuttle vectors and yeast host strains designed for efficient manipulation of DNA in Saccharomyces cerevisiae. *Genetics,* 122**,** 19-27.
SILVERSTEIN, R. A. & EKWALL, K. 2005. Sin3: a flexible regulator of global gene expression and genome stability. *Current genetics,* 47**,** 1-17.
SIMCHEN, G. 2009. Commitment to meiosis: what determines the mode of division in budding yeast? *Bioessays,* 31**,** 169-177.
SMETS, B., DE SNIJDER, P., ENGELEN, K., JOOSSENS, E., GHILLEBERT, R., THEVISSEN, K., MARCHAL, K. & WINDERICKX, J. 2008. Genome-wide expression analysis reveals TORC1-dependent and-independent functions of Sch9. *FEMS yeast research,* 8**,** 1276-1288.

SMITH, A., WARD, M. P. & GARRETT, S. 1998. Yeast PKA represses Msn2p/Msn4p-dependent gene expression to regulate growth, stress response and glycogen accumulation. *The EMBO journal,* 17**,** 3556-3564.
SMITH, H. E., DRISCOLL, S. E., SIA, R., YUAN, H. E. & MITCHELL, A. P. 1993. Genetic evidence for transcriptional activation by the yeast IME1 gene product. *Genetics,* 133**,** 775-784.
SMITH, H. E. & MITCHELL, A. P. 1989. A transcriptional cascade governs entry into meiosis in Saccharomyces cerevisiae. *Molecular and cellular biology,* 9**,** 2142-2152.
SMITH, H. E., SU, S., NEIGEBORN, L., DRISCOLL, S. E. & MITCHELL, A. 1990. Role of IME1 expression in regulation of meiosis in Saccharomyces cerevisiae. *Molecular and Cellular Biology,* 10**,** 6103-6113.
SMITH, M. H., PLOEGH, H. L. & WEISSMAN, J. S. 2011. Road to ruin: targeting proteins for degradation in the endoplasmic reticulum. *Science,* 334**,** 1086-1090.
SMITH, P. E., KROHN, R. I., HERMANSON, G. T., MALLIA, A. K., GARTNER, F. H., PROVENZANO, M., FUJIMOTO, E. K., GOEKE, N. M., OLSON, B. J. & KLENK, D. 1985. Measurement of protein using bicinchoninic acid. *Analytical biochemistry,* 150**,** 76-85.
SMOLLE, M., VENKATESH, S., GOGOL, M. M., LI, H., ZHANG, Y., FLORENS, L., WASHBURN, M. P. & WORKMAN, J. L. 2012. Chromatin remodelers Isw1 and Chd1 maintain chromatin structure during transcription by preventing histone exchange. *Nature structural & molecular biology,* 19**,** 884-892.
SOPKO, R., RAITHATHA, S. & STUART, D. 2002. Phosphorylation and maximal activity of Saccharomyces cerevisiae meiosis-specific transcription factor Ndt80 is dependent on Ime2. *Molecular and cellular biology,* 22**,** 7024-7040.
SOUSHKO, M. & MITCHELL, A. P. 2000. An RNA-binding protein homologue that promotes sporulation-specific gene expression in Saccharomyces cerevisiae. *Yeast,* 16**,** 631-639.
SPRAGUE JR, G. 1992. Pheromone response and signal transduction during the mating of Saccharomyces cerevisiae. *The molecular and cellular biology of the yeast Saccharomyces: gene expression***,** 657-744.
STANBROUGH, M. & MAGASANIK, B. 1995. Transcriptional and posttranslational regulation of the general amino acid permease of Saccharomyces cerevisiae. *Journal of bacteriology,* 177**,** 94-102.
STANBROUGH, M. & MAGASANIK, B. 1996. Two transcription factors, Gln3p and Nil1p, use the same GATAAG sites to activate the expression of GAP1 of Saccharomyces cerevisiae. *Journal of bacteriology,* 178**,** 2465-2468.
STANBROUGH, M., ROWEN, D. W. & MAGASANIK, B. 1995. Role of the GATA factors Gln3p and Nil1p of Saccharomyces cerevisiae in the expression of nitrogen-regulated genes. *Proceedings of the National Academy of Sciences,* 92**,** 9450-9454.
STEBER, C. M. & ESPOSITO, R. E. 1995. UME6 is a central component of a developmental regulatory switch controlling meiosis-specific gene expression. *Proceedings of the National Academy of Sciences,* 92**,** 12490-12494.
STEVENS, F. J. & ARGON, Y. Protein folding in the ER. Seminars in cell & developmental biology, 1999. Elsevier, 443-454.
STRICH, R., SUROSKY, R. T., STEBER, C., DUBOIS, E., MESSENGUY, F. & ESPOSITO, R. E. 1994. UME6 is a key regulator of nitrogen repression and meiotic development. *Genes & development,* 8**,** 796-810.
STUART, D. & WITTENBERG, C. 1998. CLB5 and CLB6 are required for premeiotic DNA replication and activation of the meiotic S/M checkpoint. *Genes & development,* 12**,** 2698-2710.
SU, S. & MITCHELL, A. P. 1993. Identification of functionally related genes that stimulate early meiotic gene expression in yeast. *Genetics,* 133**,** 67-77.

SUKA, N., SUKA, Y., CARMEN, A. A., WU, J. & GRUNSTEIN, M. 2001. Highly specific antibodies determine histone acetylation site usage in yeast heterochromatin and euchromatin. *Molecular cell,* 8**,** 473-479.

SWINNEN, E., WANKE, V., ROOSEN, J., SMETS, B., DUBOULOZ, F., PEDRUZZI, I., CAMERONI, E., DE VIRGILIO, C. & WINDERICKX, J. 2006. Rim15 and the crossroads of nutrient signalling pathways in Saccharomyces cerevisiae. *Cell division,* 1**,** 1-8.

TAKAHATA, S., YU, Y. & STILLMAN, D. J. 2009. The E2F functional analogue SBF recruits the Rpd3 (L) HDAC, via Whi5 and Stb1, and the FACT chromatin reorganizer, to yeast G1 cyclin promoters. *The EMBO journal,* 28**,** 3378-3389.

TALANIAN, R. V., MCKNIGHT, C. J. & KIM, P. S. 1990. Sequence-specific DNA binding by a short peptide dimer. *Science,* 249**,** 769-771.

TAMAKI, H., MIWA, T., SHINOZAKI, M., SAITO, M., YUN, C.-W., YAMAMOTO, K. & KUMAGAI, H. 2000. GPR1 regulates filamentous growth through FLO11 in yeast Saccharomyces cerevisiae. *Biochemical and biophysical research communications,* 267**,** 164-168.

TANG, W., RU, Y., HONG, L., ZHU, Q., ZUO, R., GUO, X., WANG, J., ZHANG, H., ZHENG, X. & WANG, P. 2015. System-wide characterization of bZIP transcription factor proteins involved in infection-related morphogenesis of M agnaporthe oryzae. *Environmental microbiology,* 17**,** 1377-1396.

THEVELEIN, J., GELADÉ, R., HOLSBEEKS, I., LAGATIE, O., POPOVA, Y., ROLLAND, F., STOLZ, F., VAN DE VELDE, S., VAN DIJCK, P. & VANDORMAEL, P. 2005. Nutrient sensing systems for rapid activation of the protein kinase A pathway in yeast. Portland Press Ltd.

THEVELEIN, J. M. & DE WINDE, J. H. 1999. Novel sensing mechanisms and targets for the cAMP–protein kinase A pathway in the yeast Saccharomyces cerevisiae. *Molecular microbiology,* 33**,** 904-918.

TKACH, J. M., YIMIT, A., LEE, A. Y., RIFFLE, M., COSTANZO, M., JASCHOB, D., HENDRY, J. A., OU, J., MOFFAT, J. & BOONE, C. 2012. Dissecting DNA damage response pathways by analysing protein localization and abundance changes during DNA replication stress. *Nature cell biology,* 14**,** 966-976.

TODA, T., CAMERON, S., SASS, P., ZOLLER, M. & WIGLER, M. 1987. Three different genes in S. cerevisiae encode the catalytic subunits of the cAMP-dependent protein kinase. *Cell,* 50**,** 277-287.

TODA, T., UNO, I., ISHIKAWA, T., POWERS, S., KATAOKA, T., BROEK, D., CAMERON, S., BROACH, J., MATSUMOTO, K. & WIGLER, M. 1985. In yeast, RAS proteins are controlling elements of adenylate cyclase. *Cell,* 40**,** 27-36.

TORRES, J., DI COMO, C. J., HERRERO, E. & DE LA TORRE-RUIZ, M. A. 2002. Regulation of the cell integrity pathway by rapamycin-sensitive TOR function in budding yeast. *Journal of Biological Chemistry,* 277**,** 43495-43504.

TRAVERS, K. J., PATIL, C. K., WODICKA, L., LOCKHART, D. J., WEISSMAN, J. S. & WALTER, P. 2000. Functional and genomic analyses reveal an essential coordination between the unfolded protein response and ER-associated degradation. *Cell,* 101**,** 249-258.

TREININ, M. & SIMCHEN, G. 1993. Mitochondrial activity is required for the expression of IME1, a regulator of meiosis in yeast. *Current genetics,* 23**,** 223-227.

TSUCHIYA, D., YANG, Y. & LACEFIELD, S. 2014. Positive feedback of NDT80 expression ensures irreversible meiotic commitment in budding yeast. *PLoS genetics,* 10**,** e1004398.

TSUKIYAMA, T., PALMER, J., LANDEL, C. C., SHILOACH, J. & WU, C. 1999. Characterization of the imitation switch subfamily of ATP-dependent chromatin-remodeling factors in Saccharomyces cerevisiae. *Genes & development,* 13**,** 686-697.

TURNER, R. & TJIAN, R. 1989. Leucine repeats and an adjacent DNA binding domain mediate the formation of functional cFos-cJun heterodimers. *Science,* 243**,** 1689-1694.
TZAMARIAS, D., PU, W. T. & STRUHL, K. 1992. Mutations in the bZIP domain of yeast GCN4 that alter DNA-binding specificity. *Proceedings of the National Academy of Sciences,* 89**,** 2007-2011.
UETZ, P., GIOT, L., CAGNEY, G., MANSFIELD, T. A., JUDSON, R. S., KNIGHT, J. R., LOCKSHON, D., NARAYAN, V., SRINIVASAN, M. & POCHART, P. 2000. A comprehensive analysis of protein–protein interactions in Saccharomyces cerevisiae. *Nature,* 403**,** 623-627.
UPPALA, J. K., SATHE, L., CHAKRABORTY, A., BHATTACHARJEE, S., PULVINO, A. T. & DEY, M. 2022. The cap-proximal RNA secondary structure inhibits preinitiation complex formation on HAC1 mRNA. *Journal of Biological Chemistry,* 298.
URBAN, J., SOULARD, A., HUBER, A., LIPPMAN, S., MUKHOPADHYAY, D., DELOCHE, O., WANKE, V., ANRATHER, D., AMMERER, G. & RIEZMAN, H. 2007. Sch9 is a major target of TORC1 in Saccharomyces cerevisiae. *Molecular cell,* 26**,** 663-674.
VAN ANKEN, E., PINCUS, D., COYLE, S., ARAGÓN, T., OSMAN, C., LARI, F., PUERTA, S. G., KORENNYKH, A. V. & WALTER, P. 2014. Specificity in endoplasmic reticulum-stress signaling in yeast entails a step-wise engagement of HAC1 mRNA to clusters of the stress sensor Ire1. *Elife,* 3**,** e05031.
VAN DE VELDE, S. & THEVELEIN, J. M. 2008. Cyclic AMP-protein kinase A and Snf1 signaling mechanisms underlie the superior potency of sucrose for induction of filamentation in Saccharomyces cerevisiae. *Eukaryotic cell,* 7**,** 286-293.
VAN HEECKEREN, W. J., SELLERS, J. W. & STRUHL, K. 1992. Role of the conserved leucines in the leucine zipper dimerization motif of yeast GCN4. *Nucleic acids research,* 20**,** 3721-3724.
VAN NULAND, A., VANDORMAEL, P., DONATON, M., ALENQUER, M., LOURENÇO, A., QUINTINO, E., VERSELE, M. & THEVELEIN, J. M. 2006. Ammonium permease-based sensing mechanism for rapid ammonium activation of the protein kinase A pathway in yeast. *Molecular microbiology,* 59**,** 1485-1505.
VERSELE, M., DE WINDE, J. H. & THEVELEIN, J. M. 1999. A novel regulator of G protein signalling in yeast, Rgs2, downregulates glucose-activation of the cAMP pathway through direct inhibition of Gpa2. *The EMBO journal,* 18**,** 5577-5591.
VERSHON, A. K. & PIERCE, M. 2000. Transcriptional regulation of meiosis in yeast. *Current opinion in cell biology,* 12**,** 334-339.
VIDAL, M. & GABER, R. F. 1991. RPD3 encodes a second factor required to achieve maximum positive and negative transcriptional states in Saccharomyces cerevisiae. *Molecular and cellular biology,* 11**,** 6317-6327.
VIDAN, S. & MITCHELL, A. P. 1997. Stimulation of yeast meiotic gene expression by the glucose-repressible protein kinase Rim15p. *Molecular and Cellular Biology,* 17**,** 2688-2697.
VINCENT, J. A., KWONG, T. J. & TSUKIYAMA, T. 2008. ATP-dependent chromatin remodeling shapes the DNA replication landscape. *Nature structural & molecular biology,* 15**,** 477-484.
VINSON, C., MYAKISHEV, M., ACHARYA, A., MIR, A. A., MOLL, J. R. & BONOVICH, M. 2002. Classification of human B-ZIP proteins based on dimerization properties. *Molecular and cellular biology,* 22**,** 6321-6335.
VOELKEL-MEIMAN, K., MOUSTAFA, S. S., LEFRANÇOIS, P., VILLENEUVE, A. M. & MACQUEEN, A. J. 2012. Full-length synaptonemal complex grows continuously during meiotic prophase in budding yeast.

VOGELAUER, M., WU, J., SUKA, N. & GRUNSTEIN, M. 2000. Global histone acetylation and deacetylation in yeast. *Nature,* 408**,** 495-498.
WAGNER, C., DIETZ, M., WITTMANN, J., ALBRECHT, A. & SCHÜLLER, H. J. 2001. The negative regulator Opi1 of phospholipid biosynthesis in yeast contacts the pleiotropic repressor Sin3 and the transcriptional activator Ino2. *Molecular microbiology,* 41**,** 155-166.
WALSH, G. 2010. Post-translational modifications of protein biopharmaceuticals. *Drug discovery today,* 15**,** 773-780.
WALSH, R. B., KAWASAKI, G. & FRAENKEL, D. 1983. Cloning of genes that complement yeast hexokinase and glucokinase mutants. *Journal of bacteriology,* 154**,** 1002-1004.
WALTER, P. & RON, D. 2011. The unfolded protein response: from stress pathway to homeostatic regulation. *science,* 334**,** 1081-1086.
WANG, H. & JIANG, Y. 2003. The Tap42-protein phosphatase type 2A catalytic subunit complex is required for cell cycle-dependent distribution of actin in yeast. *Molecular and cellular biology,* 23**,** 3116-3125.
WARD, M. P. & GARRETT, S. 1994. Suppression of a yeast cyclic AMP-dependent protein kinase defect by overexpression of SOK1, a yeast gene exhibiting sequence similarity to a developmentally regulated mouse gene. *Molecular and cellular biology,* 14**,** 5619-5627.
WARD, M. P., GIMENO, C. J., FINK, G. R. & GARRETT, S. 1995. SOK2 may regulate cyclic AMP-dependent protein kinase-stimulated growth and pseudohyphal development by repressing transcription. *Molecular and cellular biology,* 15**,** 6854-6863.
WEDAMAN, K. P., REINKE, A., ANDERSON, S., YATES III, J., MCCAFFERY, J. M. & POWERS, T. 2003. Tor kinases are in distinct membrane-associated protein complexes in Saccharomyces cerevisiae. *Molecular biology of the cell,* 14**,** 1204-1220.
WEINSTOCK, K. G. & BALLOU, C. E. 1987. Tunicamycin inhibition of epispore formation in Saccharomyces cerevisiae. *Journal of bacteriology,* 169**,** 4384-4387.
WELIHINDA, A. A. & KAUFMAN, R. J. 1996. The unfolded protein response pathway in Saccharomyces cerevisiae: oligomerization and trans-phosphorylation of Ire1p (Ern1p) are required for kinase activation. *Journal of Biological Chemistry,* 271**,** 18181-18187.
WELIHINDA, A. A., TIRASOPHON, W., GREEN, S. R. & KAUFMAN, R. J. 1998. Protein serine/threonine phosphatase Ptc2p negatively regulates the unfolded-protein response by dephosphorylating Ire1p kinase. *Molecular and Cellular Biology,* 18**,** 1967-1977.
WELIHINDA, A. A., TIRASOPHON, W. & KAUFMAN, R. J. 1999. The cellular response to protein misfolding in the endoplasmic reticulum. *Gene Expression The Journal of Liver Research,* 7**,** 293-300.
WELIHINDA, A. A., TIRASOPHON, W. & KAUFMAN, R. J. 2000. The transcriptional co-activator ADA5 is required for HAC1 mRNA processing in vivo. *Journal of Biological Chemistry,* 275**,** 3377-3381.
WILLIAMS, R. M., PRIMIG, M., WASHBURN, B. K., WINZELER, E. A., BELLIS, M., DE MENTHIERE, C. S., DAVIS, R. W. & ESPOSITO, R. E. 2002. The Ume6 regulon coordinates metabolic and meiotic gene expression in yeast. *Proceedings of the National Academy of Sciences,* 99**,** 13431-13436.
WIMALASENA, T. T., ENJALBERT, B., GUILLEMETTE, T., PLUMRIDGE, A., BUDGE, S., YIN, Z., BROWN, A. J. & ARCHER, D. B. 2008. Impact of the unfolded protein response upon genome-wide expression patterns, and the role of Hac1 in the polarized growth, of Candida albicans. *Fungal genetics and biology,* 45**,** 1235-1247.

WINGFIELD, P. 1998. Protein precipitation using ammonium sulfate. *Current protocols in protein science,* 13**,** A. 3F. 1-A. 3F. 8.
WINGFIELD, P. T., STAHL, S. J., PAYTON, M. A., VENKATESAN, S., MISRA, M. & STEVEN, A. C. 1991. HIV-1 Rev expressed in recombinant Escherichia coli: purification, polymerization, and conformational properties. *Biochemistry,* 30**,** 7527-7534.
WINTER, E. 2012. The Sum1/Ndt80 transcriptional switch and commitment to meiosis in Saccharomyces cerevisiae. *Microbiology and Molecular Biology Reviews,* 76**,** 1-15.
WU, C., WHITEWAY, M., THOMAS, D. Y. & LEBERER, E. 1995. Molecular Characterization of Ste20p, a Potential Mitogen-activated Protein or Extracellular Signal-regulated Kinase Kinase (MEK) Kinase Kinase from Saccharomyces cerevisiae (∗). *Journal of Biological Chemistry,* 270**,** 15984-15992.
WULLSCHLEGER, S., LOEWITH, R. & HALL, M. N. 2006. TOR signaling in growth and metabolism. *Cell,* 124**,** 471-484.
XIA, X. 2020. RNA-Seq approach for accurate characterization of splicing efficiency of yeast introns. *Methods,* 176**,** 25-33.
XIAO, Y. & MITCHELL, A. P. 2000. Shared roles of yeast glycogen synthase kinase 3 family members in nitrogen-responsive phosphorylation of meiotic regulator Ume6p. *Molecular and cellular biology,* 20**,** 5447-5453.
XIE, J., PIERCE, M., GAILUS-DURNER, V., WAGNER, M., WINTER, E. & VERSHON, A. K. 1999. Sum1 and Hst1 repress middle sporulation-specific gene expression during mitosis in Saccharomyces cerevisiae. *The EMBO journal,* 18**,** 6448-6454.
XU, L., AJIMURA, M., PADMORE, R., KLEIN, C. & KLECKNER, N. 1995. NDT80, a meiosis-specific gene required for exit from pachytene in Saccharomyces cerevisiae. *Molecular and cellular biology,* 15**,** 6572-6581.
XUE, Y., BATLLE, M. & HIRSCH, J. P. 1998. GPR1 encodes a putative G protein-coupled receptor that associates with the Gpa2p Gα subunit and functions in a Ras-independent pathway. *The EMBO journal,* 17**,** 1996-2007.
YAMAMOTO, K., GONZALEZ, G., BIGGS, W. R. & MONTMINY, M. 1988. Phosphorylation-induced binding and transcriptional efficacy of nuclear factor CREB. *Nature,* 334**,** 494-498.
YEHESKELY-HAYON, D., KOTLER, A., STARK, M., HASHIMSHONY, T., SAGEE, S. & KASSIR, Y. 2013. The roles of the catalytic and noncatalytic activities of Rpd3L and Rpd3S in the regulation of gene transcription in yeast. *PLoS One,* 8**,** e85088.
YU, J., ANGELIN-DUCLOS, C., GREENWOOD, J., LIAO, J. & CALAME, K. 2000. Transcriptional repression by blimp-1 (PRDI-BF1) involves recruitment of histone deacetylase. *Molecular and cellular biology,* 20**,** 2592-2603.
YUN, C.-W., TAMAKI, H., NAKAYAMA, R., YAMAMOTO, K. & KUMAGAI, H. 1997. G-protein coupled receptor from yeastSaccharomyces cerevisiae. *Biochemical and biophysical research communications,* 240**,** 287-292.
YUN, C.-W., TAMAKI, H., NAKAYAMA, R., YAMAMOTO, K. & KUMAGAI, H. 1998. Gpr1p, a Putative G-Protein coupled receptor, regulates glucose-dependent cellular cAMP level in yeastsaccharomyces cerevisiae. *Biochemical and biophysical research communications,* 252**,** 29-33.
ZAMAN, S., LIPPMAN, S. I., SCHNEPER, L., SLONIM, N. & BROACH, J. R. 2009. Glucose regulates transcription in yeast through a network of signaling pathways. *Molecular systems biology,* 5**,** 245.
ZARAGOZA, O. & GANCEDO, J. M. 2000. Pseudohyphal growth is induced in Saccharomyces cerevisiae by a combination of stress and cAMP signalling. *Antonie Van Leeuwenhoek,* 78**,** 187-194.

ZHANG, W., DU, G., ZHOU, J. & CHEN, J. 2018. Regulation of sensing, transportation, and catabolism of nitrogen sources in Saccharomyces cerevisiae. *Microbiology and Molecular Biology Reviews,* 82**,** e00040-17.

ZHENG, X.-F. & SCHREIBER, S. L. 1997. Target of rapamycin proteins and their kinase activities are required for meiosis. *Proceedings of the National Academy of Sciences,* 94**,** 3070-3075.